Ecological Modelling and Energy DSS

CES TECHNICAL REPORT 131, August 2013

T.V. Ramachandra	**N.V. Joshi**	**Uttam Kumar**
Gautam Krishnadas	G.R.Rao	Bharath H. Aithal
Bharath Settur	Rajsri Ray	Shwetmala
Dhanpal G	Gururaja K V	Amit S. Yadav

Mandhala, Moolbari and MeGad Watersheds

CES Technical Report 131

August 2013

Energy & Wetlands Research Group
Centre for Ecological Sciences,
Indian Institute of Science,
Bangalore - 560012, INDIA

Web: http://ces.iisc.ernet.in/energy/
http://ces.iisc.ernet.in/biodiversity

Email: cestvr@ces.iisc.ernet.in,
energy@ces.iisc.ernet.in

Ecological Modelling and Energy DSS

Sl no	Content	Page no.
1	Characterisation of Landscape with Forest Fragmentation Dynamics: Moolbari Watershed	1
2	Landscape Dynamics in Mandhala Watershed, Himachal Pradesh	21
3	Land Surface Temperature Analysis of Himachal Pradesh through Multi-Resolution, Spatio –Temporal Data	34
4	Predictive Distribution Modeling for Rare Himalayan Medicinal Plant *Berberis aristata* Dc.	42
5	Flora and Faunal Distribution in Three Selected Micro Watersheds of Western Himalaya	54
6	Above Ground Biomass and Biomass Productivity of Three Micro Watersheds across Altitudinal Gradients in Western Himalaya	84
7	Above Ground Standing Biomass of Three Micro Watersheds in Himachal Pradesh	105
8	Solar Potential Assessment in the Himalayan Landscape	250
9	Spatial Analysis of Wind Energy Potential in Himachal Pradesh	270
10	Regional Bioenergy Planning for Sustainability in Himachal Pradesh, India	286
	Publications	323

Characterisation of Landscape with Forest Fragmentation Dynamics: Moolbari watershed

Abstract

Land cover (LC) and land use (LU) dynamics induced by human and natural processes play a major role in global as well as regional patterns of landscapes influencing biodiversity, hydrology, ecology and climate. Changes in LC features resulting in forest fragmentations have posed direct threats to biodiversity, endangering the sustainability of ecological goods and services. Habitat fragmentation is of added concern as the residual spatial patterns mitigate or exacerbate edge effects. LU dynamics are obtained by classifying temporal remotely sensed satellite imagery of different spatial and spectral resolutions.

This paper reviews five different image classification algorithms using spatio-temporal data of a temperate watershed in Himachal Pradesh, India. Gaussian Maximum Likelihood classifier was found to be apt for analysing spatial pattern at regional scale based on accuracy assessment through error matrix and ROC (receiver operating characteristic) curves. The LU information thus derived was then used to assess spatial changes from temporal data using principal component analysis and correspondence analysis based image differencing. The forest area dynamics was further studied by analysing the different types of fragmentation through forest fragmentation models. The computed forest fragmentation and landscape metrics show a decline of interior intact forests with a substantial increase in patch forest during 1972 - 2007.

Key words: Land cover, algorithms, ROC curve, spatial change, correspondence analysis, forest fragmentation

Introduction

Landscape refers to a portion of heterogeneous territory composed of sets of interacting ecosystems and are characterised essentially by its dynamics that are partly governed by human activities. The physical state of the earth's immediate surface in terms of vegetation, soil, water, and human-made structures (e.g. buildings) at any instant of time constitute land cover (LC). Land use (LU) refers to the way humans and their habitat use land resources, usually with assent on the functional role of land for economic activities. LC changes in the recent times have influenced economics, environment, culture, and demography at regional levels. Consequences of LC changes such as forest fragmentation pose serious threats to biodiversity and endanger the sustainability of ecological goods and services. The change is LC and LU types can be obtained from multi-satellite sensor spatio-temporal data using efficient classification algorithms and pattern recognition techniques [1]. The classification algorithms can either be unsupervised or supervised. In the former, no training data is utilised for classification. Instead the classifiers examine the unknown pixels in an image and aggregate them into comparatively well-separated spectral classes based on the natural groupings or clusters. In the latter case, the analyst has training data which is used to train the classifier and also the outcome of the classification is validated with the independently collected test data.

Numerous statistical classification algorithms exist, each one having a genesis behind its evolution. Depending on the nature of the data sources and methodology, multi-source, multi-sensor, multi-temporal, multi-frequency or multi-polarisation data are being used [2, 3, 4]. In most of the cases, the algorithms perform well with high degrees of accuracy, however, in an undulating terrain, where there is a large variation in spectral response due to high relief and shadow, the performance of a classifier deteriorates. Another major problem with these classifiers is their inability to classify data at different measurement scales and units due to invalid assumptions of statistical distributions. Temporal analysis of the spatial data provides an idea of the extent of changes happening in the landscape. LU details derived from temporal remote sensing (RS) data offer potential for assessing the changes in land uses, forest fragmentation and its impact on biodiversity, economics, greenhouse gas emission and hydrology. Spatial LU maps indicate only the location and type of forest, and further analyses are needed to quantify forest fragmentation. Hence, fragmentation of forests was assessed to understand the implication of temporal dynamics on forest habitats. Forest fragmentation is the process whereby a large, contiguous area of forest is both reduced in area and divided into two or more fragments. The decline in the size of the forest and the increasing isolation between the two remnant patches of the forest has been the major cause of declining biodiversity [5]. The primary concern is direct loss of forest area, and all disturbed forests are subject to "edge effects" of one kind or another. Forest fragmentation is of additional concern, insofar as the edge effect is mitigated by the residual spatial pattern [6]. In this context, objectives of this communication is to

(i.) evaluate the performance of the different classification techniques (for land use analysis).

(ii.) analyse the landscape dynamics using temporal RS data.

(iii.) model the forest fragmentation in the landscape.

Material and Methods

DATA

Survey of India (SOI) toposheets of 1:50000 and 1:250000 scales were digitised to derive base layers. Ground control points (GCPs) for geo-rectification and training data for supervised classification of RS data were collected through field investigations using a handheld GPS. Google Earth data (http://earth.google.com) were used pre and post classification and also for validation. The RS data used for the study are Landsat MSS (79 m, 4 bands, acquired: November 15, 1972), Landsat TM (30 m, 6 bands, acquired: October 9, 1989), Landsat ETM+ (30 m, bands 1-5 and 7, band 8 - Panchromatic of 15m, acquired: October 15, 2000) and IRS LISS-III (23.5 m, 3 bands, acquired: May 9, 2007). Landsat data were downloaded (from http://glcf.umiacs.umd.edu/data/) and IRS data were procured from National Remote Sensing Centre, Hyderabad, India. Bands were geocorrected with the known GCP's, and projected to geographic latitude-longitude with WGS-84 datum, followed by masking and cropping of the study area. Landsat data (of 1972) were resampled to 60 m, Landsat TM data of 1989 and IRS LISS III were resampled to 15 m using nearest neighbourhood technique.

Study area: Moolbari watershed is situated in Shimla district, Himachal Pradesh, India as a part of Yamuna river basin and encompasses an area of 13.41 sq. km. from 31.07-31.17°N 77.05-77.15°E (figure 1). The altitude ranges from 1400 – 2000 m amsl.

Figure 1: Moolbari watershed

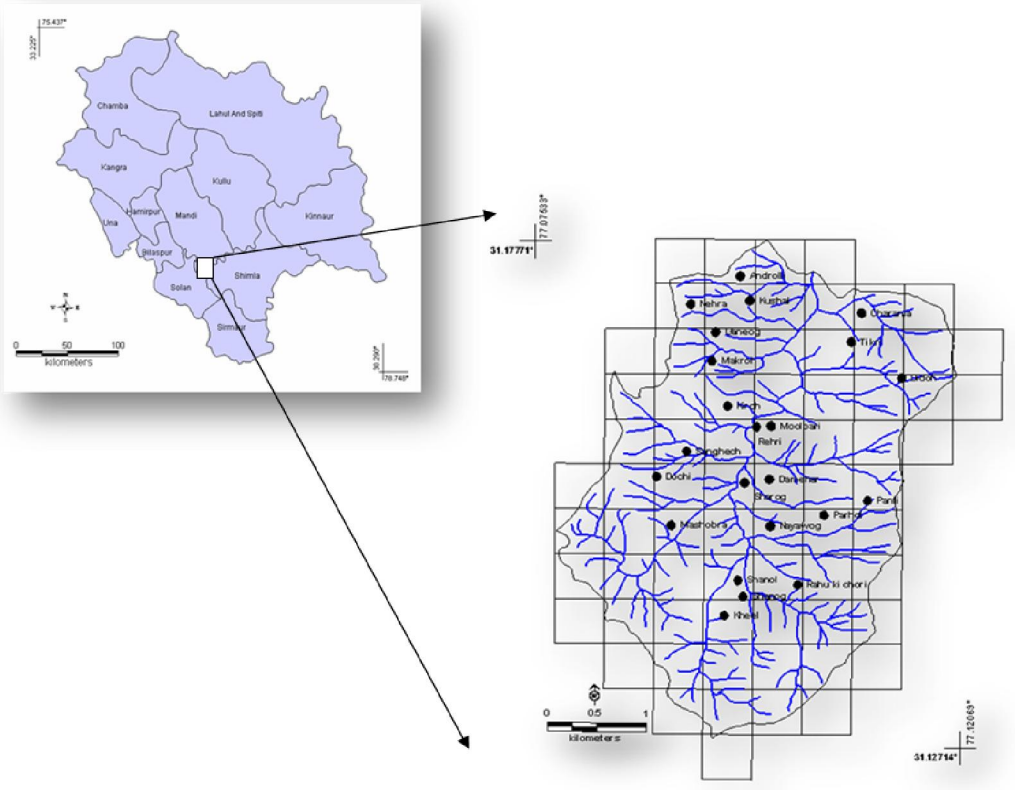

The vegetation in Moolbari is of mid-temperate comprising mixed deciduous (up to 1500 m) and sub-tropical pine forest (above 1500 m) in two different altitudinal ranges. There are reserve forests managed by state forest department, insofar cutting of trees is prohibited. However, lopping and collection of fallen wood for household purposes by the villagers are noted.

METHODS

The methods adopted in the analysis involve principal component analysis (PCA) based fusion, Land cover (LC), Land use (LU) analyses, change detection and forest fragmentation analysis.

1. Image Fusion: This was done using PCA fusion to increase the spatial resolution of multichannel image by introducing an image with a higher resolution. PC analysis was performed separately on the 6 bands of Landsat TM of 1989 (of spatial resolution 15 m) and 4 bands of Landsat MSS data of 1972 (of spatial resolution 60 m). PC1 of Landsat TM 1989 was stretched to have same mean and variance as that of PC1 of Landsat MSS using equation 1 [7].

$$DN_{new\_image} = \frac{\sigma_{ref}}{\sigma_{old}}(DN_{old} - \mu_{old}) + \mu_{ref} \quad (1)$$

where DN_{new_image} is the image that has same mean and variance as that of principal component (PC) 1 of Landsat MSS, μ_{ref} and σ_{ref} refers to the mean and standard deviation of PC1 of Landsat MSS. DN_{old}, μ_{old} and σ_{old} represent the digital number, mean and standard deviation of PC1 of Landsat TM (1989).

PC1 of Landsat MSS was replaced with PC1 of higher resolution Landsat TM of 1989 as it contains the information which is common to all bands while the spectral information is unique for each band. PC1 accounts for maximum variance which can maximise the effect of the high resolution data in the fused image. Finally, high-resolution multispectral images were determined by performing the inverse PCA transformation. Similarly, Panchromatic band at 15 m resolution was fused with the 6 bands (at 30 m) of Landsat ETM+ (2000). With this, the RS data corresponding to 4 time periods were at a uniform spatial resolution of 15 m for easy analysis, consistency and multi-date pixel to pixel comparison. These data were used subsequently for LU classification and spatial change analysis.

2. Land cover (LC): NDVI was computed to segregate regions under vegetation, soil and water using NIR and Red bands of temporal data.

3. LU classification: The classification techniques evaluated on temporal data (with diverse spatial and spectral resolutions) are: Gaussian Maximum Likelihood Classifier (GMLC), Minimum distance to means, Mahalanobis distance, Parallelepiped and Binary Encoding (BE).

(i.) **GMLC –** It quantitatively evaluates both the variance and covariance of the category spectral response patterns when classifying an unknown pixel [8], assuming the distribution of data points to be Gaussian. The distribution of a category response pattern can be completely described by the mean vector and the covariance matrix. The statistical probability of a given pixel value being a member of a particular class are computed. After evaluating the probability in each category, the pixel is assigned to the most likely class (highest probability value).

(ii.) **Minimum distance to Means –** Here, the mean spectral value in each band for each category is determined [8, 9]. These values comprise the mean vector for each category. A pixel of unknown identity may be classified by computing the distance between the value of the unknown pixel and each of the category means. After computing the distances, the unknown pixel is assigned to the closest class.

(iii.) **Mahalanobis distance –** When the covariance matrices for all of the classes are identical but otherwise arbitrary [1, 10], samples fall in hyperellipsoidal clusters of equal size and shape, the cluster for the i^{th} class being centred about the mean vector μ_i. The optimal decision rule to classify a feature vector **x** would be to measure the squared Mahalanobis distance $(x-\mu_i)^t \Sigma^{-1}(x-\mu_i)$ from **x** to each of the mean vectors, and assign **x** to the closest category.

(iv.) **Parallelepiped classifier –** Parallelepiped classifier [11] is a multidimensional analogy of the box classifier [12]. It allows multi-dimensional boxes that are used for multispectral

bands. Each box in the parallelepiped classifier is formed by the maximum (max.) and minimum (min.) values in each training class data in each band. For multispectral bands, the parallelograms will be obtained. The sensitivity or category variance is introduced by considering the range of values in each category training set defined by the highest (max.) and lowest (min.) digital number in each band. An unknown pixel is classified according to the decision region in which it lies [8]. The class signatures come from the analyst defined training sites. A pixel is classified as a member of a class if and only if all of its band information or signature falls within the corresponding ranges of the bands defined by that class.

(v.) **BE** –The most primitive and natural preprocessing of spectral data for qualitative identification is binary (one bit) encoding [13, 14]. Hamming distance, which is the binary equivalent of the Euclidean distance, is used as a dissimilarity metric. The vector for an individual spectrum represents a point in hamming space with unit edge in a hypercube. Since only 0 and 1 are assigned to peak intensities, all of the spectral points lie only on the corners (vertices) of the hypercube. Hamming distance between two spectral points is equal to the number of mismatches between the binary encoded data vectors (spectra) being compared and is the same as the result obtained by application of the logical exclusive OR operator (XOR) to the two spectra.

Accuracy assessment of these techniques was done using error matrix and receiver operating characteristic (ROC) curves to choose the best classifier.

4. LU change detection: This is performed by change/no-change recognition followed by boundary delineation on images of multi time periods [15]. Changes across a period of 35 years were analysed through PCA, correspondence analysis (CA) and Normalised Difference Vegetation Indices (NDVI) differencing based change detection.

(i.) **PCA** – PCA is effective for change detection [16, 17] and is implemented on bi-temporal multispectral images. The major components of the time two image are subtracted from the corresponding components of the time one image to obtain differences related to changes in LU. Changes are detected at the lower-end and higher-end tails of the PC difference image pixels distribution histogram.

(ii.) **CA transformation** – In CA [18], data table is transformed into a table of the contribution using Pearson chi-square statistic. Pixel (x_{ij}) values are initially converted to proportions (p_{ij}) by dividing each pixel (x_{ij}) value by the sum (x_{++}) of all the pixels in the data set. This threshold in a new dataset of proportions (Q) with the size of (rxc). Row weight p_{i+} is equal to x_{i+} / x_{++}, where x_{i+} is the sum of values in row i. Vector [p_{i+}] is of size (r). Column weight p_{+j} is equal to x_{+j}/ x_{++}, where x_{+j} is the sum of values in column j. Vector [p_{+j}] is of size (c). The Pearson chi-square statistic χ^2_p, is a sum of squared χ_{ij} values, computed for every cell ij of the contingency table. q_{ij} values were used instead of χ_i values to form the matrix $\overline{Q}_{r\times c}$ so that $q_{ij} = \chi_{ij} / \sqrt{x_{++}}$ and eigenvalues would be smaller than or equal to 1. Multispectral data are then transformed into the component space using the matrix of eigenvectors. Image differencing is applied to CA components to perform change detection.

(iii.) **NDVI differencing –** In NDVI differencing [19, 20], areas of change can be identified through the subtraction of the NDVI image of one date from the NDVI image of another date. However, NDVI technique produces limited discriminating abilities in areas less dominated by vegetative ground cover types.

5. Forest Fragmentation: Forest fragmentation analysis was done to quantify the type of forest in the study area - patch, transitional, edge, perforated, and interior based on the classified images. Additionally, landscape metrics were computed to understand the fragmentation process at a patch and class level. These metrics along with the state of the forest fragmentation index was used to quantify and investigate the fragmentation process.

Forest fragmentation statistics and the total extent of forest and its occurrence as adjacent pixels is computed through fixed-area windows surrounding each forest pixel, which is used to classify the window by the type of fragmentation. The result is stored at the location of the centre pixel. Thus, a pixel value in the derived map refers to between-pixel fragmentation around the corresponding forest location [21]. Forest fragmentation category at pixel level is computed through *Pf* (the ratio of pixels that are forested to the total non-water pixels in the window) and *Pff* (the proportion of all adjacent (cardinal directions only) pixel pairs that include at least one forest pixel, for which both pixels are forested. Pff estimates the conditional probability that, given a pixel of forest, its neighbour is also forest. Based on the knowledge of Pf and Pff [21], six fragmentation categories: (1) interior, when Pf = 1.0; (2), patch, when Pf < 0.4; (3) transitional, when 0.4 < Pf < 0.6; (4) edge, when Pf > 0.6 and Pf – Pff > 0; (5) perforated, when Pf > 0.6 and Pf – Pff < 0, and (6) undetermined, when Pf > 0.6 and Pf = Pff are mapped.

Based on these forest fragmentation indices, Total forest proportion (TFP: ratio of area under forests to the total geographical extent excluding water bodies), weighted forest area (WFA) and Forest continuity (FC) are computed. TFP provides a basic assessment of forest cover in a region ranging from 0 to 1. Weighted values for the weighted forest area (WFA) are derived from the median Pf value for each fragmentation class as given by equation 2 below:

$$\text{WFA} = (1.0 * \text{interior}) + (0.8 * (\text{perforated} + \text{edge} + \text{undetermined}) + (0.5 * \text{transitiojnal}) + (0.2 * \text{patch}) \quad (2)$$

$$FC = \frac{weighted\ forest\ area}{total\ forest\ area} * \frac{area\ of\ largest\ interior\ forest\ patch}{total\ forest\ area} \quad (3)$$

TFP designations are as per Vogelmann (1995) [22] and Wickham *et al.*(1999) [23]; Forest fragmentation become more severe as forest cover decreases from 100 percent towards 80 percent. Between 60 and 80 percent forest cover, the opportunity for re-introduction of forest to connect forest patches is the greatest, and below 60 percent, forest patches become small and more fragmented. The FC regions were evenly split and designated as high forest continuity (above 0.5) or low forest continuity (below 0.5). FC value examines only the forested areas within the analysis region. The rationale is that given two regions of equal forest cover, the one with more interior forest would have a higher weighted area, and thus be less fragmented. To separate further regions based on the level of fragmentation, the weight area ratio is multiplied by the ratio of the largest interior forest patch to total forest area for the region. FC ranges from 0 to 1.

Results and discussion

NDVI was computed with the temporal data of 1972, 1989, 2000 and 2007 for land cover analysis to delineate area under green (agriculture, forest and plantations /orchards) and non-green (builtup land, waste / barren rock and stones). This shows the reduction of region under vegetation by 5.59% during three decades.

Further analyses of four datasets were done using Iterative Self-Organising Data (ISO data) [24, 25] clustering to understand the number of probable classes. It indicated that the mapping of the classes could be done accurately, giving an overall good representation of what was observed in the field. Initially 25 clusters were made, and clusters were merged one by one to produce a map with three distinct classes: forest, agriculture and barren land that were the dominant categories in the study area. Signature separability of the LU classes was done using Transformed divergence (TD) matrix and Bhattacharrya (or Jeffries-Mastusuta) distance and spectral graphs (figure 2). Both the TD and Jeffries-Mastusuta measures are real values between 0 and 2, where '0' indicates complete overlap between the signatures of two classes and '2' indicates a complete separation between the two classes. Both measures are monotonically related to classification accuracies. The larger the separability values, the better the final classification results. The possible ranges of separability values are 0.0 to 1.0 (very poor); 1.0 to 1.9 (poor); 1.9 to 2.0 (good). Very poor separability (0.0 to 1.0) indicates that the two signatures are statistically very close to each other [26]. Figure 2 shows that all the classes are well separable except barren and agriculture in band 4 of Landsat TM/ETM and IRS LISS-III data. Supervised classification was performed for land use analysis based on the training data uniformly distributed representing / covering the study area using the five algorithms. GMLC output is shown in figure 3. The error matrix [27] is given in table 1 and ROC curves [28] were plotted for each class (figure 4) to assess the accuracy of the classified data.

Table 1: Overall accuracy and kappa statistics for each classifier (OA - Overall Accuracy)

Algorithm	1972		1989		2000		2007	
	OA	Kappa	OA	Kappa	OA	Kappa	OA	Kappa
GMLC	88.95	0.84	88.52	0.85	80.85	0.76	88.36	0.83
Mahalanobis distance	84.41	0.76	77.78	0.74	80.66	0.77	72.27	0.69
Minimum distance	79.66	0.75	86.33	0.79	76.53	0.59	85.01	0.81
Parallelepiped	82.55	0.74	77.33	0.73	56.70	0.53	76.66	0.72
BE	75.16	0.68	86.00	0.81	61.20	0.56	79.73	0.68

Figure 2: Spectral signature separability for various sensor data

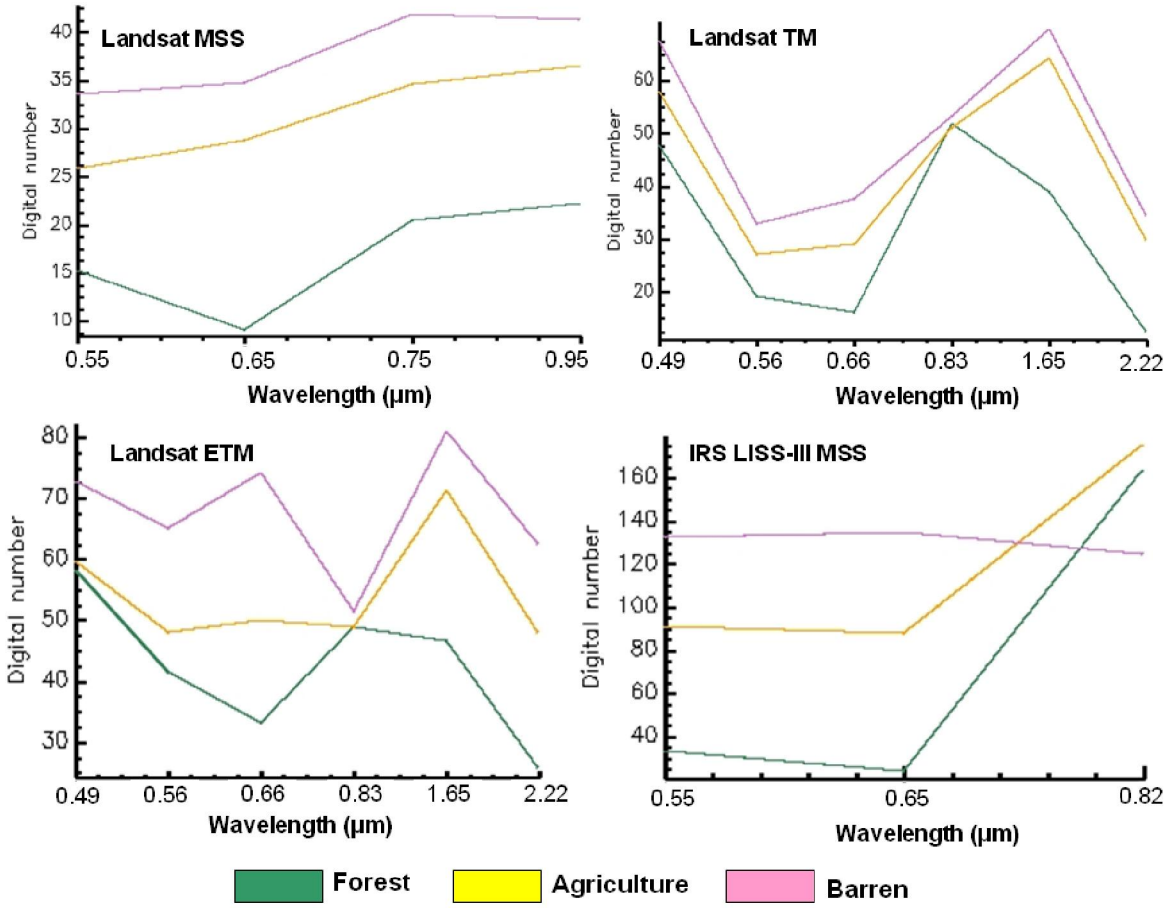

Figure 3: GMLC based LU classification using (A) Landsat MSS, 1972, (B) Landsat TM, 1989, (C) Landsat ETM, 2000 and (D) IRS LISS-III, 2007

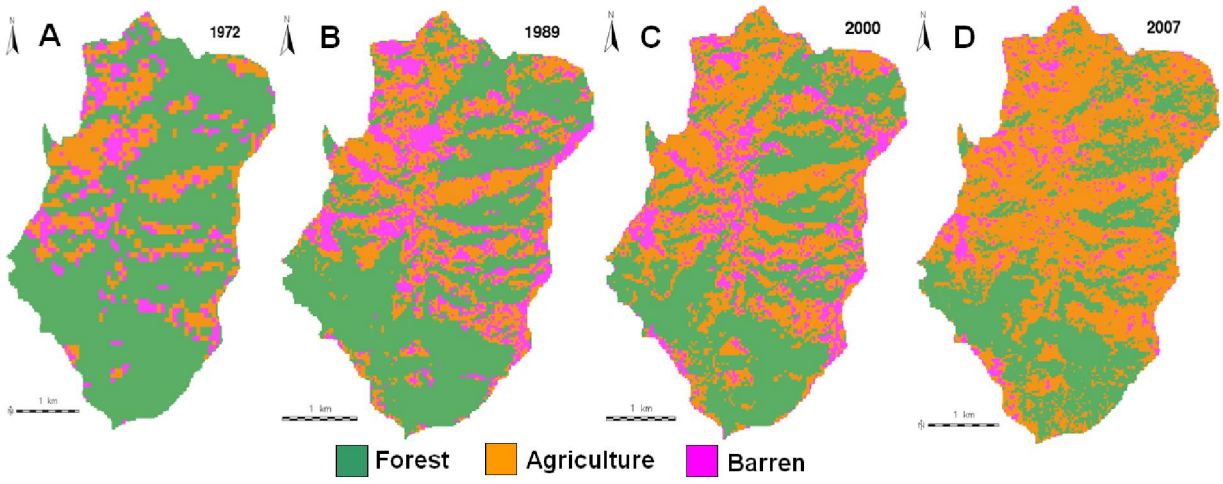

ROC curve helped in visualising the performance of a classification algorithm as the decision threshold could be varied algorithm-wise for each class. The best possible classification would yield a point in the upper left corner or coordinate (0,1) of the ROC space, representing 100% sensitivity (all true positives are found) and 100% specificity (no false positives are found). The (0,1) point is also called a *perfect classification*. A completely random guess would give a point along a diagonal line (*line of no-discrimination*) from the left bottom to the top right corners. The diagonal line divides the ROC space in areas of good or bad classification. Points above the diagonal line indicate good classification results, while points below the line indicate wrong results [29].

Figure 4: ROC curves for [A] Forest (1972); [B] Agriculture (1972); [C] Barren (1972); [D] Forest (2007); [E] Agriculture (2007); [F] Barren (2007) for the five different classifiers

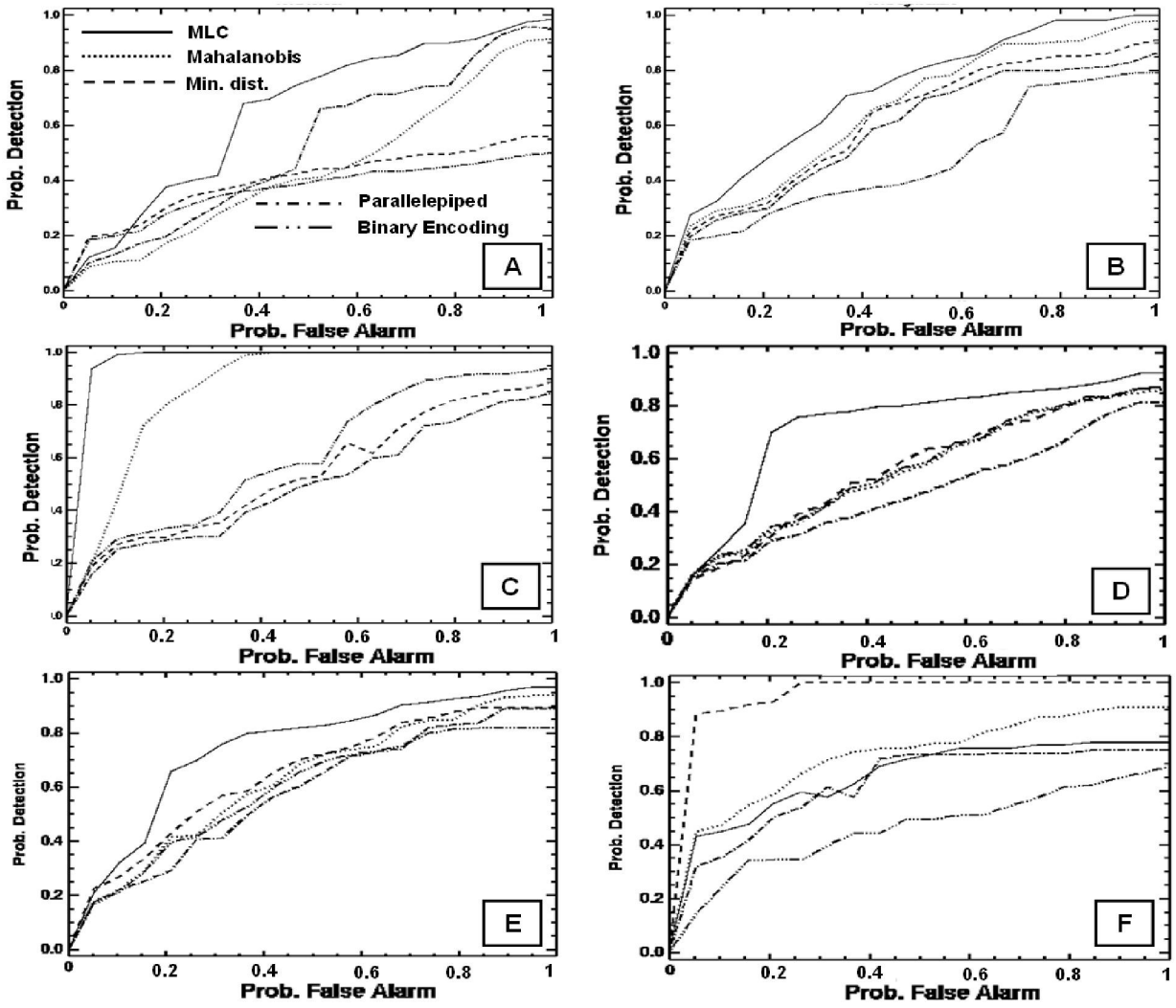

There is a good agreement between results obtained from error matrix and ROC curves to the ranking of the performance of the classification algorithms. They indicate that GMLC is the best performing algorithm for different sensor datasets (table 2). This conventional per-pixel, spectral-based classifier constitutes a historically dominant approach to RS-based automated LU and LC derivation [30, 31]. In fact, this aids as "benchmark" for evaluating the performance of novel classification algorithms [32].

Table 2: Ranking of algorithms based on Overall accuracy

Rank	1972	1989	2000	2007
1	MLC	MLC	MLC	MLC
2	Mahalanobis	Min. dist. to mean	Mahalanobis	Min. dist. to mean
3	Parallelepiped	Binary Encoding	Min. dist. to mean	Binary Encoding
4	Min. dist. to mean	Mahalanobis	Binary Encoding	Parallelepiped
5	Binary Encoding	Parallelepiped	Parallelepiped	Mahalanobis

Results of all these algorithms are valid only for the particular architecture or parameter settings tested although there may be other architectures that offer better performance. Selection of parameters is done based on the training data, evaluation, and test set methodology. Finally, for one particular application, the best way to select a classifier and its operational point is to use the Neyman-Pearson method of selecting the required sensitivity and then maximising the specificity with this constraint (or vice versa). The spectral signature curve for IRS LISS-III shows confusion between barren and agriculture. A similar result was obtained in the Jeffries-Matusita matrix with the separability values of 1.4 (poor separability). This was also observed while performing the clustering on LISS-III data.

The analysis showed GMLC to be better among the five algorithms. However, the successful application of GMLC is dependent upon having delineated correctly the spectral classes in the image data of interest. This is necessary because each class is to be modelled by a normal probability distribution. GMLC can obtain minimum classification error under the assumption that the spectral data of each class is normally distributed. The disadvantage is that it require its' every training set to include at least one more pixel than the number of bands. If a class happens to be multimodal, and this is not resolved, then clearly the modelling cannot be very effective. Mahalanobis distance is similar to any other statistical classifier and uses Mahalanobis distance as a metric. It takes into account errors associated with prediction measurement such as noise, by using the feature covariance matrix to scale features according to their variances. This classifier performed well on 1972 and 2000 images. Minimum distance to means is mathematically simple and computationally efficient. However, it has more error of omission and commission. It is insensitive to different degrees of variance in spectral response data. Therefore it should not be used where spectral classes are close to one another in the measurement space and have high variance. Although Parallelepiped algorithm did not perform very well, it is known for its good computational speed. When pixels are within overlapped region of parallelogram, then it may perform unsatisfactorily as pixels will end up unclassified and lead to error of omission. BE did

not perform very well for any dataset. However, this technique has been reported useful for high spectral resolution data where high-speed spectral signature matching is required. In order to effectively use this technique for spectral clustering, one must account for spectra which are relatively flat and devoid of absorption features.

Spatial change in LU pattern from 1972 to 2007 is shown in table 3. There is a decline of forest patches (48%) during the last three decades due to increasing agricultural practices. Agricultural area has significantly increased from 264 hectares (1972) to 779 hectares (2007). Barren area has increased by 23% (during 1972 to 2000). Barren land mainly constitutes the rocks, stones, and built ups. However, the proportion of barren land in 2007 is less compared to earlier classified images as some pixels corresponding to barren areas with grass cover showed similar spectral aspects as agriculture, which can be ascertained from figure 5.

Figure 5: FCC of Landsat MSS (1972), Landsat TM (1989), Landsat ETM (2000) and LISS-III (2007). FCC of 2007 shows similar reflectance of barren/stone and agricultural patch leading to confusion between these two classes

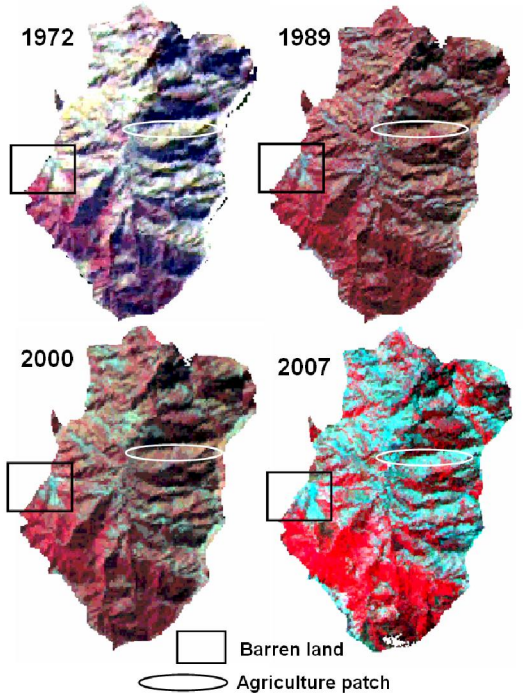

Difference of temporal PCs, CA-PC's, NDVI images and bands (rescaled from -1 to 1) showed similar results. To see the change in forest and agriculture, the NIR band of 1972 (T1) and 2007 (T2) were used which have the advantage of highlighting vegetation pixels because of the maximum reflectance by the green plants. The two NIR bands were first normalised by subtracting the image minimum and dividing by the image data range. Normalised temporal maps were then subtracted (T2 – T1) to see the absolute change in pixel values and were then converted to relative difference map with values ranging from -1 to +1 with 0 representing no change, -1 representing negative change and positive values representing increase in the value of the digital number of pixels from 1972 to 2007.

Table 3: LU change from 1972, 1989, 2000 and 2007

Year	Area	Forest	Agriculture	Barren
1972	**Ha**	925	264	152
	%	68.97	19.67	11.35
1989	**Ha**	706	398	229
	%	52.97	29.84	17.18
2000	**Ha**	591	555	187
	%	44.37	41.63	14.00
2007	**Ha**	474	779	88
	%	35.38	58.08	6.54

In both the images of the non-standardized PCA, PC1 had the highest information having all bands with unequal variances. CA puts less emphasis on bands that have low polarisation. Higher is the importance given to that band in the calculation of the between-pixel distances if more number of pixels are polarised in a band. First two components of CA explained approximately 99% of the total inertia in both images (table 4). Total inertia is a measure of how much the individual pixel values are spread around the centroid.

Table 4: Eigen structure of 1972 and 2007 data after PCA and CA transformation

PCA		Landsat MSS (1972)			IRS LISS-III (2007)		
		Comp1	Comp2	Comp3	Comp1	Comp2	Comp3
	Band 1	0.3175	0.3370	0.8863	-0.3589	0.5657	0.7424
	Band 2	0.5484	0.6973	-0.4616	-0.4747	0.5742	-0.6670
	Band 3	0.7736	-0.632	-0.0366	0.8037	0.5918	-0.0624
	Eigenvalues	168.50	9.3156	0.9892	2.9085	1.5724	0.0291
	Proportion	94.23	5.20	0.57	64.49	34.87	0.64
	Cumulative	94.23	99.43	100	64.49	99.36	100
Correspondence Analysis		Landsat MSS (1972)			IRS LISS-III (2007)		
		Comp1	Comp2	Comp3	Comp1	Comp2	Comp 3
	Band 1	0.5155	0.8569	0.00001	0.6710	0.1153	0.7325
	Band 2	0.6059	-0.365	0.7071	0.6866	0.2762	-0.6725
	Band 3	0.6059	-0.365	-0.7071	0.2799	-0.9541	-0.1061
	Eigenvalues	0.2681	0.0119	-0.0001	0.2595	0.0765	0.0040
	Proportion	95.71	4.25	0.036	76.32	22.5	1.176
	Cumulative	95.71	99.96	100	76.32	98.82	100

Detailed change detection tabulation was done between two classified images of 1972 and 2007. The analysis focuses primarily on the initial state classification changes – that is, for each initial state class (in 1972), it identifies the classes into which those pixels changed in the final state image (in 2007). Changes are reported as pixel counts, area and percentages in table 5 that list the *initial state classes in the columns* and the *final state classes in the rows* for the paired initial and final state classes. The rows contain all of the final state classes (2007) which are required for complete accounting of the distribution of pixels that changed classes.

Table 5: LU change detection statistics (1972 to 2007)

Final State (2007)		**Initial State (1972)**				
		Forest	**Agriculture**	**Barren**	**Row Total Column**	**Class Total Column**
Forest	Pixels	**23025**	1924	1797	26766	26766
	Area (Ha)	519.13	43.38	40.52	603.03	603.03
	Percent	38.71	3.23	3.02	44.96	44.96
Agriculture	Pixels	**18209**	6993	4159	**29361**	**29361**
	Area (Ha)	410.55	157.66	93.77	661.99	661.99
	Percent	30.61	11.76	6.99	49.36	49.36
Barren	Pixels	**1136**	1436	803	3375	3375
	Area (Ha)	25.61	32.38	18.12	76.09	76.09
	Percent	1.91	2.41	1.35	5.67	5.67
Class Total Row	Pixels	**42370**	**10350**	**6759**		
	Area (Ha)	955.29	233.42	152.39		
	Percent	71.23	17.41	11.36		
Class Changes Row	Pixels	**19345**	3357	5956		
	Area (Ha)	436.16	75.76	134.27		
	Percent	32.52	5.65	10.01		
Image Difference Row	Pixels	**-15604**	**+19011**	-3348		
	Area (Ha)	-352.27	+428.57	-76.3		
	Percent	-26.27	+31.95	-4.32		

For each initial state class (i.e., each column), the table indicates how these pixels were classified in the final state image. In table 5, 18209 pixels (410.55 ha) initially classified as forest (in 1972) changed into agriculture class in the final state image (2007). 23025 pixels were classified as forest in the initial state image (in 1972). The *Class Total Row* indicates the total number of pixels in each initial state class, (42370 in the Forest column = 23025+18209+1136. similarly there are 10350 pixels in agriculture and 6759 pixels in barren class) in 1972. The *Class Total*

Column indicates the total number of pixels in each final state class (29361 pixels were classified as agriculture in the final state image).

The *Row Total Column* is simply a class-by-class summation of all the final state pixels that fell into the selected initial state classes. Sometimes this may not be the same as the *Class Total Column* (i.e. final state class total) because it is not required that all initial state classes be included in the analysis. For example, if there was a fourth class "water" in 1972 and were absent in 2007 classified image or not considered while classification then the *Row Total Column* would not be equal to *Class Total Column* because total number of pixels in any final state class will not be equal to summation of all the final state pixels in that class. The difference in the *Row Total Column* and *Class Total Column* are due to those pixels. However, in the present case, *Row total Column* indicates that there is no unclassified pixel as same numbers of pixels are also reported in the *Class Total Column*.

The *Class Changes Row* indicates the total number of initial state pixel that changed classes. In table 5, the total class change for forest is 19345 pixels. In other words, 19345 pixels that were initially classified as forest changed into final state classes other then forest. To confirm that this is correct, the number of initial forest classified pixels 23025 are subtracted from the forest class total 42370, which is 19345. The *Image Difference Row* is the difference in the total number of equivalently classed pixels in the two images, computed by subtracting the initial state class totals from the final state class totals (i.e. *Class Total Column - Class Total Row*). An image difference that is positive indicates that the class size increased. The table shows that there is a decrease of 15604 pixels (352.27 ha) in forest class and there has been an increase of 19001 pixels (428.57 Ha) in agriculture class.

Temporal analysis revealed large scale LC changes in the region. To understand the level of changes, fragmentation analysis was done, which would help in assessing the state of fragmentation and its implications. In this regard, Pf and Pff in a fixed-area window of 3 x 3 were computed [21] to identify forest fragmentation categories given in figure 6 and table 6.

Table 6: Forest fragmentation types details

	1972		1989		2000		2007	
	Ha	**%**	**Ha**	**%**	**Ha**	**%**	**Ha**	**%**
Interior	788.88	87.42	508.87	73.41	320.65	65.02	246.00	52.61
Perforated	75.60	8.38	62.68	9.04	66.29	11.32	45.48	9.72
Edge	28.63	3.17	85.68	12.36	91.54	15.64	110.50	23.63
Transitional	9.29	1.03	35.75	5.16	46.63	7.96	53.35	11.41
Patch	0.00	0.00	0.22	0.03	0.32	0.05	12.31	2.63
Total	902.40	100	693.21	100	385.42	100	467.63	100

Figure 6: Forest fragmentation map (A) 1972, (B) 1989 (C) 2000 (D) 2007

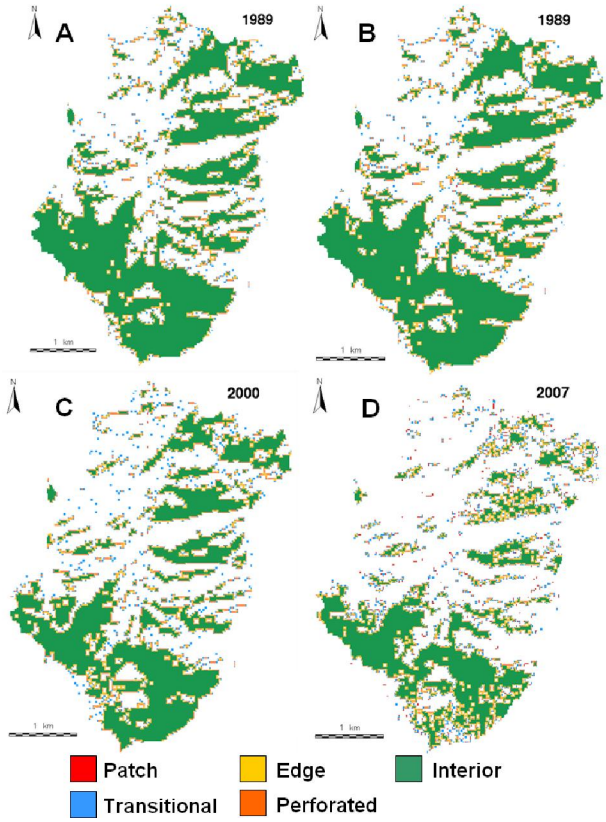

The case of Pf = 1 (interior) represents a completely forested window for which Pff is also 1. When Pff is larger than Pf, the implication is that forest is clumped; the probability that an immediate neighbour is also forest is greater than the average probability of forest within the window. Conversely, when Pff is smaller than Pf, the implication is that whatever is nonforest is clumped. The difference (Pf-Pff) characterises a gradient from forest clumping (edge) to nonforest clumping (perforated). When Pff = Pf, the model cannot distinguish forest or nonforest clumping. To understand the fragmentation process, 10 spatial metrics – Number of patches (NP), Patch density (PD), Total edge (TE), Edge Density (ED), Largest shape index (LSI), Shannon diversity index (SHDI) were calculated at landscape level using Fragstats [33].

Quantitative assessment of the pattern of forest fragmentation and its trends showed that interior forest has declined by 68.81%. Patch forest which was absent in 1972 image has increased up to 12 ha in 2007 and interior forest has decreased from 789 ha in 1972 to 246 ha in 2007. The values of TFP and FC for the temporal data were plotted that specifies six conditions of forest fragmentation in figure 7. The amount of forest and continuity were high in 1972 and declined in 2007.

Figure 7: Six forest fragmentation conditions based on the values for Total Forest Proportion and Forest calculated for a region

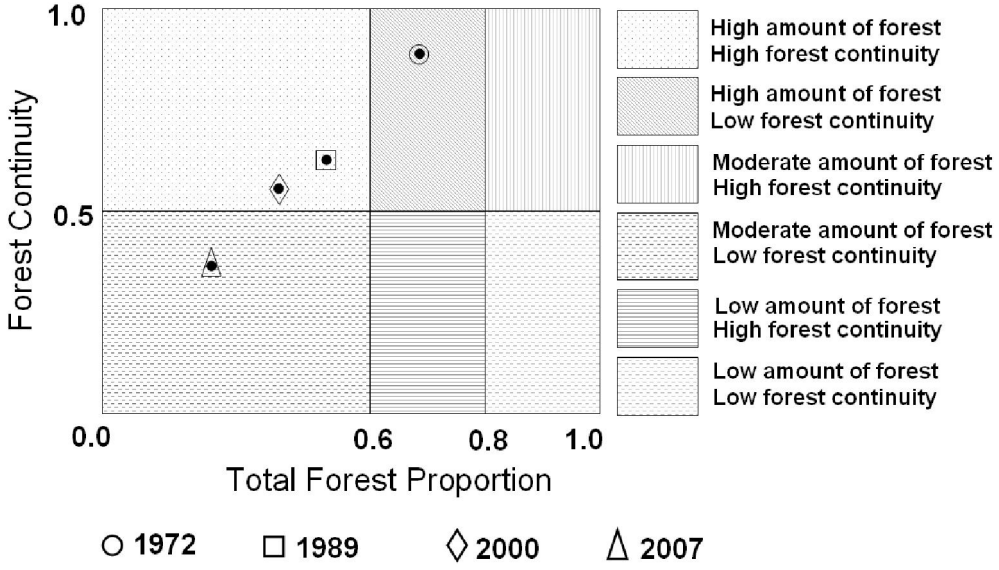

Forest in Moolbari watershed was more contiguous earlier (in 1972), with less number of patches than that of 2007. There was a single contiguous patch of forest, which is now more fragmented with interspersion of agriculture land and reduced area (925 ha in 1972 to 474 ha) in 2007. Individually, the largest patch in 1972 was 907 ha, while in 2007, the largest patch is 273 ha. Number of patches and patch density, which are the direct measure of fragmentation effect also increased over years. Table 7 details the fragmentation metrics calculated at landscape level.

Table 7: Forest fragmentation indices for 1972 to 2007

Index →	NP	PD	TE	ED	LSI	SHDI
1972	41	1.75	57206.51	24.43	3.46	0.14
1989	95	4.06	78993.03	33.74	4.58	1.48
2000	152	6.49	86560.50	36.97	4.97	2.00
2007	212	9.05	100043.80	42.73	5.67	2.10

From this analysis, it is clear that Moolbari watershed in the ecologically fragile Himalaya is under the severe influence of forest fragmentation, necessitating immediate interventions involving integrated watershed management strategies. The results highlight higher anthropogenic fragmentation in the watershed closer to villages than remote areas.

8. Conclusion

LU classification algorithms were reviewed to assess the best classifier in an undulating terrain. Error matrix along with ROC curves provided a richer measure of classification performance showing that GMLC is superior with overall accuracy of 89% (1972 and 1989), 81% (2000) and 88% (2007). The study showed reduction of region under vegetation by 5.59% during 35 years.

Change detection methods revealed a declining trend of forest patches (48%) during the last three decades due to increasing agricultural practices which have significantly increased from 264 ha (1972) to 779 ha (2007). Barren area has increased by 23% (during 1972 to 2000).

Forest fragmentation model showed that interior forest has declined by 68.81% (from 789 ha in 1972 to 246 ha in 2007). Patch forest which was absent in 1972 image has increased up to 12 ha in 2007. Forested area is negatively correlated to all the indices, hinting that decreased forest area has more fragmented patches. Patches come from many sources, ranging from our abilities to visualise and delineate what they represent, to their usage as conceptual units and patch dynamics models and to societal biases such as land ownership and anthropogenic activities. The analysis places patches into perspective as one identifiable element along a continuum of forest fragmentation, and suggest that more attention should be given for the conservation of interior forests and restoration of patch forests for the sustainability of watershed, livelihood and food security.

Acknowledgement

We are grateful to the NRDMS division, DST, Ministry of Science and Technology, Government of India for the financial assistance and to National Remote Sensing Centre (NRSC), Hyderabad for providing the remote sensing data. Landsat data was downloaded from http://glcf.umiacs.umd.edu/data/). We thank Dr.Rana and his team at Shimla for the support during the field data collection.

References

[1] R. O. Duda, P. E. Hart and D. G. Stork, "Pattern classification," A Wiley-Interscience Publication, Second Edition, ISBN 9814-12-602-0, 2000.

[2] M. K. Arora and S. Mathur, "Multi-source classification using artificial neural network in rugged terrain", *GeoCarto International,* , Vol. 16, No. 3, 2001, pp. 37-44.

[3] R. M. Rao and M. K. Arora, "Overview of image processing, Advanced Image Processing Techniques for Remotely Sensed Hyperspectral Data," (Varshney, P. K., and Arora, M. K., editors), Springer-Verlag, 2004, pp. 51-85.

[4] G. Simone, A. Farina, F. C. Morabito, S. B. Serpico and L. Bruzzone, "Image fusion techniques for remote sensing applications," *Information Fusion*, Vol. 3, No. 1, 2002, pp. 3-15.

[5] J. D. Hurd, E. H. Wilson, S. G. Lammey and D. L. Civco, "Characterization of Forest Fragmentation and Urban Sprawl using time sequential Landsat Imagery," In ASPRS 2001 Annual Convention, St. Louis, MO, April 23-27, 2001.

[6] M. G. Turner, "Landscape ecology: the effect of pattern on process," *Annual Review of Ecology and Systematics*, Vol. 20, 1989, pp. 171-197.

[7] Z. Wang, D. Ziou, C. Armenakis, D. Li and Q. Li, "A Comparative Analysis of Image Fusion Methods," *IEEE Transactions on Geoscience and Remote Sensing*, Vol. 43, No. 6, 2005, pp. 1391-1402.

[8] T. M. Lillesand and R. W. Kiefer, "Remote Sensing and Image Interpretation," Fourth Edition, John Wiley and Sons, New York, 2002.

[9] M, E. Hodgson, "Reducing the Computational Requirements of the Minimum-Distance Classifier," *Remote Sensing of Environment,* Vol. 25, No. 1, 1998, pp. 117-128.

[10] M. Wölfel and H. K. Ekenel, "Feature Weighted Mahalanobis Distance: Improved Robustness for Gaussian Classifiers," In 13th European Signal Processing Conference, EUSIPCO, Antalya, Turkey, September, 2005; http://www.eurasip.org/Proceedings/Eusipco/Eusipco2005/defevent/papers/cr1853.pdf.

[11] C-C. Hung and B-C. Kuo, "Multispectral Image Classification Using Rough Set Theory and the Comparison with Parallelepiped Classifier In Geoscience and Remote Sensing Symposium," IGARSS 2007 Geoscience and Remote Sensing Symposium, IGARSS 2007 Proceedings, IEEE International Publication, pp. 2052-2055.

[12] R. A. Schowengerdt, "Remote Sensing: Models and Methods for Image Processing," Academic Press, San Diego, CA, USA, 2nd Ed, 1997.

[13] A. S. Mazer, M.Martin, M. Lee and J. E. Solomon, "Image Processing Software for Imaging Spectrometry Data Analysis," *Remote Sensing of Environment*, Vol. 24, No. 1, 1988, pp. 201-210.

[14] D. R. Scott, "Effects of Binary Encoding on Pattern Recognition and Library Matching of Spectral Data, *Chemometrics and Intelligent Laboratory Systems*, Vol. 4, 1998, pp. 47-63.

[15] D. Lu, P. Mausel, E. Brondizio and E. Moran, "Change detection techniques," *International Journal of Remote Sensing*, Vol. 25, No. 12, 2004, pp. 2365-2407.

[16] T. Fung and E. LeDrew, "Application of principal component analysis for change detection," *Photogrammetric Engineering and Remote Sensing*, Vol. 53, No. 12, 1987, pp. 1649-1658.

[17] R. D. Macleod and R. G. Congalton, "A quantitative comparison of change-detection algorithms for monitoring eelgrass from remotely sensed data," *Photogrammetric Engineering and Remote Sensing*, Vol. 64, No. 3, 1998, pp. 207-216.

[18] H. I. Cakir, K. Khorram, S. A. C. Nelson, "Correspondence analysis for detecting land cover change," *Remote Sensing of Environment*, Vol. 102, 2006, pp. 306–317.

[19] J. G. Lyon, D. Yuan, R. S. Lunetta and C. D. Elvidge, "A change detection experiment using vegetation indices," *Photogrammetric Engineering and Remote Sensing*, Vol. 64, 1998, pp. 143–150.

[20] J. R. Jensen, "Introductory digital image processing: A remote sensing perspective," Prentice-Hall, New Jersey, 2004, pp. 467-494.

[21] K. J. Riitters, R. O' Neill. Wickham, B. Jones and E. Smith, "Global-scale patterns of forest fragmentation," *Conservation Ecology*, Vol. 4, No. 2, 2000. http://www. consecol.org/vol4/iss2/art3/

[22] J. E., Vogelmann, "Assessment of forest fragmentation in southern New England using remote sensing and geographic information system technology," *Conservation Biology*, Vol. 9, No. 2, pp. 439-449.

[23] J. D. Wickham and K. B. Jones, K. H. Ritters, T. G. Wade and R. V. O'Neill, "Transition in forest fragmentation: implications for restoration opportunities at regional scales," *Landscape Ecology*, vol. 14, 1999, pp. 137-145.

[24] A. K. Jain and R. C. Dubes, "Algorithms for Clustering Data," Prentice Hall, Englewood Cliffs, NJ, 1988.
[25] PCI Geomatics Corp., ISOCLUS-Isodata clustering program; http://www.pcigeomatics.com/cgi-bin/pcihlp/ISOCLUS
[26] J. A. Richards, "Remote Sensing Digital Image Analysis," Springer-Verlag, Berlin, 1986, pp. 206-225.
[27] J. B. Campbell, "Introduction to Remote Sensing," Taylor and Francis, New York, 2002.
[28] T. Fawcett, "An introduction to ROC analysis," *Pattern Recognition Letters*, Vol. 27, 2006, pp. 861-874.
[29] A. P. Bradley, "The use of the area under the ROC curve in the evaluation of machine learning algorithms," *Pattern Recognition,* Vol. 30, No. 7, 1997, pp. 1145-1159.
[30] J. Gao, H. F. Chen, Y. Zhang and Y. Zha, "Knowledge-based approaches to accurate mapping of mangroves from satellite data," *Photogrammetric Engineering & Remote Sensing*, Vol. 70, No. 12, 2004, pp. 1241-1248.
[31] D. B. Hester, H. I. Cakir, S. A. C. Nelson and S. Khorram, "Per-pixel Classification of High Spatial Resolution Satellite Imagery for Urban Land-cover Mapping," *Photogrammetric Engineering & Remote Sensing,* Vol. 74, No. 4, 2008, pp. 463-471.
[32] M. Song, D. L. Civco and J. D. Hurd, "A competitive pixel-object approach for land cover classification," *International Journal of Remote Sensing*, Vol. 26, 2005, pp. 4981-4997.
[33] K. McGarigal, S. A. Cushman, M. C. Neel and E. Ene, "FRAGSTATS: Spatial Pattern Analysis Program for Categorical Maps," Computer software program produced by the authors at the University of Massachusetts, Amherst, 2002; http://www.umass.edu/landeco/research/fragstats/fragstats.html

Landscape Dynamics in Mandhala Watershed, Himachal Pradesh

Abstract: Inventorying, mapping and monitoring landscape dynamics is essential for the sustainable management of natural resources including land and water. This work uses the temporal remote sensing data (1982, 1989, 2000 and 2007) for understanding landscape dynamics of Mandhala watershed in an ecologically fragile Himalayan region. Changes in land use and land cover are studied through established change detection techniques such as principal component analysis, correspondence analysis and NDVI based image differencing. Changes in forest land use are characterized by developing a forest fragmentation model involving various spatial metrics. The forest fragmentation and landscape metrics illustrate an increase in patch forests after 2000 and decline in the interior dense forest (90.4% to 33.4%) suggesting immediate policy interventions to restore the degraded landscape which had telling influence on local ecology, biodiversity and hydrology.

Keywords: landscape, land use change detection, forest fragmentation, watershed, multivariate analysis, Western Himalaya

1. Introduction

Land use and Land cover (LULC) information is a vital input for various developmental, environmental and resource planning applications at regional as well as global scale process models. LULC dynamics are analysed through changes in the state of an object or phenomenon by observing it at different times (Singh, 1989). Timely and accurate change detection of natural resources constitutes the foundation for greater understanding of the relationships and interactions between human and natural phenomena. It enables monitoring temporal dynamics of spatial aspects involving diverse ecosystems, forest changes, etc. Furthermore, remote sensing data pertaining to LULC provide spatio-temporal information of agricultural crops, wastelands, seasonal dynamics of wetlands/surface water bodies, forest, vegetation etc. which helps in analyzing reliably the landscape dynamics (Kandrika and Roy, 2008).

Land use (LU) change can be obtained from multi satellite sensor data (spatio temporal data) using pre-classification or post-classification and pattern recognition algorithms (Duda et al., 2005). These classification algorithms can be either supervised, unsupervised, hybrid of soft classification techniques. In addition to the normal routine methods of estimating the LULC change in a landscape, landscape metrics or spatial metrics are being used in recent times particularly in landscape ecology (Gustafson, 1998). Spatial metrics are spatially consistent and provide detailed information about structures and patterns (Herold et al., 2005) and are being used to quantify shape and pattern of vegetation in natural landscape based on categorical, patch-based representation at a landscape, class and patch level (McGarigal and Marks, 1995). Computation of spatial metrics using multi-scale or temporal datasets, aids in assessing the changes in the degree of spatial heterogeneity. Thus, the information derived from several change detection techniques along with spatial metrics on temporal scales help in understanding the change phenomenon that benefits the planning and management towards a sustainable use of land resources. In this context, the present paper analyses the spatio-temporal landscape dynamics of Mandhala, a medium altitude, temperate watershed in Himachal Pradesh, India.

Main objectives are to understand landscape dynamics through (i) LULC analysis using temporal remote sensing data (1972, 1989, 2000 and 2007) and (ii) computation of spatial metrics including forest fragmentation indices.

2. Tools and Techniques

This includes fusion of multi-resolution data (of different spectral and spatial resolutions), classification of data to derive land use parameters, fragmentation analysis to understand the process of fragmentation at the landscape level and computation of spatial metrics to capture landscape dynamics.

2.1. Image Fusion

Earth observation satellites provide data at different spatial, spectral and temporal resolutions. Satellites, such as IRS (LISS III) have a high spatial resolution panchromatic (PAN) band (5.8 m) and low resolution multispectral (MS) bands (G, R, NIR of 23.5 m) in order to support both spectral and best spatial resolution while minimising on-board data handling needs (Cakir and Khorram, 2008). For many applications, the fusion of these data from multiple sensors aids in delineating objects with comprehensive information due to the integration of spatial information present in the PAN image and spectral information present in the low resolution MS data. Here we have used the *À Trous algorithm based wavelet transform (ATW)* for image fusion (Nunez et al., 1999).

2.2. Image Classification

The extraction of LU information from remote sensing data is often difficult since it is closely associated with the human intervention for which the data need to be obtained from other sources (Kandrika and Roy, 2008). Keeping all the requirements and constraints in view, Gaussian Maximum Likelihood classifier (GMLC) is a parametric classifier used for classifying the satellite data.

2.3. Change detection

LU change detection is performed by change/no-change recognition followed by boundary delineation on images of two different time periods (Zhang and Zhang, 2007; Lu et al., 2004). Change/no-change recognition extracts changes from an unchanged background. The pixel patches marked as changed are then checked and the boundaries are delineated to extract the changed areas. A variety of change detection algorithms such as Principal Component Analysis (Zhang and Zhang, 2007), Correspondence Analysis (Cakir et al., 2006) and image differencing (Lyon et al., 1998) have been tested to recognise LU changes from bi-temporal images.

2.4. Forest fragmentation

Forest fragmentation is the process whereby a large, contiguous area of forest is both reduced in area and divided into two or more fragments (Meyer and Turner, 1994). The primary concern is direct loss of forest area, and all disturbed forests are subject to edge effects of one kind or another. Forest fragmentation metrics with the total extent of forest and its occurrence as adjacent pixels is computed through fixed-area windows surrounding each forest pixel. The

result is stored at the location of the centre pixel. It is computed through *Pf* (the ratio of pixels that are forested to the total non-water pixels in the window) and *Pff* (the proportion of all adjacent (cardinal directions only) pixel pairs that include at least one forest pixel, for which both pixels are forested). Based on the knowledge of Pf and Pff, six fragmentation categories were mapped (Riitters et al., 2000): (i) interior, for which Pf = 1.0; (ii), patch, Pf < 0.4; (iii) transitional, 0.4 < Pf < 0.6; (iv) edge, Pf > 0.6 and Pf – Pff > 0; (v) perforated, Pf > 0.6 and Pf – Pff < 0, and (vi) undetermined, Pf > 0.6 and Pf = Pff.

3. Study area

Mandhala watershed (figure 1) lies in Solan district, Himachal Pradesh, India (76°50'04" to 76°53'47" E and 30°53'40.7" to 30°56'18.5" N) and falls in lower Shiwalik range in the Himalayas at 400-1100 amsl spread over an area of 14.5 sq km, characterized by dry evergreen forests. Degradation of forest is evident from the dominant cover of invasive exotic species *Lantana camera*. Trees of *Holoptelia integrifolia, Dalbergia sisoo, Morus nigra*, etc. occur along the field bunds and other open lands.

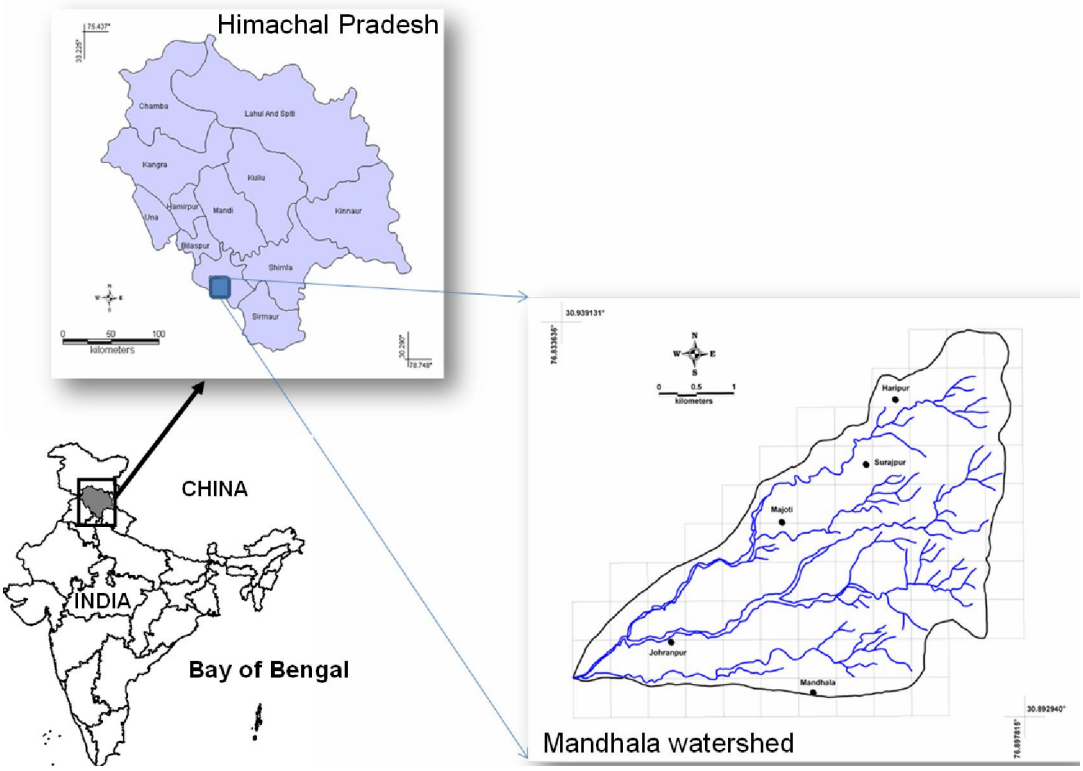

Figure 1: Study area: Mandhala Watershed.

The Western Himalayan climate is differentiated by the effect of altitude, topography and geographical trend causing reduced precipitation, extreme temperatures and increasing snowfall (Gaston et al., 1983). The forests in the watersheds are managed as reserve forest by the state forest department, cutting of trees is prohibited, still lopping and collection of fallen wood for household and industrial purposes were noticed during the field survey.

4. Methods

The methods adopted in the analysis included image fusion, LULC analyses, change detection using temporal data and temporal forest fragmentation analysis.

4.1. Data Preprocessing: Base layers like district boundary, drainage network, water bodies, etc. were mapped from the Survey of India (SOI) toposheets of scale 1:50000. Landsat bands, IRS LISS III MS bands were geocorrected with the known ground control points (GCP's) and projected to geographic latitude-longitude with WGS-84 as the datum, followed by masking and cropping of the study region (region of interest – ROI). Resampling of the data using nearest neighbourhood technique were carried out for (i) bands 1- 4 of Landsat (1972) data to 79 m, (ii) bands 1-6 of Landsat TM (1989) to 30 m, (iii) bands 1-5 and 7 of Landsat ETM (2000) to 30 m and band 8 to 15 m, (iv) IRS LISS-III MS (2007) bands 1-3 to 23.5 m and IRS PAN band to 5.8 m. IRS PAN band of 5.8 m spatial resolution was merged with the LISS-III MS bands of 2007 using Multi-resolution analysis based on the wavelet transformation (Nunez et al., 1999). Landsat ETM+ PAN band (band 8) of 15 m spatial resolution was fused with bands 1, 2, 3, 4, 5 and 7 of the same satellite. Subsequently, all bands were resampled to 5.8 m for consistency and easier comparison of LU class statistics across the data sets.

4.2. LULC analysis: NDVI was computed to segregate regions under vegetation, soil and water. Signature separation corresponding to the LU classes was done using Transformed divergence (TD) matrix and Bhattacharrya (or Jeffries-Mastusuta) distance. Both the TD and Jeffries-Mastusuta measures are real values between 0 and 2, where '0' indicates complete overlap between the signatures of two classes and '2' indicates a complete separation between the two classes. Both measures are monotonically related to classification accuracies. The larger the separability values, the better the final classification results (Richards, 1986). Supervised classification using MLC with the training sets uniformly distributed representing / covering the study area was performed on the four temporal datasets. Accuracy assessment was done using error matrix by computing producer's accuracy, user's accuracy, overall accuracy and Kappa statistics (Campbell, 2002; Lillesand and Kiefer, 2002) by overlaying the test data not used in classification. Receiver operating characteristic (ROC) curves were plotted to assess the accuracy of the classified data (Fawcett, 2006). In the absence of historical data, the classified images of 1972, 1989 and 2000 were validated by visual interpretation using the tone, texture and other interpretation keys from the false colour composite images.

4.3. Spatial change analysis: Pixel to pixel change was mapped for each category from 1972 to 2007 using PCA - Principal Component Analysis (Zhang and Zhang, 2007), CA - Correspondence Analysis (Cakir et al., 2006) and NDVI image differencing (Lyon et al., 1998). The absolute and relative changes on the original bands of the two time periods were also computed. If there is a change between the two dates, the pixel had either negative or positive values. However, subtle change in brightness values between two dates also occur due to atmospheric conditions at different dates, sensor differences, etc., even after radiometric normalisation. Brightness values of no-change areas were distributed around the mean value of each difference image.

4.4. Forest fragmentation analysis: Pf and Pff in a kernel of 3 x 3 were computed (Riitters et al., 2000) to identify forest fragmentation categories. Based on these forest fragmentation indices (Hurd et al., 2002) Total forest proportion (TFP: ratio of area under forests to the total

geographical extent excluding water bodies), weighted forest area (WFA) and Forest continuity (FC) were computed. TFP provides an extent of forest cover in a region ranging from 0 to 1. Weighted values for the weighted forest area (WFA) are derived from the median Pf value for each fragmentation class as given by equation 1 and FC is computed by equation 2.

$$WFA = (1.0 * interior) + (0.8 * (perforated + edge + undertermined) + (0.5 \mid transitiojnal) \mid (0.2 * patch) \quad (1)$$

$$FC = \frac{weighted\ forest\ area}{total\ forest\ area} * \frac{area\ of\ largest\ interior\ forest\ patch}{total\ forest\ area} \quad (2)$$

Six patch level metrics – largest patch index, number of patches, patch density, total edge, edge density and landscape shape index were calculated using Fragstats (McGarigal et al., 2002).

5. Results and Discussion

Temporal NDVI analysis shows reduction of region under vegetation by 7.27% from 1972 to 2000 and a decrease of 4.72% from 1972 to 2007. Histograms were generated to ascertain the number of likely LU categories based on the number of distinguishable peaks. Six distinct classes: agriculture, settlement, forest, plantation/orchard, barren land and water were the dominant categories in the study area. Signatures were assessed using spectral graphs which showed that forest and plantation/orchard classes have high peaks in the NIR band and are therefore distinguishable from other classes. In band 3 of Landsat MSS settlement and dry river bed were not distinguishable, whereas in Landsat ETM+ for the same band, river bed was not easily distinguishable from barren land/stony/waste. In LISS III, settlement and barren land signatures were not separable in band 3. All other classes were well separable. Supervised classification (figure 2) with the percentage statistics are listed in table 1.

Table 1: Spatio-temporal LU estimates

	Class→ Area ↓	Agriculture	Built-up	Forest	Plantation / Orchard	Barren land	Water	Total
1972	Area (Ha)	215.88	-	855.21	204.25	15.02	115.42	1405.8
	Area (%)	15.36	-	60.84	14.53	1.07	8.21	100
1989	Area (Ha)	559.39	3.26	395.28	267.39	117.17	63.29	1405.8
	Area (%)	39.79	0.23	28.12	19.02	8.33	4.50	100
2000	Area (Ha)	495.80	104.41	467.76	209.54	13.66	114.62	1405.8
	Area (%)	35.27	7.43	33.27	14.91	0.97	8.15	100
2007	Area (Ha)	249.81	98.74	318.17	640.45	55.15	43.45	1405.8
	Area (%)	17.77	7.02	22.63	45.66	3.92	3.09	100

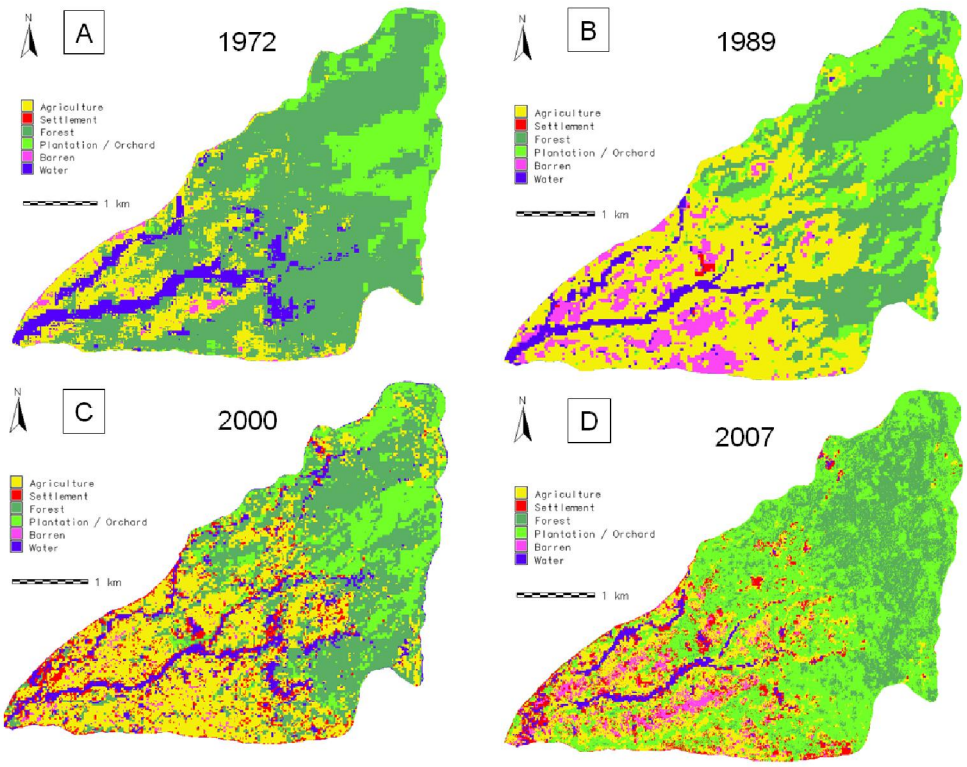

Figure 2: Classification using (A) Landsat MSS, 1972, (B) Landsat TM, 1989, (C) Landsat ETM, 2000 and (D) IRS LISS-III, 2007.

Accuracy assessment is listed in table 2. ROC curves for each class for the temporal dataset in figure 3 show the performance of the classifier as the decision threshold is varied for each class to obtain the best classified output. At any point on the curve is a possible operational point for the classifier and so was evaluated in the same manner as accuracy. There is a good agreement between results obtained from error matrix and ROC curves.

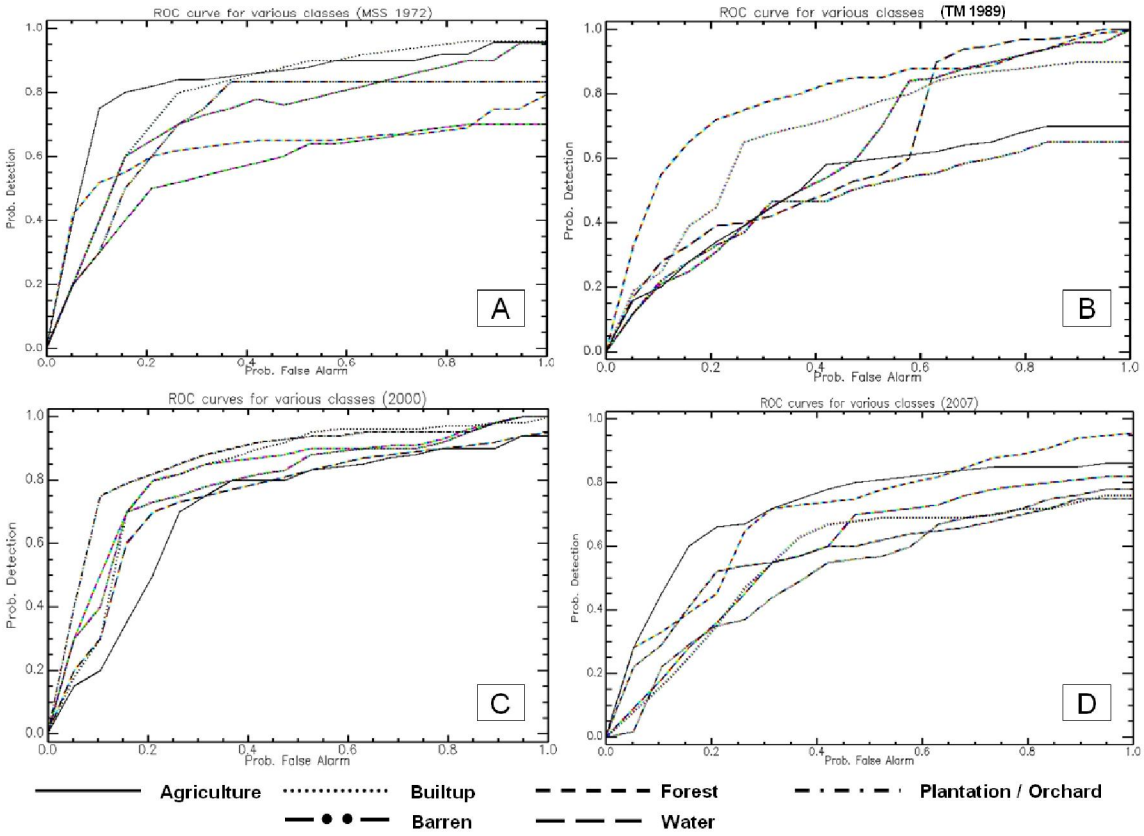

Figure 3: ROC curves for [A] Landsat MSS-1972; [B] Landsat TM – 1989; [C] Landsat ETM+ - 2000; [D] LISS-III - 2007.

Table 2: Accuracy assessment for classified images

Class	1972		1989		2000		2007	
Accuracy→	PA*	UA*	PA	UA	PA	UA	PA	UA
Agriculture	70	75	80	83	87	84	90	85
Builtup	60	65	76	71	83	82	86	81
Forest	86	81	85	80	91	87	90	85
Plantation/ Orchard	73	78	85	77	87	85	91	87
Barren	80	82	84	84	80	79	88	86
Water	83	82	78	75	83	82	83	78
OA*	78.52		80.78		83.78		86.52	
Kappa	0.7735		0.8066		0.8217		0.8667	

*PA - Producer's Accuracy, UA - User's Accuracy, OA - Overall Accuracy

Results obtained from MLC classification are comparable to the ground condition for the 2007 classified image. The successful application of MLC is dependent upon having delineated correctly the spectral classes in the image data of interest. This is necessary since each class is to

be modeled by a normal probability distribution. If a class happens to be multimodal, and this is not resolved, then clearly the modelling cannot be very effective. MLC can obtain minimum classification error under the assumption that the spectral data of each class is normally distributed. The disadvantage of this technique is that it requires every training set to have at least one more pixel than the number of bands used in classification.

Forest patches have declined from 61 ha (in 1972) to 23 ha (in 2007) with the conversions of forest for agricultural activities, which has significantly increased by ~20% from 1972 to 2000. However, the percentage area pertaining to agriculture has decreased to 17% in 2007. One of the reasons is that agricultural area and fallow land were invaded by an exotic weed – *Lantana camera* which is an invasive species that thrives in warm, high rainfall areas where it forms dense thickets that exclude native species through shading and allelopathic effects, leading to complete dominance of the under storey and eventually overshooting the main canopy. The thickets impede access, alter availability of fodder for wild animals and reduce regeneration potential displacing natural scrub communities. Lantana encroaches agricultural land, reduces the carrying capacity of pastures. Its distribution has adversely affected not only many species of economic and ecological importance but ecosystem also. Plantation has increased considerably from ~15% (1972) to ~46% (2007). These include Babool, *Acacia catechu* and shrubs as a government measure to retain greenery in the area. Barren lands mainly constitute rocks, stones and open lands. Some of the barren land pixels show similar reflectance as that of dry river bed and the signatures often mix with settlements causing confusion during classification. Hence the proportion of barren land is less compared to earlier classified images (from 1989 to 2007).

Change detection involved differencing images of two time periods between PCs, CA components, NDVI and bands (rescaled from -1 to 1) that showed similar results. In both the images of the standardised PCA, PC1 had the highest information having all bands with unequal variances. CA puts less emphasis on bands that have low polarisation. The more the pixels are polarised for a band, the higher the importance given to that band in the calculation of the between-pixel distances (Greenacre, 1984). The first two components of CA explained approximately 99% of the total inertia in both temporal images (table 3). Total inertia is a measure of how much the individual pixel values are spread around the centroid. Inertia is independent of the absolute frequencies that constitute the original data, and will be identical if the data are multiplied by any constant value (Greenacre, 1984).

Table 3: Eigen structure of 1972 and 2007 data after PCA and CA transformation

		Landsat MSS (1972)			IRS LISS-III (2007)		
		Comp1	Comp2	Comp3	Comp1	Comp2	Comp3
PCA	Band 1	0.66	0.24	0.71	0.62	0.33	0.71
	Band 2	0.66	0.28	-0.70	0.62	0.36	-0.70
	Band 3	0.37	-0.93	-0.02	0.49	-0.87	-0.01
	Eigenvalues	2.14	0.82	0.03	2.44	0.55	0.01
	Proportion	72	27	1	81.25	18.26	0.48
	Cumulative	72	98	100	81.25	99.51	100

		Landsat MSS (1972)			IRS LISS-III (2007)		
		Comp1	Comp2	Comp3	Comp1	Comp2	Comp 3
Correspondence Analysis	Band 1	0.62	0.24	0.75	0.58	0.27	0.77
	Band 2	0.60	0.47	-0.65	0.58	0.53	-0.62
	Band 3	0.51	0.85	-0.15	0.57	-0.81	-0.15
	Eigenvalues	2.50	0.50	0.006	2.96	0.037	0.0002
	Proportion	83.23	16.57	0.2	98.76	1.23	0.0066
	Cumulative	83.23	99.80	100	98.76	99.99	100

Detailed change detection tabulation was done between two classified images of 1972 and 2007 focusing primarily on the initial state classification changes – that is, for each initial state class, it identifies the classes into which those pixels changed in the final state image. The total class change for agriculture is 135.81 ha. There is a decrease of 537.03 ha in forest class and there has been an increase of 436.22 ha in plantation / orchard class. Forest fragmentation maps along with associated statistics based on the temporal forest maps (LU analysis) are presented in figure 4 and table 4.

Table 4: Forest fragmentation types details

	1972		1989		2000		2007	
	Ha	**%**	**Ha**	**%**	**Ha**	**%**	**Ha**	**%**
Interior	751.89	90.36	337.83	86.45	336.83	75.24	106.06	33.35
Perforated	48.00	5.77	38.96	9.97	73.85	16.50	20.98	6.60
Edge	25.58	3.07	9.53	2.44	24.02	5.37	122.07	38.39
Transitional	6.66	0.80	4.45	1.14	12.97	2.90	46.01	14.47
Patch	-	-	-	-	0.01	0.00	22.85	7.19
Total	832.15	100	390.78	100	447.68	100	318.01	100

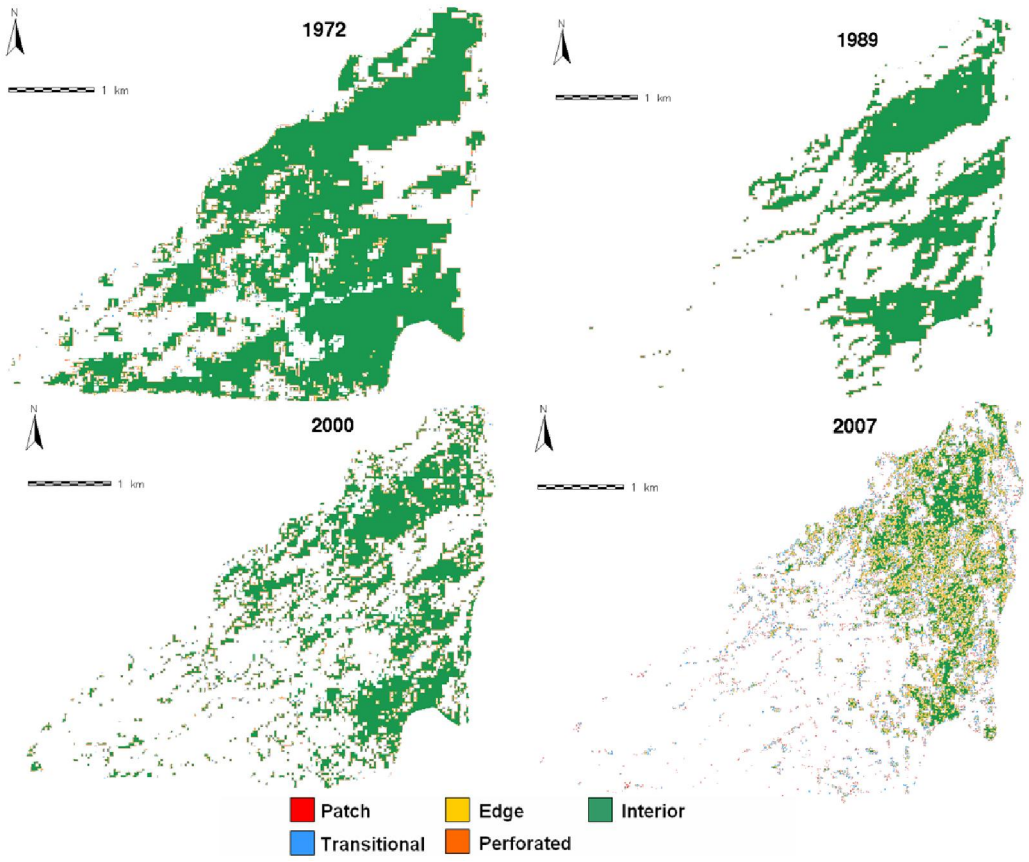

Figure 4: Forest fragmentation maps for 1972, 1989, 2000 and 2007.

Total forest proportion (TFP) and forest continuity (FC) is listed in table 5 and are depicted in figure 5. The forest fragmentation metrics analysis showed that largest forest patch is continuously decreasing consequently increasing the number of small patches and patch density. Due to increasing number of patches, more edges are getting developed with increasing edge density and the landscape shape is becoming more complex with time.

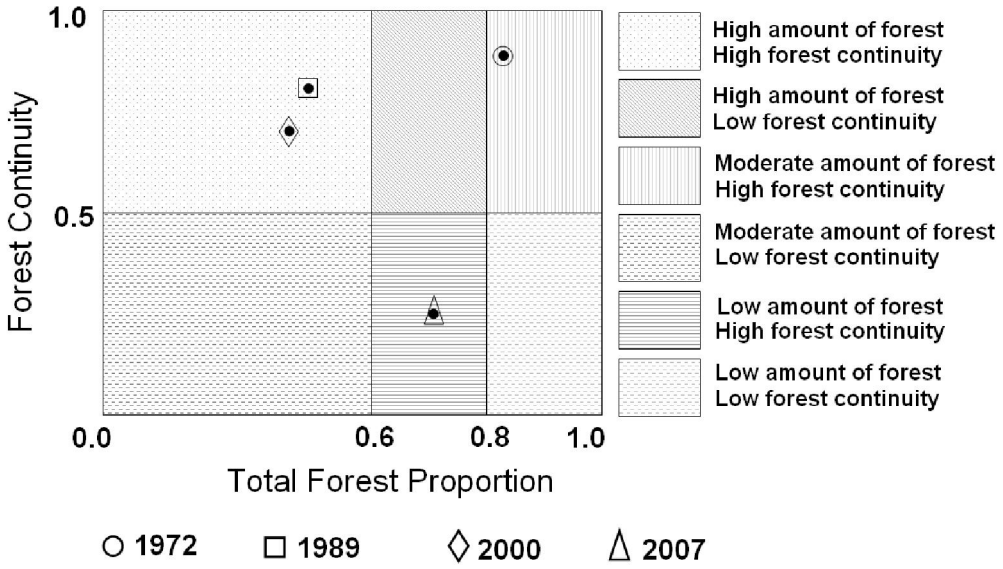

Figure 5: Six forest fragmentation conditions based on the values for TFP and FC.

Table 5: Total forest area and weighted forest area

	1972	1989	2000	2007
TFP	0.82	0.49	0.53	0.70
FC	0.88	0.84	0.71	0.26

The results of this study based on the temporal remote sensing data supplemented with the field data indicate that Mandhala watershed is degrading due to intense anthropogenic activities. When anthropogenic causes of fragmentation are considered, forest are more likely to be disturbed and fragmented where climate is hospitable, soil is productive and access is easy. Mandhala watershed is under the severe influence of forest fragmentation, calling for immediate protection measures from the concerned authorities.

5. Conclusions

Temporal remote sensing data showed reduction of vegetation by 7% from 1972 to 2000 and a decrease of 4.72% from 1972 to 2007. The reason for increase in vegetation from 2000 to 2007 is the spread of invasive species *Lantana camera* in and around the watershed. Change detection methods revealed a declining trend of forest patches (38%) during the last three decades due to increase in plantation and settlement area which was absent in 1972 and has significantly increased to ~7% (99 ha) in 2007. Forest fragmentation model showed that interior forest has declined by 57% (from 752 ha in 1972 to 106 ha in 2007). Patch forest which was absent till 2000, has increased up to 23 ha in 2007. Patches comes from many sources, ranging from our abilities to visualise and delineate what they represent, to their usage as conceptual units and patch dynamics models and to societal biases such as land ownership and anthropogenic

activities. However, forest fragmentation which is degrading the ecosystem of the watershed requires immediate protection measures from the concerned authorities.

References

1. Cakir, H. I., and Khorram, S., Pixel Level Fusion of Panchromatic and Multispectral Images Based on Correspondence Analysis. *Photogrammetric Engineering & Remote Sensing* **2008***, 74(2)*, 183-192.
2. Cakir, H. I., Khorram, S., Nelson, S.A.C., Correspondence analysis for detecting land cover change. *Remote Sensing of Environment* **2006**, *102*, 306–317.
3. Campbell, J. B., *Introduction to Remote Sensing*; Taylor and Francis: New York, **2002**.
4. Duda, R.O., Hart, P.E., and Stork, D.G., *Pattern classification*, 2nd Ed., john Wiley & Sons, Inc: Canada, **2005**.
5. Fawcett, T. An introduction to ROC analysis. *Pattern Recognition Letters* **2006**, *27*, 861-874.
6. Gaston, A. J., and Garson, P. J., and Hunter, M. L., The status and conservation of forest wildlife in Himachal Pradesh, Western Himalaya. *Biological conservation* **1983**, *27*, 291-314.
7. Greenacre, M., Theory and applications of correspondence analysis, Academic Press: London, **1984**.
8. Gustafson, E. J., Quantifying landscape spatial pattern: What is the state of the art? *Ecosystem* **1998**, *1*, 143-156.
9. Herold, M., Couclelis, H., and Clarke, K.C., The role of spatial metrics in the analysis and modeling of urban land use change. *Computers, Environment and Urban Systems* **2005**, *29*, 369-399.
10. Hurd, J. D., Wilson, E. H., and Civco, D. L., Development of a Forest Fragmentation Index to Quantify the rate of forest change. *In ASPRS-ACSM Annual Conference and FIG XXII Congress*, April 22-26, **2002**.
11. Kandrika, S., and Roy, P. S., Land use land cover classification of Orissa using multi-temporal IRS-P6 awifs data: A decision tree approach. *International Journal of Applied Earth Observation and Geoinformatics* **2008**, *10*, 186-193.
12. Lillesand, T. M., Kiefer. R. W., *Remote Sensing and Image Interpretation*, 4th Ed.; John Wiley and Sons: New York, **2002**.
13. Lu, D., Mausel, P., Brondizio, E., and Moran, E. Change detection techniques. *International Journal of Remote Sensing* **2004**, *25(12)*, 2365-2407.
14. Lyon, J. G., Yuan, D., and Lunetta, R. S., Elvidge, C.D.; A change detection experiment using vegetation indices. *Photogrammetric Engineering and Remote Sensing* **1998**, *64*, 143-150.
15. McGarigal, K., Cushman, S.A., Neel, M.C., and Ene, E., FRAGSTATS: Spatial Pattern Analysis Program for Categorical Maps. *Computer software program produced by the authors at the University of Massachusetts, Amherst*, **2002**. Available at: http://www.umass.edu/landeco/research/fragstats/fragstats.html
16. McGarigal, K., and Marks, B. J. FRAGSTATS: spatial pattern analysis program for quantifying landscape structure. *USDA Forest Serv. Gen. Tech. Rep. PNW-351*, **1995**.
17. Meyer, W. B., and Turner, B. L., *Changes in land use and land cover: a global perspective,* Cambridge University Press: Cambridge, UK, **1994**.

18. Nunez, J., Otazu, X., Fors, O., Prades, A., Pala, V., and Arbiol, R., Multiresolution-Based Image Fusion with Additive Wavelet Decomposition. *IEEE Transactions of Geoscience and Remote Sensing* **1999***, 37(3)*, 1204-1221.
19. Richards, J. A., *Remote Sensing Digital Image Analysis*, Springer-Verlag: Berlin, **1986**.
20. Riitters, K., Wickham, J., O' Neill, R., Jones, B., and Smith, E., Global-scale patterns of forest fragmentation. *Conservation Ecology* **2000**, *4(2).*
21. Singh, A., Digital change detection techniques using remotely sensed data. *International Journal of Remote Sensing* **1989,** *10***,** 989-1003.
22. Zhang, J., Zhang, Y. Remote Sensing research issues of the National Land Use Change Program of China. *Photogrammetry & Remote Sensing* **2007**, *62(6)*, 461-472.

Land Surface Temperature Analysis of Himachal Pradesh through Multi-Resolution, Spatio –Temporal data

Abstract.

Rapid changes in the land use and land cover of a region have become a major environmental concern in recent times. This has lead to unsustainable development with the reduction of green spaces and also changes in local climate and formation of urban heat islands (UHI). Monitoring and management of land use dynamics would help in land use planning and mitigation of environmental impacts. The main goal of this paper is to quantify the changes in the land cover and consequent changes in land surface temperature. Land use and land cover dynamics were assessed using temporal remote sensing data (Landsat Thematic Mapper and Enhanced Thematic Mapper data) of Himachal Pradesh, India. The thermal infrared bands of the Landsat data were used to retrieve Land Surface Temperature. The results revealed that there was a huge increase in Urban Area (including Barren land), which is the causal factor for the changes in Land Surface Temperature. Overall, Remote sensing and Geographic Information System technologies were effective approaches for monitoring and analyzing urban growth patterns and evaluating their impacts on Land Surface Temperature.

Keywords : Land Surface Temperature, Landsat, Land Use, Land cover, NDVI.

Introduction

Land cover changes induced by human and natural processes play a major role in global as well as at regional scale patterns of the climate and biogeochemistry of the Earth system. Studies have revealed of changes in water cycling process between land and atmosphere due to the large scale land cover changes, affecting the local to regional climate. Geoninformatics technologies such as remote sensing and geographic information systems are very effective in measuring monitoring and predicating the land use/cover changes (Qihao Weng, 2009; Enner *et al*., 2010). Timely information with higher accuracy of landuse (LU) Land cover (LC) changes is crucial for long-term planning, economic development, and sustainable management(Zhang *et al*., 2010) of natural resources. The analysis of temporal remote sensing data helps in understanding the land cover changes and its impact on the environment. The thermal infrared bands of remote sesning data of space borne sensors help to retrieve Land Surface Temperature (LST). Land surface temperature is the measure of the heat emision from land surface due to various activities associated with the land surface. Increase in paved land cover is an indication of concentrated human activities, which often leads to increased LST's (Ramachandra and Kumar, 2009). Increased LST in certain urban pockets in comparison to its surroundings consequent to the increase in paved surfaces is known as urban heat island (UHI) phenomenon (Landsbeg, 1981; Gallo and Owen, 1998, Li et al., 2004).

Detection of the thermal charecteristics of land surface using remote sensing data of space borne sensors and the analysis of land surface temperature (LST) has been reported earlier (Rao, 1972). Spatio-temporal data were used to develop models of land surface atmosphere exchange, and to analyze the relationship between temperature and land use and land cover (LULC) in urban areas (Voogt and Oke, 2003) highlighting the relationship between LST and surface characteristics such as vegetation indices (Carlson et al., 1994; Carlson 2007; Owen et al., 1998). Also, the studies reveal the effect of biophysical factors on LST by using vegetation fraction instead of qualitative LULC classes (Gallo and Tarpley, 1996; Owen et al., 1998; Dousset and Gourmelon, 2003). The vegetation index–LST relationship has also been used to retrieve surface biophysical parameters (Carlson et al., 1994), to extract sub-pixel thermal variations (Kustas et al., 2003), and to analyze land cover dynamics (Lambin and Ehrlich, 1996). Many investigators have observed a negative relationship between vegetation index and LST, leading to further research into two major pathways, namely, statistical analysis of the relationship and the temperature/vegetation index (TVX) approach. TVX is a multi-spectral method of combining LST and a vegetation index (VI) to monitor their associations.

Land surface and atmospheric temperatures rises by various antropogenic activities like increased land surface coverage by artificial materials, energy consumption, which have a high heat capacity and conductivity, and is also associated with the decreases in vegetation and water surfaces, which are the major factors that reduce surface temperature through evapo-transpiration (Kato and Yamaguchi., 2005). Temperatures can be monitored through space borne remote sensing(rs) sensors, which account for the top of the atmosphere (TOA) radiances in the thermal infrared (TIR) region. TOA radiance is the net radiance of the emitted radiance from the earth's surface upwelling radiance from the atmosphere, and downwelling radiance from the sky. The brightness temperatures (also known as blackbody temperatures) can also be derived from the TOA radiance (Dash et al., 2002). These brightness temperatures account for the various properties of the land surface , the amount and nature of vegetation cover , the thermal properties and moisture content of the soil (Friedl, 2002). However, lack of knowledge of spectral emissivity can introduce an error which ranges from 0.2 to 1.2k for mid-latitude summers and 0.8 to 1.4k for the winter conditions for an emissivity of 0.98 and at the ground height of 10km (Dash et al., 2002). Two approaches have been developed to recover LST from multispectral TIR imagery (Schmugge et al., 1998) as on date. The first approach utilises the radiative transfer equation to correct the at sensor radiance to surface radiance, followed by an emissivity model to separate the surfaces radiance into temperature and emissivity (Friedl, 2002). The second approach applies the split window technique for sea surfaces to land surfaces. Assuming that the emmisivity in the channels used for the split window is similar (Dash et al., 2002). TIR region corresponding to 8-14 μm in the electromagnetic spectrum is being used quantifying the thermal urban environment.

Landsat satellites, are one of the most widely used for environmental studies. Landsat thematic mapper is composed by seven bands, six of them in the visible and near infrared, and only one

band located in the thermal infrared region (with an effective wavelength of 11.457 µm) is used for LST retrieval. Possesing only one thermal band might be stated as an disadvantage/limitation in order to obtain LST as it does not allow the application of a split-window method (Sobrino et al., 1996) neither a temperature/emissivity separation method (Gillespie et al., 1998; Snyder et al., 1998) to obtain information about the emissivity spectrum of natural surfaces.

The objective here is to investigate the Land Surface Temperature with Land use dynamics to understand the Urban Heat Island phenomenon in Himachal Pradesh considering Multi -senor, Multi-resolution and temporal RS data acquired through space borne sensors. This involved:

1) Temporal LU change analysis (during 1989 to 2005)
2) Computation of LST and NDVI (Normalised Difference Vegetation Index) from Landsat Tm(1989) and Landsat ETM(2000) and Landsat ETM+(2005) Data;
3) Investigation of the role of NDVI in LST;

Study area: This analysis has been carried out for Himachal Pradesh, which lies between the Latitudes :30^{o} 22' 40"N to 30^{o} 12' 40"N, Longitude:75^{o} 47' 55"E to 79^{o} 04' 20"E (figure 1). LST was computed for a region lies between the latitudes: 30^{o} 18' 30"N to 30^{o} 10' 30"N and Longitude: 76^{o} 19' 35"E to 78^{o} 59' 10"E and covers Shimla.

Figure 1: Study area - Himachal Pradesh, India

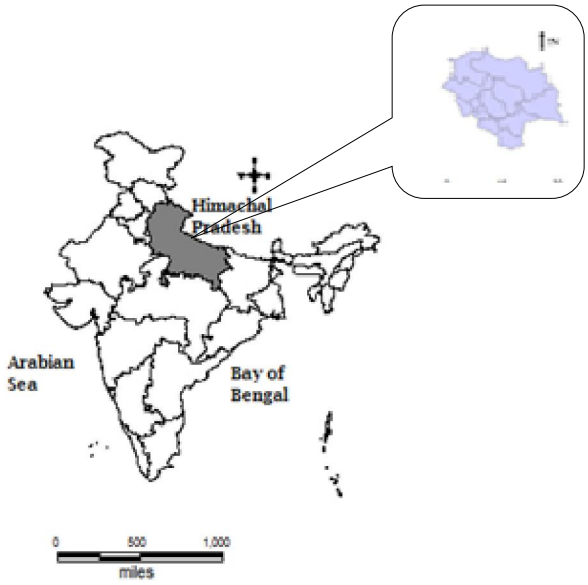

Himachal comprises of 12 dıstrıcts ın total, coverıng the area of 55,673 sq km. Its total population is 6,077,248 as per 2001 census. Shimla is the state capital of Himachal Pradesh, with its population around 7,21,745 as per 2001 census with geographical area of 5131 sq. km. Density of population in Himachal Pradesh is 109 per sq. kms. Himachal Pradesh is one of the Major Indian state undergoing rapid urbanisation. Labour Force has about 49.3% of total population employed in Industrial sectors. Industries located in Himachal as on 31/03/2010 are

36845 (micro, small, medium and large Enterprises) of which 444 are in medium and large scale industries.

Data: The data used were from Landsat series thematic mapper (28.5m) and enhanced thematic mapper (28.5m) data acquired over years 1989 to 2010. Collateral data includes google earth imagery (http://earth.google.com) and Survey of India top sheets.

Methodology: The RS data used to study the temporal changes in landscape pattern were Landsat Thematic Mapper (TM), Landsat Enhance TM Plus (ETM+) of 1989 to 2006. The data were georeferenced, rectified and cropped pertaining to the study area. Landsat ETM+ bands of 2010 were corrected for the SLC-off by using image enhancement techniques, followed by nearest-neighbour interpolation.

A. Land use and land cover analysis: This was carried out using data of Landsat satellite using Supervised Pattern classification using Maximum likelihood classifier. This method has already been proved as a superior method as it uses various classification decisions using Probability and Cost functions (Duda et al., 2000). Mean and covariance matrix are computed using estimate of Maximum likelihood estimator. Application of this method resulted in accuracy of about 75% in all the datasets. For the purpose of accuracy assessment, a confusion matrix was calculated. Land Use was computed using the temporal data through open source program GRASS: Geographic Resource Analysis Support System (http://grass.fbk.eu/)
B. Calculation of Land surface Temperature from Landsat data: LST was computed (Weng etal.,2004) from TIR bands (Landsat TM and ETM). Emissivity corrections for specified LC is carried out using surface Emissivity as per Synder et al.,(1998); Stathopoplou et al., (2007) and land surface temperature is calculated as per Artis and Carnahan (1982) and Carnahan and Larson, 1990.

$$T_s = \frac{T_B}{1 + (\lambda \times T_B / \rho) \ln \varepsilon} \qquad \text{……. ……. 1}$$

Where, λ the wavelength of emitted radiance for which the peak response and average of the limiting wavelength (λ = 11.5μm) (Markham and Barkar, 1985) were used, ρ=1.439 x 10^{-2} mk and E=Spectral Emissivity.

LC was determined through the computation of Normalised Difference Vegetation Index (**NDVI)** using Landsat visible Red (0.63 – 0.69 μm) and near-infrared band (0.76 – 0.9 μm) bands of Landsat TM/ETM. NDVI was computed in order to calculate emissivity for computing LST.

NDVI is given by

$$NDVI = \frac{(Band\ 4\ -\ Band\ 3)}{(Band\ 4\ +\ Band\ 3)}$$

……. (2)

Results and Discussion

The Classified images from 1989 – 2006 showed an overall accuracy of 76%. Land Use changes were more prominent in the area during the last 2 decades consequent to increase in Barren land as indicated in Table 1 and Represented in Figure 2. The LU analysis shows that there has been 55% increase in urban and open areas during 1989-2000 and 39% increase during 2000-2005, and 18.92% increase during 2005-06. This land cover changes has also influenced the local climate. The minimum (min) and maximum (max) temperature was found to be -2º C and 31º C from Landsat Data as tabulated in the Table 2. The analysis showed that there has been an increase in Temperature from 1989 to 2006 as evident from temporal analysis.

Figure 2. Land use classification in 1989, 2000, 2005 and 2006

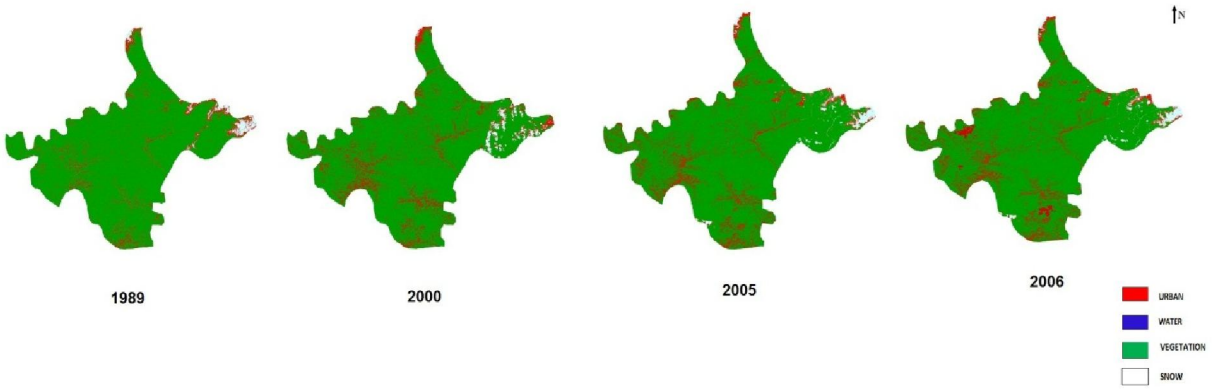

Table 1: Land use changes in Himachal Pradesh

Class	Area in Hectares (1989)	Area in Hectares (2000)	Area in Hectares (2005)	Area in Hectares (2006)
Water	16485.679	16039.310	10669.536	9454.235
Vegetation	1774602.387	1537166.846	1250625.535	1050875.265
Snow	142757.716	107648.808	99234.989	98756.325
Rock and Urban	491566.388	764532.924	1064898.297	1266326.257
Total	2425412.172	2425412.172	2425412.172	2425412.172

Table 2: Land surface Temperature changes in Himachal Pradesh

Year	Temperature (Maximum) in Degree Celsius	Temperature (Minimum) in Degree Celsius
1989	27	3
2000	28	-1
2005	30	-1
2006	31	-2

The temperature drawn by the study are, in the year 1989 minimum 3^0 C and maximum 27^0 C, where as in the year 2006 the minimum -2^0 C and maximum 31^0 C (given in Table 2), which highlights that LU characteristics play a significant role in maintaining the ambient temperature and also in the regional heat island phenomenon. Correlation analysis shows that the vegetation and water bodies are negatively correlated with temperature suggesting that these LU aid as heat sinks and hence maintains the regional climate. The population of this region exceeds its carrying capacity and is exerting pressure on the local natural resources such as land, water, etc. (MOEF,1992; Graymorea *et al*., 2009).

Conclusion:

The LU analysis shows that there has been 55% increase in urban and open areas during 1989-2000 and 39% increase during 2000-2005, and 18.92% increase during 2005-06. This land cover changes has also influenced the local climate. The minimum (min) and maximum (max) temperature was found to be -2º C and 31º C. This study clearly shows that the rate of increase in the urbanisation leads to change in the Land Surface Temperature. The increase in the temperature is in the range of 3^0 C to 4^0 C during 1989 to 2010. Change detection techniques from multi-resolution images integrating spectral, structural and textural features to generate changed patches and change attribute is also desirable and a challenging area of research.

Acknowledgement

We are grateful to NRDMS Division, The Ministry of Science and Technology, Government of India for the financial support.

References

1) Artis, D.A., and Carnahan, W.H., 1982, Survey of emissivity variability in thermography of urban areas. *Remote Sensing of Environment*, **12,** 13-329.
2) Carnahan, W.H., and Larson, R.C., 1990, An analysis of an urban heat sink. *Remote Sensing of Environment*, **33,** 65-71.
3) Carlson, T. N., Gillies, R. R., and Perry, E. M., 1994., A method to make use of thermal infrared temperature and NDVI measurements to infer surface water content and fractional vegetation cover. Remote Sensing Reviews, 9, 161−173.
4) Carlson, T. N., 2007. An overview of the so-called "Triangle Method" for estimating surface evapotranspiration and soil moisture from satellite imagery. Sensors, 7,1612−1629.
5) Dousset, B., and Gourmelon, F., 2003., Satellite multi-sensor data analysis of urban surface temperature and land cover. ISPRS Journal of Photogrammetry and Remote Sensing, 58,43−54.
6) Duda, R.O., Hart, P.E., and Stork, D.G., 2000, *Pattern Classification*, A Wiley-Interscience Publication, Second Edition, ISBN 9814-12-602-0.
7) Friedl, M.A., 2002, Forward and inverse modeling of land surface energy balance using surface temperature measurements. *Remote Sensing of Environment*, **79,** 344-354.
8) Gallo, K. P., and Tarpley, J. D., 1996., The comparison of vegetation index and surface temperature composites for urban heat island analysis. International Journal of Remote sensing, 17, 3071−3076.
9) Gallo, K.P., and Owen, T.W., 1998, Assessment of urban heat island: A multi-sensor perspective for the Dallas-Ft. Worth, USA region. *Geocarto International*, **13,** 35– 41.
10) Kato, S., and Yamaguchi, Y., 2005, Analysis of urban heat-island effect using ASTER and ETM+ Data: Separation of anthropogenic heat discharge and natural heat radiation from sensible heat flux. *Remote Sensing of Environment*, **99**, 44–54.
11) Kustas,W. P., Norman, J.M., Anderson,M. C., and French, A. N., 2003., Estimating subpixel surface temperatures and energy fluxes from the vegetation index-radiometric temperature relationship. Remote sensing of Environment, 85, 429−440.
12) Lambin, F. F., and Ehrlich, D., 1996., The surface temperature–vegetation index space for land use and land cover change analysis. International Journal of Remote Sensing, 17, 463−487.
13) Landsat 7 science data user's handbook, Landsat Project Science Office, Goddard Space Flight Center, 2002, URL: http://ltwww.gsfc.nasa.gov/IAS/handbook/handbook_toc.html (last accessed: 25 March, 2008).
14) Li, F., Jackson, T.J., Kustas, W., Schmugge, T.J., French, A.N., Cosh, M.L., Bindlish, R., 2004, Deriving land surface temperature from Landsat 5 and 7 during SMEX02/SMACEX. *Remote Sensing of Environment*, **92,** 521 – 534.

15) Markham, B.L., and Barker, J.K., 1985, Spectral characteristics of the LANDSAT Thematic Mapper Sensors. *International Journal of Remote Sensing*, **6,** 697-716.
16) Owen, T. W., Carlson, T. N., and Gillies, R. R., 1998., Assessment of satellite remotely sensed land cover parameters in quantitatively describing the climatic effect of urbanization. International Journal of Remote sensing, 19, 1663−1681.
17) Ramachandra, T.V., and Kumar, U., Land Surface Temperature with land cover dynamics: Multi resolution, spatio – temporal data analysis of greater Bangalore, International journal of geoinfomatics, vol5, No 3. September 2009.
18) Rao, P. K., 1972, Remote sensing of urban heat islands from an environmental satellite, Bulletin of the American Meteorological Society, 53, 647−648.
19) Schmugge, T., Hook, S.J., and Coll, C., 1998, Recovering surface temperature and emissivity from thermal infrared multispectral data. *Remote Sensing of Environment*, **65,** 121– 131.
20) Snyder, W.C., Wan, Z., Zhang, Y., and Feng, Y.Z., 1998, Classification based emissivity for land surface temperature measurement from space. *International Journal of Remote Sensing*, **19,** 2753– 2774.
21) Sobrino J.A et al., 2004,Land surface temperature retrieval from LANDSAT TM 5. Remote Sensing of Environment, 90, 434– 440.
22) Stathopoplou, M., Cartalis, C., and Petrakis, M., 2007, Integrating CORINE Land Cover data and landsat TM for surface emissivity definitions: an application for the urban areas of Athens, Greece. *International Journal of Remote Sensing,* **28,** 3291-3304.
23) Voogt, J. A., and Oke, T. R., 2003., Thermal remote sensing of urban climate. Remote Sensing of Environment, 86, 370−384.
24) Weng, Q., Lu, D., and Schubring, J., 2004, Estimation of land surface temperature – vegetation abundances relationship for urban heat island studies. *Remote Sensing of Environment*, **89,** 467-483.
25) *WUP (World Urbanization Prospects): The 2005 Revision*, Population Division, Department of Economic and Social Affairs, UN.
26) http://himachal.nic.in/industry/getinfon.htm
27) Zhang, J., and Zhang, Y., 2007, Remote Sensing research issues of the National Land Use Change Program of China. *Photogrammetry & Remote Sensing*, **62(6),** 461-472.

Predictive distribution modeling for rare Himalayan medicinal plant *Berberis aristata* DC.

Abstract –

Predictive distribution modelling of *Berberis aristata* DC a rare, threatened plant with high medicinal values has been done with an aim to understand its potential distribution zones in Indian Himalaya Region. Bioclimatic and topographic variables were used to develop the distribution model with the help of three different algorithms viz. Genetic Algorithm for Rule-set Production (GARP), Bioclim and Maximum Entropy (MaxEnt). MaxEnt has predicted wider potential distribution (10.36%) compared to GARP (4.63%) and Bioclim (2.44%). Validation confirms that these outputs are comparable to the present distribution pattern of the *B. aristata*. This exercise highlights that this species favours western Himalaya. However GARP and MaxEnt's prediction of eastern Himalayan states (i.e. Arunachal Pradesh, Nagaland and Manipur) are also identified as potential occurrence places require further exploration.

Keywords

Berberis aristata, Bioclim, Distribution modeling, GARP, Indian Himalayan Region, MaxEnt

Introduction-

The Indian Himalayan Region (IHR) harbours a wide spectrum of biodiversity which is reflected in diverse groups of flora, fauna and microorganisms. It supports about 8000 species of angiosperms of which 40% are endemics and the region is aptly considered as "hotspot" of Indian flora as well as part of the recently announced Himalaya "hotspot" (Nayar, 1996; Conservation International, 2007). The presence of rich biodiversity is mainly attributed to diverse habitat types influenced by wide altitudinal range (300 – 8000 m), varied rainfall and precipitation, temperature regime and complex topographical features (Samant et al., 1998).

The vast number of medicinal plants present in the region is an integral part of the livelihood of local communities. Apart from their medicinal usage, many plants are used as edible items, source for oil, fodder, fuel and timber which has been documented for a long time (Singh et al., 1984; Olsen and Larsen, 2003). However, the exponential increment of natural resource utilization, booming market demand and environmental changes nowadays put the medicinal plant resources under serious threat of existence (Ved et al., 2003). The growing list of rare, threatened and endangered plants of the region is a direct outcome of these consequences.

The raising awareness towards the importance of Himalayan biodiversity and alarming rate at which they are being exploited from natural habitats leads to initiate various conservation actions to mitigate such uncontrolled resource exploitation and its management (Arunachalam et al., 2004; Rana and Samant, 2010). As a part of the conservation and management programme, species distribution and its ecological characteristic features must be taken into consideration for species protection / restoration activities (Hirzel et al., 2004; Sanchez-Cordero et al., 2005; Martinez-Meyer et al., 2006). Himalayan region requires special attention in this regard, as frequent environmental changes take place because of its mountainous nature. The enormous variation in the altitude, latitude and longitude of the Himalayas has added to the multiplicity of habitats and provides diverse microclimates and ecological niches for all the

living beings (Karan, 1989; Carpenter, 2005; Anonymous, 2006). Although information on plant distribution and their environmental association in IHR are available to some extent, there is a gap in understanding species ecological amplitude and its application in systematic management of resources.

Berberis aristata, a well known medicinal plant in IHR and its occurrence is reported from middle altitude areas (1800-3000 m) of the state of Uttarakhand and Himachal Pradesh (Samant et al., 1998; Chauhan, 1999). It is a spinescent shrub, 3-6 m in height with obovate to elliptic, toothed leaves, yellow flowers in corymbose racemes and oblong-ovoid, bright red berries. The extract from root-barks, roots and lower stem-wood, (known as Rasanjana or Rasaut or Rasavanti) is used as stomachic, laxative, hepato-protective, antipyretic and in other ailments (Wang et al., 2004; Shahid et al., 2009; Semwal et al., 2010). It is useful in eye diseases particularly in conjunctivitis, indolent ulcers and in hemorrhoids (Rashmi et al., 2008). The plant is mostly collected from wild areas, and its agro-technique, cultivation is poorly known. Therefore, high demand for local usage as well as for pharmaceuticals creates a serious pressure on the natural resource which already categorized the plant as endangered (Srivastava et al., 2006; Ali et al., 2008). As a remedial measure, exploration of new resource, conservation of the existing resources and establishment of cultivation are of prime importance for what systematic planning and management is essential and where distribution modeling can play a key role.

Predictive distribution models aid in forecasting the spatial occurrence of species, especially, habitat suitability or realized niche based on the data from traditional field work in conjunction with climatic and topographic factors (such as slope, elevation, and precipitation) (Pearson, 2007). This habitat suitability or niche prediction is done through various algorithms or principles which usually integrate the species occurrence information and environmental data to find out the possible favourable places. A number of algorithms are available nowadays for performing the task and each unique to their data requirement, statistical methods and ease of use.

We selected Genetic Algorithm for Rule-set Production (GARP), Bioclim and Maximum Entropy (MaxEnt) methods for our study because of their predictive abilities and wide usage.

Precise prediction of the distribution of endemic and endangered species is useful for decision makers, especially for those whose conservation and management activities involve large areas but constrained by resources to carry out detail exploration / investigation. Potential distribution of species prioritises the favourable biogeographic areas to lead the conservation / management activity in a more focused way. The advantages of distribution modeling is manifold like, explaining basic ecological phenomenon behind species distribution, understanding biogeography and dispersal barriers, verification of the earlier presence records, explored the yet uncovered regions, assessment of impacts of environmental changes over species distribution, conservation planning and reserve system design (Peterson, 2006; Guisan and Thuiller, 2005; Johnson, 2005). Considering the extent of plant distribution and diversity in India, available data related to ecology and environmental preference still represents a small fraction of this vast field especially distribution modelling (Ganeshaiah et al., 2003; Irfan Ullah et al., 2007; Giriraj et al., 2008).

In our study, we developed predictive distribution models of *Berberis aristata* using three different modeling techniques, GARP, Bioclim and MaxEnt to know its potential distribution in Indo-Himalayan region.

Materials and Methods –

Study area

Indian Himalayan Region (IHR) ranges from Jammu & Kashmir to Arunachal Pradesh including Himachal Pradesh, Uttarakhand, Sikkim, Darjeeling district of West Bengal. North East states (i.e. Assam,

Meghalaya, Manipur, Nagaland, Mizoram and Tripura) are also included as part of eastern Himalaya as per available literature (Samant et al., 1998; WWF-US, 2005) (Fig 1.).

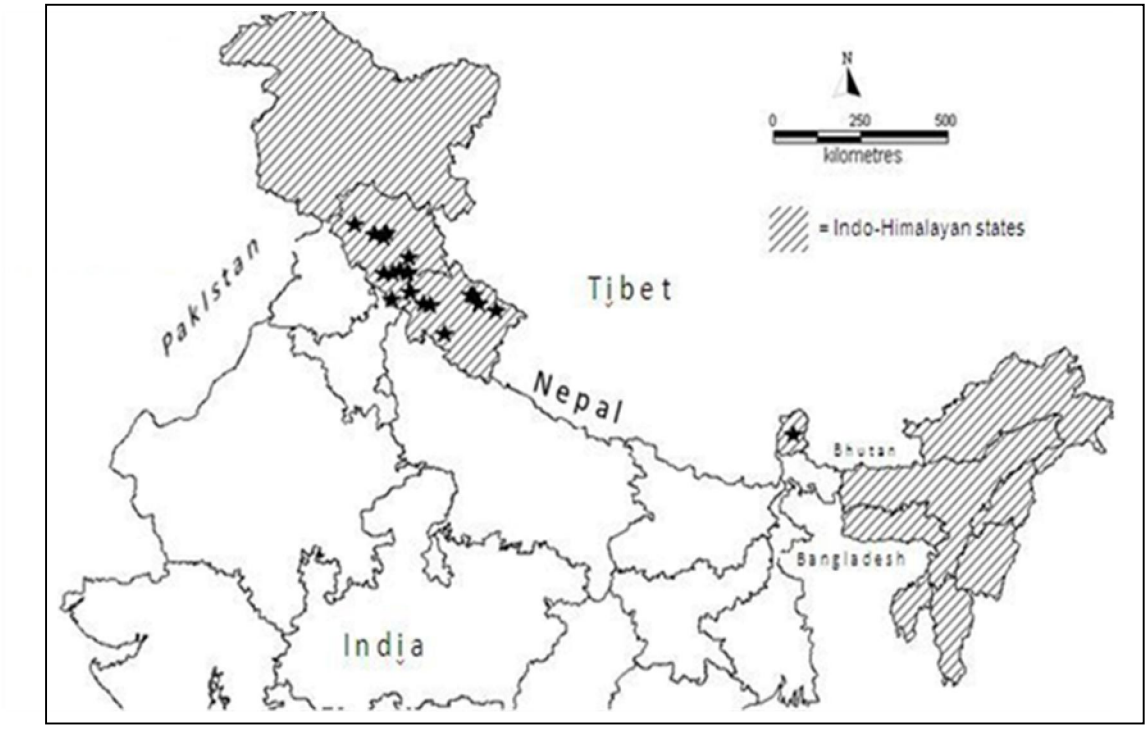

Figure 1: Study area : Indo – Himalayan Region (= occurrence points for *B.aristata*)

Species occurrence data

Twenty one occurrence points of *Berberis aristata* were shortlisted from a collection of field survey done at Moolbari watershed area of Himachal Pradesh, India and secondary data available from published literatures (Uniyal, 2002; Chhetri et al., 2005 and Anonymous, 2007-2008) (Fig 1.). Moolbari watershed is situated in Shimla district, Himachal Pradesh, India and encompasses an area of 13.41 sq. km from 31.07-31.17^0 N and 77.05-77.15^0 E. Field study was conducted by following standard ecological methods and the species was identified with the help of keys (published flora) in addition to the consultation of herbarium samples and discussion with the Himalayan flora experts.

Environmental data

For environmental information, 19 bioclimatic variables derived from globally interpolated datasets (source: http://www.worldclim.org) representing annual trends, seasonality and extreme or limiting environmental factors, were used for the modelling study which are presumed to be maximum relevant to plant existence (Pearson and Dawson, 2003; Irfan Ullah et al., 2007). The WorldClim climate layers were created by interpolating observed climate from climate stations around the world, using a thin-plate smoothing spline set to a resolution of approximately 1 km, over the 50-year period from 1950 to 2000 (Hijmans et al., 2005). Additioinally, we used aspect, slope, altitude (http://edc.usgs.gov/products/elevation/gtopo30/hydro/asia.html and http://www.worldclim.org) and landcover (GLC 2000), in the model development (Table1). All analyses were conducted at the 1 x 1 km pixels spatial resolution of the environmental data sets since, bioclimatic variables with finer than 1 km

resolution is not available at this moment. All environmental data layers were finally cropped for the study area (Indian Himalayan Region) to perform the modeling experiment.

Model development-

We followed three different modeling techniques for our study. The open Modeller desktop version 1.0.9 was used for GARP (GARP with best subsets – Desktop GARP implementation) and Bioclim techniques. Maxent 3.3.1 used for performing Maxent algorithm (downloaded from http://www.cs.princeton.edu/~schapire/maxent/). A brief description of the techniques is mentioned below.

GARP is a genetic algorithm that creates ecological niche models for species. The models describe environmental conditions under which the species should be able to maintain populations. For input, GARP uses a set of point localities where the species is known to occur and a set of geographic layers representing the environmental parameters that might limit the species' capabilities to survive. Details of the modeling algorithm can be found in Stockwell and Peters, 1999. In our study, we assigned 50% of the occurrence points as training data for developing the model while rest of the data has been used as intrinsic test data. For other parameters, we used default values available in open Modeler i.e. commission threshold = 50% of distribution models, omission threshold = 20% of the models with least omission error and resample value = 2,500.

Bioclim is one of the earlier modeling techniques, tallying species occurrence points for each environmental variable including 95% of the distribution (i.e. excluding extreme 5% of the distribution) along each ecological dimension. Details of the algorithm can be obtained from Busby (1991).

Table 1. Environmental Variables used in the model development

Variables	Details
BIO1	Annual mean temperature
BIO2	Mean diurnal temperature range [mean of monthly (max temp–min temp)]
BIO3	Isothermality (P2/P7) (×100)
BIO4	Temperature seasonality (standard deviation×100)
BIO5	Max temperature of warmest month
BIO6	Min temperature of coldest month
BIO7	Temperature annual range (P5–P6)
BIO8	Mean temperature of wettest quarter
BIO9	Mean temperature of driest quarter
BIO10	Mean temperature of warmest quarter
BIO11	Mean temperature of coldest quarter
BIO12	Annual precipitation

BIO13	Precipitation of wettest month
BIO14	Precipitation of driest month
BIO15	Precipitation seasonality (coefficient of variation)
BIO16	Precipitation of wettest quarter
BIO17	Precipitation of driest quarter
BIO18	Precipitation of warmest quarter
BIO19	Precipitation of coldest quarter
Slope	Slope value from digital elevation model (http://edc.usgs.gov)
Aspect	Aspect value from digital elevation model (http://edc.usgs.gov)
Altitude	Elevation above sea level (m)
Landcover	Global landcover map

The maximum entropy (MaxEnt) approach estimates a species' environmental niche by finding a probability distribution that is based on a distribution of maximum entropy (with reference to a set of environmental variables) (Phillips et al., 2006). Default values of different parameters, maximum iterations = 500, convergence threshold = 0.00001 and 50% of data points were used as random test percentage in our study.

Model validation -

Prediction accuracy of all three model outputs was measured through receiver operating characteristics (ROC) analysis because of its wider application in the modeling studies despite some recent arguments (Lobo et al., 2008; Boubli and Lima, 2009; VanDerWal et al., 2009; Yates et al., 2010). ROC plot can be generated by putting the sensitivity values, the true positive fraction against the false positive fraction for all available probability thresholds. A curve which maximizes sensitivity against low false positive fraction values is considered as good model and is quantified by calculating the area under the curve (AUC). An AUC statistic closer to1.0 indicates total agreement between the model and test data and considered as good model. An AUC with value closer to 0.5 considered to be no better than random.

Result and Discussion –

Predictions of the potential distribution of *Berberis aristata* in Indo-Himalayan region are comparable based on its current distribution in the region. Model outputs are varied according to the modeling techniques (Fig 2 A, B and C).

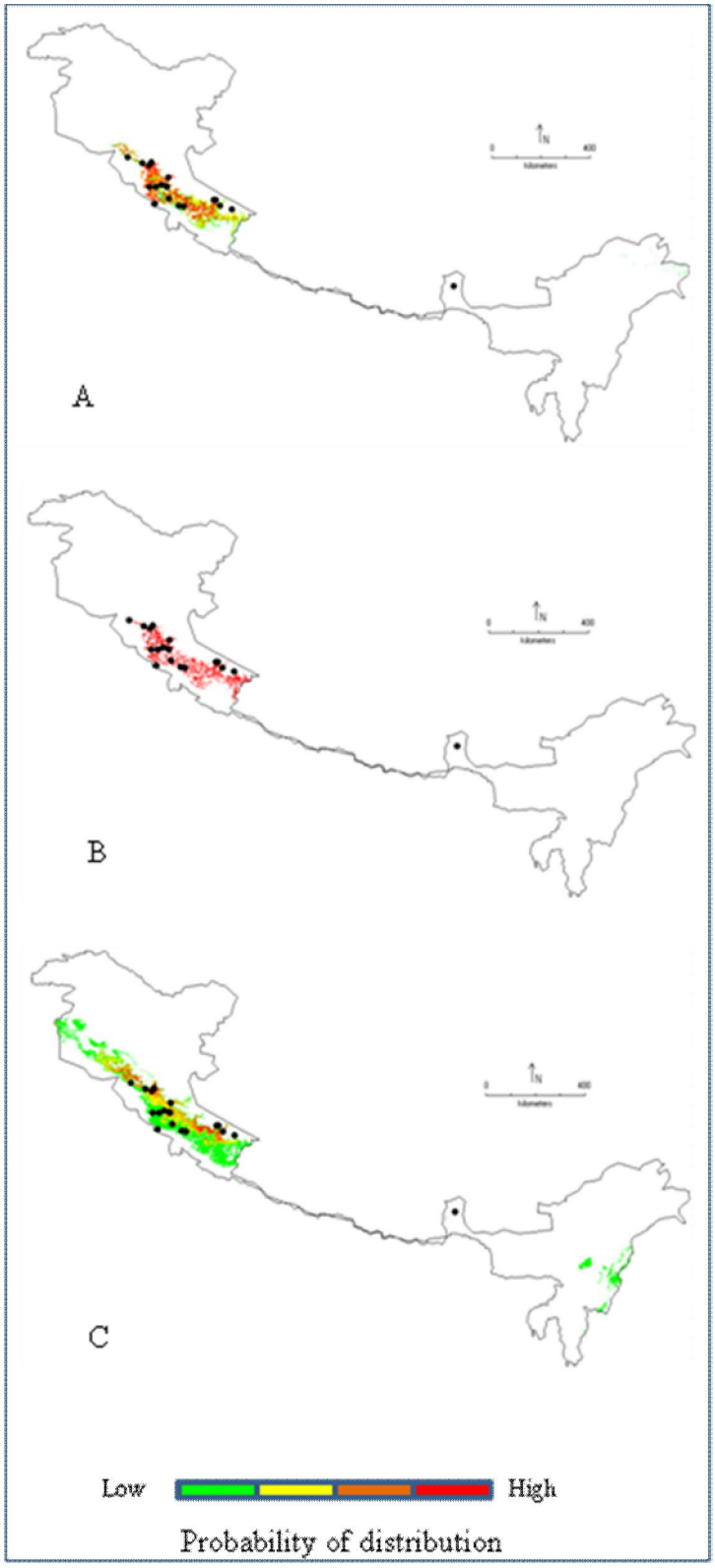

Fig 2. Modelling outputs from three different algorithms

A = GARP, B = Bioclim, C = MaxEnt

Both the GARP and MaxEnt models show distribution spread in western and eastern Himalayan states of India. On the contrary, Bioclim output is restricted in western Himalayan region i.e., Himachal Pradesh and Uttarakhand. . All three models show higher accuracy and AUC value near 1.0 with low omission error (Table 2).

Table 2. Comparative details of the modeling outputs

Parameters	Modelling techniques		
	GARP	Bioclim	Maxent
Accuracy	86.66	100	-
AUC value	1.0	1.0	0.969 (training set) 0.947 (test set)
Omission error	0.142	0	-
Total distribution (% of total area)	4.63	2.44	10.36
High probability area (% of total distribution)	29.65	100	6.27

Modelling outputs reveal that, MaxEnt has predicted largest area (10.36% of Indo-Himalayan region) under potential distribution in comparison to GARP (4.63%) and Bioclim (2.44%). However, Bioclim has higher high probability regions (100%) than GARP and MaxEnt (i.e. 29.65% and 6.27% respectively). Both GARP and MaxEnt have shown a wider range of distribution from low to high probability in Himachal Pradesh, Uttarakhand, Jammu-Kashmir, Arunachal Pradesh, Nagaland and Manipur whereas, Bioclim distribution is restricted as high probability areas in Himachal Pradesh and Uttarakhand.

The jackknife test of variable importance in MaxEnt has identified the precipitation of driest quarter (bioclimatic variable 17) as the most important environmental variable in model development. This variable has highest predictive value or gain when used in isolation. Other variables like precipitation of coldest quarter (bioclimatic variable 19), temperature seasonality (bioclimatic variable 4), mean temperature of coldest quarter (bioclimatic variable 11) and minimum temperature of coldest month (bioclimatic variable 6) also have considerable predictive value with regard to distribution of *Berberis aristata.*

Potential distribution maps show various possibilities for conservation and management of this valuable plant species. Clustering of high probability areas in the North-western states around the

occurrence points indicate the suitability of the region for further exploration as well as reintroduction / conservation program as it satisfies fundamental niche requirement of the species. Considering the mountainous inhospitable nature of the Himalayan region, targeting high probability regions for future exploration could increase the probability of success in the venture. Earlier endevours involving field surveys / exploration based on model outputs had helped in discovering new populations as well as allied species (Raxworthy et al., 2003; Siqueira et al., 2009). This prior information on species probable distribution in the area certainly helps in judicious utilization of resources and time. On the other hand, new areas like eastern Himalayan states have come out as potential occurrence sites for the species as evidenced through GARP and MaxEnt outputs. At present we have only one occurrence record from this site (i.e. Sikkim) but further studies may improve the candidature of the region as favorable site for the *Berberis aristata*. This idea gets support from available literature on *Berberis* spp. distribution in India, where several other species of *Berberis* viz,, *B. asiatica var asiatica*, *B. parisepala, B. macrosepala var macrosepala, B. insignis, B. dasyclada* etc. have been reported from north eastern Himalayan states (Sharma et al., 1993). The presence of other species in the region may open up the possibilities for *B. aristata* as several studies have indicated niche conservatism among the closely related species (Peterson, 1999). However, this could only be verified after field exploration and collection of information.

This exercise could be useful for comparing natural resource distribution pattern and conservation / management strategies to protect them. Application of species distribution modeling in conservation area planning and management is widely used nowadays (Araujo and Williams, 2000; Ortega-Huerta and Peterson, 2004; Pearson, 2007). By knowing the potential distribution region, especially the high probability areas (here it is part of Uttarakhand and Himachal Pradesh), it is possible to design conservation priority zone / resource management zone with an emphasis on species ecological boundary. This approach from ecological viewpoint makes species survival and management easier and more efficient than other practices.

Acknowledgement

We are grateful to the Ministry of Science and Technology, Government of India and Indian Institute of Science for the financial assistance. We thank Mr. G.R. Rao, Vishnu Mukri and Dr. Archana Singh (NBPGR, Shimla, Himachal Pradesh) for suggestions during the field investigations. Special thanks to Mr. Uttam Kumar and Mr. Bharath Setturu for their help in GIS analysis.

Reference

Ali M, A.R. Malik,and K.R. Sharma : Vegetative propagation of *Berberis aristata* DC. An endangered Himalayan shrub. J. *Med. Pl. Res*. **12**, 374-377 (2008).

Anonymous: Forest Research Institute (FRI), Dehradun, India. (2007-2008).

Anonymous: THE MOUNTAIN ECOSYSTEMS [Environment and Forest Sector] for Eleventh Five Year Plan. Report. Planning Commission, Government of India, November 2006

Araújo M.B. and P.H. Williams: Selecting areas for species persistence using occurrence data. *Biol. Conserv*. 96, 331-345 (2000)

Arunachalam, A,, R. Sarmah, D. Adhikari,M. Majumder and M.L. Khan: Anthropogenic threats and biodiversity conservation in Namdapha nature reserve in the Indian Eastern Himalayas. *Curr. Sci*, **87**, 447-454 (2004)

Boubli, J.P.and M.G. de Lima, : Modeling the Geographical Distribution and Fundamental Niches of *Cacajao* spp. and *Chiropotes israelita* in Northwestern Amazonia via a Maximum Entropy Algorithm. *Int. J. Primatol.* **30**,217–228 (2009)

Busby, J.R: BIOCLIM - a bioclimate analysis and prediction system. *In*: Nature conservation: cost effective biological surveys and data analysis (*Eds.*: C.R. Margules and M.P. Austin). CSIRO, pp. 64-68 (1991).

Carpenter, C.: The environmental control of plant species density on a Himalayan elevation gradient. *J. Biogeogr.* **32**, 999–1018 (2005)

Chauhan, N.S.: Medicinal and Aromatic plants of Himachal Pradesh. Indus Publishing Company, New Delhi. Pp.114-117 (1999).

Chhetri D.R., P. Parajuli, and G.C. Subba : Antidiabetic plants used by Sikkim and Darjeeling Himalayan tribes, *Ind. J. Ethnopharmacol.,* **99**, 199–202 (2005).

Conservation International: Biodiversity Hotspots (2007). Website: http://www.biodiversityhotspots.org

Ganeshaiah, K.N., N. Barve, N. Nath, K. Chandrashekara, M. Swamyand R. Uma Shaanker. : Predicting the potential geographical distribution of the sugarcane woolly aphid using GARP and *DIVA*-GIS. *Curr. Sci*., **85**, 1526-1528 (2003).

Giriraj, A., M. Irfan-Ullah, B.R. Ramesh, P.V. Karunakaran, A. Jentsch, and M.S.R. Murthy: Mapping the potential distribution of *Rhododendron arboreum* Sm. ssp. *Nilagiricum* (Zenker) Tagg (Ericaceae), an endemic plant using ecological niche modelling. *Curr. Sci*., **94**, 1605-1612 (2008).

Global Land Cover 2000 (GLC 2000) database. European Commission, Joint Research Centre, (2003). http://gem.jrc.ec.europa.eu/products/glc2000/glc2000.php

Guisan, A, and W. Thuiller: Predicting species distribution: offering more than simple habitat models. *Ecol. Lett.* **8**, 993-1009 (2005)

Hijmans, R. J., S. Cameron, J. Parra, P. Jones and A. Jarvis: Very high resolution interpolated climate surfaces for global land areas. *Int. J. Clim*. **25**,1965–1978 (2005).

Hirzel, A.H., B. Posse, P. Oggier, Y. Crettenand, C. Glenz, R. Arlettaz: Ecological requirements of reintroduced species and the implications for release policy: the case of the bearded vulture. *J. Appl. Ecol* **41**, 1103–1116 (2004)

Irfan-Ullah M., A. Giriraj, M.S.R Murthy and A.T. Peterson: Mapping the geographic distribution of Aglaia bourdillonii Gamble (Meliaceae), an endemic and threatened plant, using ecological niche modelling. *Biodivers. Conserv*., **16**, 1917–1925 (2007).

Johnson, C.J. and M.P. Gillingham: An evaluation of mapped species distribution models used for conservation planning. *Environ Conserv.,* **32**, 117-128 (2005)

Karan, P.P.: Environment and Development in Sikkim Himalaya: A Review. *Hum*. *Ecol*. **17**, 257-271 (1989)

Lobo, J.M., A. Jime´nez-Valverde and R. Real: AUC: a misleading measure of the performance of predictive distribution models. *Glob Ecol Biogeogr.,* **17**,145–151 (2008)

Martínez-Meyer, E., A.T. Peterson, J.I. Servín and L.F. Kiff: Ecological niche modelling and prioritizing areas for species reintroductions. *Oryx*, **40**, 411-418 (2006)

Nayar, M.P: "Hot spots" of endemic plants of India, Nepal and Bhutan. Tropical Botanic Garden and Research Institute. Palode, Thiruvananthapuram, Kerala, India, pp. 252 (1996).

Olsen, C.S. and H.O. Larsen: Alpine medicinal plant trade and Himalayan mountain livelihood strategies. *Geo. J*., **169**, 243-254 (2003).

Ortega-Huerta, M.A. and A.T.Peterson: Modelling spatial patterns of biodiversity for conservation prioritization in North-eastern Mexico. *Divers Distrib.,***10,** 39-54 (2004)

Pearson, R.G. and T.P. Dawson: Predicting the impacts of climate change on the distribution of species: are bioclimatic envelope models useful? *Global. Ecol.Biogeogr*., **12**, 361-371(2003).

Pearson, R.G: Species distribution modelling for conservation educators and practitioners. Synthesis. American Museum of Natural History (2007). Available at http://ncep.amnh.org

Peterson, A.T., J. Soberon and V.S. Cordero: Conservatism of ecological niches in evolutionary time. *Science*, **285**, 1265-1267 (1999).

Peterson, A.T: Uses and requirements of ecological niche models and related distributional models. *Biodivers. Info*., **3**, 59 – 72 (2006).

Phillips, S.J, M. Dudik and R.E. Schapire: A maximum entropy approach to species distribution modeling. In *Proceedings of the 21st international conference on machine learning*, pp. 655-662 (2004). AMC Press, New York.

Phillips, S.J., R.P. Anderson and R.E. Schapire: Maximum entropy modeling of species geographic distributions. *Ecol. Model*. **190**, 231- 259.(2006)

Rana, M.S. and S.S. Samant: Threat categorisation and conservation prioritisation of floristic diversity in the Indian Himalayan region: A state of art approach from Manali Wildlife Sanctuary. *J. Nat. Conserv.,* **18**, 159-168 (2010)

Rashmi, A. Rajasekaran and J. Pant: The genus Berberis Linn.: A Review. *Phcog Rev*, **2**, 369-385 (2008).

Raxworthy, C.J., E. Martinez-Meyer, N. Horning, R.A. Nussbaum, G.E. Schneider, M. A. Ortega-Huerta and A.T. Peterson: Predicting distributions of known and unknown reptile species in Madagascar. *Nature* **426**, 837-841 (2003)

Samant. S.S, U. Dhar and L.M.S. Palni: Medicinal plants of Indian Himalaya: diversity, distribution potential values. Gyanodaya Prakashan, Nainital, India, pp.163 (1998).

Sánchez-Cordero, V., V. Cirelli, M. Munguía and S. Sarkar: Place prioritization for biodiversity representation using species' ecological niche modeling. *Biodivers. Inf.*, **2**, 11-23 (2005)

Semwal, B.C., J. Gupta, S. Singh, Y. Kumar and M. Giri: Antihyperglycemic activity of root of Berberis aristata DC. in alloxan-induced diabetic rats. International Journal of green Pharmacy DOI: 10.4103/0973-8258.56288

Shahid, M., T. Rahim, A. Shahzad, T.A. Latif, T. Fatma, M. Rashid, A. Raza and S. Mustafa: Ethnobotanical studies on Berberis aristata DC. root extracts. *African J. Biotechnol.* **8**, 556–563, (2009)

Sharma, B.D., N.P. Balakrishnan, R.R. Rao and P.K. Hajra (eds.): Flora of India. Botanical Survey of India, Kolkata, India. **1**, 351-405 (1993).

Singh J.S., U. Pandey and A.K. Tiwari : Man and forests: A central Himalayan case study. *Ambio*, **13**, 80-87 (1984).

Siqueira, M.F., G. Durigan, P.M. Ju´nior and A.T. Peterson: Something from nothing: Using landscape similarity and ecological niche modeling to find rare plant species. *J. Nat. Conserv*., **17** , 25—32 (2009)

Srivastava, S.K, V. Rai, M. Srivastava, A.K.S. Rawat and S. Mehrotra: Estimation of heavy metals in different B*erberis* species and its market samples. *Environ. Monit. Assess.,* **116,** 315–320 (2006)

Stockwell D. R. B. and D. Peters: The GARP modeling system: Problems and solutions to automated spatial prediction. *Int. J. Geogr. Inf. Sci.,* **13**, 143–158 (1999).

Uniyal V.P: Nanda Devi Expedition (Report). Wildlife Institute of India, Dehradun (2002)

VanDerWal, J., L.P. Shoo, C. Graham and S.E. Williams: Selecting pseudo-absence data for presence-only distribution modeling: How far should you stray from what you know? *Ecol. Model.,* **220**, 589–594, (2009)

Ved D.K., G.A. Kinhal , K. Ravikumar , V. Prabhakaran , U. Ghate, R. Vijaya Sankar and J.H. Indresha (eds.) : Conservation Assessment and Management Prioritisation for the medicinal plants of Himachal Pradesh, Jammu & Kashmir and Uttaranchal. Foundation for Revitalisation of Local health Traditions (FRLHT), Bangalore, India (2003).

Wang, F., H.Y. Zhou, G. Zhao, L. Fu, L. Cheng, J. Chen and W. Yao: Inhibitory effects of berberine on ion channels of rat hepatocytes. *World. J. Gastroenterol.,* **10**, 2842-2845 (2004)

WWF-US, Asia Program: Ecosystem Profile: Eastern Himalayas Region. Website: www.cepf.net/Documents/final.ehimalayas.ep.pdf (2005).

Yates, C.J., A. McNeill, J. Elith and G.F. Midgley: Assessing the impacts of climate change and land transformation on *Banksia* in the South West Australian Floristic Region. Diversity Distrib., **16**, 187–201(2010)

Flora and faunal distribution in three selected micro watersheds of Western Himalaya

SUMMARY

Ecological status of a particular region is determined by assessing its biodiversity, prevailing conditions of the environment and their interactions. Such an assessment is carried out through the estimation of species composition and their relative abundance with reference to space and time in a region. Prioritising the region, based on these, helps to evaluate and emphasise the protection needs of a habitat, considering its local and global distribution, habitat preference and threats to species and habitats. In this regard, field sampling of flora through 34 belt transects of 1000 sq.m in three micro watersheds (Mandhala, Moolbari and Megad, Himachal Pradesh) of Western Himalaya, yielded a total of 2276 individuals from 75 woody species belonging to 38 families. Among these families, Fabaceae was species rich (7 species) followed by Rosaceae (5), Pinaceae (5) and Moraceae (5). *Quercus leucotriphora* had highest individuals (811) followed by *Q. glauca* (394), *Acacia catechu* (157), *Myrica esculenta* (73), *Pinus roxbhurghii* (72), *Abies pindrow* (70) and *Flacourtia indica* (68). Among the three micro watersheds, Mandhala was species rich with 43 species followed by Moolbari (39) and MeGad (9). In Mandala most of the species are thorny shrubs and rarely attain tree forms due to severe anthropogenic disturbances, which also yielded very low basal area. Moolbari had the highest basal area, which had dominant species *Quercus leucotricophora* and *Q. glauca*. MeGad, a high altitude area was mostly dominated by *Abies pindrow, Picea smithiana,* and *Pinus wallichiana*.

Faunal investigations enumerated 115 butterfly species, 14 amphibian and 136 bird species. Butterflies in the region were oriental and palaearctic in origin representing nine families. Nympahlidae is dominant (32 sp.) followed by Pieridae (19 sp.), Lycaenidae (16 sp.), Satyridae and Papilionidae (12 sp. each) and Hesperridae (10 sp.). Similarly, we observed 14 species amphibians belonging to 5 families. *Paa minica* is vulnerable and *Amolops chakrataensis* is data deficient according to IUCN status and these two are endemics of Himalayan foot hills. Among the three watersheds, Mandhala, lying in Shivaliks has higher diversity followed by Moolbari. We did not encounter any amphibians in MeGad microwatershed during Aug-Sept 07. In total 136 bird species were recorded from three watersheds, the maximum number of bird species occurred in Mandhala region (104) followed by Moolbari (57) and Me Gad (35). Eight species were found in all three watersheds, ranging from an altitude of 400 m to 4000 m.

INTRODUCTION

Three watersheds , viz., Mandhala, Moolbari and Me Gad representing lower, middle and upper Himalayas respectively in the state of Himachal Pradesh were chosen by the Ministry of Science and Technology, Government of India for implementing a coordinated, multi disciplinary and multi institutional program “Bio-geo database and ecological modeling for western Himalayas”..

The Himalayas are rich in natural resources; however over the years, Himalayan environment is increasingly being threatened due to various unplanned human activities with excessive exploitation of natural resources. It is imperative to develop strategies for sustainable management to commensurate with the increasing human pressure on the natural resources.

Himachal Pradesh is an important part of Western Himalaya covering about 11% of total Himalayan land mass. Mountain ranges in the state include Shivaliks and Trans–Himalayas with altitudes ranging from about 350–7000 m above mean sea level. Winter (December–February), pre-monsoon (March–June),

monsoon (July–September) and post-monsoon (October–Novermber) are major seasons in the region. Precipitation varies from snowfall to rainfall that ranges from 1000-2500 mm. Temperature varies from sub-zero ranges of -30° to -40°C (in winter) at higher altitudes, whereas in the plains it ranges between 8° to 40°C. Many rivers like Beas, Sutlej, Chenab, Ravi and Yamuna originate from this region.

The climate is distinguished in three axes: (i) a vertical axis determined by the effect of altitude on temperature; (ii) a transverse axis determined by topography along which rain shadow effects cause decreasing precipitation and increasingly extreme (continental) temperature fluctuations from SW to NE across the main ranges; (iii) a longitudinal axis determined by a geographical trend of decreasing monsoon precipitation (June September) and increasing winter snowfall (December-April) from SW to NW along all the ranges. The third axis is important in determining major ecological trends over the entire length of the Himalayan chain, but it is less important than the other two axes in determining the ecology of localities within the Western Himalayas. (Gaston et al.,1983)

The enormous variations in the altitude, latitude and longitude of the Himalayas have added to the multiplicity of habitats and provide diverse microclimates and ecological niches for all the living beings. The Western Himalayan region which includes Jammu and Kashmir, Himachal Pradesh and hilly regions of Uttar Pradesh receives very less rain compared to its eastern counterpart, the Eastern Himalayas. As a result the Western Himalayan flora in due course of time has evolved and established itself as drought resistant and cold loving while the Eastern Himalayan flora has developed into moist evergreen type. Also, the Western Himalayan flora is species deficient whereas, the eastern Himalayan flora is species rich. The vegetation of Himachal Pradesh can be broadly classified into

(i) Tropical-below 1000 m
(ii) Sub-tropical- between 1800-2000 m
(iii) Temperate- between 1800- 3500 m
(iv) Subalpine- between 3500-4000 m
(v) Alpine- above 4000 m

However, these may overlap depending upon the location, topography and climatic conditions.

(i) *Tropical vegetation*

a) *Moist mixed deciduous Sal forests*: These forests occur in Shivalik ranges and slopes of lesser Himalayas up to an altitude of about 1000 m.
b) *Mixed deciduous forests*: These occur on exposed slopes up to an altitude of 1500 m.

(ii) *Subtropical vegetation*

a) *Subtropical Pine forest*: *Pinus roxbhurgii* predominate such forests. In moist conditions broad-leaved elements such as evergreen oaks occur in association with other broad leaved species.
b) *Subtropical dry evergreen forest*: These are scrub forests of small leaved evergreen trees dominated by shrubby elements and several thorny species which are more prominent on hot dry exposed slopes.

(iii) *Temperate vegetation*

a) *Himalayan moist temperate forest*: These are predominantly coniferous forests.
b) *Himalayan dry temperate forest*: These types of forests are found in the inner Himalayan ranges with very less rainfall and precipitation is mainly in the form snowfall during winter months. Generally, conifers predominate in such forests.

(iv) *Subalpine vegetation*

The subalpine vegetation appears above the timber line or tree limit. The vegetation is in the form of stunted, scattered bushes.

(v) *Alpine vegetation*

Alpine vegetation can be divided into three types based on the species composition and climatic conditions, etc. as:

a) *Moist alpine scrubs*: Such scrubs are commonly found in rocky places, ridges and stony slopes.

b) *Alpine meadows*: Alpine meadows present some of the spectacular and colourful view of the Himalayan flora in the flowering season. Only some specialised types of herbaceous elements are seen as the climatic conditions are extremely severe and hostile at an altitude of 4000 m or above.
c) *Alpine or stony desert*: Beyond alpine vegetation, which begins above timber line or tree line and constitutes up to 4500 m or even up to 5000 m lies zone of alpine desert. The most dominant elements of this zone are lichens and mosses with some associated herbaceous elements.

Fauna

Compared to eastern Himalayan region, Western Himalaya is species poor. There is a comprehensive account on available faunal species from this region (Mehta, 2005). This includes lower organisms from protozoans to mammals. This study focuses on three faunal components namely butterflies, amphibians and birds.

***Butterflies*:** Insects are particularly useful in the evaluation of landscapes for biological conservation (Kim 1993; Samways 1994). Among the diversity of insects, butterflies are ideal subjects for ecological study in landscapes (Thomas and Malorie 1985; Pollard and Yates 1993). In temperate regions, butterfly taxonomy and natural history are relatively well understood and most species can be reliably identified in the field. Butterflies are probably the best-known invertebrate taxa with an estimated 20,000 species worldwide and a prominent place in conservation programmes and biodiversity assessments (Stork *et al.*, 2003). Furthermore, they are represented by a diverse yet relatively small number of species exhibiting a wide spectrum of ecological characteristics. Butterflies are particularly sensitive to environmental variation (Scoble 1992). Positive relations have been found between butterfly diversity and environmental variables such as plant diversity (Erhardt 1985; Thomas and Malorie 1985; Leps and Spitzer 1990; Spitzer *et al.*, 1997), habitat complexity (Molina and Palma 1996), landscape structure (Wood and Samways 1992), topographic and moisture gradients (Kremen 1992), and climate (Pollard and Yates 1993; Parmesan 1996). Furthermore, inventorying and monitoring of butterflies has proven useful in the evaluation of terrestrial landscapes for biological conservation (Samways 1994). Examples include habitat assessment and classification (New 1991; Pollard and Yates 1993; New et al. 1995), as well as evaluation of the effects of land use (Erhardt 1985; Swengel 1996) and urbanisation (Kremen 1992; Blair and Launer 1997).

The Himalayan butterfly fauna is well documented since mid-nineteenth century viz., Carlo von-Hugel (1844-1848); Hardwick's collections were described by Doubleday and Gray (1846) and Rodtenbacker (1848). Besides collections were also made by Lt. Colonel A. M. Lang from North Western Himalayas and A. G. Young from Kullu, which were included by Major G.F.L. Marshall and L. de Niceville in the *The Butterflies of India, Burma and Ceylon* (vols. 1 to 3: 1882-1890), and Rev. J.H. Hocking from Kangra district and were published by Moore, F. (1882). Subsequently, these were included in publications by Evans (1932), and Talbot (1939, 1947). De Rhe-Philipe (1931) was probably the first to publish a comprehensive list of 246 butterflies of Shimla hills and later Wynter-Blyth (1940-1946) listed as many as 294 species of butterflies from Shimla hills. These were also included in the book *Butteflies of the Indian Region* (1957). Mani (1986) described 377 species of butterflies except Hesperiidae from Himalaya. The recent work on Western Himalayan Butterflies was recorded by Arora *et al.* (2005), which provides a comprehensive list of 288 butterflies form Himachal Pradesh (2005).

***Amphibians*:** Amphibians are the only vertebrate group to have dual life stages, one in water and the other on land. Coupled with this, they are ectotherms and skin breathers, which make them highly sensitive to ecological changes in the surroundings. They are the group with the highest proportion of species threatened with extinction (Beebee and Griffiths, 2005). Both for understanding the reasons of decline in their global population as well as to have a proper conservation initiative, there is a need for studies that focus on the processes that drive patterns of distribution and abundance of amphibians.

Diversity of amphibians in India is about 240 species (Global Amphibian Asssement, 2006), with Himalayan ranges and Western Ghats harbouring most of them. Despite such diversity, systematic studies on them are very few, especially in the temperate regions of Himalayas. For the entire state of Himachal Pradesh, 17 species of amphibians have been reported so far (Mehta, 2005).

***Birds*:** The Himalayan birds species accounts for more than 60% of birds found in India and species differ greatly in abundance, geographical range, mobility and detectability. The Eastern Himalayas is more rich and diverse in bird species, while, the western Himalayas is also known for rare and endemic birds like the pheasants, visiting cranes and breeding warblers. This constitutes a distinct assemblage sandwiched between the tropical forests of the Indian plains and the palaearctic steppes of the Tibetan plateau. The fauna of the alpine zone has much in common with that of adjacent Tibet, whilst many of the species typical of the subtropical foothills are also represented on the plains to the south. The intermediate temperate zone, a narrow ribbon of land 50-100 km wide and more than 2000 km long, contains the highest proportion of characteristic Himalayan species (Gaston et al., 1983). Although a description of the avifauna of the region is already available (Inskipp, 1989; Inskipp and Inskipp, 1998), no quantitative data has been published on bird habitat use.(Laiolo et al 2003)

Objectives

The major objectives of this study are:

1. Diversity and distribution of flora in the three micro watersheds
2. Diversity and distribution of selected fauna, namely butterfly, amphibians and birds in the region

Materials and Methods

Study area: Details of the geography of the study area are given in Table 1. These three micro watersheds form a part of Chandrabagha, Sutlej and Yamuna river basins.

Table 1. Geographical details of studied micro watersheds.

Micro watersheds	District	Main watershed	Latitude (°N)	Longitude (°E)	Altitude (m amsl)	Area (sq.km)
Mandhala	Solan	Yamuna	30.87-30.97	76.82-76.92	400-1100	14.5
Moolbari	Shimla	Sutlej	31.07-31.17	77.05-77.15	1400-2000	10
MeGad	Lahaul and Spiti	Chandrabhaga	32.64-32.74	76.46-76.74	2900-4500	45

Mandhala: This area has mixed deciduous forests in an altitude below 1100 m. The prominent trees and shrubs found here are *Flacourtia montana, Acacia catechu, Grewia optiva, Toona ciliata, Albizia procera, Haldina cordifolia, Acacia* sp*., Lannea coramandelica, Mitragyma parviflora*, along with *Nyctanthus arbor-tristis, Carissa apaca, Dodonaea viscose* and *Woodfordia fruticosa*. Most of the forests here have been deforested and hill ranges are completely covered with *Lantana camera* an exotic invasive weed. Also scattered trees of *Holoptelia integrifolia, Dalbergia sisoo, Morus nigra*, etc. occur along the field bunds and other open lands.

Moolbari: Vegetation in this watershed consists of mixed deciduous (till an altitude of 1500 m) and sub-tropical pine forest (beyond 1500 m). Apart from *Pinus*, other species are *Pyrus pashia, Rubus ellipticus, Berberis* sp, and in moist localities species of *Quercus leucotrichophora* and *Q. glauca* and *Rhododendron arboretum*. Exposed hill slopes in pine forests have *Euphorbia royleana*. Between 1800-2300 m, oak forests species such as *Quercus leucotrichophora*, *Q. glauca* dominate along with *Rhododendron arboretum, Lyonia ovalifolia, Persia* sp*., Myrica esculenta*, *Acer oblongum, Cedrus deodar,*etc.

MeGad:

This watershed lies in cold desert and comprises of temperate, sub-alpine and alpine vegetation.

- *Temperate vegetation*: It consists of woody trees at an altitude of 2500-3200 m such as *Pinus wallichiana, Juniperus recurva, Picea smithiana, Abies pindrow*, *Cedrus deodara* . Along the streams and irrigated canals are planted trees of *Salix* and *Poplar* sp.
- *Sub-alpine vegetation:* It consists of stunted, scattered bushes of *Juniperus communis, Berberis* sp., etc along with herbaceous species such as *Ranunculus, Pedicularis, Potentilla, Polygonum, Geranium, Anemone, Corydalis*, etc.
- *Alpine Vegetation:* Up to 4000 m only herbaceous species such as *Swertia, Silene, Potentilla, Cordalis, Taraxacum, Astralagus, Rheum, Polygonum, Artimisia, Primula* etc., occur. Alpine meadows provide one of the most spectacular and colourful view. Majority of the alpine meadows are perennial in nature and perenate through rhizomes, root stocks, runners, suckers, bulbs, tubers or bulbils. Common herbaceous species here are *Saxifraga, Arenaria, Aster, Polygonum, Primula, Potentilla, Selinum, Taraxicum, Astralagus, Geranium, Senecio, Saussurea, Swertia, Erigeron, Corydalis, Rheum,* etc. Terrestrial orchids such as *Goodyera, Malaxis,* etc., are also seen here.

Methods:

Vegetation **Sampling:** Systematic sampling was carried out in all three micro watersheds (Moolbari, Mandhala, and MeGad) With belt transects of 250 x 4 m. In each transect, for each tree GBH in cm (Girth at Breast Height, approximately at 130 cm above ground) and height in m is noted along with its identification. Unidentified plants were labelled and pressed in herbaria for later identification.

Coordinates were marked using GPS (Global Positioning System) at every 100 metres interval and at the start and end points in each transect. Litter weight is measured in four 1 m X 1 m quadrat within each transect. Using densiometer, canopy cover is measured at start, end point and at 100 metre intervals in each transect. Also, relative humidity and air temperature was taken at every 100 m and at the start and end of the transect.

Faunal Sampling

Butteflies**:** In selected localities, transect based sampling (250x4 m) as well as opportunistic sampling of butterflies was carried out. Most of the butterflies were identified in the field and others were photographed and identified later with the available keys.

Amphibian**:** Amphibians are highly seasonal and majority of them breed during monsoon. Hence, we searched and identified amphibians during July-August 2007 in major land-use categories like waterbodies (streams of 1° and 2°), forests, agriculture fields, and open area between 19:00-21:00 h. We have invested 2 man-hour searches on each night. Number of individuals, sampling co-ordinates and habitat characteristics were also noted.

Birds**:** Time constrained sampling of 1 hour in each habitat types during morning and evening was carried out. The co-ordinates were taken at the start and end point of transects using GPS and species alongwith their numbers were also recorded

Table 1: Showing the equations for calculating IVI

Index	Equation	Remarks	References
Density	Number of species A / Area sampled (m^2)	Compactness with which a species exists in an area.	Elzinga et al, (2001)
Relative Density	Density of species A x 100 / Total density of all species		
Dominance	Basal area of species A / Area sampled (m^2)	The occupancy of a species over an area	
Relative dominance	Dominance of species A x 100 / Total dominance of all species		
Frequency	Number of quadrats with species A / Total number of quadrats sampled	The repeated occurrence of a species	Elzinga et al, (2001)
Relative Frequency	Frequency of species A x 100 / Total frequency of all species		
Important Value Index	R. density + R. frequency + R. basal area		
Abundance	Number of individuals of a species x 100 / Number of sampling units		
Numerical species Richness	S-1 / log N	S= Number of species N= Number of Individuals	Magurran A.E,1988
Simpson Diversity index	$D=\sum n_i (n_i-1) / N(N-1)$	N_i= Number of individuals in each species N= Total number of individuals	
Simpson dominance index	$D=\sum(n_i/N)^2$		
Shannon Weiner's Index	$H'=-\sum P_i \ln P_i$	$P_i= n_i/N$	
Pielou's evenness measure	$E=H'/\log S$	H'= Shannon-Weiner's index S= Number of species	

RESULTS AND DISCUSSION

Vegetation

Woody species in the three micro watersheds is detailed in Table 2. Transects are named with first two letters of the microwatershed (Ma stands for Mandhala, Mo-Moolbari and Me for MeGad). Transect wise analysis in each of the micro watershed is discussed below.

Mandhala: 11 transects were laid in Mandhala water shed area. Total individuals recorded in these transects were 447 with the highest number of individuals (84) recorded in Ma-6. *Acacia catechu* with higher number of individuals constitute a dominant species. This species was planted earlier by forest department under afforestation programme. Lower number of individuals were recorded in Ma-5 and Ma-10 with severe degradation. Species richness was more in Ma-2 with 21 species and lowest in Ma-9 with 3 species. Basal area was highest in Ma-2 and lowest in Ma-7. Table 3 details transect-wise data for all three micro watersheds. The higher species diversity and basal area in Ma-2 can be attributed to the fenced protection provided by the farmers residing in the region that has ensured the survival of saplings. Hills adjoining this transect without fencing were totally barren, filled with impenetrable thickets of *Lantana* shrubs.

The highest diversity was in Ma-2, which also has highest Shannon value of 2.6, Simpson diversity of 0.9 and dominance value of 0.09. The least diversity was in Ma-8 dominated by *Acacia catechu* with Shannon value of 0.63 and dominance of 0.73. *Acacia catechu* had the highest IVI of 61.19, followed by *Flacourtia indica* (28.51), *Mangifera indica,* (26.04), *Odina* (19.07), and *Anogeissus latifolia* (15.35) as listed in Table 4. Dominating deciduous trees in the region are *Acacia catechu*, *Flacourtia indica, Anogeissus latifolia* and *Odina wodiyer*.

Moolbari: Total number of species (15 species) and number of individuals (188) was high in Mo-15, which is *Rhododendron arboreum* and *Quercus* mixed forest. Mo-4 was species deficient (5 species) as these forests were dominated by *Quercus glauca*. Mo-1 had the highest basal area contributed mainly by *Quercus glauca* followed by *Quercus leuchotrichophora*. Mo-15 showed highest Pielou species richness value of 2.67, while it was lowest in Mo-4 with 0.92. Shannon diversity was highest in Mo-15 (1.72). This is due to the presence of several evergreen species such as *Persea, Euonymous, Myrica* sp etc., in the valleys. The higher slopes generally has *Quercus* species, mixed with *Rhododendron*. With dominance value of 0.73, Mo-11 showed the highest species dominance and had low Simpson value (0.34). This higher dominance is mainly due to *Quercus leucotrichophora*, which has 92 individuals and only 16 individuals of all other species.

The higher dominance of *Quercus leucotricophora* is reflected in the IVI value of 109.40, which is the highest for Moolbari water shed (Table 5). This is followed by *Quercus glauca* with 62.18. *Pinus roxburghii* is found extensively covering some of the slopes and has an IVI of 16.49. Mixed with these dominant species are species of *Acer oblongum* with IVI of 13.39, *Myrica esculenta* with 13.01. *Rhododendron arboreum* with IVI of 9.08 mostly occurred in Mo-15, which is relatively wetter compared to other transects. Other species such as *Cedrus deodara* with IVI of 8.01 occured in valleys and *Pyrus pashia* with 6.98 is scattered throughout the watershed.

MeGad: This micro watershed is relatively species poor. However, basal area was highest in Me-7 with 4.05 contributed by *Abies pindrow* and *Pinus wallichiana*. The lowest basal area was in Me-5 with 0.27, predominantly sub-alpine grasslands with scattered trees. The overall species diversity in MeGad was very low with Shannon diversity of 0.9 in Me-1, with only 4 species in entire transect. Me-5 is a alpine grassland and cultivated in some areas had only one species with lowest diversity.

Abies pindrow with 94.61 and *Pinus wallichiana* with 83.30 show a very high IVI value (Table 6). These are followed by *Picea smithiana* (58.58) and *Salix denticulate* (27.34).

Table 2. Woody species with habitats in all three micro watersheds

Sl	Species	Family	Habit
1	*Abies pindrow*	Pinaceae	Tree
2	*Acacia catechu*	Mimosaceae	Tree
3	*Acacia leucophloea*	Mimosaceae	Tree
4	*Acacia nilotica*	Mimosaceae	Tree
5	*Acer oblongum*	Aceraceae	Tree
6	*Adina cordifolia*	Rubiaceae	Tree
7	*Albizzia lebbeck*	Fabaceae	Tree
8	*Anogeissus latifolia*	Combretaceae	Tree
9	*Azadirchta indica*	Meliaceae	Tree
10	*Bambusa sp*	Poaceae	Shrub
11	*Bauhinia variegata*	Fabaceae	Tree
12	*Berberis aristata*	Berberidaceae	Tree
13	*Butea monosperma*	Fabaceae	Tree
14	*Carissa spinarium*	Apocynaceae	Shrub
15	*Cassia fistula*	Fabaceae	Tree
16	*Cassia sp*	Fabaceae	Tree
17	*Cedrus deodara*	Pinaceae	Tree
18	*Celtis australis*	Ulmaceae	Tree
19	*Cornus capitata*	Cornaceae	Tree
20	*Cupressus torulosa*	Cupressaceae	Tree
21	*Dalbergia sissoo*	Fabaceae	Tree
22	*Diospyrus montana*	Ebenaceae	Tree
23	*Dodonea viscosa*	Sapindaceae	Tree
24	*Eucalyptus sp*	Myrtaceae	Tree
25	*Euonymus hamiltoniaus*	Celastraceae	Tree
26	*Euonymus sp*	Celastraceae	Tree
27	*Euonymus tingens*	Celastraceae	Tree
28	*Euphorbia roylena*	Euphorbiaceae	Shrub
29	*Ficus nemoralis*	Moraceae	Tree
30	*Ficus pumila*	Moraceae	Tree
31	*Ficus racemosa*	Moraceae	Tree
32	*Ficus sp*	Moraceae	Tree
33	*Flacourtia indica*	Flacourtiaceae	Tree
34	*Grewia optiva*	Tiliaceae	Tree
35	*Grewia sp*	Tiliaceae	Tree
36	*Hamiltonia suaveolens*	Rubiaceae	Tree
37	*Holoptilia integrifolia*	Ulmaceae	Tree
38	*Ipomea carnea*	Convolvulaceae	Shrub
39	*Jasminum multiflora*	Oleaceae	Shrub
40	*Juglans regia*	Juglandaceae	Tree
41	*Juniperus macropoda*	Cupressaceae	Tree
42	*Lannea coromandelica*	Anacardiaceae	Tree
43	*Lantana camara*	Verbenaceae	Shrub
44	*Leucena leucocephala*	Fabaceae	Tree

45	*Lyonia ovalifolia*		Tree
46	*Malus baccata*	Rosaceae	Tree
47	*Mangifera indica*	Anacardiaceae	Tree
48	*Mitragyna parviflora*	Rubiaceae	Tree
49	*Morus nigra*	Moraceae	Tree
50	*Murraya koengii*	Rutaceae	Tree
51	*Myrica esculenta*	Myricaceae	Tree
52	*Nyctanthus arbor-tristis*	Nyctaginaceae	Tree
53	*Persea sp*	Lauraceae	Tree
54	*Phoenix sylvestris*	Arecaceae	Palm
55	*Picea smithiana*	Pinaceae	Tree
56	*Pinus roxbhurghii*	Pinaceae	Tree
57	*Pinus wallichiana*	Pinaceae	Tree
58	*Pistachia integrima*	Anacardiaceae	Tree
59	*Prunus cerasoides*	Rosaceae	Tree
60	*Punica granatum*	Rosaceae	Tree
61	*Pyrus pashia*	Rosaceae	Tree
62	*Quercus glauca*	Fagaceae	Tree
63	*Quercus leucotrichophora*	Fagaceae	Tree
64	*Randia sp*	Rubiaceae	Shrub
65	*Rhamnus sp*	Rhamnaceae	Shrub
66	*Rhododendron arboreum*	Ericaceae	Shrub
67	*Rubus ellipticus*	Rosaceae	Shrub
68	*Salix denticulate*	Salicaceae	Tree
69	*Syzygium cumini*	Myrtaceae	Tree
70	*Toona ciliate*	Meliaceae	Tree
71	*ui-species*		
72	*Vitis vinifera*	Vitaceae	Climber
73	*Woodfordia fruticosa*	Lythraceae	Shrub
74	*Zanthoxylum alatum*	Rutaceae	Shrub
75	*Zizypus mauritiana*	Rhamnaceae	Shrub

Table 3. Micro watershed wise Vegetation analysis

Watershed	Transect	Species	Individuals	Basal area (m^2)	Shannon's	sim-div	Pielou
Mandala	**Ma-1**	16	66	0.597	2.113	0.79	0.762
	Ma-2	21	77	1.242	2.655	0.901	0.872
	Ma-3	16	43	0.899	2.403	0.872	0.867
	Ma-4	13	29	0.406	2.240	0.861	0.873
	Ma-5	5	9	0.538	1.465	0.741	0.910
	Ma-6	12	84	0.569	1.454	0.572	0.585
	Ma-7	5	11	0.071	1.160	0.562	0.720
	Ma-8	6	76	0.432	0.637	0.264	0.356
	Ma-9	3	27	0.553	0.727	0.412	0.662
	Ma-10	6	9	0.261	1.677	0.790	0.936
	Ma-11	8	16	0.210	1.890	0.820	0.909
Moolbari	**Mo-1**	10	158	3.471	1.564	0.707	0.679
	Mo-2	11	129	3.137	1.428	0.658	0.595
	Mo-3	7	89	3.059	1.095	0.593	0.563
	Mo-4	5	75	2.198	0.694	0.354	0.431
	Mo-5	9	85	2.388	1.256	0.563	0.572
	Mo-6	6	83	2.335	1.057	0.577	0.590
	Mo-7	6	101	2.407	1.107	0.552	0.618
	Mo-8	6	66	2.509	1.325	0.652	0.740
	Mo-9	11	64	1.668	1.330	0.563	0.555
	Mo-10	8	79	1.458	1.454	0.682	0.699
	Mo-11	6	108	1.131	0.626	0.268	0.349
	Mo-12	8	62	1.351	1.298	0.621	0.624
	Mo-13	12	131	3.235	1.002	0.405	0.403
	Mo-14	13	102	2.695	1.480	0.631	0.577
	Mo-15	15	188	2.893	1.727	0.759	0.638
	Mo-16	7	58	0.730	1.301	0.626	0.669
MeGad	**Me-1**	4	39	2.050	0.908	0.523	0.655
	Me-2	3	31	2.361	0.923	0.564	0.840
	Me-3	3	31	3.507	0.668	0.398	0.608
	Me-4	3	18	1.995	0.426	0.204	0.388
	Me-5	1	1	0.207	0	0	0
	Me-6	3	22	2.520	0.937	0.558	0.853
	Me-7	2	30	4.056	0.637	0.444	0.918
All	Mandhala	446	43	6.664	2.688	0.842	0.706
	Moolbari	1649	39	39.94	1.805	0.695	0.493
	MeGad	177	9	16.70	1.428	0.720	0.650

Discussion

Mandhala, Moolbari, and Me Gad micro watersheds had a total of 2276 individuals from 75 woody species from 34 belt transects. A total of 38 families were recorded, of which Fabaceae had the highest number of species (7), followed by Rosaceae, Pinaceae and Moraceae (5 each). The highest number of individuals per species was *Quercus leucotriphora* with 811 individuals followed by *Q.glauca* (394),

Acacia catechu (157), *Myrica esculenta* (73), *Pinus roxbhurghii* (72), *Abies pindrow* (70) and *Flacourtia indica* (68).

Species richness was highest in Mandhala (45 species) followed by Moolbari (39) and MeGad (9). Although Mandala had the highest species diversity, it had lowest dominance. Most of the species are thorny shrubs and rarely attain tree forms due to severe anthropogenic disturbances in this watershed, hence very low basal area is observed compared to number of other species. In Moolbari, which had the highest basal area (39.94) was mainly contributed by *Quercus leucotricophora* and *Q. glauca*. In Mandhala, the negligible basal area found was due to absence of large trees as in Moolbari or MeGad, due to the earlier deforestation and extensive encroachment of forestland by obnoxious weed *Lantana camara*. This shrub has totally covered the lower slopes in Mandhala making it an unsuitable habitat for wildlife as well as domesticated animals. Also regeneration of forest plant species has totally ceased due to the permanent cover created by this bush.

Overall *Quercus* species dominated in the Moolbari watershed area, while deciduous species such as *Acacia catechu, Flacourtia indica* dominated in Mandala watershed. MeGad, a high altitude area was dominated by *Abies pindrow, Picea smithiana,* and *Pinus wallichiana*, which is reflected in the IVI values (Table 4, 5, and 6).

Table 4: IVI for woody species in Mandhala watershed.

Sl	Species	IVI
1	*Acacia catechu*	61.19
2	*Flacourtia indica*	28.51
3	*Mangifera indica*	26.04
4	*Lannea coromandelica*	19.07
5	*Anogeissus latifolia*	15.35
6	*Dalbergia sissoo*	9.45
7	*Mitragyna parviflora*	9.39
8	*Grewia optiva*	8.58
9	*Cassia fistula*	7.99
10	*Woodfordia fruticosa*	7.88
11	*Azadirachta indica*	7.42
12	*Eucalyptus*	7.18
13	*Butea monosperma*	6.28
14	*Dodonea viscosa*	6.24
15	*Murraya koenigii*	4.96
16	*Carissa spinarium*	4.78
17	*Syzgium cumini*	4.74
18	*Phoenix sylvestris*	4.73
19	*Adina cordifolia*	4.68
20	*Species 1*	4.54
21	*Acacia nilotica*	3.84
22	*Ficus racemosa*	3.72
23	*Pinus roxbhurghii*	3.50
24	*Randia sp*	2.99
25	*Acacia leucophloea*	2.97
26	*Zanthoxylum alatum*	2.81
27	*Holoptilia integrifolia*	2.64
28	*Morus nigra*	2.54

29	*Albizzia lebbeck*	2.51
30	*Bambusa sp*	2.14
31	*Species 4*	2.09
32	*Species 2*	2.09
33	*Leucena leucocephala*	1.92
34	*Diospyros montana*	1.71
35	*Jasminum multiflora*	1.64
36	*Pyrus pashia*	1.44
37	*Hamiltonia suveolens*	1.42
38	*Zizypus mauritiana*	1.42
39	*Punica granatum*	1.41
40	*Species 5*	1.27
41	*Nyctanthus arbor-tristis*	1.18
42	*Ipomea carnea*	1.18
43	*Lantana camara*	1.16

Table 5: IVI of Woody species from Moolbari watersheds

Sl	**Species**	**IVI**
1	*Quercus leucotricophora*	109.40
2	*Quercus glauca*	62.18
3	*Pinus roxburghii*	16.49
4	*Acer oblongum*	13.39
5	*Myrica esculenta*	13.01
6	*Rhododendron arboreum*	9.08
7	*Cedrus deodara*	8.01
8	*Pyrus pashia*	6.98
9	*Grewia sp*	6.04
10	*Pistachia integrima*	5.74
11	*Lyonia ovalifolia*	5.32
12	*Species A*	4.57
13	*Euonymus tingens*	3.51
14	*Punica granatum*	3.23
15	*Euphorbia roylena*	2.72
16	*Species 1*	2.53
17	*Ficus nemoralis*	2.02
18	*Berberis aristata*	1.78
19	*Euonymus hamiltoniaus*	1.78
20	*Bauhinia variegate*	1.74
21	*Prunus cerasoides*	1.73
22	*Celtis australis*	1.69
23	*Persea sp*	1.65
24	*Grewia optiva*	1.59
25	*Cupressus torulosa*	1.29
26	*Euonymus sp*	1.17
27	*Tiliaceae*	1.17
28	*Toona ciliata*	1.12
29	*Species C*	0.89
30	*X sp*	0.87
31	*Hypericum*	0.86

32	*Ficus pumila*	0.85
33	*Species D*	0.83
34	*B sp*	0.82
35	*Ficus sp*	0.80
36	*Cornus capitata*	0.79
37	*Vitis vinifera*	0.79
38	*Rhamnus sp*	0.79
39	*Rubus ellipticus*	0.78

Table 6: IVI of Woody species in MeGad watershed.

Sl	Species	IVI
1	*Abies pindrow*	94.61
2	*Pinus wallichiana*	83.30
3	*Picea smithiana*	58.58
4	*Salix denticulate*	27.34
5	*Juglans regia*	9.70
6	*Malus baccata*	7.72
7	*ui-Krown*	7.07
8	*Cassia sp*	5.85
9	*Juniperus macropoda*	5.83

Faunal diversity

Butterfly

The present study enumerated 115 butterfly species of oriental and palaearctic origin representing nine families. Nympahlidae is the dominant family (32 sp.) followed by Pieridae (19 sp.), Lycaenidae (16 sp.), Satyridae and Papilionidae (12 sp. each), Hesperridae (10 sp.), Danaidae (8 sp.), Erycidae (4 sp.) and Acraeidae (2 sp.). Table 7, 8, 9 and 10 details the list of butterflies in the three micro watersheds.

- The family Papilionidae is commonly known as Swallowtail family, comprising some of the larger butterflies. In the study area, this family representing two sub-families viz., Parnasiinae (Apollos) and Papilioninae. Three species of apollos namely *Parnassius hardwickii hardwickii* (Common Blue Apollo) in Moolbari watershed and *Parnassius delphius* (Banded Apollo) and *Parnassius charltonius* (Regal Apollo) in the open grassy and rocky areas of Megad watershed were seen. The sub-family Papilioninae represented by *Papilio protenor protenor* (Spangle) and *Chilasa agestor* (Tawny Mime).
- The Family Pieridae commonly known as Whites or Yellows seen in MeGad watershed are *Pieris brassicae nepalensis* (Large Cabbage White), *Aporia nabellica* (Dusky Blackvein), *Pontia daplidice moorei* (Bath White) and *Colias* sp. (Clouded yellows).

- More species of the family Satyridae and Nymphalidae were recorded during the survey. *Nymphalis* (*Aglais*) *kashmirensis* (Common Tortoiseshell), *Nymphalis* (*Aglais*) *ladakensis* (Ladakh Tortoiseshell), *Vanessa indica* (Red Admiral), *Kaniska canace canace* (Blue Admiral), *Aulocera* sp. (Satyrs), *Callerebia* sp. (Arguses) and *Melitaea arceisa* (Blackvein Fritillary) were recorded in Moolbari and Megad watersheds.
- Family Erycinidae is commonly known as family of Beaks, Punches and Judies, which are represented by *Dodona durga* (Common Punch), *Lybithea* sp. (Beaks) in Moolbari and *Abisara echerius suffusa* (Plum Judy) in Mandhala watershed.
- Lycaenidae is commnly known as family of Blues are represented by *Heliophorus sena* (Sorrel Sapphire), *Tajuria cippus* (Peacock Royal) and *Chrysozephyrus* sp. (Hairstreak) in Moolbari

watershed and *Lycaena kasyapa* (Green Copper) and *Polyommatus stoliczkanus janetae* (Common Meadow Blue) in Megad watershed.

Table 7: Butterfly species in Moolbari Watershed (Shimla Dist.)

Sl. No.	Family	Common Name	Species
1	Papilionidae	Common Blue Apollo	*Parnassius hardwickii hardwickii* (Gray 1831)
2	Papilionidae	Common Peacock	*Papilio polyctor polyctor* (Boisduval 1836)
3	Papilionidae	Common Mormon	*Papilio polytes romulus* (L., 1758)
4	Papilionidae	Common Lime	*Papilio demoleus* (L., 1758)
5	Papilionidae	Spangle	*Papilio protenor protenor* (Cramer 1775)
6	Papilionidae	Common Bluebottle	*Graphium serpedon* (L., 1758)
7	Papilionidae	Common Mime	*Chilasa clytia clytia* (L., 1758)
8	Papilionidae	Tawny Mime	*Chilasa agestor* (Gray 1831)
9	Pieridae	Spot Puffin	*Appias lalage* (Doubleday 1842)
10	Pieridae	Striped Albatross	*Appias libythea* (Fabricius 1775)
11	Pieridae	Common Gull	*Cepora nerissa phryne* (Fabricius 1775)
12	Pieridae	Common Emigrant	*Catopsilia pomona* (Fabricius 1775)
13	Pieridae	Mottled Emigrant	*Catopsilia pyranthe pyranthe* (L., 1758)
14	Pieridae	Small Grass Yellow	*Eurema brigitta rubella* (Wallace 1867)
15	Pieridae	Spotless Grass Yellow	*Eurema laeta laeta* (Boisduval 1836)
16	Pieridae	Common Grass Yellow	*Eurema hecabe* (L., 1758)
17	Pieridae	White Orange Tip	*Ixias marianne* (Cramer 1779)
18	Pieridae	Yellow Orange Tip	*Ixias pyrene* (L., 1764)
19	Pieridae	Indian Cabbage White	*Pieris canidia* (Sparrman) *indica* (Evans 1926)
20	Danaidae	Plain Tiger	*Danaus chrysippus* (L., 1758)
21	Danaidae	Common Tiger	*Danaus genutia* (Cramer 1779)
22	Danaidae	Common Indian Crow	*Euploea core core* (Cramer 1780)
23	Danaidae	Striped Blue Crow	*Euploea mulciber mulciber* (Cramer 1777)
24	Danaidae	Chestnut Tiger	*Parantica sita sita* (Kollar 1844)
25	Danaidae	Blue Tiger	*Tirumala limniace* (Cramer 1775)
26	Danaidae	Dark Blue Tiger	*Tirumala septentrionis* (Butler 1874)
27	Satyridae	Lilacine Bushbrown	*Mycalesis francisca sanatana* (Moore 1857)
28	Satyridae	Dark-brand Bushbrown	*Mycalesis mineus mineus* (L., 1758)
29	Satyridae	Common Three ring	*Ypthima asterope* (Moore 1886)
30	Satyridae	Large Three ring	*Ypthima nareda nareda* (Kollar 1844)
31	Nymphalidae	Indian Tortoiseshell	*Nymphalis* (*Aglais*) kashmirensis (Kollar 1844)
32	Nymphalidae	Ladakh Tortoiseshell	*Nymphalis* (*Aglais*) ladakensis (Moore1878)
33	Nymphalidae	Indian Fritillary	*Argyreus hyperbius hyperbius* (L., 1765)
34	Nymphalidae	Common Castor	*Ariadne merione* (Cramer 1777)
35	Nymphalidae	Himalayan Sergeant	*Athyma opalina* (Kollar 1844)
36	Nymphalidae	Common Sergeant	*Athyma perius* (L., 1758)
37	Nymphalidae	Studded Sergeant	*Athyma asura* (Moore 1858)
38	Nymphalidae	Indian Purple	*Mimathyma ambica ambica* (Kollar 1844)

		Emperor	
39	Nymphalidae	Common Map	*Cyrestis thyodamas thyodamas* (Boisduval 1836)
40	Nymphalidae	Common Siren	*Hestina persimilis* (Westwood 1850)
41	Nymphalidae	Gaudy Baron	*Euthalia lubentina* (Cramer 1777)
42	Nymphalidae	Great Eggfly	*Hypolimnas bolina* (L., 1758)
43	Nymphalidae	Danaid Eggfly	*Hypolimnas misippus* (Linn.)
44	Nymphalidae	Chacolate Pansy	*Junonia iphita* (Cramer 1779)
45	Nymphalidae	Yellow Pansy	*Junonia hierta* (Fabricius 1798)
46	Nymphalidae	Blue Pansy	*Junonia orithya* (L., 1758)
47	Nymphalidae	Lemon Pansy	*Junonia lemonias persicaria* (Fruhstorfer)
48	Nymphalidae	Peacock Pansy	*Junonia almana* (L., 1758)
49	Nymphalidae	Orange Oakleaf	*Kallima inachus* (Boisduval 1846)
50	Nymphalidae	Blue Admiral	*Kaniska canace canace* (L., 1763)
51	Nymphalidae	Common Sailer	*Neptis hylas* (L., 1758)
52	Nymphalidae	Common Leopard	*Phalanta phalanta* (Drury 1773)
53	Nymphalidae	Common Nawab	*Polyura athamas athama* (Drury 1773)
54	Nymphalidae	Painted Lady	*Vanessa cardui* (L., 1758)
55	Nymphalidae	Indian Red Admiral	*Vanessa indica* (Herbst 1794)
56	Acraeidae	Tawny Coster	*Acraea terpsicore* (L., 1758)
57	Acraeidae	Yellow Coster	*Acraea issoria* (Hubner 1819)
58	Erycinidae	Common Punch	*Dodona durga* (Kollar, 1844)
59	Erycinidae	Common Beak	*Lybythea celtis lepita* (Moore 1858)
60	Erycinidae	Club Beak	*Lybithea myrrha* (Godart 1819)
61	Lycaenidae	Common Copper	*Lycaena phlaeas* (L., 1761)
62	Lycaenidae	Brown Argus	*Aricia agestis nazira* (Moore 1865)
63	Lycaenidae	Common Pierrot	*Castalius rosimon* (Fabricius 1775)
64	Lycaenidae	Hairstreak	*Chrysozephyrus* sp.
65	Lycaenidae	Sorrel Sapphire	*Heliophorus sena* (Kollar 1844)
66	Lycaenidae	Pale Grass Blue	*Pseudozizeeria maha* (Kollar 1844)
67	Lycaenidae	Peacock Royal	*Tajuria cippus* (Fabricius 1798)
68	Lycaenidae	Tiny Grass Blue	*Zizula hylax* (Fabracius 1775)
69	Hesperiidae	Rice Swift	*Borbo cinnara* (Wallace 1866)
70	Hesperiidae	Tricolour Pied Flat	*Coladenia indrani indrani* (Moore 1865)
71	Hesperiidae	Large Branded Swift	*Pelopidas sinensis* (Mabille 1877)
72	Hesperiidae	Small Branded Swift	*Pelopidas mathias mathais* (Fabricius 1798)
73	Hesperiidae	Yellow-spot Swift	*Polytremis eltola* (Hewitson 1869)
74	Hesperiidae	Indian Skipper	*Spialia galba* (Fabricius 1793)
75	Hesperiidae	Indian Palm Bob	*Suastus gremius* (Fabricius 1798)
76	Hesperiidae	Dark Palm Dart	*Telicota pythias* (Mabille)
77	Hesperiidae	Grass Demon	*Udaspes folus* (Cramer 1775)

Table 8: Butterfly species in Mandhala watershed (Solan District)

Sl. No.	Family	Common Name	Species
2	Papilionidae	Common Peacock	*Papilio polyctor polyctor* (Boisduval 1836)
3	Papilionidae	Common Mormon	*Papilio polytes romulus* (L., 1758)
1	Papilionidae	Common Lime	*Papilio demoleus* (L., 1758)
4	Papilionidae	Tailed Jay	*Graphium agamemnon* (L., 1758)
5	Papilionidae	Common Jay	*Graphium doson* (C & R Felder 1864)
6	Pieridae	Common Gull	*Cepora nerissa phryne* (Fabricius 1775)
7	Pieridae	Common Emigrant	*Catopsilia pomona* (Fabricius 1775)
8	Pieridae	Common Jezebel	*Delias eucharis* (Drury 1773)
9	Pieridae	Small Grass Yellow	*Eurema brigitta rubella* (Wallace 1867)
10	Pieridae	Common Grass Yellow	*Eurema hecabe* (L., 1758)
11	Pieridae	Yellow Orange Tip	*Ixias pyrene* (L., 1764)
12	Pieridae	Common Wanderer	*Pareronia valeria* (Cramer 1776)
13	Pieridae	Indian Cabbage White	*Pieris canidia* (Sparrman) *indica* (Evans 1926)
14	Danaidae	Plain Tiger	*Danaus chrysippus* (L., 1758)
15	Danaidae	Common Tiger	*Danaus genutia* (Cramer 1779)
16	Danaidae	Common Indian Crow	*Euploea core core* (Cramer 1780)
17	Danaidae	Glassy Tiger	*Parantica aglea* (Stoll 1782)
18	Danaidae	Blue Tiger	*Tirumala limniace* (Cramer 1775)
19	Danaidae	Dark Blue Tiger	*Tirumala septentrionis* (Butler 1874)
20	Satyridae	Common Evening Brown	*Melanitis leda leda* (Fabricius 1775)
21	Satyridae	Common Bushbrown	*Mycalesis perseus* (Fabricius 1775)
22	Satyridae	Nigger	*Orsotriaena medus* (Fabricius 1775)
23	Satyridae	Common Three ring	*Ypthima asterope* (Moore 1886)
24	Satyridae	Common Five ring	*Ypthima baldus baldus* (Fabricius 1775)
25	Nymphalidae	Indian Fritillary	*Argyreus hyperbius hyperbius* (L., 1765)
26	Nymphalidae	Common Castor	*Ariadne merione* (Cramer 1777)
27	Nymphalidae	Common Sergeant	*Athyma perius* (L., 1758)
28	Nymphalidae	Common Baron	*Euthalia aconthea garuda* (Cramer 1777)
29	Nymphalidae	Great Eggfly	*Hypolimnas bolina* (L., 1758)
30	Nymphalidae	Danaid Eggfly	*Hypolimnas misippus* (Linn.)
31	Nymphalidae	Commander	*Limenitis procris* (Cramer 1777)
32	Nymphalidae	Chacolate Pansy	*Junonia iphita* (Cramer 1779)
33	Nymphalidae	Yellow Pansy	*Junonia hierta* (Fabricius 1798)
34	Nymphalidae	Blue Pansy	*Junonia orithya* (L., 1758)
35	Nymphalidae	Lemon Pansy	*Junonia lemonias persicaria* (Fruhstorfer)
36	Nymphalidae	Peacock Pansy	*Junonia almana* (L., 1758)
37	Nymphalidae	Grey Pansy	*Junonia atlites* (L., 1763)
38	Nymphalidae	Common Sailer	*Neptis hylas* (L., 1758)
39	Nymphalidae	Common Leopard	*Phalanta phalanta* (Drury 1773)
40	Nymphalidae	Painted Lady	*Vanessa cardui* (L., 1758)
41	Acraeidae	Tawny Coster	*Acraea terpsicore* (L., 1758)
42	Erycinidae	Plum Judy	*Abisara echerius suffusa* (Moore 1882)
43	Lycaenidae	Common Pierrot	*Castalius rosimon* (Fabricius 1775)

44	Lycaenidae	Gram Blue	*Euchrysops cnejus* (Fabricius 1798)
45	Lycaenidae	Common Cerulean	*Jamides celeno* (Cramer 1775)
46	Lycaenidae	Pale Grass Blue	*Pseudozizeeria maha* (Kollar 1844)
47	Hesperiidae	Common Small Flat	*Sarangesa dasahara dasahara* (Moore 1865)
48	Hesperiidae	Grass Demon	*Udaspes folus* (Cramer 1775)

Table 9: Butterfly species in Megad watershed (Lahul and Spiti District)

Sl. No.	Family	Common Name	Species
1	Papilionidae	Banded Apollo	*Parnassius delphius* (Eversmann 1843)
2	Papilionidae	Regal Apollo	*Parnassius charltonius* (Gray 1852)
3	Pieridae	Indian Cabbage White	*Pieris canidia* (Sparrman) *indica* (Evans 1926)
4	Pieridae	Large Cabbage White	*Pieris brassicae nepalensis* (Doubleday)
5	Pieridae	Dusky Blackvein	*Aporia nabellica* (Boisduval 1838)
6	Pieridae	Butler,s Dwarf	*Baltia butleri* (Moore 1882)
7	Pieridae	Fiery Clouded Yellow	*Colias eogene eogene* (Felder 1865)
8	Pieridae	Dark Clouded Yellow	*Colias fieldii* (Menetries 1855)
9	Pieridae	Bath White	*Pontia daplidice moorei* (Rober)
10	Satyridae	Doherty's Satyr	*Aulocera loha* (Doherty 1886)
11	Satyridae	Common Satyr	*Aulocera swaha swaha* (Kollar 1844)
12	Satyridae	Ringed Argus	*Callerebia annada* (Moore 1858)
13	Satyridae	Mountain Argus	*Callerebia shallada* (Lang 1880)
14	Nymphalidae	Ladakh tortoiseshell	*Nymphalis* (*Aglais*) ladakensis (Moore1878)
15	Nymphalidae	Large Silverstripe or Himalayan Fritillary	*Childrena childreni* (Gray 1861)
16	Nymphalidae	Common Map	*Cyrestis thyodamas thyodamas* (Boisduval 1836)
17	Nymphalidae	Siren	*Hestina* sp.
18	Nymphalidae	Blackvein Fritillary	*Melitaea arceisa* (Bremer 1861)
19	Nymphalidae	Sailer	*Neptis* sp.
20	Nymphalidae	Indian Red Admiral	*Vanessa indica* (Herbst 1794)
21	Lycaenidae	Green Copper	*Lycaena kasyapa* (Moore 1865)
22	Lycaenidae	Plains Cupid	*Chilades pandava pandava* (Horsfield 1829)
23	Lycaenidae	Common Meadow Blue	*Polyommatus stoliczkanus janetae* (Evans 1927)
24	Lycaenidae	Hairstreak	*Thecla* sp.
25	Lycaenidae	UI*	-
26	Lycaenidae	UI*	-

Note: *– refers to unidentified species.

Table 10: Butterfly species from Three watersheds of Himachal Pradesh.

Sl. No.	Family	Species	Moolbari	Mandhala	Megad
1	Papilionidae	*Parnassius hardwickii hardwickii*	+		
2		*Parnassius delphius*			+
3		*Parnassius charltonius*			+
4		*Papilio polyctor polyctor*	+	+	
5		*Papilio polytes romulus*	+	+	
6		*Papilio demoleus*	+	+	
7		*Papilio protenor protenor*	+		
8		*Graphium serpedon*	+		
9		*Graphium agamemnon*		+	
10		*Graphium doson*		+	
11		*Chilasa clytia clytia*	+		
12		*Chilasa agestor*	+		
13	Pieridae	*Appias lalage*	+		
14		*Appias libythea*	+		
15		*Cepora nerissa phryne*	+	+	
16		*Catopsilia pomona*	+	+	
17		*Catopsilia pyranthe pyranthe*	+		
18		*Eurema brigitta rubella*	+	+	
19		*Eurema laeta laeta*	+		
20		*Eurema hecabe*	+	+	
21		*Ixias marianne*	+		
22		*Ixias pyrene*	+	+	
23		*Pieris canidia indica*	+	+	+
24		*Pieris brassicae nepalensis*			+
25		*Delias eucharis*		+	
26		*Pareronia valeria*		+	
27		*Aporia nabellica*			+
28		*Baltia butleri*			+
29		*Colias eogene eogene*			+
30		*Colias fieldii*			+
31		*Pontia daplidice moorei*			+
32	Danaidae	*Danaus chrysippus*	+	+	
33		*Danaus genutia*	+	+	
34		*Euploea core core*	+	+	
35		*Euploea mulciber mulciber*	+		
36		*Parantica sita sita*	+		
37		*Tirumala limniace*	+	+	
38		*Tirumala septentrionis*	+	+	
39		*Parantica aglea*		+	
40	Satyridae	*Mycalesis francisca sanatana*	+		
41		*Mycalesis mineus mineus*	+		
42		*Mycalesis perseus*		+	
43		*Ypthima asterope*	+	+	
44		*Ypthima nareda nareda*	+		
45		*Ypthima baldus baldus*		+	
46		*Melanitis leda leda*		+	

47		*Orsotriaena medus*		+	
48		*Aulocera loha*			+
49		*Aulocera swaha swaha*			+
50		*Callerebia annada*			+
51		*Callerebia shallada*			+
52	Nymphalidae	*Nymphalis* (*Aglais*) kashmirensis	+		
53		*Nymphalis* (*Aglais*) ladakensis	+		+
54		*Argyreus hyperbius hyperbius*	+	+	
55		*Ariadne merione*	+	+	
56		*Athyma opalina*	+		
57		*Athyma perius*	+	+	
58		*Athyma asura*	+		
59		*Mimathyma ambica ambica*	+		
60		*Cyrestis thyodamas thyodamas*	+		+
61		*Hestina persimilis*	+		
62		*Hestina* sp.			+
63		*Euthalia lubentina*	+		
64		*Euthalia aconthea garuda*		+	
65		*Hypolimnas bolina*	+	+	
66		*Hypolimnas misippus*	+	+	
67		*Junonia iphita*	+	+	
68		*Junonia hierta*	+	+	
69		*Junonia orithya*	+	+	
70		*Junonia lemonias persicaria*	+	+	
71		*Junonia almana*	+	+	
72		*Junonia atilites*		+	
73		*Kallima inachus*	+		
74		*Kaniska canace canace*	+		
75		*Neptis hylas*	+	+	
76		*Neptis* sp.			+
77		*Phalanta phalanta*	+	+	
78		*Polyura athamas athama*	+		
79		*Vanessa cardui*	+	+	
80		*Vanessa indica*	+		+
81		*Limenitis procris*		+	
82		*Childrena childreni*			+
83		*Melitaea arceisa*			+
84	Acraeidae	*Acraea terpsicore*	+	+	
85		*Acraea issoria*	+		
86	Erycinidae	*Dodona durga*	+		
87		*Lybythea celtis lepita*	+		
88		*Lybithea myrrha*	+		
89		*Abisara echerius suffusa*		+	
90	Lycaenidae	*Lycaena phlaeas*	+		
91		*Lycaena kasyapa*			+
92		*Aricia agestis nazira*	+		
93		*Castalius rosimon*	+	+	
94		*Chrysozephyrus* sp.	+		
95		*Heliophorus sena*	+		

96		*Pseudozizeeria maha*	+	+		
97		*Tajuria cippus*	+			
98		*Zizula hylax*	+			
99		*Euchrysops cnejus*		+		
100		*Jamides celeno*		+		
101		*Chilades pandava pandava*				+
102		UI				+
103		UI				+
104		*Polyommatus stoliczkanus janetae*				+
105		*Thecla* sp.				+
106	Hesperiidae	*Borbo cinnara*	+			
107		*Coladenia indrani indrani*	+			
108		*Pelopidas sinensis*	+			
109		*Pelopidas mathias mathais*	+			
110		*Polytremis eltola*	+			
111		*Spialia galba*	+			
112		*Suastus gremius*	+			
113		*Telicota pythias*	+			
114		*Sarangesa dasahara dasahara*		+		
115		*Udaspes folus*	+	+		

Amphibians

Diversity: In the present study, 14 species were observed belonging to 5 families and diversity is listed in Table 10. Of the 5 families, Dicroglossidae represents 7 species, followed by Bufonidae (4) and Microhylidae, Ranidae and Rhacophoridae (1 species each). Six species are first reported from this study.

Distribution: Table 11 details the relative abundance from three watersheds. Figure 1 depicts few amphibians recorded during this study. Mandhala watershed located in the Shivaliks is bestowed with numerous ponds, pools, streams and rivers. Most of the streams and river drain off the rainwater as soon as it rains, without any water retaining in the streams. Only ponds and pools retain water for considerable time and could be one of the reasons that majority of the amphibians observed from the regions are pool breeders dominated by *Euphlyctis cyanophlyctis*, *Microhyla ornata*, *Fejervarya* sp. and *Polypedates maculates*. *Sphaerotheca breviceps*, a burrowing frog was observed in the dry beds of river. *Euphlyctis cyanophlyctis* was found in both streams as well as in pools. Moolbari watershed belongs to the mid Himalayan ranges and many streams originate forming a network. As it has higher elevation and more streams, frogs that breed in streams predominate the region. *Paa minica* was observed in almost all streams with water, and having canopy cover. In agriculture fields and forested areas, *Bufo himalayanus* and *Duttaphrynus melanostictus* were recorded. Altitude and extreme temperature in MeGad watershed appears inhospitable to amphibians as it is evident from their absence while recordings during this fieldwork.

Table 11. Amphibian diversity in the three micro watersheds of Himachal Pradesh.

Species#	**Mandhala**	**Moolbari**	**Megad**	**IUCN status**
Bufonidae				
Bufo himalayanus	0	1	0	Least concern
Bufo sp.	1	1	0	
*Bufo stomaticus**	1	1	0	Least concern

Duttaphrynus melanosticuts	1	1	0	Least concern
Microhylidae				
Microhyla ornate	1	0	0	Least concern
Dicroglossidae				
Euphlyctis cyanophlyctis	1	0	0	Least concern
*Fejervarya limnocharis**	0	1	0	Least concern
Fejervarya sp.	1	0	0	Least concern
Hoplobatrachus crassus	1	0	0	Least concern
*Hoplobatrachus tigerinus**	1	0	0	Least concern
Paa minica	1	1	0	Vulnerable
Sphaerotheca breviceps	1	0	0	Least concern
Ranidae				
Amolops chakrataensis	0	1	0	Data deficient
Rhacophoridae				
Polypedates maculates	1	0	0	Least concern
Species richness	10	6	0	

Nomenclature based on Frost et al (2006)
* Observation by Zoological Survey of India.

Table 12. Relative abundance (individuals/hour of search) of amphibians recorded during the study.

Species	Mandhala	Moolbari	MeGad
Bufonidae			
Bufo himalayanus	0	1	0
Bufo sp.	15		
Duttaphrynus melanosticuts	1	10	0
Microhylidae			
Microhyla ornate	2	0	0
Dicroglossidae			
Euphlyctis cyanophlyctis	39	0	0
Fejervarya rufescens	5	0	0
Hoplobatrachus crassus	2	0	0
Paa minica	1	8	0
Sphaerotheca breviceps	2	0	0
Ranidae			
Amolops chakrataensis	0	1	0
Rhacophoridae			
Polypedates maculates	4	0	0
Shannon's index	1.43	1.01	0
Simpson's index	2.8	2.41	0

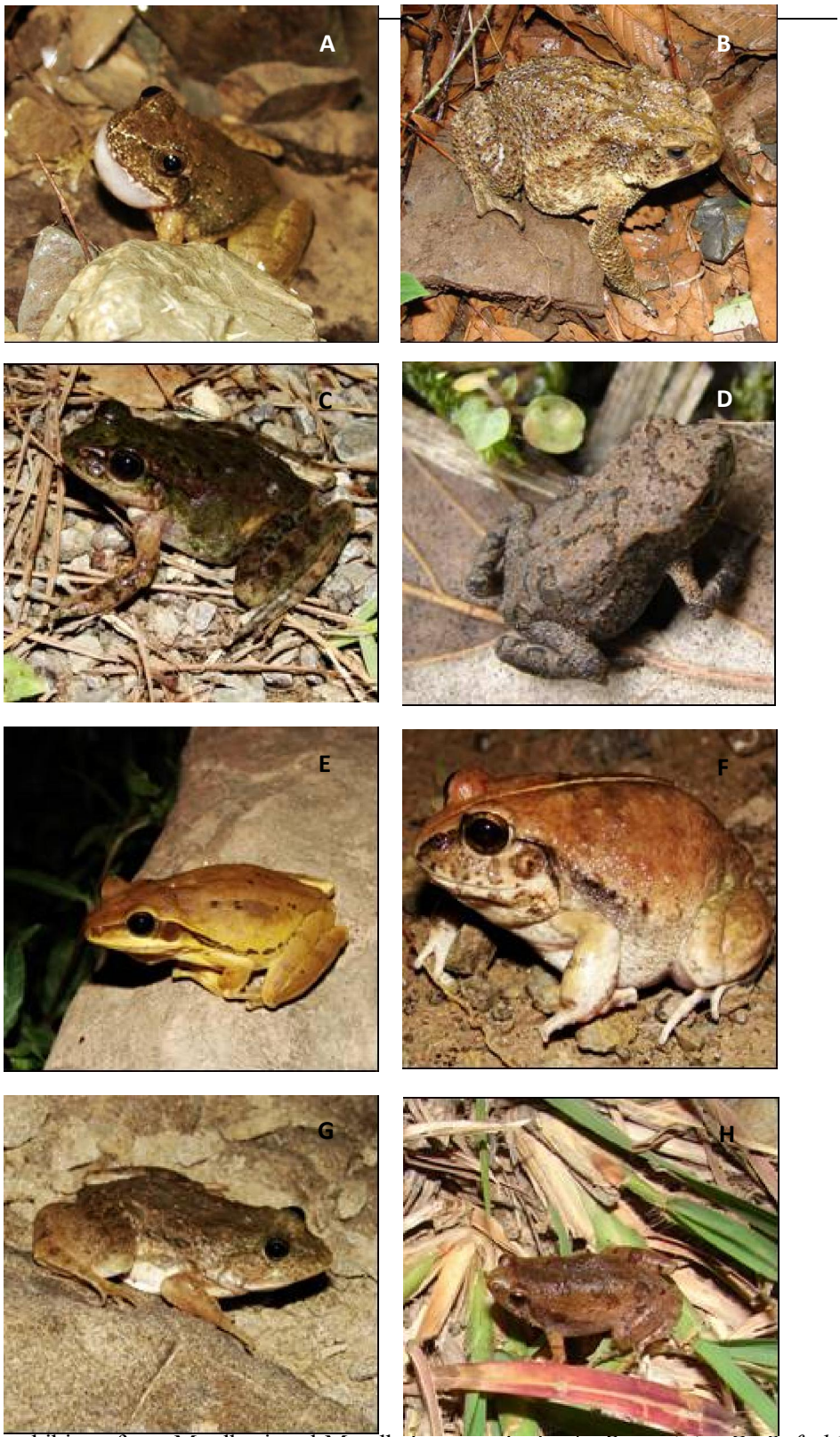

Figure 1. Amphibians from Moolbari and Mandhala watersheds. A. *Paa minica* B. *Bufo himalayanus* C. *Amolops chakrataensis* D. *Bufo sp.* E. *Polypedates maculates* F. *Sphaerotheca breviceps* G. *Euphlyctis cyanophlyctis* H. *Microhyla ornata*

Avifaunal Diversity and Richness

Sampling was done in different habitat types: forests, glacier, agriculture and forests, riverine, and agriculture. Habitatwise speces richness is given in Table 13, 14 and 15 for Moolbari, MeGad and Mandhala watersheds respectively. In total, 136 bird species were recorded in three watersheds. Mandhala watershed records highest number of species (105) followed by Moolbari (57) and Megad (35).

Table 16 lists 8 species of birds common to all three watersheds, in an altitude of 400 to 4000 m. Table 17 provides the list of 31 species common to Mandhala and Moolbari watershed, in the altitudanal range of 400 to 2000 m. Table 18 lists nine species common to Moolbari and MeGad Watersheds. The distribution of bird species in the three watersheds is summarised in Table 19.

The habitat wise study revealed that bird species richness is more in forest patches of Mandhala and MeGad Watersheds, whereas, forest and agriculture mixed habitats in Moolbari had more species.

Table 13: Habitat wise bird species richness in Moolbari watershed

Habitat	Number of Species
Forest	25
Forest and Agriculture	33
Riverine	35
Agriculture	21

Table 14: Habitat wise bird species richness in MeGad watershed

Habitat type	Number of species
Forest	29
Glacier	11
Village and Agriculture	23

Table 15: Habitat wise bird species richness in Mandhala watershed

Habitat	Number of Species
Forest	65
Agriculture	47
Riverine	43
Agriculture and Forestry	42

Table 16: Bird species in all three watersheds

1	*Parus Xanthogenys*	Black lored tit
2	*Phylloscopus fuscatus*	Dusky warbler
3	*Parus major*	Great tit
4	*corvus splendens*	house crow
5	*Passer domesticus*	house sparrow
6	*Corvvus macrorhynchos*	Jungle crow
7	*Streptopelia orientalis*	Oriental turtle dove
8	*columba livia*	rock pigeon

Table 17: Bird species common to Mandhala and Moolbari watersheds

Sl. No	Scientific Name	Common name
1	*Terpsiphone paradisi*	Asian Paradise Flycatcher
2	*hypsipetes leucocephalus*	Black Bulbul
3	*Ictinaetus malayensis*	Black Eagle
4	*Parus Xanthogenys*	Black Lored Tit
5	*Acridotheres tristis*	Common Myna
6	*Phylloscopus fuscatus*	Dusky Warbler
7	*Streptopelia decaocto*	Eurasian Collared Dove
8	*Parus major*	Great Tit
9	*Merops orientalis*	Green Bee Eater
10	*Treron sphenura*	Wedge Tailed Green Pigeon
11	*Seicercus xanthoschistos*	Grey Hooded Warbler
12	*Pycnonotus leucogenys*	Himalayan Bulbul
13	*corvus splendens*	House Crow
14	*Passer domesticus*	House Sparrow
15	*Turdoides striatus*	Jungle Babbler
16	*Corvvus macrorhynchos*	Jungle Crow
17	*Lophura leucomelanos*	Kalij Pheasant
18	*Eudynamys scolopacea*	Koel
19	*Copsychus saularis*	Magpie Robin
20	*Treron bicincta*	Orange Breasted Green Pigeon
21	*Streptopelia orientalis*	Oriental Turtle Dove
22	*Nectarinia zeylonica*	Purple Rumped Sunbird
23	*Nectarinia asiatica*	Purple Sunbird
24	*Gallus gallus*	Red Jungle Fowl
25	*Hirundo daurica*	Red Rumped Swallow
26	*Pycnonotus cafer*	Red Vented Bulbul
27	*columba livia*	Rock Pigeon
28	*Streptopelia chinensis*	Spotted Dove
29	*Athene brama*	Spotted Owllet
30	*Halcyon smyrnensis*	White Breasted Kingfisher
31	*Zosterops palpebrosus*	White Eye

Table 18: Bird Species common to Moolbari and MeGad watersheds

1	*Parus Xanthogenys*	Black Lored Tit
2	*Phylloscopus fuscatus*	Dusky Warbler
3	*Parus major*	Great Tit
4	*corvus splendens*	House Crow
5	*Passer domesticus*	House Sparrow
6	*Corvvus macrorhynchos*	Jungle Crow
7	*Streptopelia orientalis*	Oriental Turtle Dove
8	*columba livia*	Rock Pigeon
9	*Myophonus caeruleus*	Blue Whistling Thrush

Table 19: Comparative distribution of bird species in the three watersheds

Scientific names	species	number	Mandhala	Moolbari	MeGad
Ocyceros biprostris	Indian Grey Hornbill	11	-	+	-
Dicrucrus leucophaeus	Ashy drango	1	-	+	-
Prinia socialis	ashy prinia	7	+	-	-
Terpsiphone paradisi	Asian paradise flycatcher	10	+	+	-
Stachyris pyrrhops	Black chinned babbler	2	+	-	-
Francolinus francolinus	Black Francolin	2	+	-	-
Certhia himalayana	bar tailed tree creeper	6	-	+	-
Hirundo rustica	Barn swallow	9	-	-	+
Ploceus philippinus	Baya weaver	4	+	-	-
hypsipetes leucocephalus	Black bulbul	31	+	+	-
Dicrucrus macrocercus	Black drongo	83	-	+	-
Ictinaetus malayensis	black eagle	7	+	+	-
Parus Xanthogenys	Black lored tit	13	+	+	+
Phoenicurus ochruros	Black redstart	2	-	+	-
Elanus caeruleus	black shouldered kite	1	+	-	-
Psittacula roseata	blossom headed parakeet	6	-	+	-
Nyctyornis athertoni	Blue bearded bee eater	2	-	+	-
Monticola cynclorhynchus	Blue capped rock thrush	2	-	+	-
Megalaima asiatica	blue throated barbet	1	-	+	-
Myophonus caeruleus	Blue whistling thrush	30	-	+	+
Sturnus pagodarum	brahminy myna	8	+	-	-
Megalaima zeylanica	brown headed barbet	1	-	+	-
bubulcus ibis	cattle egret	13	+	-	-
Motacilla citreola	citrine wagtail	5	-	-	+
Turdoides caudatus	common babbler	6	+	-	-
Falco tinnunculus	common kestrel	1	-	-	+
Alcedo atthis	Common Kingfisher				
Acridotheres tristis	common myna	146	+	+	-
Megalaima haemacephala	coppersmith barbet	4	+	-	-
Centropus sinensis	Greater coucal	2	+	-	-
Melophus lathami	crested bunting	14	+	-	-
Spilornis cheela	crested serpent eagle	1	+	-	-
Aethopyga siparaja	crimpson sunbird	1	+	-	-

Phylloscopus fuscatus	Dusky warbler	33	+	+	+
Streptopelia decaocto	eurasian collared dove	1	+	+	-
Carduelis carduelis	European goldfinch	2	-	-	+
Rhipidura aureola	White browed fantail	1	+	-	-
Serinus pusillus	fire fronted serin	23	-	-	+
Dicaeum agile	Thick billed flowerpecker	2	+	-	+
Oriolus oriolus	golden oriole	9	+	-	-
Parus major	Great tit	3	+	+	+
Merops orientalis	green bee eater	3	+	+	-
Treron sphenura	Wedge tailed green pigeon	12	+	+	-
Prinia hodgsonii	Grey breasted prinia	31	+	-	-
Dendrocopos canicapillus	grey capped pygmy woodpecker	2	-	+	-
Culicicapa ceylonensis	Grey headed flycatcher	3	-	+	-
Seicercus xanthoschistos	grey hooded warbler	19	+	+	-
Saxicola ferrea	Grey bushchat	1	-	+	-
Lanius minor	Lesser grey shrike	7	-	-	+
Dendrocitta formosae	Grey tree pie	7	-	+	-
Hierococcyx varius	Common hawk cuckoo	8	+	-	-
Megalaima virens	Himalayan barbet	4	-	+	-
Pycnonotus leucogenys	Himalayan bulbul	151	+	+	-
Dendrocopos himalayensis	Himalayan woodpecker	2	-	+	-
Upupa epops	hoopoe	11	+	-	+
corvus splendens	house crow	11	+	+	+
Passer domesticus	house sparrow	185	+	+	+
Apus affinis	house swift	17	+	-	-
Phylloscopus humei	hume's warbler	6	-	-	+
Cuculus micropterus	indian cuckoo	6	+	-	-
Pavo cristatus	Indian peafowl	15	+	-	-
Saxicoloides fulicata	indian robin	64	+	-	-
Aegithina tiphia	iora	2	+	-	-
Turdoides striatus	jungle babbler	133	+	+	-
Corvvus macrorhynchos	Jungle crow	142	+	+	+
Lophura leucomelanos	Kalij pheasant	15	+	+	-
Eudynamys scolopacea	Koel	15	+	+	-
Bubo bubo	Eurasian Eagle owl	2	-	-	+
Streptopelia sengalensis	laughing dove	1	+	-	-
Phylloscopus chloronotus	lemon rumped warbler	14	-	-	+
Dinopium javanense	lesser flameback woodpecker	3	+	-	-
Sylvia curruca	lesser white throat	2	-	-	+
Picus chlorolophus	Lesser yellow nape woodpecker	3	-	+	-
Phalacrocorax niger	little carmorant	3	+	-	-
Egretta garzetta	little egret	21	+	-	-
Tachybaptus ruficollis	little grebe	2	+	-	-
Copsychus saularis	magpie robin	5	+	+	-
Spizaetus nipalensis	mountain hawk eagle	1	+	-	-
Treron bicincta	Orange breasted green pigeon	2	+	+	-
Streptopelia orientalis	Oriental turtle dove	47	+	+	+
Anthus rufulus	paddyfield pipit	2	-	-	+

Milvus migrans	paraiah kite	3	+	-	-
Psittacula eupatria	alexandrine parakeet	6	+	-	-
Francolinus pondicerianus	Grey Francolin	6	+	-	-
Falco peregrinus	peregrine falcon	11	-	-	+
Saxicola caprata	pied bushchat	26	+	-	-
Clamator jacobinus	pied cuckoo	5	+	-	-
Psittacula cyanocephala	Plum headed parakeet	4	+	-	-
Ardeola grayii	pond heron	2	+	-	-
Nectarinia zeylonica	purple rumped sunbird	3	+	+	-
Nectarinia asiatica	Purple sunbird	39	+	+	-
Urochssa erythrorhyncha	Red billed blue magpie	21	-	+	-
Streptopelia tranquebarica	red collard dove	2	+	-	-
Gallus gallus	Red jungle fowl	3	+	+	-
Hirundo daurica	Red rumped swallow	48	+	+	-
Pycnonotus cafer	Red vented bulbul	73	+	+	-
Vanellus indicus	Red wattled lapwing	4	+	-	-
Acrocephalus dumetorum	Blyth's reed warbler	1			
Sterna aurantia	river tern	1	+	-	-
columba livia	rock pigeon	201	+	+	+
Psittacula krameri	rose ringed parakeet	26	+	-	-
Lanius schach	Long tailed shrike	91	-	-	+
Oenanthe pleschanka	rufous tailed wheatear	13	-	-	+
Tringa stagnatilis	Marsh sandpiper	1	-	-	+
Lophura nycthemera	Silver pheasant	6	-	+	-
Ficedula tricolor	Slaty blue flycatcher	1	-	+	-
Psittacula himalayana	Slaty headed parakeet	52	-	+	-
Megalaima viridis	White cheeked barbet	10	+	-	-
Streptopelia chinensis	Spotted dove	49	+	+	-
Enicurus maculatus	Spotted forktail	2	-	-	+
Lonchura punctulata	spotted munia	11	+	-	-
Athene brama	spotted owllet	3	+	+	-
Saxicola torquata	Common stone chat	2	-	+	-
Garrulax lineatus	streaked laughing thrush	35	-	+	-
Aethopyga gouldiae	MRS Gould's Sunbird	1	+	-	-
Orthohotomus sutorius	tailor bird	8	-	+	-
Dendrocitta vagabunda	tree pie	15	+	-	-
Sitta frontalis	velvet fronted nuthatch	2	-	-	+
Eumyias thalassina	Verditer flycatcher	2	-	+	-
Tichobroma muraria	wallcreeper	2	-	+	-
Chlidonias hybridus	whiskered tern	1	-	-	+
Lonchura malabarica	Indian silverbill	2	+	-	-
Dicrurus caerulescens	white bellied drongo	4	+	-	-
Halcyon smyrnensis	White breasted kingfisher	12	+	+	-
Chaimarrornis leucocephalus	white capped redstart	5	-	-	+
Zosterops palpebrosus	White eye	24	+	+	-
Parus nuchalis	white naped tit	2	-	-	+
Garrulux albogularis	White throated laughing thrush	6	-	+	-
Hirundo smithii	wire tailed swallow	16	-	+	-

Prinia flaviventris	yellow bellied prinia	1	+	-	-
Dendrocopos mahrattensis	Yellow crowned woodpecker	1	-	+	-
Chrysomma sinense	yellow eyed babbler	4	+	-	-
Carduelis spinoides	Yellow breasted greenfinch	36	-	-	+
Phoenicoptera treron	Yellow footed green pigeon	4	+	-	-
Motacilla flava	yellow wagtail	15	-	-	+
Acridotheres fuscus	Jungle myna				

Acknowledgements:

We are grateful to The Department of Science and Technology and Ministry of Science and technology for funding this project. We thank Dr. J.C.Rana at NBPGR who was instrumental in getting our accommodations at CPRI rest house, coordinating the meeting and fieldwork and for his support in procuring data from various other organisations. Dr.Pradeep, Dr.Verma.V.L are acknowledged for the useful discussions during the meeting and for letting us know more about NBPGR. We thank Dr. Archana Singh and Prashanth Bhasim, who accompanied us for the field identification of flora.

We thank the Director, Himachal Pradesh remote sensing agency and Mr.Thapa and other staff involved in this project for explaining the remote sensing part of this project and providing us with valuable data. We also thank Dr. J.C.Sharma for providing us with a report on Mandhala soil types.

We thank Mr.Rajesh Sharma, Block development officer at panchayat office, who took the trouble for us in procuring information related to people living below poverty line for various districts. Mr. R.S. Rathore and Mr.S.S.Thakur are acknowledged for their help in data collection at the Directorate of Agriculture, Shimla.

The D.F.O., Shimla Mr.Naresh Kumar IFS is duly acknowledged for his kind permission to visit the forest areas and also for providing us with working plans and compartment history data. We are thankful to the R.F.O., Dhami range and other field staff of the forest department. The D.F.O., Solan and D.F.O., Keylong are also acknowledged for their kindness in granting us permission to visit the forest areas and collect data. We are grateful to the people of Himachal for the warm welcome and the help we received during the entire fieldwork days.

Reference

1. Ali.S , 1989, Book of Indian birds , Second edition, Bombay Natural history Society publication.
2. Murti, S.K. 2001. Flora of Cold Deserts of Western Himalaya- Vol-1. Botanical survey of India, Calcutta.
3. Chowdhery, H.J. 1999. Himachal Pradesh. In Floristic diversity and Conservation strategies in India, Vol-2. Eds. V.Mudgal, P.K. Hajra. Botanical survey of India, Calcutta.
4. Aswal, B.S., Mehrotra, B.N. 1994. Flora of Lahaul-Spiti (A cold desert in North-West Himalaya). Bishen Singh Mahendra Pal Singh. Dehra Dun.
5. Arora, G.S., Mehta H.S., Walia V. 2005. Insecta: Lepidoptera (Butterflies). *In:* Fauna of Western Himalaya (Part-2)-Himachal Pradesh (ed. Director), Zoological Survey of India, Kolkata, pp. 157-180.

6. Blair, R.B. Launer, A.E. 1997. Butterfly diversity and human land use: Species assemblages along an urban gradient. Biological Conservation. 80: 113–125.
7. Erhardt, A, 1985. Diurnal Lepidoptera: Sensitive indicators of cultivated and abandoned grassland. Journal of Applied Ecology. 22: 849–861.
8. Evans, W.H. 1932. The Identification of Indian Butterflies (2nd ed.), 454 pp., 32 pls. Bombay Natural History Society, Bombay.
9. Gaston A.J, Garson. P.J, and Hunter M.L, 1983, The status and conservation of forest wildlife in Himachal Pradesh, Western Himalayas, Biological Conservation, 29; pp- 291-314
10. Grimmet, R., Inskipp, C., Inskipp, T., 1998. Birds of the Indian Subcontinent. Oxford University Press, Oxford, UK.
11. Kim, K. C. 1993. Biodiversity, conservation, and inventory: Why insects matter. Biodiversity and Conservation. 2: 191–214.
12. Kremen, C. 1992. Assessing the indicator properties of species assemblages for natural areas monitoring. Ecological Applications. 2: 203–217.
13. Leps, J. Spitzer, K. 1990. Ecological determinants of butterfly communities (Lepidoptera, Papilionidae) in the Tam Dao Mountains, Vietnam. Acta Entomologica Bohemoslovaca. 87: 182–194.
14. Laiolo Paulo, 2003, Diversity and structure of the bird community overwintering in the Himalayan subalpine zone: is conservation compatible with tourism?, *Biological Conservation*, ;115; pp- 251-262
15. Manel Stea Phanie , Diasx J.M. , Buckton S.T. And Ormerod S.J, 1999, Alternative methods for predicting species distribution: an illustration with Himalayan river birds, *Journal of Applied Ecology* ; 39; pp- 734-747
16. Mani, M.S. 1986. Butterflies of the Himalaya. Oxford & IBH Publishing Co. New Delhi.
17. Molina, J.M, Palma, J.M. 1996. Butterfly diversity and rarity within selected habitats of western Andalusia, Spain (Lepidoptera: Papilionoidea and Hesperioidea). Nota Lepidopterologica. 78: 267–280.
18. New, T.R. 1991. Butterfly Conservation. Oxford University Press, South Melbourne, Australia.
19. New, T.R.,Pyle, R.M., Thomas, J.A., Thomas, C.D., Hammond, P.C. 1995. Butterfly Conservation Management. Annual Review of Entomology 40: 57–83.
20. Parmesan, C. 1996. Climate and species range. Nature. 382: 765–766.
21. Pollard, E., Yates, T.J. 1993. Monitoring Butterflies for Ecology and Conservation. Chapman & Hall, London.
22. Samways, M.J. 1994. Insect Conservation Biology. Chapman & Hall, London.
23. Scoble, M.J. 1992. The Lepidoptera: Form, Function and Diversity. Oxford University Press, New York.
24. Spitzer, K. Jaros, J., Havelka, J., Leps, J. 1997. Effect of small-scale disturbance on butterfly communities of an Indochinese montane rainforest. Biological Conservation. 80: 9–15.
25. Stork, N.E., Srivastava, D.S., Watt, A.D., Larsen, T.B. 2003. Butterfly diversity and silvicultural practice in lowland rainforests of Cameroon. Biodiversity and. Conservation. 12: 387–410.
26. Swengel, A.B. 1996. Effects of fire and hay management on abundance of prairie butterflies. Biological Conservation. 85(2): 73–85.
27. Thomas, C.D., Malorie, H.C. 1985. Rarity, species richness, and conservation: Butterflies of the Atlas Mountains in Morocco. Biological Conservation. 33: 95–117.
28. Wood, P.A., Samways, M.J. 1992. Landscape element pattern and continuity of butterfly flight paths in an ecologically landscaped botanic garden, Natal, South Africa. Biological Conservation. 58: 149–166.

29. Wynter-Blyth, M.A. 1940-1946. A list of the butterflies of the Shimla hills, Journal of Bombay Natural History Society., 41: 716-741; 1945, 45: 256-257: 1946, 46: 735-736.
30. Wynter-Blyth, M.A. 1957. Butterflies of the Indian Region, pp.523, 1-72 plates. Bombay Natural History Society, Bombay.
31. Mehta, H.S. 2005. *Fauna of Western Himalaya (Part 2) Himachal Pradesh*. (ed. Director). Zoological Survey of India, Kolkata. pp
32. Mehta, H.S. 2005. *Amphibia*. In: Fauna of Western Himalaya (Part 2) Himachal Pradesh. (ed. Director). Zoological Survey of India, Kolkata.
33. Beebee, T.J.C., Griffiths, R.A. 2005. The amphibian decline crisis: A watershed for conservation biology? Biological Conservation, 125: 271-285 doi:10.1016/j.biocon.2005.04.009

Above ground biomass and biomass productivity of three micro watersheds across altitudinal gradients in Western Himalaya

Introduction

Bioresources

Bioresources are the resources we derive from living things around, bioresources play an important role in our system, as our dependency for food, fodder, energy etc.,

Bioresource in an ecosystem has two broad components, standing crop (living biomass) and litter. The former is the amount present in living components of the vegetation whereas the latter is an estimate of the dead plant parts which subsequently undergo the decomposition process. The primary step in the build up of biomass is photosynthesis. In this process, sunlight is absorbed by chlorophyll in the chloroplasts of green plant cells and is utilized by the plant to produce carbohydrates from water and carbon dioxide (Johansson *et al.* 1993). The process can be represented by the following equation.

$$6CO_2 + 6H_2O \xrightarrow{\text{sunlight}} C_6H_{12}O_6 + 6O_2$$

Biomass residues are the organic by-products of food, fibre and forest production. The most significant potential sources of biofuels are residues, wood resources from natural forests and biomass from managed plantations. Animal wastes like dung, skin, meat, bones and horns are well used in production of manure for agriculture. These animal residues can also be used as significant bioresources.

Of the different renewable energy sources, biomass appears to be the most important in terms of technical and economic feasibility during the next few decades in developing countries (Hall and Scrase, 1998). Regional policymakers, particularly those who consider options for meeting the energy needs at regional level require accurate assessment of bioresources. Biomass in all its form provides about 14% of the world's energy (Hall et al.,1992). The annual per capita biomass energy consumption in developing countries is in range of 0.4 to 2 tonnes of wood. Most of the energy needs in India is met by biomass and bioenergy. The dependency on forest resources is high in developing countries like India, which has an estimated 328.73 Mha area that be used for biomass production under various classes like cropland, forests, plantation etc. (Bhattacharya *et al*., 2003). The projected biomass demand for India is around 516 Mt/yr. There is a clear need to develop indigenous energy sources, especially biomass resources in the developing countries, because of the growing rural energy problems. With the depletion of the non renewable energy there is an increase in demand for finding new ways to use renewable energy resources. The

degree of dependence of rural communities on forests for their biomass needs varies depending on the degree and proximity of the forests (Ravindranath *et al*., 1991).

Energy from biomass has significant potential for more efficient production in the short term and for long-term inter fuel substitution. The biomass productivity is more in tropical forests than in the temperate region (Whittaker, 1975), but most of the tropical countries are developing nations and do require Bioresources to meet its needs especially in the rural area. This potential is particularly great in lower income developing countries with highly productive ecosystems.

Biomass

Biomass is defined as the total amount of aboveground living organic matter in trees expressed as oven-dry tons per unit area. The biomass is expressed in terms of weight per unit area, grams/square centimetre in case for microbes to tonnes/ha in case of forest or plantation biomass. Biomass estimation of vegetation in general, forests in particular has received serious attention over the last few decades for the very reason that components of climate change are associated with change in the biomass of a region. From ecosystem perspectives, biomass estimation helps in ecosystem productivity, energy and nutrient flows, and for assessing the contribution of changes in forest lands to the global carbon cycle. The potential carbon emission that could be released to the atmosphere due to degradation of forest and forest resource, deforestation and conversion of forested area into other land-use can be determined by biomass estimation. Hence, the precise estimation of biomass becomes necessary for understanding the importance of forest at regional scale.

Biomass can be categorised broadly as woody, non-woody and animal residues. Woody biomass comprises forests, agro-industrial plantations, bush trees, urban trees and farm trees. Wood, bark, branches and leaves constitute the above ground woody biomass. Woody biomass is generally a high valued commodity and has diverse uses such as timber, raw material for pulp and paper, pencil and matchstick industries, and cooking fuel. Woody biomass is derived from sources like forests, plantations and from wastelands.

Non-woody biomass comprises crop residues like straw, leaves and plant stems (agro-wastes), processing residues like saw dust, bagasse, nutshells and husks, and domestic wastes (food, sewage, etc.). They are harvested at the village level and are essentially used either as fodder or cooking fuel and animal residues constitutes the waste from animal husbandry These traditional fuels are especially important in developing countries, where they meet a large portion, of energy needs (Ramachandra *et al.,* 2004).

The actual energy content measured as the heating values is an important characteristic of biomass when it is considered as an energy source. It measures the quality of fuel in combustion applications. For woody biomass resources, the moisture content of the wood impedes the available energy, while for non-woody biomass, the ash content and the moisture content affect its energy values.

Forest Biomass

Forests play an important role in global carbon cycling, since they are large pools of carbon as well as potential carbon sinks and sources to the atmosphere. Accurate estimation of forest biomass is required for greenhouse gas inventories and terrestrial carbon accounting. The needs for reporting carbon stocks and stock changes for the Kyoto Protocol have placed additional demands for accurate surveying methods that are verifiable, specific in time and space, and that cover large areas at acceptable cost (Krankina *et al*. 2004; Patenaude *et al*. 2005; UNFCCC, 1997).

Biomass production and accumulation integrate plant responses to biotic and abiotic features of their environment. Forest biomass varies over climatic zone, altitude and region (Brown *et al*., 1989). Plant biomass is therefore a metric fundamental to understanding and managing forest ecosystems, whether to estimate primary production, nutrient pools, species dominance, responses to experimental manipulation, or fuel loads for fire. In recognition of its central importance, models of ecosystem processes often include plant biomass or biomass-related variables as inputs and outputs (Northup *et al.* 2005). Forest biomass is important for both commercial (timber, non-timber forest produce, etc.) and non-commercial (e.g., fuel wood assessment) uses. This is useful in national development planning, as well as in scientific uses such as studies of ecosystem productivity, energy and nutrient flows, and for assessing the contribution of changes in tropical forest lands to the global carbon cycle. Hence, estimating forest biomass helps in assessing fuel wood stock, carbon stock (Lugo, 1982; Brown *et al.,* 1989), and are equally important in estimation of forest productivity and carbon fluxes, assessing sequestration of carbon in wood, leaves and roots (Cole and Ewel, 2006), etc.

Characterizing the composition, structure and function of ecosystems is done through the assessment of the above ground biomass (AGB), which is of value not only for theoretical understanding of energy and element flows within the ecosystem, but also from a more practical point of view, as an indicator of ecological impacts.

Evaluation of the patterns, processes and dynamics of C cycling in forest ecosystems at local, regional and global scales (Luo *et al*., 2002) are done through the assessment of Net primary productivity (NPP) and biomass productivity. Net primary production is the difference between total photosynthesis (Gross Primary Production, GPP) and total plant respiration in an ecosystem. Alternatively, NPP is defined as the total new organic matter produced during a specified interval. NPP is usually defined as the balance between the light energy fixed through photosynthesis and lost through respiration and mortality, representing the net C uptake from the atmosphere into vegetation. Biomass productivity indicates the amount of biomass (leaf litter, dead wood, twigs, etc) available on renewable basis, which depends on the species, type of ecosystem, etc.

Plantations

Biomass from plantations has been recognised as a viable alternative to conventional energy resources. The establishment of forest plantations for the production of biomass, to be used as an energy source has attracted considerable interest since the late 1970's. The productivity of these plantations depends on different factors such as species, soil quality, rainfall, silvicultural practice, planting space, etc., and varies from 0.8 to 6.0 t/ha/yr for tropical countries. In India, faster growing tree species like poplar, *Eucalyptus*, *Acacia*, etc., are preferred in social forestry or *adhoc* afforestation programmes wherein a quicker yield is given over a short period of time. However, biomass production from plantations, have varying results.

In case of India, the productivity of *Eucalyptus* species for barren uncultivable land is estimated to be 3 t/ha/yr (air dry) due to degraded land condition. A productivity of 6.6 t/ha/yr has been assumed as the productivity for short rotation plantation on other land categories. The productivity of plantations with genetic improvement of seeds is assumed to be 8 t/ha/yr and the addition of fertilisers is assumed to enhance the productivity to 12 t/ha/y (Bhattacharya *et al*., 2003). Above ground biomass (standing biomass) in plantations of Himalayan region has given an estimate of 273 t/ha for an age of 25 years. Standing biomass in a central Indian plantation of monoculture *Gmelina arborea* is estimated as 3.6 t/ha for one year old plot to 56.4 t/ha for 6 year old plot (Swamy *et al*., 2004).

Karmacharya and Singh (1992) estimated the productivity and biomass of a teak plantation in India, they developed a regression equation of type log Y= a+ b log X, where Y is biomass component of the tree (kg) and X is the girth at breast height (GBH in cm). The predicted and the initial estimates were strongly correlated ($r=0.99$, $df= 32$, $P< 0.001$). Total aboveground biomass increased from 25 t/ha at 4 years to 77 t /ha at 30 years. Teak trees showed measurable and varying annual girth increments. Mean annual increment varied with girth class, being maximum (6.7 cm/yr) in the 15-20 cm girth class and minimum (1.7 cm/yr) in the greater than 70 cm girth class.

Agriculture

Biomass from agriculture is very significant; tonnes of agricultural residues are produced each year after the harvest season. Earlier these residues were used to make agricultural manure, but with advanced technology, biogas and electricity are being produced**.**

Biomass in Himalaya

In the Himalaya, vegetation ranges from tropical monsoon forest to alpine meadow and scrub, across elevation gradients. The Himalayan forest biomass is important as a large population of hill folk are still dependent on forest biomass to meet their daily requirement (Singh and Singh,

1991). The trend in biomass in the Himalayan region shows an increase in biomass with increase in altitude for different strands up to an altitude of 2700 m and shows decrease hence on, as the vegetation above 3000 m is sparse and are mostly of alpine grassland types at above 3500 m (Singh *et al*., 1994). *Pinus roxburghii* Sarg. (chir pine) forest are dominant along the low-to-mid montane belt of Central and Western Himalaya (Chaturvedi and Singh, 1987) with high regeneration potential, growth rate, establishing in degraded habitats, pipe like boles and high volumes. A sustained regeneration and growth in the presence of older plants is required for better growth of any plant community (Ramakrishnan *et al.*, 1981).

Knowledge on ecological processes and biotic pressure helps in understanding the persistence of long-lived plant communities, as disturbance is widespread all over the Himalaya (Singh and Singh, 1991). Humans have made considerable impacts in the Himalayan region, estimating such changes accurately would be of particular value to Himalayan people, whose subsistence agriculture depends on forest productivity to maintain livestock and soil fertility.

Factors Influencing Biomass

Forest degradation and/or fragmentation have significant impacts on the biomass of forest stand. Recent concerns about global warming and the carbon sequestration potential of tropical rainforests highlight the importance of regenerated secondary forests and their role as a carbon sink. Fire can also have a high toll on the biomass of forests. In the humid tropics, if fire kills large primary tree species, the burned area becomes dominated by a few pioneer tree species and the lost biomass is unlikely to be completely restored. In addition, degraded lands without parent trees may not have the potential for succession leading to replacement. Therefore, biomass recovery in such areas is quite slow and there may be limits to the potential above ground biomass.

In India, large areas of primary tropical forests are either degraded to different degrees or converted to other uses, like agriculture, urban and industrial development. Major causes of this degradation are habitat destruction, over exploitation, pollution and species introduction. Forest destruction is considered as one of the most serious environmental and economic problems for many countries in the tropical and sub-tropical regions of the world (Sharma, 1996). In India, 72% of existing forest has lost the capacity for regeneration. However, tropical forests have high regenerating capacity and if protection measures are extended they can recover very well (Behera *et al.,* 2006). Lopping intensity has proven to have impact on biomass of forests, leading to reduction in growth of tree girth and production of leafy biomass (Bhat *et al.,* 1995).

Biomass Estimation

The total inventory is divided into land and water. Land is divided into forest and non forest, and forest into productive and unproductive. For an assessment of forest biomass, forest inventory is

most commonly used and it differs depending on scope and purpose. Inventories are being designed to obtain information on other uses of the forest like recreation, grazing, wildlife and water conservation. It is designed to measure forest biomass rather than or in addition to traditional volume. Species specific equations that describe relationships between plant attributes and biomass are more accurate and flexible. Furthermore, it is preferable to use region or site-specific relationships where possible. Species size–biomass relationships could differ as plants alter allocation patterns in response to soil, climate and disturbance. Changes in structure and composition of vegetation are often accompanied by changes in biomass.

Destructive Methods

Forest biomass varies over climatic zone, altitude and region (Brown *et al.,* 1989; 1991) and there is no standard method to estimate biomass. Different methods are used for different study region. The methods that have been developed so far include the destructive and non-destructive sampling and most are based on harvested methods (Utsov *et al*., 1997). The destructive sampling involves harvesting reasonable samples and estimating wood density and AGB. The next stage involves deriving the probable relationship between the parameters *viz.,* tree girth, height with AGB. Destructive sampling provides reasonably accurate yield, but cannot be carried in all situations, hence biomass estimation through indirect method from basal area, height, etc is adapted nowadays.

Non-destructive Methods

In non-destructive techniques, forest biomass is estimated mathematically, using functions (based on earlier experiments involving parameters such as tree girth, height, etc), which relate the diameter of a tree to its biomass- or parts of its biomass- (leaves, bark, bole wood etc). Much work has been done to make the necessary measures and calculations to prepare these functions for many species (Jenkins *et al*., 2004). Brown *et al*., (1997) arrived at a non-destructive sampling strategy through the biomass estimation methods for the forests of the tropical region, based on regression models that were derived from known samples, which were cut and measured. Advances in the field of remote sensing and GIS, has given further boost to these techniques in estimating forest biomass over large region.

A protocol for forest biomass assessment based on the allometric equations will involve four steps (Ketterings *et al.,* 2000):

i) choosing a suitable functional form for the allometric equation;

ii) choosing suitable values for any adjustable parameters in the equation;

iii) field measurements of the input variables such as tree diameter (DBH), height, etc., and

iv) using the allometric equation to give the above ground biomass of individual tree and summation to get area estimates.

A detailed summary of biomass density studies in tropical forests, from lowland to montane and from wet to very dry zones, was made by Brown and Lugo (1982). Olson *et al.,* (1983), produced a global map of the biomass density of all ecosystem types, including disturbed and undisturbed forests at a 0.5° x 0.5° grid-scale of resolution.

AGB as given in equation 1, is computed considering VOB (volume of biomass)/ha and accounting for volume-weighted average wood density and biomass expansion factor (Brown and Lugo 1992). Above ground biomass is given by:

AGB(t/ha) = VOB * WD * BEF .....Equation 1

where WD = volume-weighted average wood density (1 ton of oven-dry biomass per m^3 green volume) and BEF = biomass expansion factor (ratio of aboveground oven-dry biomass of trees to oven-dry biomass of inventoried volume).

Wood density is expressed in units of mass of wood per unit of volume (either tons/m^3 or grams/cm^3) at 12% moisture content. Reyes *et al.,* (1992) derived the relationship between wood density with 12% moisture content to wood density based on oven-dry mass per green volume and is given by Y = 0.0134 + 0.800X (r^2= 0.99; number of data points n = 379), where Y is wood density based on oven-dry mass/green volume and X is wood density based on 12% moisture content. The term BEF is defined as the ratio of total aboveground oven-dry biomass density of trees with diameter at breast height (DBH) ≥10cm to the oven-dry biomass density of the inventoried volume and is given by BEF = Exp{3.213 - 0.506*Ln(BV)} for BV < 190 t/ha (sample size = 56, adjusted r^2 = 0.76) or BEF=1.74 for BV>=190t/ha where BV is biomass of inventoried volume in t/ha, calculated as the product of VOB/ha (m^3/ha) and wood density (t/m^3).

Another approach for AGB estimation is by regression models considering varioius components like tree top, foliage, branches, bole, stump and root using known samples. One desirable attribute of tree biomass equation is that they be additive, i.e., the sum of the biomass of components is equal to the total tree biomass for a given species.

The tree biomass equations are similar to tree volume equations relating volume and biomass with variables like height (H) and Diameter at Breast Height (DBH).

$V= a +b D^2H$ .....Equation 2

$B= a + bD^2H$ .....Equation 3

V is volume , B is biomass (Kg), D is DBH (cm)and H is height of tree (metre).

There are also other regression models relating biomass with variables using log values (Brown *et al*., 1997) as listed below

.

$Y=\exp\{a+b*\ln(D)\}$ .....Equation 4

$Y=10^{\{-a+\log_{10}(BA)\}}$ .....Equation 5

$Y=a+b(D)+c(D^2)$.....Equation 6

$Y=\exp\{a+b*\ln(D)\}$ .....Equation 7

Remote Sensing and GIS Techniques

Remote sensing is the art of acquiring information from an object without coming in actual contact with it. Many methods have been developed to estimate and map forest biomass from remotely sensed data (Foddy *et al*., 2001). Satellite remote sensing is the only way to acquire synoptic views over the huge expanses of inaccessible tropical forests. Forested land covers in the tropics are being differentiated using satellite digital and photographic data. Also, it can be used to differentiate secondary forests from primary forests and non-forested areas in the tropics.

Vegetation indices have, in particular, been used widely in land-cover analysis. A vegetation index expresses the remotely sensed response observed in two or more wavebands as a single value that is related to the biophysical variable of interest (Mather, 1999). An index may be easily applied to the imagery and thereby produce a representation of the spatial distribution of the biophysical variable of interest. Numerous indices have been proposed (Mather, 1999) but the most popular is the NDVI (Normalised difference vegetation index), which is given by:

NDVI = (IR - R)/(IR + R),

where, IR and R represent the near-infrared and red wavebands, respectively. There are, however, problems with the use of vegetation indices such as the NDVI. First, the relationship between the vegetation index and biomass is asymptotic and this can limit the ability of the index to represent accurately vegetation with a large biomass (Ripple, 1985). Secondly, it is essential that the remotely sensed data be accurately calibrated, typically to radiance, if the calculated index values are to be correctly interpreted and compared (Mather, 1999). Thirdly, the sensitivity of vegetation indices to biomass has been found to vary between environments (Ringrose *et al*., 1994). Fourthly, most vegetation indices fail to use all the spectral data available. Typically, a vegetation index uses only the data acquired in two spectral wavebands, yet the sensor typically acquires the spectral response in several additional wavebands.

Massanda *et al*., (2003) gave a method to estimate biomass using remote sensing, aerial photography and allometric equations. Photogrammetric methods were used in order to measure tree height and tree crown diameter, using aerial photographs. The measurements were then transformed to biomass, using an allometric equation generated through trees that were cut and oven dried and weighed. Luther *et al*., (2006) developed a model called BIOCLUST to estimate biomass from forest type and structure using Landsat TM imagery. This technique is useful in estimating and mapping biomass of large areas with maximum accuracy.

Biomass in Tropical Region

Regression models were developed by researchers in the tropical region (Brown *et al.* 1997), for estimating above ground biomass through non destructive measures and measures from forest inventories. The biomass regression equations can provide estimates of biomass per tree. The equation developed were regardless of species and was done zone wise: dry zone where rainfall is considerably less than potential evapotranspiration (e.g. <1500 mm rain/year and a dry season of several months), moist or where rainfall approximately balances potential evapotranspiration (e.g. 1500-4000 mm rain/year and a short dry season to no dry season), and wet or where rainfall is in excess of potential evapotranspiration (e.g. >4000 mm rain/year and no dry season). Probable relationship between AGB and Girth of trees were derived based on field samples in various climatic zones are listed in Table 1.

Table 1. Regression models for estimating AGB in various climatic zones.

Climatic zone	**Range D(cm)**	**#trees**	**Equation**	**Adjusted r^2**	**Equation Number**
Dry	5-40	28	Y=exp{1.996+2.32*ln(D)}	0.89	8
	3-30	191	Y=10^{-0.535+$\log_{10}$ (BA)}	0.94	9
Moist	5-148	170	Y=42.69-12.800(D)+1.242(D^2)	0.84	10
			Y=exp{-2.134+2.530*ln(D)}	0.97	11
Wet	4-112	169	Y=21.297-6.953(D)+0.740(D^2)	0.92	12

Note: Y=AGB (in kg), D=diameter at breast height, BA=basal area (in sq.cm).

The drawbacks associated with this technique are – a) use of trees of various girth classes, b) wide and often uneven-width diameter classes, c) multiple branching and buttresses and selection of the appropriate average diameter to represent a diameter class, and d) missing smaller diameter classes. To overcome the potential problem of the lack of large trees, equations were selected that were expected to behave reasonably up to 150 cm or so or upon extrapolation somewhat beyond this limit (Brown *et al*. 1989).

Murali *et al*., (2000) compiled equations for estimating biomass in tropical forest, which are listed in Table 2.

Table 2. List of AGB (Y in t/ha) equations for tropical forest.

Parameters	**Linear**	**Log**
Deciduous (n=11)	Y=-73.55+10.73(basal area) (r^2=0.82; % error =48)	Y=-1168.66+429.63*ln(basal area) (r^2= 0.87; % error = 24.98)
Evergreen (n=84)	Y=-2.81+6.78(basal area) (r^2=0.53; %error =74)	Y=3.51+0.036*ln(basal area) (r^2=0.28; % error=79.5)
Deciduous (n=10)	Y=11.27+6.03(basal area)+1.83(height) (r^2=0.94; % error = 49)	Y=-766+452.19*ln(basal area)-166.66*ln(height) (r^2=0.94; %error=28.94)
Evergreen (n=52)	Y=34.97+10.98(basal area)-6.77(height) (r^2=0.94; % error= 80)	Y=-961.65+276.85*ln(basal area)+86.32*ln(height) (r^2=0.53; % error = 88.89)
Deciduous (n=10)	Y=-160.64-0.025(density)+15.4(basal area) (r^2=0.92; % error=27.8)	Y=-957.1-44.07*ln(density)+460.63*ln(basal area) (r^2=0.91; % error=31)
Evergreen (n=52)	Y=120.67-0.01(density)+5.73(basal area) (r^2=0.6; %error 60.6)	Y=-142.24-47.65*ln(density)+230.54*ln(basal area) (r^2=0.57; % error=26.4)
Deciduous (n=10)	Y=227.2+0.03(density)-3.54(height) (r^2=0.46; % error = 123)	Y=-439.2+40.3*ln(density)-134.17*ln(height) (r^2=0.14; % error =12.9)
Evergreen (n=40)	Y=5.74-0.14(density)+0.312(height) (r^2=0.6; % error=88.26)	Y=-142.24-47.65*ln(density)+230.63*ln(height) (r^2=0.49;% error =98)
Deciduous (n=10)	Y=-56.8-0.015(basal area)+13.6(height)-4.21(density) (r^2=0.92; %error =27.8)	Y=-760.94-6.4*(basal area)+455.05*ln(height)-155.82*ln(density) (r^2=0.94;% error = 26.62)
Evergreen (n=39)	Y=123.26-0.008(basal area)+5.63(height)-0.27(density) (r^2=0.62; % error=86.79)	Y=-631.98-32.75*(basal area)+288.87*ln(height)+52.20*ln(density) (r^2=0.59; % error=95.16)

Path coefficient analysis based on parameters of the above equations showed that only basal area has significant correlation with biomass, compared to height and density. Deciduous forests had higher correlation between biomass and basal area.

Biomass estimate throughout the tropical region varied from 30–900 t/ha based on species composition, age and level of degradation in forest. Behera and Mishra (2006) noted the variation in AGB over age of strand in recovering tropical sal (*Shorea robusta*) forests of Eastern Ghats of India. Table 3 lists regression models and estimated AGB based on the same.

Table 3. Regression models and estimated AGB for tropical forests

Forest types	**Parameters**	**Equations**	**Adjusted r^2**	**Estimated AGB (t/ha)**	**Equation #**
Deciduous (N=11)	BA	AGB= -73.55 + 10.73 (BA)	0.82	65-352	13
Tropical dry (N=2410)	D, H, ρ	AGB = 0.112 + ($\rho D_{BH}^2 H_T$) ln(AGB)=a + ln ($D^2H\rho$)	0.99		14
Tropical dry (N=104)	BA	AGB = -0.5352+ $\log_{10}$(BA)	0.95	39.69 to 170.02	15
Tropical dry evergreen (N=5 each species)	BA	AGB = - 12.05 + 0.876 (BA).	0.98	73.06 to 173.10	16
Tropical dry evergreen	BA, H	AGB= 11.27+ 6.03 (BA) +1.83 (H)	0.94		17
Tropical wet (N=315)	D	AGB=Exp(2.4257 ln(DBH) - 2.5118		397 ±30	18

Note: BA=Basal area (cm); D=Diameter at breast height (cm); H=Height(m); ρ= Wood density

Chave *et al*. (2005, equation 14), derived a biomass estimation equation for tropical dry forests, which draws upon data from 404 trees from India, Australia and Mexico (refer table 3). Mani and parthasarathy (2006, equation 16, 17) developed regression equation for inland and coastal tropical dry evergreen forests of peninsular India. The above ground biomass varied from 39.69 to 170.02 t/ha and by inclusion of height (in m), it varied from 73.06 to 173.10 t/ha. Aboal *et al*., (2004, equation 13), derived the allometric relationship based on samples of different tree species and stand above ground biomass in an island, and the estimated AGB varied from 65 to 352 t/ha. Haripriya (2000) reported the above ground biomass of Indian forests to be in range of 14 to 210 t/ha, with a mean of 67.4 t/ha. According to this study, most of the biomass is concentrated in lower diameter classes of potentially large species, thus making it potential to sequester carbon over a long period of time. Nascimento and Laurence (2001, equation 18), estimated AGB of Amazon forests as 397 t/ha ±30 t/ha. A significant result in this study was biomass varied widely within the large study region, hence biomass estimation should be extensive. Tropical forest biomass based on published literatures (listed in Table 4) shows that the AGB ranges from 78.1 – 689.7 t/ha (Brown and Lugo, 1992) and for Indian region it ranges between 14-210 t/ha (Haripriya, 2004).

Table 4. Estimated AGB for various Tropical forests.

Forest type	Biomass (t/ha)
Tropical pre-montane wet forest	475.3-689.7
Tropical lower montane rain forest	552.8
Tropical montane wet forest	374.0-415.8
Tropical wet forest	171.7-501.3
Tropical moist forest	324.2-473.7
Tropical pre-montane moist forest	170.3
Subtropical wet forest	271.8
Subtropical moist forest	157.0-290.8
Subtropical dry forest	78.1-89.8
Tropical forest India	14.0-210.0

Source: Brown and Lugo (1992) and Haripriya (2004)

Biomass in Temperate Region

Johnson and Risser (1974) estimated AGB of temperate oak forest, based on Whittaker *et al.,* (1967). The biomass obtained was 245 t/ha, which is comparable to the estimate of 100 to 500 t/ha for a broad range of temperate deciduous forests. Whittaker (1975) gave estimated values for fir forests in temperate region to be around 360-440 t/ha, and for pine forest in range of 130-210 t/ha (equations 20, 21). Wang (2005) developed allometric equations (#19) for ten co-occurring species based on destructive sampling of temperate region in China. Humus layer biomass ranged from 67.0 to 153 t/ha at different sites in the temperate forest. AGB estimates for temperate forest are listed in Table 5.

Table 5. AGB equations for temperate regions based on forest types or stands.

Forest type	Parameters	Equations	Estimated AGB (t/ha)	Equation #
Temperate	AGB, D	$\log_{10}AGB = a+b(\log_{10} D)$	67-153	19
Temperate fir	AGB, D	AGB =a+bD	360-440	20
		AGB =a+ b $\log_{10}$ D		
Temperate pine	AGB, D	AGB =a+bX	130-210	21
		AGB =a+ b $\log_{10}$ D		
Temperate deciduous			245	

Note: AGB=Above ground biomass (t/ha), D=diameter at breast height (cm)

Luo *et al.,* (1996) have derived regression equations for China and Tibet plateau comprising temperate forests and are listed in Table 6. The AGB estimate varies from 14-727 t/ha for various forest types with the maximum value for evergreen broad leaved forest type. The regression equations were calculated for individual species of the temperate region, as well for a forest type or stand, which are listed in Table 6.

Table 6. AGB equations for individual species of the temperate region

Species	Equation	Equation #	Ref
Cupressus torulosa	AGB=-2.8232+.9268D	22	Luo *et al*., 2002
Ficus nemoralis	$AGB=7.5*10^{-2}*(D)^{2.6}$	23	Hiratsuka *et al*., 2006
Lyonia ovalifolia	lnAGB=-2.155+2.356*lnD	24	Mohns *et al*., 1988
Myrica esculenta	AGB=-2.286+2.496D	25	Mohns *et al*., 1988
Pinus roxburghii	AGB=23.9124+.5232D	26	Luo *et al*., 2002
Pinus roxburghii	AGB=-5.106+3.022D	27	Mohns *et al*., 1988
Pinus roxburghii	AGB=-6.398+2.655D	28	Chaturvedi and Singh, 1987
Pyrus pashia	lnAGB=.043+2.072lnD	29	Mohns *et al*., 1988
Quercus glauca	$AGB=1.8409D^{0.89262}$	30	Luo *et al*., 2002
Rhododendron arboreum	lnAGB=-1.628+2.24lnD	31	Mohns *et al*., 1988
Quarcus species	AGB=0.113+2.4572D	32	www.classes.yale.edu
Acer sp.	AGB=.01008+2.5735D	33	www.classes.yale.edu
Vitis	AGB=.0617+2.5328D	34	www.classes.yale.edu

Note: D=diatmeter at breast height (cm)

Biomass in Himalayan forest

Garkoti and Singh (1995), studied the variation in biomass and productivity in a central Himalayan forest region through an altitudinal gradient using 10m X 10m quadrat in each strata. Singh and Singh (1991), developed allometric equation for different parts of the tree, in addition to interspecies allometric equation for non-dominant tree species. Rana *et al*., (1989) estimated AGB in an altitudinal gradient of 300-2200m in the central Himalayas as 199 to 787 t/ha. The representative forest communities are sal *(Shorea robusta* Gaertn. F.) between 300 and 900 m; chir pine *(Pinus roxburghii*)/mixed-broadleaf forest from 900 to 1200 m; chir-pine forest from 1200 to 1800 m; mixed banj-oak *(Quercus leucotrichophora*)/chir-pine forest from 1500 to 2000 m; and mixed-oak *(Quercus* sp.) forests between 1800 and 2500 m (Table 7).

Table 7. Estimated AGB for various Himalayan region.

Forest type	Estimated AGB (t/ha)	Reference
Central Himalaya	199 - 787	Rana *et al*.,1988
Eastern Himalaya	368 - 682	Sundriyal *et al*., 1996
Central Himalaya	40 - 308	Garkoti and Singh 1995
Nepal Himalaya	2.5 - 27.5	Mohns *et al*., 1988

The biomass distribution in trees were in the range of 40 to 60% in the bole, and is found to be low in oak forest than others, this is comparable to Negi *et al.*, (1983). The allocation of biomass to branches was greater (40-45.2%) in oak-dominated forest compared with the other forests as dominance of leader shoot over the laterals was less marked in oaks than in the others. The contribution of foliage to the above-ground biomass was 3.4-5.1%, which falls in the range 2.6-9.3% reported for certain temperate and tropical forests of the world (Johnson and Risser, 1974; Whittaker, 1975; Singh, 1979; Negi *et al*., 1983; Rawat, 1988).

The range of forest biomass (199-787 t/ha) in the Central Himalaya (up to 2200-m elevation) was comparable to the range of biomass (200-600 t/ha) generally found in the mature forests of the world (Whittaker, 1975). The tree biomass in chir-pine forest and chir-pine/mixed-broadleaf forest (respectively, 199 t/ha and 192 t/ha) was similar to that of a 38-year-old chir-pine forest of this region studied by Chaturvedi and Singh (1982).

The biomass of various strand within a temperate watershed in Sikkim region varied from 368 to 682 t/ha with a mean of 596 t/ha (Sundriyal and Sharma, 1996). Negi and Tadoria (1993) estimated the biomass consumption as 442 kg/person/year in rural Garhwal Himalayas. Such high dependency on forest biomass has led to considerable degradation in the forests of the Himalayan region. Singh *et al*., (1994) compiled the biomass estimation in different Himalayan region, which are listed in Table 8.

Table 8. Species wise AGB and Net Productivity in Himalayan forests.

Forest type	Elevation (m)	Density (#/ha)	Basal area (sq.m/ha)	Biomass (t/ha)	Net productivity (t/ha/yr)
Shorea robusta	300	443	56.4	710	15.5
Shorea robusta	350	726	41	455	18.8
Pinus roxburghii	1300	700	45.4	29	18.7
Pinus roxburghii	1400	820	40.2	208	17
Pinus roxburghii	1600	1630	25	113	7.6
Pinus roxburghii	1700	540	47.2	283	16
Pinus roxburghii	1750	657	37	199	17.3
Mixed oak	1850	783	40	426	15.9
Quercus leucotrichophora	1950	570	36.8	388	13.2
Quercus lanata	2150	993	60	557	17.8
Quercus lanata	2190	660	35.8	285	15.5
Quercus floribunda	2190	760	33.9	459	16.6
Quercus floribunda	2200	1107	71	782	25.1
Mixed oak	2200	598	55	344	15
Cedrus deodara	2200			451	28.2
Aesculus indica	2300	280	59.7	502	16.5
Abies pindrow	2500	350	105.6	565	17.8
Quercus semecarpifolia	2650	480	73	590	19.5
Acer cappadocicum	2750	505	35.8	305	14.5
Betula utilis	3150	700	23.2	172	12.5
Rhododendron campanulatum	3300	1180	14.9	40	7.5

The above result shows that there is a decrease in biomass after an elevation of 2400m and more abruptly after 3300m. Tree density and basal area varied in the middle altitude. Lower elevation (<1500m) strands had less mean basal area. Stands above 3000m were composed of trees of coniferous type having high basal area but low density. The lower elevation is composed of low to moderate number of small trees,

while mid elevation stands varies in tree size and density both within and among forest types, largely due to the stands of *Quercus* sp.

The relationship of tree density and total basal area varied widely, within and among forest types. In the central Indian Himalayas (foothills to 2600m elevation), AGB varied from 500-600 t/ha. However, much lower biomass estimates of 200 t/ha occurred in early successional *P. roxburghii* between 1300 and 1750 m elevation. Above 2600 m, biomass declined sharply to 170 t/ha in birch forest with rhododendrons, at 3100-3200 m elevation. At 3300m elevation in pure thickets of small-stature rhododendrons, the biomass was 40 t/ha. In two stands, one of *S. robusta* forest at 300m and the other in *Q. floribunda* forest at 2200m elevation, forest biomass exceeded 700 t/ha. These two stands appeared to represent a limit for biomass values for elevations below 2200m. Biomass values up to 2400 t/ha occurred up to 3400 m elevation in the Nepal central Himalaya forests of a given biomass occurred several hundred metres higher in Nepal than in Kumaun. In both Kumaun and Nepal, *Q. semecarpifolia* forest attained similar maximal biomass, up to 550-600 t/ha near 2600 m elevation.

Productivity

Net primary productivity (NPP) and above ground biomass (AGB) are two widely used indices in evaluation of the patterns, processes and dynamics of Carbon cycling in forest ecosystems at local, regional and global scales (Luo *et al*., 2002).

Net primary production is the difference between total photosynthesis (Gross Primary Production, GPP) and total plant respiration in an ecosystem. Alternatively, NPP is defined as the total new organic matter produced during a specified interval. NPP is usually defined as the balance between the light energy fixed through photosynthesis (gross primary productivity) and lost through respiration and mortality, representing the net Carbon uptake from the atmosphere into vegetation (Mellino *et al*., 1993).

Equations involving the basal area are used for all tree species and therefore are used to estimate the standing biomass of mixed forests. Productivity, which is the increase in weight or volume of any biomass over a period of time, can be estimated when the standing biomass estimates are available for two consecutive years. It can also be calculated, by knowing the age of the forest stand in addition to the litter available annually. Productivity is equal to standing biomass per hectare/age of a tree or the trees per forest stand. Productivity estimates are important as they help to calculate the extent of biomass that can be extracted for fuel purposes (Ramachandra *et al*., 2004)

Another method used to find the productivity of a central Himalayan forest is by collecting the litter fall, where in litter fall is recorded on a monthly basis, by collecting the litter in a 50cm X 50cm X 15cm wooden trap with nylon mesh. The litter is sorted into leaf, wood and miscellaneous components. A sample plot of 1ha is marked, where the increase in GBH is measured annually. Dry biomass increments of different tree components can be calculated using the biomass equations. The annual biomass accumulation can be calculated from the net changes in biomass. The sum of accumulation for different tree components yielded the net biomass accretion for the trees. And the weight of litter collected in a defined area annually is added to the foliage biomass accumulation to calculate foliage production. Wood reproductive parts and miscellaneous litter fall values were summed in biomass accumulation of twigs to give the productivity for an interval (Garkoti and Singh, 1995).

Clarke *et al*., (2001) developed a conceptual method to calculate NPP (net primary productivity) with two approaches.

Approach 1:

Stand Increment = (Σ Increments of surviving trees) + (Σ Increments(s) of ingrowth)

Approach 2:

Stand Increment = (Σ AGB at t_2 - Σ AGB at t_1) + (Σ Biomass of trees that died in the Interval) - [(Biomass of a minimum size tree) x (number of new trees)]

Rana *et al.*, (1989) also estimated the net primary productivity in the Himalayan region, which was in the range of 12.8-27.9 t /ha/year and was not related to the elevation. Mohns *et al.*, (1988) gave the productivity for pine forest to be 0.6-6.7 t/ha/yr. According to this study the Broad-leaved tree biomass ranged from 5.1-24.2 t/ha with productivity rates between 1.8 and 6.7 t/ha/year.

References

1. Aboal Jesus Ramon, Arevalo Jose Ramon, Fernandez Angel. 2005. Allometric relationships of different tree species and stand above ground biomass in the Gomera laurel forest (Canary Islands), *Flora*, 200: 264–274
2. Behera S K., Misra M.K. 2006. Above ground biomass in a recovering tropical sal (*Shorea robusta* Gaertn.f.) forest of Eastern Ghats, India. *Biomass and Bioenergy,* 30:509–521
3. Bhat D.M., Ravindranath N.H. 1995. Tropical forest biomass. Centre for Ecological Sciences, Indian Institute of Science, Technical report – 77.
4. Bhat D.M., Ravindranath N.H., Gadgil M., 1995. Effect of Lopping intensity on tree growth and stand productivity in tropical forest. *Journal of Tropical Forest Science,* 8: 15-23
5. Bhatt, B. P., Sachan, M. S. 2004. Firewood consumption along an altitudinal gradient in mountain villages of India, *Biomass and Bioenergy,* 27:69-75.
6. Bhattacharya, S. C., Salam, P. A., Pham, H. L., Ravindranath, N. H. 2003. Sustainable biomass production for energy in selected Asian countries, *Biomass and Bioenergy*, 25:471-482.
7. Brown S, Gillespie A. J. R., Lugo A. E. 1991. Biomass of tropical forests in South and Southeast Asia. *Canadian Journal of Forest Research*. 21: 11 1-117.
8. Brown S, Lugo A. E. 1982. Storage and production of organic matter in tropical forests and their role in the global carbon cycle. *Biotropica.* 14: 161-187.
9. Brown S. 1989, Estimating Biomass and Biomass Change of Tropical Forests: a Primer.(FAO Forestry Paper - 134): http://www.fao.org/docrep/W4095E/w4095e00.HTM
10. Brown Sandra, Schroeder Paul, Birdsey Richard. 1997. Aboveground biomass distribution of US eastern hardwood forests and the use of large trees as an indicator of forest development, *Forest Ecology and Management*. 96:37-47.
11. Brown Sandra., Schroeder Paul, Kern Jeffrey S. 1999. Spatial distribution of biomass in forests of the eastern USA, *Forest Ecology and Management*. 123: 81-90
12. Brown, S and A.E. Lugo, 1990. Tropical secondary forests, *J. Trop. Ecol.* 1990: 1–32.
13. Brown, S., 1997. Estimating biomass and biomass change of tropical forests. A primer. FAO Forestry Paper 134. Food and Agriculture Organization of the United Nations, Rome, Italy.
14. Chave J., Andalo C., Brown S., Cairns M. A., Chambers J. Q., Eamus D., Folster H., Fromard F., Higuchi N., Kira T., Lescure J.-P., Nelson B. W., Ogawa H., Puig H., Riera B., Yamakura T.,

2005. Tree allometry and improved estimation of carbon stocks and balance in tropical forests, *Oecologia*, DOI 10.1007.

15. Chave Jérôme, Condit Richard, Lao Suzanne, Caspersen John P., Foster Robin B. Hubbell Stephen P. 2003. Spatial and Temporal Variation of Biomass in a Tropical Forest: Results from a Large Census Plot in Panama, *Journal of Ecology*, 91:240-252.
16. Chaturvedi O.P and Singh J.S, 1987, The Structure and Function of Pine Forest in Central Himalaya. I. Dry Matter Dynamic, Annals of Botany 60: 237-252
17. Cole T.G., Ewel J.J. 2006. Allometric equations for four valuable tropical tree species. *Forest ecology and management*. 229:351-360. 1-9.
18. Foody Giles M; Mark E. Cutler; Julia McMorrow; Dieter Pelz; Hamzah Tangki; Doreen S. Boyd; Ian Douglas, 2001, Mapping the Biomass of Bornean Tropical Rain Forest from Remotely Sensed Data**,** *Global Ecology and Biogeography*, Vol. 10, No. 4 pp 379-387.
19. Garkoti S.C, Singh S.P, 1992. Variations in the Net primary productivity and Biomass of forests in high altitude region in the central Himalayan region. *Journal of Vegetation Science*, 1:23-28
20. Gillespie, A.J.R., Brown, S. and Lugo, A.E., 1992. Tropical forest biomass estimation from truncated stand tables. Forest Ecology and Management. 48: 69-87.
21. Hall R.J., Skakun R.S., Arsenault E.J., Case B.S., 2006. Modeling forest stand structure attributes using Landsat ETM+ data:Application to mapping of aboveground biomass and stand volume, Forest Ecology Management 225: 378-390
22. Hall, D. O. 1991. Biomass energy, *Energy Policy,* 19:711-737.
23. Hall D.O., F. Rosillo-Calle and P. de Groot, 1992, Lessons from case studies in developing countries , Biomass energy, Vol 1, pp 62-72
24. Hall, D. O.,Scrase, J. I. 1998. Will biomass be the environmentally friendly fuel of the future?, *Biomass and Bioenergy,* 15:357-367.
25. Hall, D.O., House, J.I.1994. Biomass energy development and carbon dioxide mitigation options. In: Proceeding of the International Conference: National Action to Mitigate Global Climate Change, Copenhagen, Denmark.
26. Haripriya, G. S. 2000. Estimates of biomass in Indian forests, *Biomass and Bioenergy*, 19:245-258.
27. Haripriya G.S 2004, How 'sustainable' is the 'sustainable development objective' of CDM in developing countries like India? Forest Policy and Economics-6, pp 329-343
28. Jensin C.Jennifer, David C.Chojnacky, Linda S. Heath, Richard A. birdsey, Comprehensive Database of Diameter-based Biomass Regressions for North American Tree Species, 1981, USGS Forest Services pp 1-48
29. Johnson FL, PG Risser, 1974, Biomass, Net primary productivity and synamics of six mineral elements in a Post Oak Black jack oak forest, Ecology, Vol 55 pp 1245-1258
30. Johansson T.B., Kelly, H., Reddy, A.K.N., Williams R.H. 1993. Renewable energy sources for fuels and electricity. Island Press, USA.
31. Karmacharya S.B, Singh K.P 1992. Biomass and net production in teak plantation in a dry tropical region in India. *Forest Ecology and Management* 55; 233-247
32. Ketterings Quirine M., Coe Richard, Noordwijk Meine van, Ambagau Yakub and Palm Cheryl A. 2001. Reducing uncertainty in the use of allometric biomass equations for predicting above-ground tree biomass in mixed secondary forests , Forest Ecology and Management ,146:199-209.
33. Krankina Olga N, Mark E. Harmon, Warren B. Cohen ,Doug R. Oetter, Zyrina Olga and Maureen V. Duane, 2004, Carbon Stores, Sinks, and Sources in Forests of Northwestern Russia: Can We Reconcile Forest Inventories with Remote Sensing Results? Climate Change, Vol 67: No. 2-3, pp 257-272
34. Lal, J.B. Forest Biomass Estimation, Technical Report from Forest Survey of India, Dehradun.
35. Luo tianxiang, Li wenhua, and Zhu huazhong. 2002. Estimated biomass and productivity of natural vegetation on the Tibetan plateau, Ecological Applications, 12:980–997

36. Luther, J., Fournier, R., Piercey, D., Guindon, L., Hall, R. 2006. Biomass mapping using forest type and structure derived from Landsat TM imagery, *International Journal of Applied Earth Observation and Geoinformation,* 8:173-187.
37. Mather, P.M. (1999) Computer processing of remotely sensed images, 2nd edn. Wiley, Chichester.
38. Mandal R. A. and Laake P. van. 2005. Carbon sequestration in community forests: an eligible issue for CDM (A case study of Nainital, India), Banko Janakari, 15:53-61.
39. Mani, S., Parthasarathy, N. 2007. Above-ground biomass estimation in ten tropical dry evergreen forest sites of peninsular India, *Biomass and Bioenergy,* 31: 284-290.
40. Martinez-Yrizar, A., Maass, J. M., Perez-Jimenez, L. A., Sarukhan, J. 1996. Net Primary Productivity of a Tropical Deciduous Forest Ecosystem in Western Mexico**,** *Journal of Tropical Ecology*, 12:169-175.
41. Mohns B., Applegate G.B., Gilmour D.A. 1988. Biomass and productivity estimations for community forest management: A case study from the Hills of Nepal – II. Dry matter production in mixed young stands of chir pine (*Pinus roxburghii*) and broad-leaved species. *Biomass.* 17:165-184.
42. Murali K.S., Bhat D.M. and. Ravindranath N.H. 2005. Biomass estimation equation for tropical deciduous and evergreen forests, International Journal of Agricultural Resources, Governance and Ecology, 4:81–92.
43. Murali K.S., Bhat D.M., Ravindranath N.H. 2000. Biomass Estimation Equations for Tropical Deciduous and Evergreen Forests. Centre for Ecological Sciences, Indian Institute of Science, Technical Report - 81.
44. Nascimento, H. E. M., Laurance, W. F. 2002. Total aboveground biomass in central Amazonian rainforests: a landscape-scale study, *Forest Ecology and Management,* 168:311-321.
45. Negi, A. K. Todaria, N. P. 1993. Studies on the impact of local folk on forests of Garhwal Himalaya. 1: Energy from biomass, *Biomass and Bioenergy.* 4:447-454.
46. Negi, K. S., Y. S. Rawat, and J. S. Singh. 1983. Estimation of biomass and nutrient storage in a Himalayan moist temperate forest. Canadian Journal of Forest Research 13: 1185-1196.
47. Northup B.K., Zitzer S.F., Archer S., McMurtry C.R., Boutton T.W. 2005. Above-ground biomass and carbon and nitrogen content of woodyspecies in a subtropical thornscrub parkland. *Journal of Arid Environments*. 62: 23–43
48. Olson J.S, Watts J.A, and Allison L.J, 1983, Carbon of Live vegetation of world ecosystem, National technical informative service, Springerfield.
49. Patenaude G, R Milne, TP Dawson, 2005, Synthesis of remote sensing approaches for forest carbon estimation: reporting to the Kyoto Protocol, Environmental Science and Policy, Volume 8, Issue 2, pp 161-178
50. Rai, S. N. 1984. Above ground biomass in tropical rainforests of Western Ghats. Indian For. 110:754–764.
51. Rai, S.N. and Proctor, J. 1986. Ecological studies on four forests in Karnataka, India. I. Environment, structure, floristics and Biomass, Journal of Ecology. 74:439–454.
52. Ramachandra T.V, Kamakshi B, Shruthi B.V. 2004. Bioresources status in Karnataka, Renewable And Sustainable Energy Reviews, 8:1-47
53. Rana B.S., Singh S.P. and Singh R.P. 1989. Biomass and Net Primary Productivity in Central Himalayan Forests along an Altitudinal Gradient, Forest Ecology and Management. 27:199-218.
54. Ravindranath N.H, M.R.Mohan Nayak, R.S Hariyur, and C.R Dinesh, 1991, The status of Tree biomass in a Semi arid Ecosystem, Biomass and Bioenergy Vol. I, No. I, pp**.** 9-16,
55. Rawat, Y. S., and J. S. Singh. 1988. Structure and function of oak forests in Central Himalaya. I. Dry matter dynamics. Annals of Botany 62:397-4 1 I.
56. Ripple W.J, 1985, Asymptotic reflectance characteristics of grass vegetation, photogrammetric Engineering and Remote Sensing. Vol. 51, pp. 1915-1921

57. Ringrose, S., Matheson, W., Matlala, C.J.S.S., O'Neill, T. & Werner, P.A. (1994) Vegetation spectral reflectance along a north-south vegetation gradient in northern Australia. Journal of Biogeography, 21, 33-47
58. Sharma, E., Sundriyal, R.C., Rai, S.C., Bhatt, Y.K., Rai, L.K., Sharma. R. and Rai, Y.K., 1992. Integrated watershed management: A case study in Sikkim Himalaya. Gyanodaya Prakashan. Nainital, 120 pp.
59. Sharma.M. 1996. Current environmental problems and future perspectives. *Tropical Ecology,* 37:15–20
60. Sierra Carlos A., Valle Jorge I. del, Orrego Sergio A., Moreno Flavio H., Harmon Mark E., Zapata Mauricio, Colorado Gabriel J., Herrera Marı´a A., Lara Wilson, Restrep David E. o, Berrouet Lina M, Loaiza Lina M., Benjumea John F. 2007. Total carbon stocks in a tropical forest landscape of the Porce region, Colombia, Forest Ecology and Management, 243:299-309.
61. Singh Arvind, Jha A.K. & Singh J.S. 1997. Influence of a developing tree canopy on the yield of Pennisetum pedicellatum sown on a mine spoil, Journal of Vegetation Science, 8:537-540.
62. Singh Surendra P, Adhikari Bhupendra S., Zobel Donald B. 1994. Biomass, Productivity, Leaf Longevity, and Forest Structure in the Central Himalaya, Ecological Monographs, 64: 401-421.
63. Singh Lalji and Singh J.S 1991, Species Structure, Dry Matter Dynamics and Carbon Flux of a Dry Tropical Forest in India, Annals of Botany 68: 263-273
64. Sundriyal R.C., Sharma E. 1996. Anthropogenic pressure on tree structure and biomass in the temperate forest of Mamlay watershed in Sikkim , Forest Ecology and Management, 81: 113-134
65. Sundriyal, R.C., Sharma, E., Rai, L.K. and Rai, S.C. 1994. Tree structure, regeneration and woody biomass removal in a subtropical forests of Mamaly watershed in the Sikkim Himalaya. *Vegetation,* 113: 53-63.
66. Swamy SL, A Mishra, S Puri, 2006, Comparison of growth, biomass and nutrient distribution in five promising clones of *Populus deltoides* under an agrisilviculture system, bioresources Technology, Volume 97, Issue 1: pp 57-68
67. Tiwari A.K. 1992. Component – wise biomass models for trees: A non-Harvest technique, Indian for, 118: 405-410.
68. Wang Chuankuan. 2005. Biomass allometric equations for 10 co-occurring tree species in Chinese temperate forests, Forest Ecology and Management. 222: 9–16.
69. Westman, W. E. Whittaker, R. H.1975. The Pygmy Forest Region of Northern California: Studies on Biomass and Primary Productivity, *Journal of Ecology*, 63:490-520.
70. Whittaker, R. H., Woodwell, G. M. 1968. Dimension and Production Relations of Trees and Shrubs in the Brookhaven Forest, New York. *Journal of Ecology*, 56:1-25
71. Whittaker, R. H., Woodwell, G. M.1969. Structure, Production and Diversity of the Oak-Pine Forest at Brookhaven, New York, *Journal of Ecology*, 55: 155-174
72. Whittaker, R. H. Niering, W. A.1975. Vegetation of the Santa Catalina Mountains, Arizona. V. Biomass, Production, and Diversity along the Elevation Gradient, *Ecology*; 56:771-790
73. Whittaker, R. H.1996. Forest Dimensions and Production in the Great Smoky Mountains, *Ecology*; 47:103-121
74. Xiao Chun-Wang, Ceulemans R. 2004. Allometric relationships for below- and aboveground biomass of young Scots pines, Forest Ecology and Management, 203: 177–186.
75. https://classes.yale.edu/05-06/fes519b/methods-006/FES_519_Spring_2006/ Biomass_objectives.html Last accessed on 9 May 2007

PART - II

Above Ground Standing Biomass of three micro watersheds in Himachal Pradesh

Introduction

Biomass in all its form provides about 14% of the world's energy (Hall and Challe, 1991). The dependency on forest resources is high in developing countries like India, which has an estimated 329 million hectares that can be used for biomass production under various classes like cropland, forests, plantation, etc. The projected biomass demand for India is around 516 Mt/yr (Bhattacharya *et al.* 2003).

Forests play an important role in global carbon cycling, since they are large pools of carbon as well as potential carbon sinks and sources to the atmosphere. Accurate estimation of forest biomass is required for greenhouse gas inventories and terrestrial carbon accounting. The needs for reporting carbon stocks and stock changes for the Kyoto Protocol have placed additional demands for accurate surveying methods that are verifiable, specific in time and space, and that cover large areas at acceptable cost (IPCC, 2003; Krankina *et al*. 2004; Patenaude *et al*. 2005; UNFCCC, 1997).

Forest biomass varies over climatic zone, altitude and region (Brown *et al*., 1989). Plant biomass is therefore a metric fundamental to understanding and managing forest ecosystems, whether to estimate primary production, nutrient pools, species dominance, responses to experimental manipulation, or fuel loads for fire. In recognition of its central importance, models of ecosystem processes often include plant biomass or biomass-related variables as inputs and outputs (Northup *et al.* 2005).

In the Himalaya, vegetation ranges from tropical monsoon forest to alpine meadow and scrub, across elevation gradients. The Himalayan forest biomass is important as a large population of hill folk are still dependent on forest biomass to meet their daily requirement (Singh and Singh, 1987). The trend in biomass in the Himalayan region shows an increase in biomass with increase in altitude for different strands up to an altitude of 2700 m and shows decrease hence on, as the vegetation above 3000 m is sparse and are mostly of alpine grassland types at above 3500 m (Singh *et al.* 1994)

Pinus roxburghii Sarg. (chir pine) forest are dominant along the low-to-mid montane belt of Central and Western Himalaya (Chaturvedi and Singh, 1987) due to high regeneration potential, growth rate, establishing in degraded habitats, pipe like boles and high volumes.

Disturbance has become a widespread feature in most of the forests all over the Himalaya (Singh and Singh, 1992), therefore, knowledge on ecological processes and biotic pressure can help in understanding the persistence of long-lived plant communities. A sustained regeneration and growth of all species in the presence of older plants is required for better growth of any plant community (Ramakrishnan *et al.*, 1981). Humans have made considerable impacts in the Himalayan region, estimating such changes accurately would be of particular value to Himalayan people, whose subsistence agriculture depends on forest productivity to maintain livestock and soil fertility.

For an assessment of forest biomass, forest inventory is most commonly used and it differs depending on scope and purpose. Inventories are being designed to obtain information on other uses of the forest like recreation, grazing, wildlife and water conservation. It is designed to measure forest biomass rather than or in addition to traditional volume. Species specific equations that describe relationships between plant attributes and biomass are more accurate and flexible. Furthermore, it is preferable to use region or site-specific relationships where possible. Species size–biomass relationships could differ as plants alter allocation patterns in response to soils, climate and disturbance. Changes in structure and composition of vegetation are often accompanied by changes in biomass. (Brown and Luo 1992). Forest biomass varies over climatic zone, altitude and region (Brown *et al.,* 1989, 1991)

In this report we have examined the variation in above ground standing biomass of three micro watersheds which has a forest widely used by the local people for fuel wood, fodder, and for grazing of cattle in the Himachal Pradesh region across varying altitude and vegetation types.

Methods

Study Area:

The department of Science and Technology (DST), Government of India, has taken a major initiative to create a bio-geo database and ecological modelling for western Himalayas. Initially three watersheds have been identified in Himachal Pradesh. The three micro watersheds having typical mountain village ecosystem were selected across three altitudinal zones (Figure 1). The forests in the three watersheds are managed as reserve forest by the state forest department, where cutting of trees is prohibited. However, lopping and collection of fallen wood for household purpose by the villagers are noted in all three watersheds. Spatial bounds of the respective watersheds were delineated from the digital elevation model (DEM) generated from the remote sensing data. The characteristics of the watersheds is summarised in Table 1.

Table 1. Geographical attributes of study area

Micro watersheds	District	Main watershed	Latitude (°N)	Longitude (°E)	Altitude (m amsl)	Area (sq.km)
Mandhala	Solan	Yamuna	30.87-30.97	76.82-76.92	400-1100	14.53
Moolbari	Shimla	Yamuna	31.07-31.17	77.05-77.15	1400-2000	10.50
MeGad	Lahaul and Spiti	Chandrabhaga	32.64-32.74	76.46-76.74	2900-4500	46.05

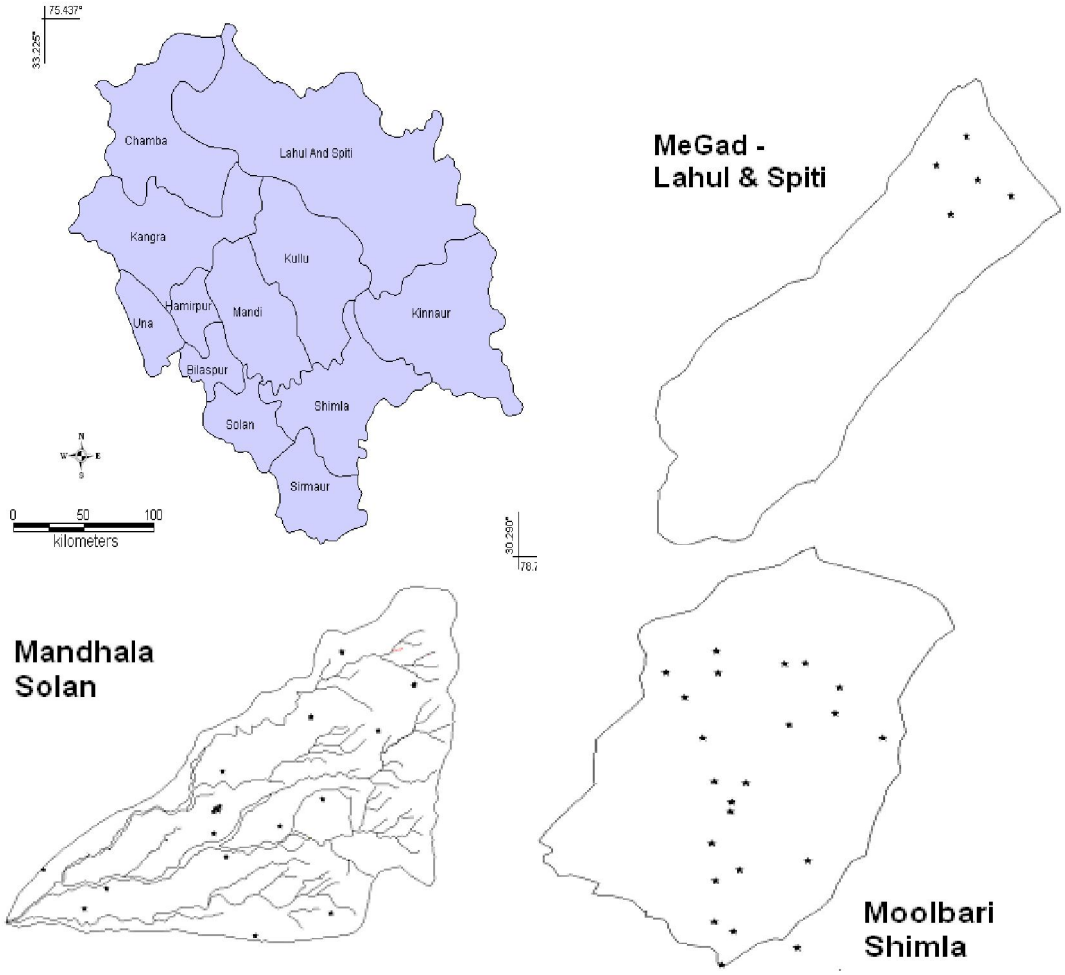

* - indicates the location of villages in the watershed

Figure 1: Boundary map of three watersheds

Climate

The climate is distinguished in three axes, in the Western Himalayas: (1) a vertical axis determined by the effect of altitude on temperature; (2) a transverse axis determined by topography along which rain shadow effects cause decreasing precipitation and increasingly extreme (continental) temperature fluctuations from SW to NE across the main ranges; (3) a longitudinal axis determined by a geographical trend of

decreasing monsoon precipitation (June-September) and increasing winter snowfall (December-April) from SW to NW along all the ranges. The third axis is important in determining major ecological trends over the entire length of the Himalayan chain, but it is less important than the other two axes in determining the ecology of localities within the Western Himalayas (Gaston *et al*., 1983).

Vegetation type

The three watersheds represent different vegetation types;

Mandhala watershed: This watershed falls in lower shiwalik range (400 - 1100m) and are characterised by dry evergreen tree species and scrub vegetation. The major tree species in this watershed is *Flacourtia montana, Acacia catechu, Grewia optiva, Toona ciliata, Albizia procera, Haldina cordifolia, Acacia* sp*., Lannea coramandelica, Mitragyma parviflora*, along with *Nyctanthus arbor-tristis, Carissa apaca, Dodonaea viscose* and *Woodfordia fruticosa*. Most of the forests here have been deforested and hill ranges completely covered with *Lantana camera* weed. Also scattered trees of *Holoptelia integrifolia, Dalbergia sisoo, Morus nigra*, etc. occur along the field bunds and other open lands.

Moolbari watershed: The vegetation here is characteristically of middle temperate type of the Himalayan region of the mid altitude ranges (1400-2000m). The vegetation in this watershed consisted of mixed deciduous and sub-tropical pine forest in two different altitudinal ranges. Former till an altitude of 1500m and later beyond 1500m. Apart from *Pinus* other species seen are *Pyrus pashia, Rubus ellipticus, Berberis* sp, and in moist localities species of *Quercus leucotrichophora* and *Q. glauca* and *Rhododendron arboretum*. On the exposed hill slopes in pine forests *Euphorbia royleana* is encountered. Between 1800-2000 m, oak forests species such as *Quercus leucotrichophora*, *Q. glauca* dominate along with *Rhododendron arboretum, Lyonia ovalifolia.*

MeGad Watershed: This watershed falls in the rain shadow region of the Himalayas (2900-4500m), and receives less than 80cm rainfall annually, there is high snowfall during winter and temperature goes to as low as -20˚C in this season. This watershed comprises of temperate, alpine and sub-alpine vegetation.

- *Temperate vegetation*: It consists of woody trees at altitude of 2500-3200 such as *Pinus wallichiana, Juniperus recurva, Picea smithiana, Abies pindrow*, *Cedrus deodara* that form the natural forests. Along the streams and irrigated canals are planted trees of *Salix* and *Popular* sp.
- *Alpine - Sub-alpine vegetation:* Mostly stunted, scattered bushes of *Juniperus communis, Berberis* sp., etc along with herbaceous elements such as *Ranunculus, Pedicularis, Potentilla, Polygonum, Geranium, Anemone, Corydalis*, etc., are commonly encountered.

Quantification of Bioresources

Vegetation Sampling to estimate Above Ground Biomass (AGB)

Belt transect of 250 x 4 m was laid randomly throughout the water shed. In each transect, for each tree GBH (Girth at Breast Height in cm) and height (in m) is noted along with its identification. Coordinates

were marked using GPS at the start and end points in each transect and at every 100m interval. Litter weight is measured in four 1m X 1m quadrat within each transect. Using densiometer, canopy cover is measured at start, end point and at 100 meter interval in each transect.

The above ground standing biomass is estimated transect wise through non-destructive sampling using standard regression models suitable for these agro-climatic zones (Brown *et al*., 1989; Schroeder *et al*., 1997) and are given in Table 2. The AGB is estimated for each transect in all three watersheds and represented as tonnes/hectare (t/ha).

Table 2. Regression models used to estimate AGB in the study region

Regression model	**Study region**	**Model #**
AGB = exp{-1.996+2.32*ln(D)}	Mandhala, MeGad	1
AGB = 10^{-0.535+log10 (BA)}	Mandhala, MeGad	2
AGB = 42.69-12.800(D)+1.242(D^2)	Moolbari	3
AGB = exp{-2.134+2.530*ln(D)}	Moolbari	4
AGB= (0.5+25000$D^{2.5}$)/($D^{2.5}$+246872)	Moolbari	5

Note: AGB=Above ground biomass (t/ha), D=diameter at breast height (cm), BA =Basal Area (sq.cm)

Results

AGB in Mandhala

Mandhala watershed falls in the lower Shiwaliks, receives low rainfall and hence are considered as dry regions. We used Model 1 and 2 from Table 2 for estimation of AGB. Table 3 provides transect-wise estimated AGB in Mandhala watershed.

Table 3. Transect-wise AGB in Mandhala watershed.

Transect #	**Basal Area (sq.cm)**	**Model 1 (t/ha)**	**Model 2 (t/ha)**
1	5969.9	31.60	17.42
2	12398.1	69.80	36.17
3	8993.1	44.79	26.24

4	4060.3	17.91	11.85
5	5386.4	33.02	15.71
6	5697.4	21.66	16.62
7	685.0	2.71	2.00
8	4317.8	15.18	12.60
9	4862.5	21.70	14.19
10	2084.4	8.92	6.08
11	2615.4	12.58	7.63
Mean±Sd	**5188.23±256.32**	**25.44±18.93**	**15.14±9.5**
Range	**685.0 - 12398.1**	**2.71 - 69.8**	**2.00 - 36.17**

Estimated AGB varied from 2.71-69.8 to 2.00-36.17 t/ha according to respective models. The variations among transects were significantly different (Analysis of Variance, ANOVA, F = 3.97, P=0.04) between Model 1 and 2, though the overall estimate is not different between the models (Students t, t=1.61, P=0.12). Figure 2 is the scatter plot of basal area against above ground biomass estimate based on Model 1 and Model 2. Model 2 mentioned in Table 4 is better suited for Mandhala water shed (n=11, R^2=1).

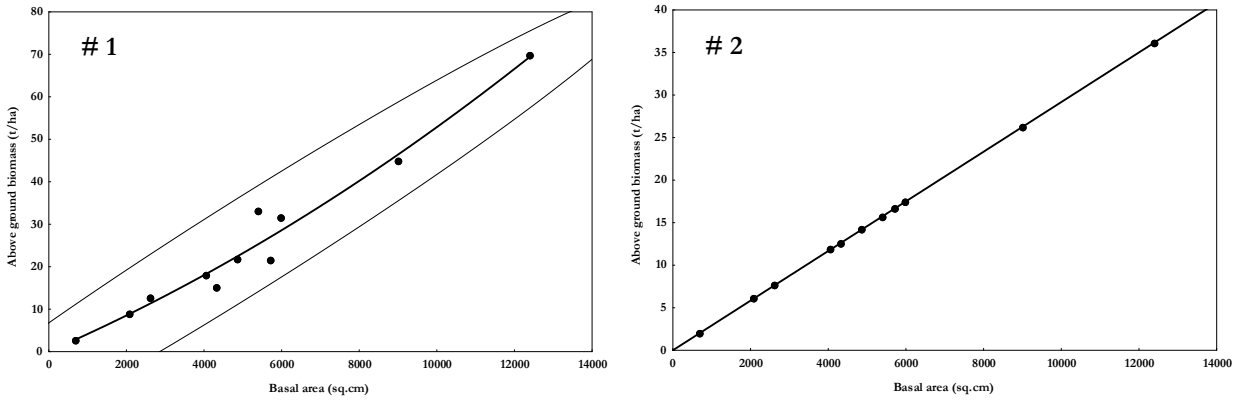

Figure 3. Scatter plot for AGB estimation in Mandhala watershed.

Table 4. AGB estimation regression models based on basal area (BA in sq.cm).

Model #	Regression model	R^2
1	AGB=0.0497+0.004(BA)+1E-7(BA^2)	0.97
2	AGB=0.0012+0.0029(BA)	1.0

AGB in Moolbari

This watershed falls in mid Himalayan ranges and receives higher rainfall (compared to Mandhala and MeGad). Regression models 3, 4 and 5 for wet region are used to estimate AGB. Table 5 provides transect-wise estimated AGB in Moolbari watershed.

Table 5. Transect-wise AGB in Moolbari watershed.

Transect #	Basal area (sq.cm)	Model 3 (t/ha)	Model 4 (t/ha)	Model 5 (t/ha)
1	25101.27	274.56	246.86	246.86
2	16690.37	157.52	134.48	102.58
3	14587.18	127.35	107.89	83.21
4	11312.74	87.26	75.88	58.90
5	13514.97	123.86	104.94	80.45
6	32371.50	285.80	240.78	185.81
7	26968.07	236.72	202.23	155.51
8	28952.87	205.99	182.35	142.79
9	7301.27	54.92	47.26	36.99
10	34736.07	261.03	228.06	177.72
11	31389.01	254.35	230.21	174.21
12	30605.41	280.61	242.64	184.45
13	22370.38	191.97	166.93	127.96
14	23891.16	199.65	175.47	134.37
15	23362.76	195.78	166.74	129.26
16	24085.99	191.40	166.70	129.16
Mean±Sd	**22952.56±8146.31**	**195.55±70.22**	**169.96±62.03**	**134.39±53.91**
Range	**7301.27-34736.07**	**54.92 – 285.80**	**47.26-246.86**	**36.99-246.86**

Variations among transects were not significant (Model 3 vs. 4, F=1.28, p=0.64; Model 3 vs. 5, F=1.7, p=0.32; and Model 4 vs. 5, F=1.32, p=0.59), indicating homogeneity among transects. Among the three models, mean AGB estimate between models were also similar, except for model 3 and 5 (Model 3 vs. 4, t=1.09, p=0.28; Model 4 vs. 5, t=1.73, p=0.094; and Model 3 vs. 4, t=2.76, p=0.009). Figure 3 is the scatter plot of basal area against above ground biomass estimate based on Models 3, 4 and 5. Table 6 lists the models with their R^2 values.

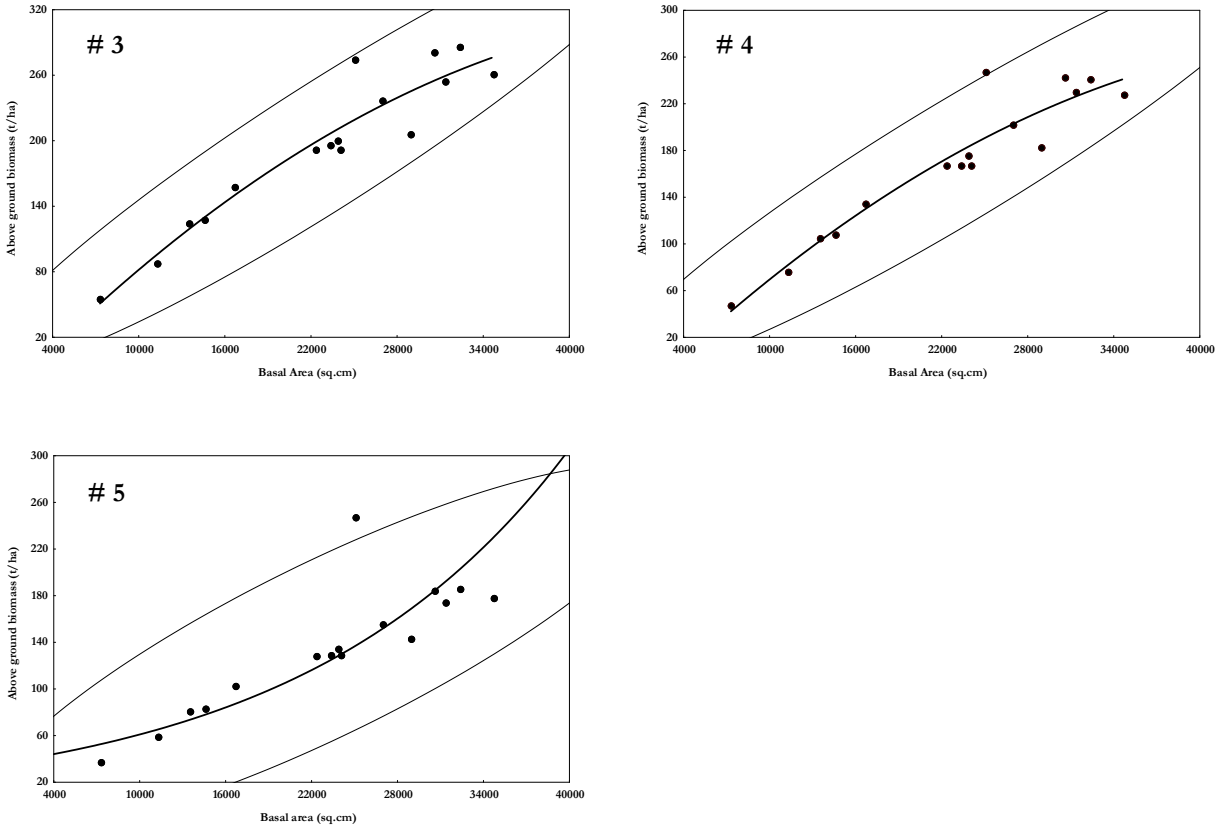

Figure 4. Scatter plot for AGB estimation in Moolbari watershed.

Table 6. AGB estimation regression models based on basal area (BA in sq.cm, n=16).

Model #	**Regression model**	**R^2**
3	AGB=-42.176+0.014(BA)-1.3E-7(BA^2)	0.91
4	AGB=-39.984+0.0121(BA) -1.0E-7(BA^2)	0.90
5	AGB=35.596$^{e5.0E-5(BA)}$	0.82

AGB was also estimated considering entire Moolbari watershed as temperate broadleaf forest and dividing further according to dominant forest type (Table 7).

Table 7. Species-wise estimate of AGB in Moolbari watershed.

Forest type	**Model**	**AGB (t/ha)**	**Reference**
Quercus forest	$AGB = 1.8409BA^{0.89262}$	221.79	Li and Luo (1996)
Pine and other conifers	AGB= 0.5168*(Volume)+33.2378	31.26	Fang *et al*., (1998)
Miscellaneous broad leaved	$AGB=0.5+25000D^{2.5}/D^{2.5}+246872$	19.17	Schroeder *et al*., (1997)
Total		**272.22**	

AGB in MeGad Watershed

For the marked reduction in precipitation, MeGad is considered as dry region for the estimation of AGB. Table 8 details the estimated AGB based on Model 1 and 2 listed in Table 2.

Table 8. Transect-wise AGB in MeGad watershed.

Transect #	**Basal Area (sq.cm)**	**Model 1 (t/ha)**	**Model 2 (t/ha)**
1	20513.61	112.70	59.85
2	23629.62	135.45	68.94
3	35090.13	221.44	102.37
4	19964.49	114.94	58.25
5	2067.44	9.06	6.03
6	25217.91	161.56	73.57
7	40590.37	248.65	118.42
Mean±Sd	**23867.65±12309.93**	**143.4±78.91**	**69.63±35.91**
Range	**2067.44-40590.37**	**9.06-248.65**	**6.03-118.42**

On comparing Model 1 vs. Model 2, mean estimate of AGB were significantly different ($t=2.25$, $P=0.044$). AGB estimates for each transect varied considerably, although not statistically significant ($F=4.83$, $P=0.08$). Figure 4 depicts basal area against AGB in MeGad watershed and regression models of the same are in Table 9.

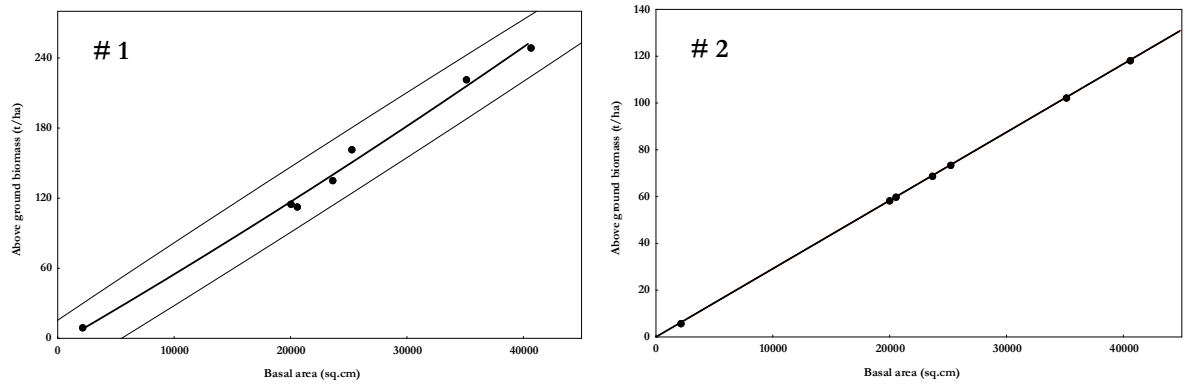

Figure 5. Scatter plot for AGB estimation in MeGad watershed.

Table 9. AGB estimation regression models based on basal area (BA in sq.cm).

Model #	Regression model	R^2
1	AGB=-4.4259+0.0058(BA)+1E-8(BA^2)	0.99
2	AGB=0.0013+0.0029(BA)	1.0

Both model 1 and 2 have significant r^2 values. Model 2 is better suited than model 1 for its simplicity in calculation. Considering different forest types, AGB estimated for MeGad are listed in Table 10. These estimates vary from 140.37 to 400.34t/ha for the region.

Table 10. Species-wise estimate of AGB in MeGad watershed.

Forest type	Model	AGB (t/ha)	Reference
Picea - *Abies* forest	AGB = 50.8634 + 0.5406(BA)	400.34	Li and Luo (1996)
Mixed conifers	AGB= 0.5168*(Volume)+33.2378	352.93	Fang *et al*., (1998)
Pines and other conifers	AGB= 0.5168*(Volume)+33.2378	336.96	Fang *et al*., (1998)
Conifers	AGB= (0.5+15000$D^{2.7}$) /($D^{2.7}$+ 364946)	140.37	Schroeder *et al*., (1997)

Validation of Biomass results:

The results of biomass estimation for the three watersheds were validated with the biomass estimation results in published literature.

Altitude range	Biomass range (Observed)	Biomass obtained
Quercus	200-550	221.79
Abies- pindrow	52-512	400.34
Pine forest	28-365	336.96
Evergreen broad leaved Quercus forest	46-727 34-516	19.17 221.79
Dry evergreen forest type	39-170	25.14

The results show that for most of the forest types in the study area, the biomass obtained is well within the range of biomass obtained in similar forests. However very low biomass is noted in Mandhala watershed, the forests of Mandhala region are highly degraded and invasive weeds like lantana and euphotorium have put constraint on the growth and regeneration of natural vegetation

Litter Weight:

The dry litter in the ground is measured in each belt transect at start point, end point and at every hundred metre interval. A plot of 1m X 1m is made and all the dry leaf litter falling within the plot is collected in a bag and weighed with a 500g spring balance.

Table 9: Values of Litter weight and canopy cover in transects

Litter weight in grams	Canopy cover in %	Litter wt	Canopy cover closed
90	32.4	110	36
80	52.16	370	76
10	0	70	74
120	53.2	170	82
45	11.6	130	92
130	91.68	120	56
20	0.16	80	54
40	25.12	90	35
170	81.28	125	4
370	75.04	0	8
120	4.32	350	72
110	33.44	0	2
80	29.28	250	76
150	81.28	0	4
260	92.72	270	96
240	91.68	0	5
310	41.76	0	4
70	72.96		

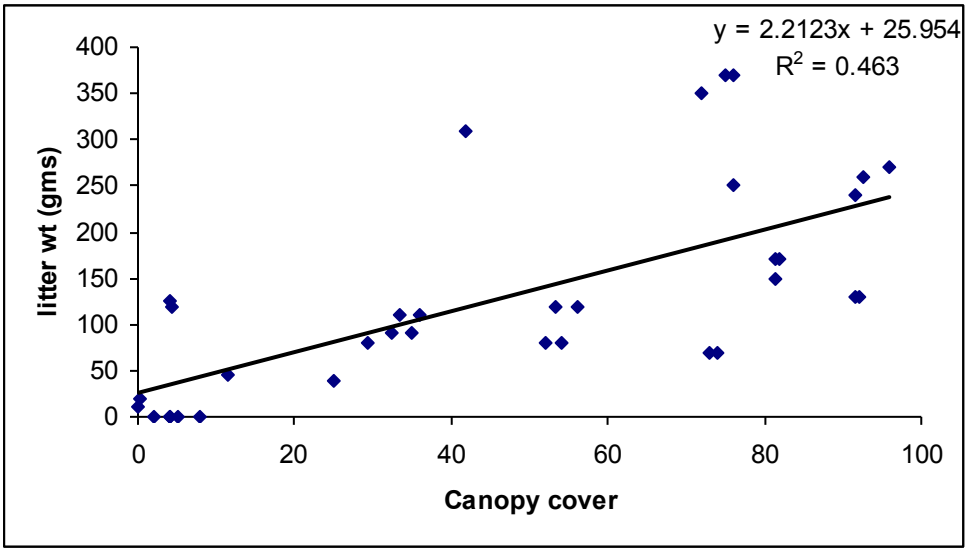

Graph 1: Litter Weight and canopy cover

A graph was plotted between the litter weight and canopy cover. A linear trend line was plotted in the graph to see the relation; though not much a significant relation is seen, increase in canopy cover will cause the litter weight to increase.

Discussion

In the Himalaya, vegetation ranges from sub-tropical monsoon forest to alpine meadow and scrub, across elevation gradients. Plant species richness in the three watersheds varied along elevation and is represented in Figure 6. The overall trend indicates a gradual increase in species richness till mid altitudinal regions and then decrease with increase in elevation. Though the polynomial relationship is not significant (r^2=0.32), but this is similar to general pattern of species richness along elevation in the Himalayas. Such pattern is evident in relative abundance of plant species.

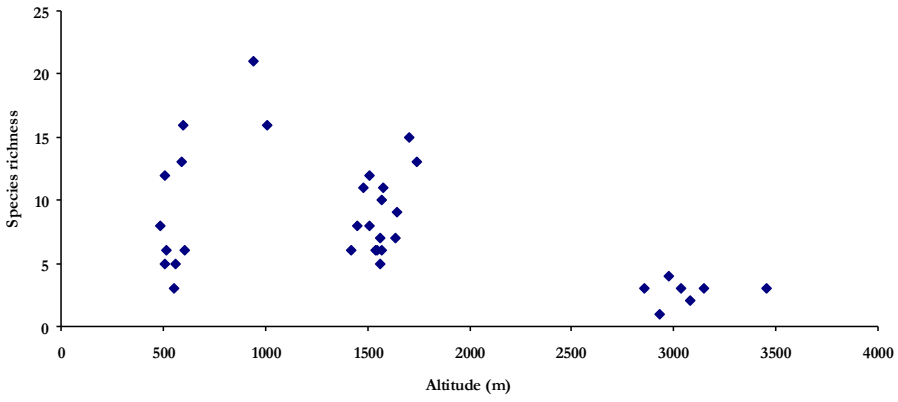

Figure 6. Plant species richness along elevation gradient in the three watersheds.

Figure 7 illustrates the trend in relative abundance (no. of individuals/1000 sq.m) of plant species in each transect against elevation gradient. It is interesting to note that, low altitude (500-1000m) and very high altitude (2700-3500m) had lesser abundance compared to mid altitude (1300-1600m).

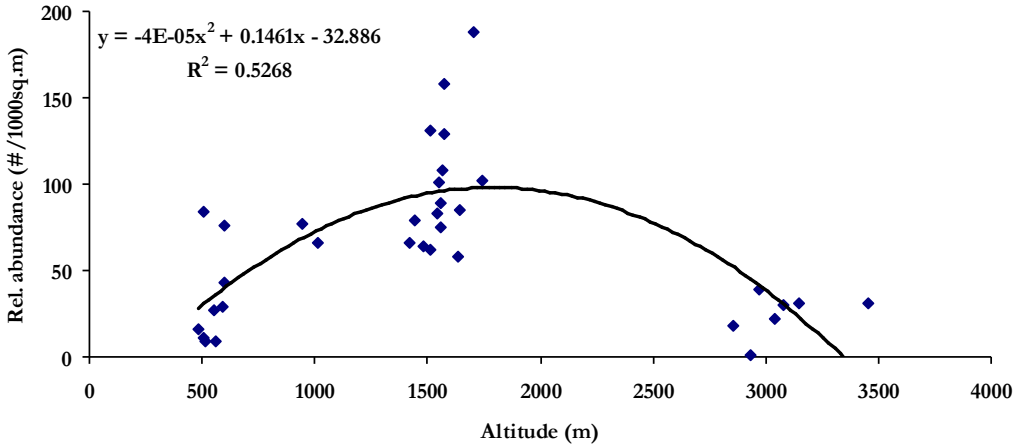

Figure 7. Relative abundance along elevation gradient in the three watersheds.

Species richness has not influenced the relative abundance in the three watersheds as evident in Figure 8 (r^2=0.26). Hence, it can be inferred here that relative abundance of the individuals in a region influences the AGB than species richness. This apparent non-influence is evident in scatter plot of species richness against AGB (Figure 9, r^2=0.005).

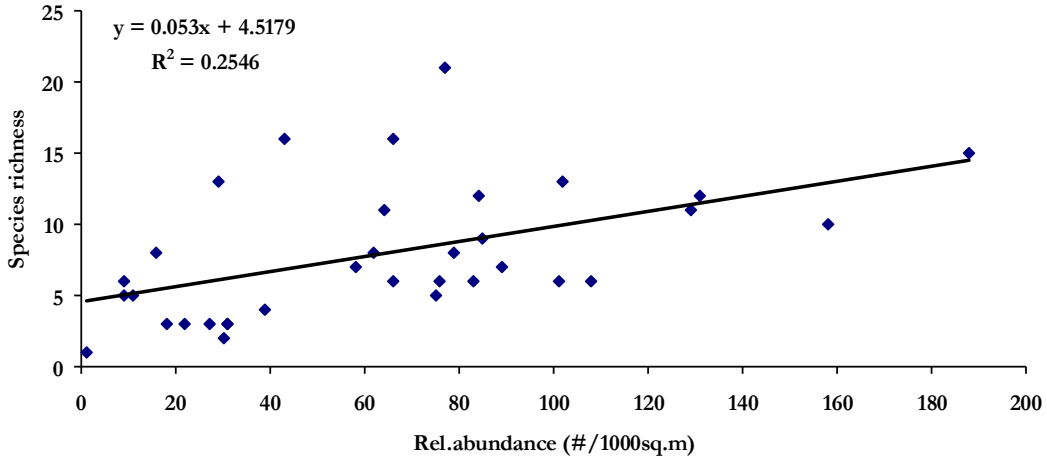

Figure 8. Scatter plot of relative abundance versus species richness in three watersheds.

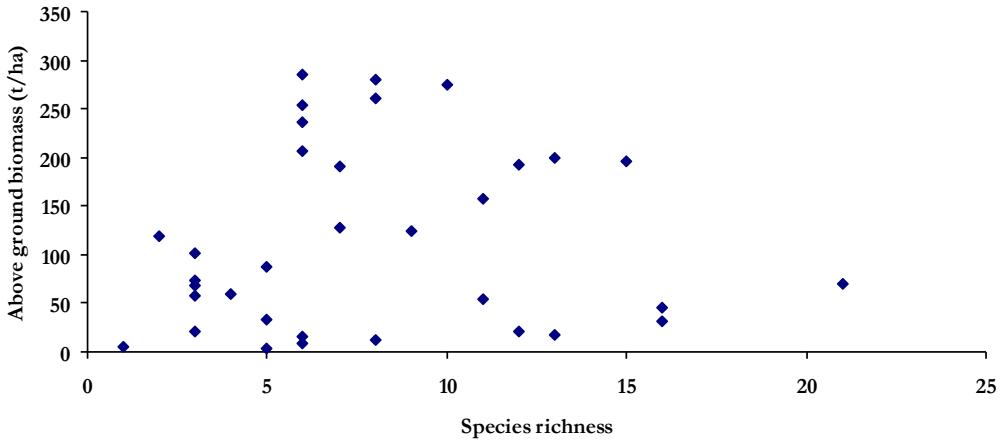

Figure 9. Scatter plot of species richness and above ground biomass in the study region.

Influence of relative abundance on the AGB estimate in the study region is illustrated in Figure 9. The apparent lower AGB estimate at higher abundance are due to plantation trees of lower girth classes from Mandhala water shed.

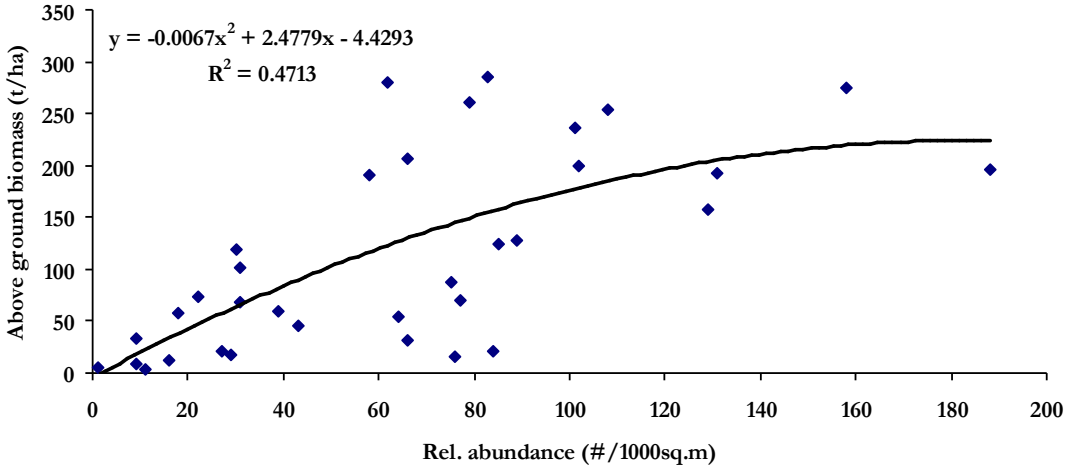

Figure 10. Scatter plot of relative abundance and above ground biomass in the study region.

The trend in biomass in the Himalayan region shows an increase in biomass with increase in altitude for different strands up to an altitude of 2700 m and shows decrease hence on, as the vegetation above 3000

m is sparse and are mostly of alpine grassland types at above 3500 m (Singh *et al.* 1994). This is evident in Figure 10 based on elevation gradient and estimated AGB in the study area.

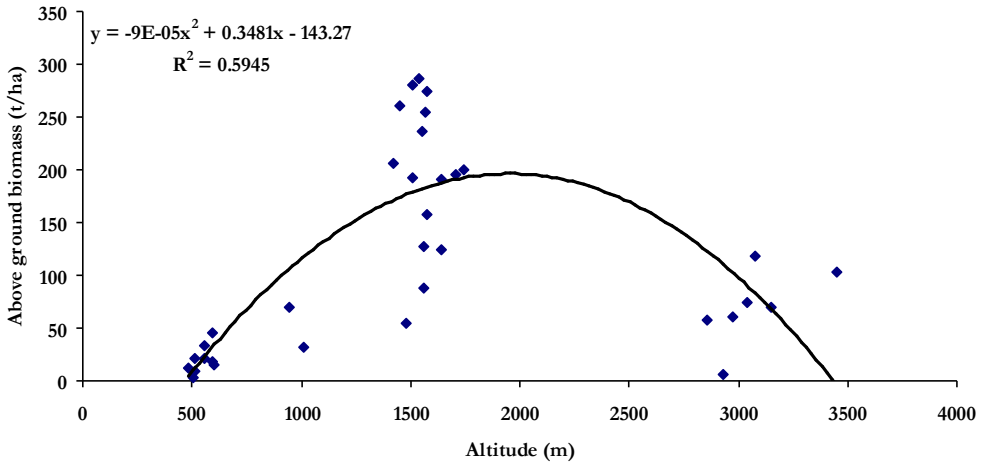

Figure 11. Scatter plot of above ground biomass against elevation gradient.

Pinus roxburghii Sarg. (chir pine) forest are dominant along the low-to-mid montane belt of Central and Western Himalaya (Chaturvedi and Singh, 1987) due to high regeneration potential, growth rate, establishing in degraded habitats, pipe like boles and high volumes.

Disturbance has become a widespread feature in most of the forests all over the Himalaya (Singh and Singh, 1992), therefore, knowledge on ecological processes and biotic pressure can help in understanding the persistence of long-lived plant communities. A sustained regeneration and growth of all species in the presence of older plants is required for better growth of any plant community (Ramakrishnan *et al.*, 1981). Humans have made considerable impacts in the Himalayan region, estimating such changes accurately would be of particular value to Himalayan people, whose subsistence agriculture depends on forest productivity to maintain livestock and soil fertility.

The distribution and dynamics of biological resources must be understood to provide a rational basis for planning and management decisions, without which conservation of these resources in the natural habitats would be impossible (Keith and Sanders, 1990; Khoshoo, 1992).

Land use patterns needs to be considered before analyzing the area that will be potentially available for biomass production, it is essential to understand the projected trends in land use pattern for the future.

Watershed approach in the Himalayan region has become acceptable in undertaking land improvement measures (Sharma *et al.*1992), however, the development has not achieved the desired pace due to lack of information available on the watershed level and because of sectoral approaches adopted by various departments working in the Himalaya (Sundriyal *et al.* 1994b).

Therefore, in many areas re-construction of disturbed ecosystems should be taken up on a priority basis, both for biodiversity conservation and for maintaining landscape productivity (Behera *et al.,* 2006)

Conclusion

The basal area, tree density and biomass per hectare is high for the watershed in the middle elevation, the mid domain effect observed in the Himalayan region is same here. The basal area and number of trees/ha for all three watershed is less than in comparison with undisturbed sites of the Himalayan region.

References:

1. Aboal, J. R.; Arevalo, J. R. & Fernandez, A. (2005), 'Allometric relationships of different tree species and stand above ground biomass in the Gomera laurel forest (Canary Islands)', *Flora - Morphology, Distribution, Functional Ecology of Plants* **200**(3), 264--274.
2. Behera S K., Misra M.K. 2006. Above ground biomass in a recovering tropical sal (*Shorea robusta* Gaertn.f.) forest of Eastern Ghats, India. *Biomass and Bioenergy* 30 :509–521
3. Bhat D.M, Ravindranath N.H, Gadgil M, 1995, Effect of Lopping intensity on tree growth and stand productivity in tropical forest. *Journal of Tropical Forest Science* 8(1): 15-23
4. Bhattacharya, S. C.; Salam, P. A.; Pham, H. L. & Ravindranath, N. H. (2003), 'Sustainable biomass production for energy in selected Asian countries', *Biomass and Bioenergy* **25**(5), 471--482.
5. Brown, S., 1997. Estimating biomass and biomass change of tropical forests. A primer. FAO Forestry Paper 134. Food and Agriculture Organization of the United Nations, Rome, Italy.
6. Brown Sandra, Schroeder Paul, Birdsey Richard. 1997. Aboveground biomass distribution of US eastern hardwood forests and the use of large trees as an indicator of forest development, *Forest Ecology and Management*. 96:37-47.
7. Brown Sandra., Schroeder Paul, Kern Jeffrey S. 1999. Spatial distribution of biomass in forests of the eastern USA, *Forest Ecology and Management*. 123: 81-90
8. Brown, S and A.E. Lugo, 1990. Tropical secondary forests, *J. Trop. Ecol.* **1990:** 1–32
9. Chave, C. Andalo, S.L. Brown, M.A. Cairns, J.Q. Chambers, D. Eamus, H. Fölster, F. Fromard, N. Higuchi, T. Kira, J.P. Lescure, B.W. Nelson, H. Ogawa, H. Puig, B. Riéra and T. Yamakura, Tree allometry and improved estimation of carbon stocks and balance in tropical forests, *Oecologia* **145** (2005), pp. 87–99.
10. Chaturvedi O.P and Singh J.S, 1987, The Structure and Function of Pine Forest in Central Himalaya. I. Dry Matter Dynamic, Annals of Botany 60: 237-252
11. Fang J Y, GG Wang, GH Liu, SL Xu,1998, Forest Biomass of China: An Estimate Based on the Biomass-Volume Relationship, Ecological Applications,8(4) pp 1084-1089
12. Garkoti S.C, Singh S.P, Variations in the Net primary productivity and Biomass of forests in high altitude region in the central Himalayan region. Journal of Vegetation Science, Vol 1, pp 23-28
13. Gaston A.J, P.J Garson, M.L Hunter Jr, 1983, The status and conservation of forest Wildlife in Himachal Pradesh in Western Himalayas, Biological Conservation, 27 pp 291-314.
14. IPCC 2003, Inter Governmental Panel on Climate Change, Report
15. Keith D A and Sanders J.M, 1990, Vegetation of the eden region, south eastern Ausralia: Species composition diversity and Structure, Journal of Vegetation Science, Vol 1: 203-232
16. Khoshoo, T.N., 1992. Plant Diversity in the Himalaya: Conservation and Utilization. G.B. Pant Memorial Lecture 1I, G.B. Pant Institute of Himalayan Environment and Development, Kosi, Almom-263443, 129 pp.

17. Krankina Olga N, Mark E. Harmon, Warren B. Cohen ,Doug R. Oetter, Zyrina Olga and Maureen V. Duane, 2004, Carbon Stores, Sinks, and Sources in Forests of Northwestern Russia: Can We Reconcile Forest Inventories with Remote Sensing Results? Climate Change, Vol 67: No. 2-3, pp 257-272
18. Luo tianxiang, Li wenhua, and Zhu huazhong. 2002. Estimated biomass and productivity of natural vegetation on the Tibetan plateau, Ecological Applications, 12:980–997
19. Northup B.K., Zitzer S.F., Archer S., McMurtry C.R., Boutton T.W. 2005. Above-ground biomass and carbon and nitrogen content of woodyspecies in a subtropical thornscrub parkland. *Journal of Arid Environments*. 62: 23–43
20. Schroeder, S. Brown, J. Mo, R. Birdsey and C. Cieszewski , Biomass estimation for temperate broadleaf forests of the US using inventory data. *Forest Science* **43** (1997), pp. 424–434
21. Sharma.M, Current environmental problems and future perspectives, *Tropical Ecology* **37** (1996), pp. 15–20
22. Sharrna, E., Sundriyal, R.C., Rai, S.C., Bhatt, Y.K., Rai, L.K., Sharma. R. and Rai, Y.K., 1992. Integrated watershed management: A case study in Sikkim Himalaya. Gyanodaya Prakashan. Nainital, 120 pp.
23. Sundriyal, R.C., Sharma, E., Rai, L.K. and Rai, S.C., 1994a. Tree structure, regeneration and woody biomass removal in a subtropical forests of Mamaly watershed in the Sikkim Himalaya. Vegetation 113: 53-63.
24. Patenaude G, R Milne, TP Dawson, 2005, Synthesis of remote sensing approaches for forest carbon estimation: reporting to the Kyoto Protocol, Environmental Science and Policy, Volume 8, Issue 2, pp 161-178
25. Singh Arvind, Jha A.K. & Singh J.S. 1997. Influence of a developing tree canopy on the yield of Pennisetum pedicellatum sown on a mine spoil, Journal of Vegetation Science, 8:537-540.
26. Singh Surendra P, Adhikari Bhupendra S., Zobel Donald B. 1994. Biomass, Productivity, Leaf Longevity, and Forest Structure in the Central Himalaya, Ecological Monographs, 64: 401-421.
27. Singh Lalji and Singh J.S 1991**,** Species Structure, Dry Matter Dynamics and Carbon Flux of a Dry Tropical Forest in India**,** Annals of Botany 68: 263-273
28. UNFCCC. 1997. "Climate Change Secretariat" [Web Page]. Available at http://www.unfccc.de/.
29. UNFCCC. 1997. Kyoto Protocol to the United Nations Framework Convention on Climate Change. Kyoto: United Nations Framework Convention on Climate Change.

Annexure – I

Biomass is defined as the total amount of aboveground living organic matter in trees expressed as oven-dry tons per unit area. Biomass estimation of vegetation in general, forests in particular has received serious attention over the last few decades for the very reason that components of climate change are associated with change in the biomass of a region. From ecosystem perspectives, biomass estimation helps in ecosystem productivity, energy and nutrient flows, and for assessing the contribution of changes in forest lands to the global carbon cycle. The potential carbon emission that could be released to the atmosphere due to degradation of forest and forest resource, deforestation and conversion of forested area into other land-use can be determined by biomass estimation. Hence, the precise estimation of biomass becomes necessary for understanding the importance of forest both at global scale as well as regional scale for their impact in climate change.

Literature review

Methods involved in estimation of above ground biomass: There are two approaches for estimating aboveground biomass (AGB) in trees, namely

- **Destructive,**
- **non-destructive**.

The destructive method involves harvesting tree samples and estimating wood density and above ground biomass followed by deriving a probable relationship between tree girth, height with above ground biomass. Rai (1984) developed equations based on destructive sampling of four tropical rainforests of Western Ghats of Karnataka and compared the regression models against D^2H and DBH (where D is diameter in cm, H is height in m and DBH is diameter at breast height in cm) , both in log and non-log models. Most of recent non-destructive methods involving allometric equations are based on earlier destructive sampling methods. Destructive sampling gives precise biomass estimation, but cannot be done in all situations and more over this requires considerable amount of trees to be cut. Hence biomass estimation through non-destructive method is adapted nowadays.

In non-destructive techniques, forest biomass is estimated mathematically, using functions which relate the diameter of a tree to its biomass- or parts of its biomass- (leaves, bark, bole wood etc). This approach is further divided into a direct approach using allometric equations, and an indirect approach using biomass expansion factors.

i) Allometry is the relation between the size of an organism and the size of any of its parts, and allometric equation is usually expressed in power-law form or in logarithmic form. Once an allometric equation has been developed, the biomass can be estimated in a forest stand using just the simple measurements of diameter.

The allometric equation's general form is usually written as,

$$y = bxa$$

or

$$\ln y = \ln b + a \ln x$$

where b is a constant, called allometric coefficient and a is the allometric exponent.

Ketterings et al. (2001) proposed allometric equation based on original data collected in field study in Indonesia. It is more flexible and reduces estimated errors due to change in site. Laurance et al. (1999) estimated above-ground dry biomass of living trees including palms in central Amazonia. The biomass attained from 231 to 492 tha^{-1}, with a mean of 356 ± 47 tha^{-1}.

ii) Biomass expansion factor and root-to-shoot ratio: To calculate living aboveground biomass in plantations, a biomass expansion factor is applied to the commercial volume of trees as well as wood density. The biomass expansion factor is the ratio of total aboveground oven-dry biomass of trees with a minimum DBH of 10 cm or more to the oven-dry biomass of the inventoried volume (Brown, 1997). Biomass expansion factors from inventories in tropical Asia, America, and Africa were reported to be 1.1 and 2.5 (Brown and Lugo 1990; Brown, 1997). Root-to-shoot ratio is expressed as the ratio of the weight of the root to the weight of the top. For instance, a high root-to-shoot ratio means that the tree has much more biomass belowground than aboveground. The equation for estimating total biomass as follows:

$$TB = [V \bullet D \bullet BEF] \bullet (1 + R)$$

where:

TB=total biomass

V=merchantable volume (see Chapter 4 in the GPG/LULUCF)

D=basic wood density

BEF=biomass expansion factor for conversion of commercial volume to aboveground biomass

R=root-to-shoot ratio

Other methods

Gillespie *et al.*, (1992) estimated AGB based on commercial inventory stand and stock tables through a variety of techniques. The most accurate method of estimating the number of stems in smaller (10-15 cm) diameter classes used the ratio of the numbers of stems in the two smallest diameter classes.

Mandal and Laake (2005) using LAI (Leaf area index) estimated AGB. LAI was extracted from the canopy photos, taken by hemispherical camera and analysed by the use of Gap Light Analyzer. They developed two linear models for above ground biomass and LAI. The LAI is related with the photosynthetically active surface (for photosynthesis etc.) which allows the tree to grow and accumulate the biomass. Now LAI is widely used as a reliable tool to develop the relationship with forest biomass (Kiniry *et al.,* 1999). Lu *et al*., (2002) developed equations based on image data and vegetative inventory data to estimate biomass in moist tropical areas in Brazilian Amazon basin. These are suitable to estimate above ground biomass of dense vegetation areas. Above ground biomass is difficult to quantify over large areas using traditional technique (direct estimation). Remote sensing has opened an effective way to estimate forest biomass and carbon (Rosenqvist et al., 2003) over large areas. Based on Lidar remote sensing technique, Lefsky (1999) developed equation of canopy structure and above ground biomass. The equation explained 84% of variance in above ground biomass ($P<0.0001$). These were validated in the temperate deciduous, temperate coniferous and boreal coniferous biomes.

Santos *et al*., (2003) proposed equation based on different polarizations of Polarimetric band Synthetic Aperture Radar data for tropical primary and secondary forests. Okuda *et al*., (2004) aerial photographs taken by satellite remote sensing and inventory data collected by destructive sampling in the same area and developed equations for in an old-growth primary forest and in a regenerating logged forest, both within the tropical rainforest of the Pasoh Forest Reserve in Peninsular Malaysia.

Above ground biomass estimate in different biomes

Tropical forest

Murphy and Lugo (1986) estimated plant biomass, based on destructive sampling of trees in dry Guanica forest of Puerto Rico. Total Above ground biomass for live plants was 44.9 tha^{-1}. Live trees (DBH $\geq$ 5 cm) had 16 tha^{-1} aboveground live biomass and 68 tha^{-1} dead biomass. Ground vegetation (DBH< 5 cm) had 28.7 tha^{-1} above ground biomass. Live woody plant biomass was 65.6 % of the total biomass, epiphytes were 0.2 %, standing dead stems were 12.2% (82% for stems DBH<5 cm), and leaf and wood litter 22%. Total biomass of live foliage for trees and ground vegetation was 4.6 tha^{-1}. Root biomass was 45 tha^{-1} or 50 percent of total live plant biomass. Approximately 70% of the root biomass was concentrated within 40 cm of the soil surface, with 57% in the upper 10 cm.

Rai and Proctor (1986) had studied four evergreen rainforest sites Agumbe, Bannadpare, Kagneri and South Bhadra at 575-800 m altitude in Karnataka, southern India. They found the total AGB to be 420-649 tha^{-1} and the root fraction to be 13.9-20.2 tha^{-1}. Girth increment data over 35 years were available for one site and these were used with biomass estimates to calculate the approximate mean annual increase of above-ground and root (>5-cm girth) biomass in the four sites. These were 6.4-11.1 tha^{-1} for aboveground material and 0.2-0.4 tha^{-1} for roots. In one plot biomass was estimated by destructive sampling of small trees (<5 cm dbh) and herbs. The combined AGB of these fractions was 7.2 tha^{-1}.They developed six allometric equations based on destructive sampling of 465 trees.

Similar allometric equations were developed by Overman *et al*., (1994) based on destructive sampling of 54 trees in terra firme forest near Araracuara in Colombia, Ares and Fownes (2000) for tropical ash (*Fraxinus uhdei*) trees growing on organic uplands soils in the island of Hawaii, Cordero and Kanninen

(2002) with 17 trees of *Bombacopsis quinata* in two different climatic zones of Costa Rica. Foliage, branch, and stem biomass were highly correlated with DBH ($r > 0.68$, $n = 17$).

Cummings *et al*., (2002) developed equations based on forest inventories and quantified the total above ground biomass (TAGB) and forest structure in 20 intact Amazonian tropical sites in Western Brazil. The TAGB of open forest ranged from 288 to 346 tha^{-1}, with a mean of 313 tha^{-1}; desce forest TAGB ranged from 298 to 533 tha^{-1}, with a mean of 377 tha^{-1}; and ecotone forests TAGB ranged from 298 to 422 tha^{-1}, with a mean of 350 tha^{-1}. Mean TAGB for all 20 sites was 341 tha^{-1}.

For mixed hard wood forest trees near Franklin, North Carolin, Elliott *et al.,* (2002) developed allometric equations. These equations were used to estimate branch and stem biomass of *Acer rubrum*, *Cornus florida*, *Liriodendron tulipifera*, *Quercus prinus*, *Quercus rubra*, *Robinia pseudoacacia* trees and to estimate biomass for all oaks and all tree species. Tiepolo et al. (2002) proposed equation based on destructive sampling of fern tree (*Cyathea* spp.) at the Atlantic Forest biome in Paraná State, Brazil. They also estimated the average carbon stock using established equations for submontane forest was 135.9 $tCha^{-1}$, lowland forest was 106.8 $tCha^{-1}$, floodplain forest was 64.12 $tCha^{-1}$, advanced/medium forest was 106.1 $tCha^{-1}$, medium secondary forest was 101.96 $tCha^{-1}$, young secondary forest was 42.89 $tCha^{-1}$, pasture strata was 2.4 $tCha^{-1}$, and for shrub land was 7.4 $tCha^{-1}$.

For moist tropical forest, Chave *et al*., (2003) estimated AGB at Barro Colorado Island, Panama. Total mean above ground biomass was 281±20 tha^{-1}. Palms contributed 1.5 tha^{-1} (*i.e.* about 0.5%). The mean AGB change over 15 years was + 0.21 $tha^{-1}year^{-1}$ with a 95% confidence of -0.68 to 0.63 $tha^{-1}year^{-1}$ and no spatial autocorrelation was found in AGB growth or mortality across subplots ($r^2 < 0.001$ in all cases). Branch falls and partial breakage of stems contributed 0.46 $tha^{-1}year^{-1}$ to the AGB loss. Trees (diameter < 10cm) contributed about 5% of AGB increment.

For dry deciduous forests of Madhya Pradesh, India, Kale *et al*., (2004) developed allometric equations based on non-destructive sampling of five species, viz. *Ziziphus xylopyra*, *Tectona grandis*, *Lannea coromandelica*, *Bauhinia racemosa*, and *Miliusa tomentosa*. These equations were validated to estimate species-specific bole biomass at the local and regional level. For developing equations they measured Circumference at breast height (cbh) and bole (cone) height of each selected tree. With the help of stem-borer, wood samples were taken from all the representative girth classes of each species. Length of each wood sample and its oven-dried weight were noted. Bole volume (V) and coefficient of dry weight (cd) were calculated and finally multiplied together to get the sample tree biomass in kilograms.

For pine forest shrub layer, Sah *et al*., (2004) developed equations based on destructive sampling 10 common hardwood species in lower Florida Keys. Total shrub biomass included plant parts of all sizes and shrub fine fuel included the biomass of leaves, reproductive parts, and stems <6.3 mm diameter. The equations were validated in estimating shrub biomass in pine forests elsewhere in the Caribbean basin, and in other dry tropical environments. Similarly, Aboal *et al*., (2005) developed allometric equations for five species (*Erica arborea*, *Ilex canariensis*, *Laurus azorica*, *Myrica faya* and *Persea indica*) in four types of laurel forest in the Garajonay National Park on Gomera Island in the Canary Islands. Biomass

were estimated using total volume of trunk, primary branches (i.e. those inserting directly to the trunk), and secondary branches and used the previously published values for the density of dry wood.

Chave *et al*., (2005) developed equations using a dataset of 2,410 harvested trees (DBH ≥ 5 cm), in 27 sites across the tropical forests in three continents: America, Asia, and Oceania. Models were tested and selected best predictive models for dry, moist, wet and mangrove forests. These are valid in the range 5–156 cm for D, and 50–1,000,000 for ρD^2H. (D is trunk diameter at 130cm above ground, H is total tree height and ρ is wood specific gravity) for broadleaf tree species. Murali *et al*., (2005) developed and tested statistically allometric equations based on data collected from published reports to estimate biomass of deciduous tropical forests.

Brandies *et al*., (2006) proposed equations based on destructive sampling of 30 trees (that were cleared for road construction) from *Bucida buceras*, *Bursera simaruba*, *Eugenia monticola*, *Krugiodendron ferreum*, *Bourreria succulenta* and *Gymnanthes lucida* at deciduous dry forest site near Ponce, Puerto Rico. Equations were established to estimate leaf, woody, and total AGB for *Bucida buceras* and mixed dry forest species and to estimate inside and outside bark total and merchantable stem volume using both diameter at breast height and total height, and diameter at breast height alone for *B. buceras*, *Bursera simaruba* and mixed dry forest species.

Temperate forest

Czapowskyj *et al*., (1985) presented equations based on destructive sampling of young black spruce (*Picea mariana*) in northern Maine. They used weighted and ordinary least squares model to construct the equations for small trees from 1 to 15 cm dbh and for trees less than 2 m in height, respectively. In complete oven dry tree biomass around 80% was above ground biomass and 20% was stump(less than 6 cm in height) and roots. Fang *et al*., (1998) proposed equations based on inventory data and statistically tested with the data sets of 758 field measurement in China. Estimated total forest biomass was 9103×106 t with the contribution of forests, special product plantations and bamboo forests was 8592×106, 326×106, and 185×106 t, respectively. The area-weighted mean biomass density was 84 tha^{-1}.

Brown *et al*., (1999) estimated biomass density and carbon stocks, using inventory data of all eastern USA forests. For hardwood forests, total biomass density was 36 to 344 tha^{-1} and mean of area-weighted was 159 t ha^{-1} and for softwood forest, total biomass density was 2 to 346 tha^{-1} and mean of area-weighted was 110 tha^{-1}. The total biomass pool was 20500 ×106 t and hardwood forests were 80% of total biomass. In Kloesterhede, Denmark, Ingerslev and Hallbäcken (1999) proposed equations based on destructive sampling of 59-year-old Norway spruce stand. They harvested five trees from each of four plots (Control, Ca MgPS, CaMgPS + NPK, and CaMgP + NPK).Biomass of stem wood, stem bark, living branches and older needles were closely correlated (r^2=0.70) with the tree size. After 9 year investigation the biomass and stem volume growth were not affected (P≤0.05) by the different treatements, but above ground biomass were increased by NPK fertilization. The amount of P in the above ground biomass increased from 2.3 kg ha^{-1} to more than 5 kg ha^{-1} after treatments.

Ponette *et al*., (2001) proposed equations based on destructive sampling of *Pseudotsuga menziesii* (Mirbel) Franco stands in French forest. Total AGB increased from ~160 tha^{-1} in the youngest stands to 360 tha^{-1} in the 54-year old stands. Stem wood biomass was 70 to 80% of total aboveground biomass. Stem bark or needles contributed ≤10% and bark contributed 30 to 60% to total stem biomass. For *Acer pensylvanicum* L. and *Castenea dentate* (Marsh.) Borkh in the Appalachian mountains of western Virginia, USA, King (2003) developed equations based on destructive sampling. Similarly, Xiao and Ceulemans (2004) based on destructive sampling for 10-year-old Scots pine (*Pinus sylvestris*). In central Japan, for temperate deciduous forest, Jia and Akiyama (2005) developed allometric equations, assessing seven components of carbon storage. The total carbon storage was 440.6 $tCha^{-1}$.

Lefsky *et al.*, (2005) used equation to calculate total aboveground biomass and the LCD (Lidar change detection) approach was applied to estimate only NPPAw (aboveground wood production) for relatively young stands in western??????. They estimated: 6.7 tha^{-1} $year^{-1}$ from the LCD approach, 6.8 $tha^{-1}year^{-1}$ from Biome-BGC, and 7.2 $tha^{-1}year^{-1}$ from the inventory approach. Biome-BGC is a daily time-step biogeochemistry model with physiologically based algorithms for photosynthesis, autotrophic respiration and heterotrophic respiration.

Zianis *et al*. (2005) presented equations for *Abies* spp, *Eucalyptus* spp., *Picea* spp and *Quercus* spp. based on the review of Europian tree species. They proposed 607 biomass equations and 30 stem volume equations. Hall et al., (2006) used BioSTRUCT (Biomass estimation from stand STRUCTture) model for AGB. This model was based on georeferenced field plots to generate empirical relationships between continuous estimates of forest structure attributes and remote sensing image data represented as spectral response variables. Average AGB estimates were within 4 tha^{-1} and stand volume was within 4 m^3/ha of field plot values, statistically similar to a validation sample data set for both AGB (P = 0.61) and stand volume (P = 0.65). Wang (2006) developed and tested statistically allometric equations based on destructive sampling of 10 species in northeastern Chinese temperate forest. These were validated with field samples and relative errors were estimated.

Above ground biomass estimate in Himalaya

In the central Himalaya region, Rana *et al*., (1989) developed equations based on destructive sampling of trees at 300-2200 m. The biomass was 199 and 787 tha^{-1} and the net primary productivity was 12.8-27.9 $tha^{-1}year^{-1}$. The net production in trees ranged between 9.1 and 25.1 tha^{-1} $year^{-1}$, respectively, in chir-pin/mixed-broadleaf forest and tilonj-dominated mixed-oak forest. Percentage net production in dominant trees in their respective forests was: 83.2-84.8% of *Shorea robusta* in sal forests; 31.1-94.7% in *Pinus roxburghii*, respectively, for chir-pine/mixed-broadleaf forest and chir-pine forest; 66.0% in *Quercus leucotrichophora* in mixed banj-oak/chir-pine forest; 70.4% in *Quercus lanuginose* in rianj-dominated mixed-oak forest; and 34.7% in *Quercus floribunda* in tilonj-dominated mixed-oak forest.

Tiwari (1992) developed and tested statistically allometric equations based on non harvest technique. Wood samples for bole were collected using stem borer and results obtained through models compared with the estimates obtained through harvest method.

Zomer and Menke (1993) proposed equation based on the site index of Himalayan alder (*Alnus nqbalensis*) and large cardamom (*Amomum subulatum*) at the Kosi and Mechi zones of the Eastern Development Region of Nepal. Tree biomass production was 14 $tha^{-1}yr^{-1}$ and after thinning standing biomass was increased in average 11 $tha^{-1}yr^{-1}$. After 25 years plantation average quantified total standing biomass was 273 tha^{-1}.

Singh *et al*., (1994) estimated the biomass and Net primary productivity in Kumaun forests of Indian central Himalaya. Biomass was 500-600 tha^{-1}, from foothills to 2600m elevation, but for *P.roxburghii* at 1300 and 1750 m was ≈200 t ha^{-1}. Above 2600m biomass was 170 tha^{-1} in birch forest with rhododendrons at 3100-3200 m elevation. At ≈3300 m elevation, the biomass was 40t ha^{-1}. In *S. robusta* forest at 300 m and in *Q. floribunda* forest at 2200 m elevation, forest biomass exceeded 700t ha^{-1}. 2400 t ha^{-1} biomass occurred at 3400 m elevation in the Nepal central Himalaya. In Kumaun and Nepal, *Q. semecarpifolia* forest attained similar maximal biomass, up to 550-600 tha^{-1} near 2600 m elevation. Total net primary productivities (NPP) were 15-20 $tha^{-1}yr^{-1}$ from the foothills to 2700 m elevation, and they declined above 2700 m. *Q. floribunda* forest and a *C.deodara* plantation forest had high productivity 25.1 and 28.2 $tha^{-1}yr^{-1}$ respectively at 2200 m.

Sundriyal and Sharma (1996) proposed equations using tree volume and specific wood density for *Quercus lamellose*, *Castanopsis tribuloides*, *Symplocos theaefolia*, *Eurya acuminate*, *Alnus nepalensis*, Other species group and total species in a temperate forest of the Mamlay watershed in Sikkim Himalaya. Tree density varied from 536 to 756 trees ha^{-1} and basal area from 39.79 m^2ha^{-1} to 81.0 m^2ha^{-1}. Net primary productivity was 8.32 $tha^{-1}y^{-1}$ for wood biomass and 1.80 $tha^{-1}y^{-1}$for floor phytomass (excluding litter). 75% of the total biomass was contributed by dicotyledons and 25% by monocotyledons and ferns. For 1-4 yr old poplar (*Populus deltoides*) plantations in the Tarai belt of the central Himalayan mountains, Lodhiyal and Lodhiyal (1997) gave allometric equations. The total vegetation biomass was 12.0 tha^{-1} for 1-yr-old and 113.0 tha^{-1} for 4-yr-old. Luo *et al*., (2002) developed the QZNPP model for estimating the Net primery Productivity (NPP) on the Tibetan plateau based on the data collected from forest and grassland inventories and ecological research sites. Garkoti (2007) generated equations based on sampling of *Acer cappadocicum* and *Meliosma dilleniaefolia* trees which were fallen due to heavy snowfall in the west central Himalayas. Total vegetation biomass was 308.3 t ha^{-1} and the annual litter fall was 6.2 t ha^{-1}.

Above ground biomass estimate in plantations

Fang *et al*., (1998) proposed equations based on inventory data and statistically tested with the data sets of 758 field measurement in China. Estimated total forest biomass was 9103×106 t with the contribution of forests, special product plantations and bamboo forests was 8592×106, 326×106, and 185×106 t, respectively. The area-weighted mean biomass density was 84 tha−1. For 19 lianas at eastern Brazilian Amazon fores, Gerwing and Farias (2000) developed equation based on harvesting of these species. Total stand above ground live biomass was estimated as 314 tha-1 of which 43 tha-1 (14%) was lianas. Liana leaf area index (LAI) varied from 1.3 m^2m^{-2} to 5.3 m^2m^{-2}.

Goel and Behl (2005) developed linear regression equations between growth parameters and productivity for 8-yr-old *Casuarina glauca* at Banthra in Lucknow, Uttar Pradesh. These equations were based on plant height (h), diameter (d^2) or both (d^2h). Height alone had relatively poor functional correlation with

yield (r^2 = 0.45). At the age of 8 years, stand productivity was 68.2 tha^{-1}(oven dry biomass) out of which relatively 80.3% of biomass was allocated to stem wood (54.8 tha^{-1}). Both branch wood (8.4 tha^{-1}) and leaves (5 tha^{-1}) contributed marginally. Similarly, Uri et al. (2007) generated equations based on destructive sampling of 8-year-old stands of silver birch growing on different soil types. The density of the studied stands varied from 3060 to 36 200 trees per ha and their above-ground biomass varied from 6.0 to 22.9 tha^{-1}.

Salis *et al*., (2006) developed equations based on destructive sampling of five species: *Protium heptaphyllum*, *Magonia pubescens*, *Diptychandra aurantiaca*, *Terminalia argentea* and *Licania minutiflora* and sampling of a miscellaneous group of 11 different less abundant species in a region of woodland savanna on Rio Negro farm in the Pantanal of Nhecolandia, Brazil. Miehle *et al*., (2006) established equation based on photosynthesis and evapotranspiration-nitrification-denitrification and decomposition forest model for 4 and 6 year old *Eucalyptus globules* in 28 permanent sample plots of southeastern Australia.

Above ground biomass estimate for other vegetation types

Sharifi *et al*., (1982) established equation based on non-destructive sampling of *Prosopis glandulosa* in the sonoran desert of California. Total above-ground biomass was 43-760 kg per plant and 1.9-8.5 kg m^{-2} canopy area. Stand biomass was 23,000 kg ha^{-1} to 3,500 kg ha^{-1}. Net above-ground primary production was 2.2 kg m^{-2} canopy for shrub forms and 5.3 kg m^{-2} canopy for tree forms. Mean stand production was 3,650 kg ha^{-1}. 51.5% of productivity was produced by new woody tissues of trunk and branches and 33.6% was produced by leaves.

Brown *et al*., (1997) used equations developed by Schroeder *et al*., (1997) to determine quantities and distribution of aboveground biomass density of US eastern hardwood trees (> 70 cm diameter). For trees, palms and lianas of primary and secondary forest in Colombia, In north Peru, for *Prosopis pallida*, Pardon and Navarro (2004) developed and tested allometric equations based on destructive sampling of 17 individuals. Singh et al. (1997) developed allometric equations based on destructive sampling of *Petlnisetum pedicellatum* at the Jayant coal mine in the Singrauli coal field. The relation was established between incident light and grass biomass under developing canopies of tree plantations on the mine spoil.

Návar et al. (2002) proposed equations based on destructive sampling of tree in the *Tamaulipan* thornscrub of northeastern Mexico. The total standing biomass was 60.31 ± 12.24 tha^{-1}, composed of leaf 2.51 ± 0.47 tha^{-1}, branch 24.44 ± 4.88 tha^{-1}, stem 9.80 ± 2.62 tha^{-1}, and root 23.56 ± 4.25 tha^{-1}.

Baker et al. (2004) used equations and updated inventory data to analyze the biomass change in 59 sites of old-growth Amazonian forest. They found that the above-ground dry biomass in trees that are more than 10 cm in diameter (AGB) has increased since plot establishment by 1.22 ± 0.43 $tha^{-1}yr^{-1}$ or 0.98 ± 0.38 $tha^{-1}yr^{-1}$, if individual plot values were weighted by the number of hectare years of monitoring.

Jepsen (2006) developed equations based on biometric data and quantitative data of fallow land trees in Sarawak, Malaysia.The biomass of fallows became saturated after 6 years at 47 t dry matter(DM)per hectare and biomass accumulated at the rate of up to 12.7 t carbon per hectare per year.

Sierra et al. (2007) developed allometric equations Tree diameter explained the variation in individual tree biomass for aboveground and belowground pools with the exception of palms, for which height was the explanatory variable.

References

1. Aboal Jesus Ramon, Arevalo Jose Ramon, Fernandez Angel. 2005. Allometric relationships of different tree species and stand above ground biomass in the Gomera laurel forest (Canary Islands), Flora 200: 264–274
2. Ares, A and JH Fownes. 2000. Comparisons between generalized and specific tree biomass functions as applied to tropical ash. New Forests 20: 277-286
3. Baker Timothy R., Phillips Oliver L., Malhi Yadvinder, Almeida Samuel, Arroyo Luzmila, Fiore Anthony Di, Erwin Terry, Higuchi Niro, Killeen Timothy J., Laurance Susan G., Laurance William F., Lewis Simon L., Monteagudo Abel, Neill David A., Vargas Percy Nunez, Pitman Nigel C. A., Silva J. Natalino M. and Martı´nez Rodolfo Va´squez, 2004, Increasing biomass in Amazonian forest plots, Phil.Trans.R.Soc.Lond.B. 359, 353-365.
4. Brandeis Thomas J., Delaney Matthew, Bernard R. Royer Parresoland Larry. 2006. Development of equations for predicting Puerto Rican subtropical dry forest biomass and volume, Forest Ecology and Management, 233:133-142 .
5. Brown, S and A.E. Lugo, 1990. Tropical secondary forests, *J. Trop. Ecol.* 1990: 1–32.
6. Brown Sandra, Schroeder Paul, Birdsey Richard. 1997. Aboveground biomass distribution of US eastern hardwood forests and the use of large trees as an indicator of forest development, Forest Ecology and Management 96:37-47.
7. Brown Sandra., Schroeder Paul, Kern Jeffrey S. 1999. Spatial distribution of biomass in forests of the eastern USA, Forest Ecology and Management 123: 81-90
8. Brown, S., 1997. Estimating biomass and biomass change of tropical forests. A primer. FAO Forestry Paper 134. Food and Agriculture Organization of the United Nations, Rome, Italy.
9. Chave Jérôme, Condit Richard, Lao Suzanne, Caspersen John P., Foster Robin B. Hubbell Stephen P. 2003. Spatial and Temporal Variation of Biomass in a Tropical Forest: Results from a Large Census Plot in Panama, The Journal of Ecology, 91:240-252.
10. Chave J., Andalo C., Brown S., Cairns M. A., Chambers J. Q., Eamus D., Folster H., Fromard F., Higuchi N., Kira T., Lescure J.-P., Nelson B. W., Ogawa H., Puig H., Riera B., Yamakura T., 2005. Tree allometry and improved estimation of carbon stocks and balance in tropical forests, Oecologia, DOI 10.1007.
11. Cordero Luis Diego Pérez and Kanninen Markku. 2002. Wood specific gravity and aboveground biomass of Bombacopsis quinata plantations in Costa Rica, Forest Ecology and Management, 165: 1-9.
12. Cummings D. L, Kauffman J. Boone, Perry David A., Hughes R. Flint. 2002. Above ground biomass and structure of rainforests in the southwestern Brazilian Amazon, Forest Ecology & Management, 163: 293-307.
13. Czapowskyj M. M., Robison D. J., Briggs R. D.,; White E. H. 1985. Component biomass equations for black spruce in Maine, Res. Pap. NE-564,

14. Elliott Katherine J., Boring Lindsay R., and Swank Wayne T. 2002. Aboveground biomass and nutrient accumulation 20 years after clear-cutting a southern Appalachian watershed, Can. J. For. Res. 32: 667-683.
15. Fang Jing-yun, Wang G.Geoff, Liu Gew-Hua, Xu Song-Ling. 1998. Forest biomass of china: an estimate based on the biomass-volume relationship, Ecological Applicntioris, 8:1084-1091
16. Garkoti S. C. 2007. Estimates of biomass and primary productivity in a high-altitude maple forest of the west central Himalayas, Ecol Res DOI 10.1007/s11284-007-0355-2.
17. Gerwing Jeffrey John and Farias Damiaão Lopes. 2000. Integrating liana abundance and forest stature into an estimate of total aboveground biomass for an eastern Amazonian forest, Journal of Tropical Ecology, 16:327-335.
18. Gillespie, A.J.R., Brown, S. and Lugo, A.E., 1992. Tropical forest biomass estimation from truncated stand tables. Forest Ecology and Management. 48: 69-87.
19. Goel V.L., Beh H.M. 2005. Growth and productivity assessment of Casuarina glauca Sieb. ex. Spreng on sodic soil sites, Bioresource Technology 96: 1399–1404.
20. Hall R.J., Skakun R.S., Arsenault E.J., Case B.S., 2006. Modeling forest stand structure attributes using Landsat ETM+ data:Application to mapping of aboveground biomass and stand volume, Forest Ecology Management 225: 378-390
21. Ingerslev Morten and Hallbäcken Leif. 1999. Above ground biomass and nutrient distribution in a limed and fertilized Norway spruce (Picea abies) plantation,Forest ecology and management, 119:21-38.
22. Jepsen Martin Rudbeck, 2006. Above-ground carbon stocks in tropical fallows, Sarawak, Malaysia, Forest Ecology and Management 225: 287–295
23. Jia Shugang and Akiyama Tsuyoshi. 2005. A precise, unified method for estimating carbon storage in cool-temperate deciduous forest ecosystems, Agricultural and Forest Meteorology, 134: 70–80
24. Kale Manish , Singh Sarnam, Roy P. S., Deosthali Vrishali and Ghole V. S. 2004. Biomass equations of dominant species of dry deciduous forest in Shivpuri district Madhya Prades Current Science, 87:pp?
25. Ketterings Quirine M., Coe Richard, Noordwijk Meine van, Ambagau Yakub and Palm Cheryl A. 2001. Reducing uncertainty in the use of allometric biomass equations for predicting above-ground tree biomass in mixed secondary forests , Forest Ecology and Management ,146:199-209.
26. King D. A. 2003. Allocation of above-ground growth is related to light in temperate deciduous saplings, Functional Ecology,17:482-488.
27. Kiniry, J. R., C. R. Tischler and G. A. Van Esbroeck. 1999. Radiation use efficiency and leaf CO_2 exchange for diverse C_4 grasses. Biomass and Bioenergy. 17:95-112.
28. Laurance William F., Fearnside Philip M., Laurance Susan G., Delamonica Patricia, Lovejoy Thomas E., Merona Judy M.Rankin-de, Chambers Jeffrey Q., Gascon Claude, 1999. Relationship between soils and Amazon forest biomass: a landscape-scale study, Forest Ecology and Management 118: 127 -138.
29. Lefsky M.A., Cohen W.B., Acker S.A., Spies T.A., Parker G.G. and Harding D., 1999. Lidar remote sensing of biophysical properties and canopy structure of forest of Douglas-fir and western hemlock, Remote Sensing of Environment. 70: 339–361.
30. Lefsky M.A., Hudak A.T., Cohen W.B. and Acker S.A. 2005. Geographic variability in lidar predictions of forest stand structure in the Pacific Northwest, Remote Sensing of Environment, 95: 532–548.
31. Lodhiyal L.S. and Lodhiyal Neelu. 1997. Variation in biomass and net primary productivity in short rotation high density central Himalayan poplar plantations, Forest Ecology and Management, 98:167- I79.
32. Luo tianxiang, Li wenhua, and Zhu huazhong. 2002. Estimated biomass and productivity of natural vegetation on the Tibetan plateau, Ecological Applications, 12:980–997

33. Lu Dengsheng, Mausel Paul, Brondizio Eduardo and Moran Emilio. 2002. Above ground biomass estimation of successional and mature forersts using TM images in the Amazon Basin, Symposium on geospatial theory, Processing and applications, Symposium sur la theorie, les traitements et les applications des donnees Geospatiales, Ottawa.
34. Mandal R. A. and Laake P. van. 2005. Carbon sequestration in community forests: an eligible issue for CDM (A case study of Nainital, India), Banko Janakari, 15:53-61.
35. Miehle P., Livesley S.J., Feikema P.M., Li C., Arndt S.K. 2006. Assessing productivity and carbon sequestration capacity of Eucalyptus globulus plantations using the process model Forest-DNDC: Calibration and validation, Ecological Modelling. 192: 83–94
36. Murali K.S., Bhat D.M. and. Ravindranath N.H. 2005. Biomass estimation equation for tropical deciduous and evergreen forests, International Journal of Agricultural Resources, Governance and Ecology, 4:81–92.
37. Murphy Peter G., Lugo Ariel E. 1986. Structure and Biomass of a Subtropical Dry Forest in Puerto Rico, Biotropica, 18:89-96.
38. Návar José, Méndez Eduardo and Dale Virginia. 2002. Estimating stand biomass in the Tamaulipan thornscrub of northeastern Mexico, Ann.For.Sci. 59:813-821.
39. Noordwijk Meine van, Rahayu Subekti, Hairiah Kurniatun, Wulan Y. C., Farida A. & Verbist Bruno. 2002. Carbon stock assessment for a forest-to-coffee conversion landscape in Sumber-Jaya (Lampung, Indonesia): from allometric equations to land use change analysis, SCIENCE IN CHINA (Series C), 45:75-86.
40. Okuda Toshinori, Suzuki Mariko, Numata Sinya, Yoshida Keiichiro, Nishimura Sen, Adachi Naoki, Niiyama Kaoru, Manokaran N., Hashim Mazlan. 2004. Estimation of above ground biomass in logged and primary lowland rainforests using 3-D photogrammetric analysis, Forest, Ecology and Management. 203:63-75
41. Overman JPM, Witte HJL, Saldarriaga JG. 1994. Evaluation of regression models for above-ground biomass determination in Amazon rainforest. Journal of Tropical Ecology 10:207-218
42. Ponette Quentin, Ranger Jacques, Ottorini Jean-Marc, Ulrich Erwin. 2001. Aboveground biomass and nutrient content of five Douglas-firs stands in France, Forest Ecology and Management, 142: 109-127.
43. Rai, S. N. 1984. Above ground biomass in tropical rainforests of Western Ghats. Indian For. 110:754–764.
44. Rai, S.N. and Proctor, J. 1986. Ecological studies on four forests in Karnataka, India. I. Environment, structure, floristics and Biomass, Journal of Ecology. 74:439–454.
45. Rana B.S., Singh S.P. and Singh R.P. 1989. Biomass and Net Primary Productivity in Central Himalayan Forests along an Altitudinal Gradient, Forest Ecology and Management. 27:199-218.
46. Rosenqvist, Å., M. Shimada, T. Igarashi, M. Watanabe, T. Tadono and H. Yamamoto. 2003. Support to multi-national environmental conventions and terrestrial carbon cycle science by ALOS and ADEOS-II—the Kyoto and Carbon Initiative Proceedings of IGARSS'03, Toulouse, France.
47. Sah J.P, Ross M.S, Koptur S. and Snyder J.R. 2004. Estimating aboveground biomass of broadleaved woody plants in the understory of Florida Keys pine forests, Forest Ecology and management, 203:319-329.
48. Salis Suzana M., Assis Marco A. , Mattos Patricia P. , PiaoAntonio C.S. 2006. Estimating the aboveground biomass and wood volume of savannawoodlands in Brazil's Pantanal wetlands based on allometric correlations, Forest Ecology and Management. 228:61–68.
49. Santos J.R., Araujo L.S., Freitas C.C., Dutra L.V., Sant'Anna S.J.S., Kuplich T.M., Gama F.F. 2003. Allometric equations for tropical forest estimation and its relationship with P-band SAR data.Geoscience and Remote sensing Symposium, 3:1948-1950.
50. Sharifi .M. Rasoul, Nilsen Erik T., and Rundel Philip W. 1982. Biomass and net primary production of prosopis glandulosa (fabaceae) in the sonoran desert of California, Amer. J. Bot. 69(5): 760-767.

51. Sierra Carlos A., Valle Jorge I. del, Orrego Sergio A., Moreno Flavio H., Harmon Mark E., Zapata Mauricio, Colorado Gabriel J., Herrera Marı´a A., Lara Wilson, Restrep David E. o, Berrouet Lina M, Loaiza Lina M., Benjumea John F. 2007. Total carbon stocks in a tropical forest landscape of the Porce region, Colombia, Forest Ecology and Management, 243:299-309.
52. Singh Arvind, Jha A.K. & Singh J.S. 1997. Influence of a developing tree canopy on the yield of Pennisetum pedicellatum sown on a mine spoil, Journal of Vegetation Science, 8:537-540.
53. Singh Surendra P, Adhikari Bhupendra S., Zobel Donald B. 1994. Biomass, Productivity, Leaf Longevity, and Forest Structure in the Central Himalaya, Ecological Monographs, 64: 401-421.
54. Sundriyal R.C., Sharma E. 1996. Anthropogenic pressure on tree structure and biomass in the temperate forest of Mamlay watershed in Sikkim , Forest Ecology and Management, 81: 113-134
55. Tiepolo Gilberto, Calmon Miguel, Feretti André Rocha. 2002. Measuring and Monitoring Carbon Stocks at the Guaraqueçaba Climate Action Project, Paraná, Brazil, Taiwan Forestry Research Institute. International Symposium on Forest Carbon Sequestration and Monitoring. Extension Series No. 153 (p 98-115).
56. Tiwari A.K. 1992. Component – wise biomass models for trees: A non-Harvest technique, Indian for, 118: 405-410.
57. Uri Veiko, Vares Aivo, Tullus Hardi and Kanal Arno 2007. Above-ground biomass production and nutrient accumulation in young stands of silver birch on abandoned agricultural landBiomass and bioenergy. 31:195-204.
58. Wang Chuankuan. 2006. Biomass allometric equations for 10 co-occurring tree species in Chinese temperate forests, Forest Ecology and Management. 222: 9–16.
59. Xiao Chun-Wang, Ceulemans R. 2004. Allometric relationships for below- and aboveground biomass of young Scots pines, Forest Ecology and Management, 203: 177–186.
60. Zianis Dimitris, Muukkonen Petteri, Mäkipaa Raisa, Mencuccini Maurizio. 2005. Biomass and Stem Volume Equations for Tree Species in Europe, Silvafennica, Monographs 4.
61. Zomer Robert, Menke John. 1993. Site Index and Biomass Productivity Estimates for Himalayan Alder-Large Cardamom Plantations: A Model Agroforestry System of the Middle Hills of Eastern Nepal, Mountain Research and Development, 13:235-255.

BIOMASS MODELS

TABLE I: HIMALAYAN FOREST

EQUATIONS	REFERENCE
1. $y = 0.0189+2.0411x$ Where, y=Above ground biomass, x=LAI values. LAI=leaf area index	Mandal et al. (2005)
2. $NPP = 20/(1+ exp [1.57716 - 0.0003026(T \times PR)])$ F = 416.1356, r= 0.8369, n= 180, P < 0.0001 Where, T=Mean annual air temperature (8°C), PR= Mean annual precipitation (mm), F=Statistical value of F distribution, r=Correlation coefficient, n=Number of sample points, P=Significance level.	Luo et al. (2002)
3. $Y = n + b. X$ Where, Y=Dry weight of a component (kg), X=dbh above ground level (cm per tree)	Lodhiyal & Lodhiyal (1997)
4. $ln\ Y=a + b\ ln\ X$ Where, Y=The dry weight of the component, X=The DBH (cm), a=The Y intercept, b=The slope or regression coefficient, ln=Natural log.	Singh & Adhikari (1995)
5. $lnY = a + blnX$ Where, Y=Dry weight, X=Circumference at breast height, a=Intercept and b=Slope of the regression line	Singh & Singh (1993)
6. $y =12.78x – 15.37$ r^2=0.73, P<0.001 **7.** $Dbh= 41.087 \times (1 – e^{(-0.077*Age)})$ r^2=0.50 **Height=27.169 × (1 – $e^{(-0.139*Age)}$)** r^2=0.49 Where, y=Total tree standing biomass (t/ha), x=Age (yr)	Zomer & Menke (1993)

8. *Foliage biomass* $$LB_j = D\ [(\sum_{i=1}^{n} t_i \cdot C_d)/\ n]$$ Where, LB_j= Foliage biomass for branch 'j'(kg), D= Number of twigs in branch 'j', n=Number of twigs sampled for branch'j', t_i= fresh weight of leaves in twig 'i'(kg), C_d=Coefficient of dry weight (t_d/ t_f), t_d=Dry weight of the foliage sample (kg), t_f=Fresh weight of the foliage sample (kg)	Tiwari (1992)
9. *Foliage biomass* $$\ln Y = a + b \ln X.$$ Where, Y=Foliage biomass (kg per tree), X= Circumference of branch at the base (cm)	Tiwari (1992)
10. *Foliage biomass* $$\ln Y = a + b_1 \ln X_1 + b_2 \ln X_2$$ Where, Y=Foliage biomass (kg per tree), X_1= Circumference of branch at the base (kg), X_2= Length of branch (cm)	Tiwari (1992)
11. *Foliage biomass* $$Y_{major} = \sum_{i=1}^{n} Y_i$$ $$Y_{minor} = DY_i$$ Where, Y_{major}=Total foliage biomass for major branches (kg), Y_i=Foliage biomass major branch 'i' (kg), Y_{minor}=foliage biomass of all the minor branches of the tree (kg), D=Total number of minor branches of the tree Y_i=Average foliage biomass per minor branch (kg)	Tiwari (1992)
12. *Twig biomass* $$TB_j = D\ [(\sum_{i=1}^{n} t_i \cdot C_d)/\ n]$$ Where, TB_j=Twig biomass for branch 'j'(kg), D=Total number of twigs in branch 'j', n=Number of twigs sampled for branch'j', t_i=Fresh weight of twig 'i'(kg), C_d= coefficient of dry weight (t_d/	Tiwari (1992)

t_f), t_d=Dry weight of the twig sample (kg), t_f=Fresh weight of the twig sample (kg)	
13. *Twig biomass* **ln Y = a + b lnX.** Where, Y=Twig biomass (kg per tree), X=Circumference of branch at the base (cm)	Tiwari (1992)
14. *Twig biomass* **ln Y = a + b_1 lnX_1 + b_2 ln X_2.** Where, Y=Twig biomass (kg per tree), X_1=Circumference of branch at the base (kg), X_2=length of branch (cm)	Tiwari (1992)
15. *Twig biomass* **n** **Y_{major}= $\sum Y_i$** **i=1** Where, Y_{major}=Total twig biomass for major branches (kg), Y_i=Twig biomass major branch 'i'(kg)	Tiwari (1992)
16. *Bole biomass* **Bole biomass(kg)= V × C_d** V = cbh ^{2} × L / 12 Π Where, V=Volume of bole (cm^3), Cbh=Circumference at breast height (cm), L=Length of bole (cm), C_d=Coefficient of dry weight=B_s / V_s, B_s=Dry weight for sample wood of bole (kg), V_s=Volume of sample wood of bole (cm^3)	Tiwari (1992)
17. *Branch biomass* **Y=C_d [V_{major} + V_{minor}]** V_{major}= C^2_i * L_i / 12 Π Where, V_{major}=Total volume of major branches (cm^3), V_{minor}=Total volume of minor branches (cm^3), Y=Total branch biomass of tree (kg), C_i=Circumference of branch 'i'(cm), C_d= Coefficient of dry weight=B_s / V_s, L_i=Length of branch'i', V_{minor}= D * C^2_i * L_i / 12 Π D=Total number of minor branches in the tree, B_s =Dry weight for sample wood of bole (kg), V_s=Volume of sample wood of bole (cm^3)	Tiwari (1992)
18. *ln Y = a + b ln X*	.

Where Y=Biomass of various tree component (kg tree^{-1}) X=Circumference at breast height (cm) Bole: r^2=0.801, a=2.1906, b=1.0193 Branch: r^2=0.896, a=1.0372, b=0.8259 Twigs: r^2=0.726, a=0.7446, b=0.7852 Leaves: r^2=0.695, a=0.5024, b=0.7338 Total above ground: r^2=0.899, a=2.1091, b=0.9406.	Tiwari (1992)
19. $Log_{10} Y=b1+b2\ Log_{10} X$ Where, Y=Biomass (100kg m^{-2}), X=Crown cover (percentage of ground covered by canopy).	Tiwari & Singh (1984)
20. *The total herb-layer production was calculated by using given formula.* $NPP = \sum_{i=1}^{m} = \delta LS + \sum_{i=1}^{n} = \delta DS,$ Where, LS and DS are the positive increments in the biomass and necromass of herbaceous live shoots and dead shoots.	Singh 1975. Did not get full article of this reference.

Reference

1. Adhikari B.S., Rawat Y.S. and Singh S.P., 1995. Structure and function of high altitude forests of central Himalaya I. Dry matter dynamics, *Ann. Bot.,* **75:** pp 237–248.
2. Hiigglund, B., 1981. Evaluation of forest site productivity. *Forestry Abstracts* 42(11): pp 515-526.
3. Lodhiyal L.S. and Lodhiyal Neelu, 1997. Variation in biomass and net primary productivity in short rotation high density central Himalayan poplar plantations, *Forest Ecology and Management,* 98: pp 167- I79.
4. Luo Tianxiang, Li Wenhua, and Zhu Huazhong, 2002. Estimated biomass and productivity of natural vegetation on the Tibetan plateau, *Ecological Applications,* 12(4): pp 980–997.
5. Singh Lalji & Singh, J.S., 1993. Importance of short-lived components of a dry tropical forest for biomass production and nutrient cycling. *J. Veg. Sci.,* 4: pp 681-686.
6. Singh R.P., 1979. Primary production and energy dynamics of tropical dry deciduous forests in Chandraprabha region, Varanasi. PhD Thesis, Banaras Hindu University, Varanasi.
7. Singh S.P. and Singh J.S., 1991. Analytical conceptual plan to reforest central Himalaya for sustainable development. *Environ. Manage.* **15**(3): pp 369–379.
8. Tiwari A. K. and Singh J. S., 1984. Mapping forest biomass in India through aerial photograph and non destructive field sampling, *Applied Geography*, 4: pp 151–165.
9. Tiwari A. K., 1992. Component-wise biomass models for trees. A nonharvest technique. *Indian For*., 118: pp 405–410.
10. Zomer Robert & John Menke, 1993. Site Index and Biomass Productivity Estimates for Himalayan Alder-Large Cardamom Plantations: A Model Agroforestry System of the Middle Hills of Eastern Nepal, *Mountain Research and Development*, 13(3): pp 235-255.

TABLE II: HIMALAYAN FOREST (SPECIES AND COMPONENTWISE)

SPECIES	REGRESSION EQUATION	REFERENCE
21. *Acer cappadocicum* Bole wood Bole bark Branch Twig Foliage Total above ground Stump root Lateral root Small root Total below ground Total (TAG + TBG)	$\ln Y = a + b \ln X$ a= - 3.5691, b=1.9690, r^2=0.949 a= - 6.5686, b=2.0288, r^2=0.942 a= - 5.4372, b=2.101, r^2=0.940 a= - 6.3664, b=2.0641, r^2=0.967 a= - 7.3873, b= 2.0375, r^2=0.935 a= - 3.3384, b= 2.0067, r^2=0.945 a= - 4.9453, b=1.9990, r^2=0.935 a= - 6.4184, b= 2.042, r^2=0.962 a= - 8.2417, b= 2.1589, r^2=0.945 a= - 3.0398, b=1.6453, r^2=0.951 a= - 3.1185, b=2.0098, r^2=0.949 Where, Y=Biomass of tree components (kg tree^{-1}), X=Circumference at breast height (cm), TAG=Total above-ground biomass, TBG=Total below-ground biomass	Garkoti (2007)
22. *Meliosma dilleniaefolia* Bole wood Bole bark Branch Twig Foliage Total above ground Stump root	$\ln Y = a + b \ln X$ a= - 5.189, b=2.4068, r^2=0.905 a= - 9.5460, b=2.7845, r^2=0.901 a= - 8.0113, b=2.8132, r^2=0.928 a= - 9.2389, b=2.7782, r^2=0.910 a= - 9.9792, b=2.8272, r^2=0.904 a= - 5.4984, b=2.5298, r^2=0.915	Garkoti (2007)

Lateral root Small root Total below ground Total (TAG + TBG)	a= - 6.0724, b=2.3659, r^2=0.826 a= - 8.9794, b=2.7827, r^2=0.900 a= - 10.125, b=2.8365, r^2=0.903 a= - 6.5767, b=2.5028, r^2=0.862 a= - 5.2281, b=2.5303, r^2=0.908 Where, Y=Biomass of tree components (kg tree^{-1}), X=Circumference at breast height (cm), TAG=Total above-ground biomass, TBG=Total below-ground biomass	
23. *Guna Chautara (pure oak forest)*	**y = 0.0189+2.0411x** r^2=0.55 Where, y=Above ground biomass, x=LAI values, LAI=Leaf area index.	Mandal & Laake (2005)
24. *Dhaili* **25.** *(Adense mixed forest)*	**y = - 0.6168+2.2928x** r^2=0.54 Where, y=Above ground biomass, x=LAI values, LAI=Leaf area index.	Mandal & Laake (2005)
26. *Abies pindrow* Whole tree (above ground) Stem (wood only) Stem(bark wood) Foliage total Twigs total Coarse stump roots Coarse lateral roots Fine roots Roots total	**ln biomass = a + b × dia + c × (ln(dia ^{d}))** a=2.0656, b=0, c=0.9781, d=1, r^2=0.98 a=1.538, b=0, c=1.0088, d=1, r^2=0.97 a= - 0.1066, b=0, c=0.8876, d=1, r^2=0.92 a=0.2464, b=0, c=0.6429, d=1, r^2=0.74 a= - 0.0146, b=0, c=0.8374, d=1, r^2=0.84 a= - 0.4874, b=0, c=1.0909, d=1, r^2=0.95 a= - 0.651, b=0, c=0.9947, d=1,r^2=0.86 a=1.0137, b=0, c=0.4604, d=1, r^2=0.72 a=0.5244, b=0, c=0.998, d=1, r^2=0.96	Jenkins et al. (2003)
27. *Poplar* (*Populus deltoides*)	**Y = a + bx** Where, Y=Biomass (kg tree^{-1}), X = Diameter at	Lodhiyal and Lodhiyal (1997)

	breast height (cm)	
Bole wood	For age=1year: a= - 0.0157, b=1.4043, r^2=0.997, P< 0.01 For age=2year: a= - 0.0075, b=2.1843, r^2=0.990, P< 0.01 For age=3year: a= - 0.0939, b=2.7312, r^2=0.994, P< 0.01 For age=4year: a= - 1.0568, b=3.9097, r^2=0.996, P< 0.01	
Bole bark	For age=1year: a= - 0.0022, b=0.1805, r^2=0.997, P< 0.01 For age=2year: a= - 0.0013, b=0.2827, r^2=0.990, P< 0.01 For age=3year: a= - 0.0129, b=0.3617, r^2=0.994, P< 0.01 For age=4year: a= - 0.1412, b=0.5237, r^2=0.996, P< 0.01	
Branch	For age=1year: a= - 0.0201, b=0.4911, r^2=0.948, P< 0.01 For age=2year: a= - 0.0024, b=0.7717, r^2=0.966, P< 0.01 For age=3year: a= - 0.2786, b=0.7803, r^2=0.944, P< 0.01 For age=4year: a= - 0.3461, b=1.0078, r^2=0.957, P< 0.01	

Twig	For age=1year: a= - 0.0084, b=0.1382, r^2=0.911, P< 0.01 For age=2year: a= - 0.0083, b=0.2479, r^2=0.930, P< 0.01 For age=3year: a= - 0.0792, b=0.2822, r^2=0.881, P< 0.01 For age=4year: a= - 0.0511, b=0.3505, r^2=0.932, P< 0.01	
Foliage	For age=1year: a= - 0.0050, b=0.5487, r^2=0.994, P< 0.01 For age=2year: a= - 0.0913, b=0.6568, r^2=0.953, P< 0.01 For age=3year: a= - 0.1569, b=0.62 19, r^2=0.954, P< 0.01 For age=4year: a= - 0.2254, b=0.8036, r^2=0.970, P< 0.01	
Stump root	For age=1year: a= - 0.0109, b=0.3916, r^2=0.987, P< 0.01 For age=2year: a= - 0.0169, b=0.5727, r^2=0.974, P< 0.01 For age=3year: a= - 0.0043, b=0.6343, r^2=0.952, P< 0.01 For age=4year: a= - 0.3371, b=0.8813, r^2=0.971, P< 0.01	
Lateral root	For age=1year: a= - 0.0048, b=0.0677, r^2=0.966, P< 0.01	

Fine root	For age=2year: a= - 0.0355, b=0.2285, r^2=0.870, P< 0.01 For age=3year: a= - 0.1579, b=0.3283, r^2=0.912, P< 0.01 For age=4year: a= - 0.2485, b=0.4733, r^2=0.925, P< 0.01 For age=1year: a= - 0.0109, b=0.0342, r^2=0.885, P< 0.01 For age=2year: a= - 0.0104, b=0.05 12, r^2=0.858, P< 0.01 For age=3year: a= - 0.0149, b=0.0706, r^2=0.824, P< 0.01 For age=4year: a= - 0.0444, b=0.0993, r^2=0.777, P< 0.05	
28. *Quercus lamellosa*	**$y = exp(- 0.948 + 0.826 \ln D^2H)$** P<0.001, r=0.947, d.f.=27, E=1.077 Where, y=Woody biomass (bole and branch)(kg), D=Diameter at breast height (cm), H=Tree height (m)	Sundriyal and Sharma (1996)
29. *Castanopsis tribuloides*	**$y = exp(0.807 + 0.595 \ln D^2H)$** P<0.001, r=0.908, d.f.=38, E=1.049 Where, y=Woody biomass (bole and branch)(kg), D=Diameter at breast height (cm), H=Tree height (m)	Sundriyal and Sharma (1996)
30. *Symplocos theaefolia*	**$y = exp(0.520 + 0.594 \ln D^2H)$** P<0.001, r=0.935, d.f.=17, E=1.066 Where, y=Woody biomass (bole and branch)(kg), D=Diameter at breast height (cm), H=Tree height (m)	Sundriyal and Sharma (1996)
31. *Eurya*	**$y = exp(l.165 + 0.514 \ln D^2H)$**	Sundriyal and Sharma

acuminata	P<0.001, r=0.860, d.f.=19, E=1.073 Where, y=Woody biomass (bole and branch)(kg), D=Diameter at breast height (cm), H=Tree height (m)	(1996)
32. *Alnus nepalensis*	**$y = \exp(- 2.847 + 0.839 \ln D^2H)$** P<0.001, r=0.967, d.f.=8, E=1.030 Where, y=Woody biomass (bole and branch)(kg), D=Diameter at breast height (cm), H=Tree height (m), d.f =Degree of freedom, r=Coefficient of correlation, E=Relative error calculated as antilog of the standard error of the natural logarithm of the y-value.	Sundriyal and Sharma (1996)
33. *Other species* group	**$y = \exp(- 0.427 + 0.719 \ln D^2H)$** P<0.001, r=0.915, d.f.=24, E=1.120 Where, y=Woody biomass (bole and branch)(kg), D=Diameter at breast height (cm), H=Tree height (m), d.f =Degree of freedom, r=Coefficient of correlation, E=Relative error calculated as antilog of the standard error of the natural logarithm of the y-value.	Sundriyal and Sharma (1996)
34. *Total species*	**$y = \exp(- 0.695 + 0.780 \ln D^2H S)$** P<0.001, r=0.909, d.f.=143, E=1.049 Where, y=Woody biomass (bole and branch) (kg), D=Diameter at breast height (cm), H=Tree height (m), S=Specific wood density (gcm^{-3}), d.f =Degree of freedom, r=Coefficient of correlation, E=Relative error calculated as antilog of the standard error of the natural logarithm of the y-value.	Sundriyal and Sharma (1996)
35. *Larix forest*	**$y = 1.6481x^{0.84788}$** P=0.001, R=0.9530, N=34 Where, y=Live biomass (MgDM/ha), x= Stem volume (m^3/ha)	Li and Luo (1996) and Luo (1996)
36. *Picea–Abies forest*	**$y= 50.8634 + 0.5406x$** P=0.001, R=0.9330, N=26	Li and Luo (1996) and Luo (1996).

	Where, y=Forest live biomass (MgDM/ha), x=Stem volume (m^3/ha)	
37. *Montane pine forest*	**y = 23.9124 + 0.5232x** P=0.001, R=0.9646, N=23 Where, y=Forest live biomass (MgDM/ha), x=Stem volume (m^3/ha)	Li and Luo (1996) and Luo (1996).
38. *Cupressus forest*	**Y = - 2.8232 + 0.9268x** P=0.001, R=0.9915, N=20 Where, y=Forest live biomass (MgDM/ha), x=Stem volume (m^3/ha)	Li and Luo (1996) and Luo (1996).
39. *Evergreen* broad-leaved forest	**y= - 1.5306 +1.1595x** P=0.001, R=0.9255, N=50 Where, y=Forest live biomass (MgDM/ha), x=Stem volume (m^3/ha)	Li and Luo (1996) and Luo (1996).
40. *Quercus forest*	**$y = 1.8409x^{0.89262}$** P=0.001, R=0.9469, N=49 Where, y=Forest live biomass (MgDM/ha), x=Stem volume (m^3/ha)	Li and Luo (1996) and Luo (1996).
41. *Populus–Betula forest*	**$y = 2.3727x^{0.79024}$** P=0.001, R=0.8976, N=42 Where, y=Forest live biomass (MgDM/ha), x=Stem volume (m^3/ha)	Li and Luo (1996) and Luo (1996).
42. *Castanopsis tribuloides*	**$y = \exp[0.511 + 0.7631n(D^2H)]$** n=12, r=0.940, P<0.001 Where, y=Wood biomass including branch and bole (kg), D=Diameter at breast height (cm), H=Height (m), S=Specific wood density (Mg/m^3), exp=Exponential	Sundriyal et al. (1994)

43. *Castanopsis indica*	**$y = exp[0.204 + 0.7691n(D^2H)]$** n=52, r=0.906, P<0.001 Where, y=Wood biomass including branch and bole (kg), D=Diameter at breast height (cm), H=Height (m), S=Specific wood density (Mg/m3), exp=Exponential	Sundriyal et al. (1994)
44. *Shorea robusta*	**$y = exp[-1.768 + 0.9451n(D^2H)]$** n=26, r=0.904, P<0.001 Where, y=Wood biomass including branch and bole (kg), D=Diameter at breast height (cm), H=Height (m), S=Specific wood density (Mg/m^3), exp=Exponential	Sundriyal et al. (1994)
45. *Schima wallichii*	**$y = exp[-1.064 +0.8881n(D^2H)]$** n=32, r=0.960, P<0.001 Where, y=Wood biomass including branch and bole (kg), D=Diameter at breast height (cm), H=Height (m), S=Specific wood density (Mg/m^3), exp=Exponential	Sundriyal et al. (1994)
46. *Other species*	**$y = exp[-0.277 + 0.906ln(D^2H)]$** n=13, r=0.618, P<0.050 Where, y=Wood biomass including branch and bole (kg), D=Diameter at breast height (cm), H=Height (m), S=Specific wood density (Mg/m^3), exp=Exponential	Sundriyal et al. (1994)
47. *Total species*	**$y = exp[1.741 + 0.6151n(D^2HS)]$** n=135, r=0.615, P<0.001 Where, y=Wood biomass including branch and bole (kg), D=Diameter at breast height (cm), H=Height (m), S=Specific wood density (Mg/m^3), exp=Exponential	Sundriyal et al. (1994)
48. *Shorea robusta* Bole Branch Twigs	**$\ln Y = a + b \ln X$** a=1.2396, b=1.1459, Sy.X=0.051, r^2=0.962 a=0.5898, b=1.0361, Sy.X=0.034, r^2=0.953 a=1.2893, b=0.7209, Sy.X=0.063, r^2=0.872 a=0.9131, b=0.6775, Sy.X=0.072, r^2=0.795	Tiwari (1992)

Leaves Total above ground	a=2.1133, b=1.0429, Sy.X=0.071, r^2=0.936 Where, Y=Biomass of various tree component (kg $tree^{-1}$), *X*=Circumference at breast height (cm)	
49. *A. latifolia* Bole Branch Twigs Leaves Total above ground	**ln Y = a + b ln *X*** a=1.425, b=1.0241, Sy.X=0.043, r^2=0.975 a= - 0.1301, b=1.1352, Sy.X=0.061, r^2=0.899 a=0.6596, b=0.8596, Sy.X=0.071, r^2=0.821 a=1.8665, b=0.5125, Sy.X=0.053, r^2=0.831 a=2.3399, b=0.9581, Sy.X=0.068, r^2=0.913 Where Y=Biomass of various tree component (kg $tree^{-1}$), *X*=Circumference at breast height (cm)	Tiwari (1992)
50. *Terminalia tomentosa* Bole Branch Twigs Leaves Total above ground	**ln Y = a + b ln *X*** a=0.6489, b=1.1065, Sy.X=0.069, r^2=0.895 a=1.1591, b=0.7670, Sy.X=0.052, r^2=0.912 a=0.9058, b=0.7536, Sy.X=0.091, r^2=0.821 a= - 0.0232, b=0.8260, Sy.X=0.081, r^2=0.851 a=1.8161, b=0.8161, Sy.X=0.075, r^2=0.933 Where Y=Biomass of various tree component (kg $tree^{-1}$), *X*=Circumference at breast height (cm)	Tiwari (1992)
51. *Terminalia chebula* Bole Branch Twigs Leaves Total above ground	**ln Y = a + b ln*X*** a=1.5228, b=0.8937, Sy.X=0.072, r^2=0.962 a=1.9849, b=0.5449, Sy.X=0.039, r^2=0.916 a=0.0941, b=0.6803, Sy.X=0.057, r^2=0.812 a= -1.1703, b=1.0552, Sy.X=0.055, r^2=0.713 a=2.7889, b=0.7198, Sy.X=0.063, r^2=0.952 Where Y=Biomass of various tree component (kg $tree^{-1}$), *X*=Circumference at breast height (cm)	Tiwari (1992)
52. *Mallotus philippensis*	**ln Y = a + b ln*X***	Tiwari (1992)

Bole Branch Twigs Leaves Total above ground	 a=0.6234, b=0.8912, Sy.X=0.059, r^2=0.899 a=1.2549, b=0.6517, Sy.X=0.066, r^2=0.812 a= -1.2571, b=1.0849, Sy.X=0.053, r^2=0.712 a= - 0.5915, b=0.8811, Sy.X=0.084, r^2=0.782 a=0.3557, b=1.1551, Sy.X=0.063, r^2=0.911 Where Y=Biomass of various tree component (kg $tree^{-1}$), *X*=Circumference at breast height (cm)	
53. *Alnus nepalensis*	**Ln (Biomass) = -3.408 + 2.744 Ln (dbh)** Where, dbh=Diameter at breast height, Biomass will be in kg.	Thapa et al. (1989)
54. *Shorea robusta* Bole Branch Twig Leaf Total	**Ln y = a + b ln x** a= - 2.83, b=1.98, r^2=0.98, S_yx=0.12, P<0.01 a= - 2.04, b=1.50, r^2=0.92, S_yx=0.19, P<0.01 a= - 2.69, b=1.46, r^2=0.98, S_yx=0.09, P<0.01 a= - 1.74, b=1.18, r^2=0.96, S_yx=0.15, P<0.01 a= - 1.79, b=1.89, r^2=0.98, S_yx=0.11, P<0.01 Where y=Biomass of tree components (kg $tree^{-1}$), x=GBH (cm)	Rana et al. (1989)
55. *Mallotus philippensis* Bole Branch Twig Leaf Total	 a= - 2.14, b=1.40, r^2=0.92, S_yx=0.30, P<0.01 a= - 2.28, b=1.22, r^2=0.96, S_yx=0.13, P<0.01 a= - 2.33, b=0.81, r^2=0.92, S_yx=0.16, P<0.01 a= - 3.86, b=1.07, r^2=0.90, S_yx=0.25, P<0.01 a= - 1.24, b=1.28, r^2=0.96, S_yx=0.14, P<0.01	Rana et al. (1989)
56. *Interspecies of sal forest* Bole	 a= - 5.03, b=2.33, r^2=0.79, S_yx=0.86, P<0.05	Rana et al. (1989)

Branch	a= - 5.21, b=2.08, r^2=0.83, S_yx=0.68, P<0.05	
Twig	a= - 4.63, b=1.68, r^2=0.48, S_yx=1.24, P<0.05	
Leaf	a= - 4.96, b=1.68, r^2=0.42, S_yx=1.42, P<0.05	
Total	a= - 4.31, b=2.21, r^2=0.69, S_yx=0.67, P<0.05	
57. *Quercus leucotrichophora*		Rana et al. (1989)
Bole	a= - 0.52, b=1.37, r^2=0.99, S_yx=0.03, P<0.01	
Branch	a= - 0.72, b=1.30, r^2=0.97, S_yx=0.01, P<0.01	
Twig	a= - 0.07, b=0.90, r^2=0.90, S_yx=0.07, P<0.01	
Leaf	a= - 0.98, b=0.85, r^2=0.30, S_yx=0.44, P<0.01	
Stump root	a= - 0.98, b=0.90, r^2=0.61, S_yx=0.11, P<0.01	
Lateral root	a= - 0.31, b=0.81, r^2=0.57, S_yx=0.14, P<0.01	
Fine root	a= - 1.33, b=0.50, r^2=0.49, S_yx=0.20, P<0.01	
58. *Quercus floribunda*		Rana et al. (1989)
Bole	a= - 1.11, b=1.52, r^2=0.91, S_yx=0.14, P<0.01	
Branch	a= - 0.99, b=1.38, r^2=0.93, S_yx=0.11, P<0.01	
Twig	a= - 1.13, b=1.27, r^2=0.81, S_yx=0.18, P<0.01	
Leaf	a= - 1.23, b=1.38, r^2=0.79, S_yx=0.22, P<0.01	
Stump root	a= - 0.25, b=1.11, r^2=0.80, S_yx=0.12, P<0.01	
Lateral root	a= - 1.59, b=1.00, r^2=0.71, S_yx=0.17, P<0.01	
Fine root	a= - 1.05, b=0.25, r^2=0.61, S_yx=0.12, P<0.01	
59. *Rhododendron arboreum*		Rana et al. (1989)
Bole	a=1.12, b=0.70, r^2=0.87, S_yx=0.19, P<0.01	
Branch	a=1.11, b=0.61, r^2=0.61, S_yx=0.35, P<0.01	
Twig		

Leaf	a=1.16, b=0.37, r^2=0.33, S_yx=0.38, P<0.01	
Stump root	a=1.19, b=0.17, r^2=0.10, S_yx=0.36, P<0.01	
Lateral root	a= - 0.12, b=0.87, r^2=0.61, S_yx=0.12, P<0.01	
Fine root	a= - 1.75, b=0.98, r^2=0.60, S_yx=0.17, P<0.01	
	a= - 0.01, b=0.41, r^2=0.57, S_yx=0.20, P<0.01	
60. *Pinus roxburghii*		Rana et al. (1989)
Bole	a= - 6.42, b=2.60, r^2=0.99, S_yx=0.06, P<0.01	
First order branch	a= - 9.83, b=2.98, r^2=0.98, S_yx=0.09, P<0.01	
Other branches	a= - 9.34, b=2.63, r^2=0.96, S_yx=0.11, P<0.01	
Leaf	a= - 6.11, b=1.87, r^2=0.95, S_yx=0.09, P<0.01	
Stump root	a= - 7.22, b=2.45, r^2=0.98, S_yx=0.10, P<0.01	
Lateral root	a= - 9.16, b=2.59, r^2=0.97, S_yx=0.11, P<0.01	
Fine root	a= - 9.10, b=2.07, r^2=0.94, S_yx=0.14, P<0.01	
61. *Interspecies of other forest*		Rana et al. (1989)
Bole	a= - 0.86, b=1.43, r^2=0.92, S_yx=0.06, P<0.01	
Branch	a= - 0.91, b=1.33, r^2=0.91, S_yx=0.05, P<0.01	
Twig	a= - 0.51, b=1.03, r^2=0.80, S_yx=0.09, P<0.01	
Leaf	a= - 1.11, b=1.04, r^2=0.76, S_yx=0.10, P<0.01	
Stump root	a= - 0.10, b=0.95, r^2=0.79, S_yx=0.11, P<0.01	
Lateral root	a= - 2.25, b=1.00, r^2=0.72, S_yx=0.14, P<0.01	
Fine root	a= - 2.07, b=0.53, r^2=0.72, S_yx=0.20, P<0.01	

Reference:

1. Garkoti S. C., 2007. Estimates of biomass and primary productivity in a high-altitude maple forest of the west central Himalayas, Ecol Res DOI 10.1007/s11284-007-0355-2.
2. Jenkins Jennifer C., Chojnacky David C., Heath Linda S. and Birdsey Richard A., 2003. Comprehensive Database of Diameter-based Biomass Regressions for North American Tree

Species, United States Department of Agriculture Forest Service Northeastern Research Station, General Technical Report NE-319.
3. Li, W.-H., and T.-X. Luo, 1996. Biomass and productivity of forests in China. Pages 80–133 *in* W.-H. Li and F. Li, editors. Research of forest resources in China. In Chinese. Chinese Forestry Publisher, Beijing, China.
4. Luo, T.-X., 1996. Patterns of net primary productivity for Chinese major forest types and their mathematical models. [In Chinese.] Dissertation. Commission for integrated survey of natural resources, Chinese Academy of Sciences, Beijing, China.
5. Lodhiyal L.S. and Lodhiyal Neelu, 1997. Variation in biomass and net primary productivity in short rotation high density central Himalayan poplar plantations, *Forest Ecology and Management,* 98: pp167- I79.
6. Mandal R. A. & Laake P. van, 2005. Carbon sequestration in community forests: an eligible issue for CDM (A case study of Nainital, India), *Banko Janakari*, 15(2): pp 53-61.
7. Rana B.S., Singh S.P. and Singh R.P., 1989. Biomass and Net Primary Productivity in Central Himalayan Forests along an Altitudinal Gradient, *Forest Ecology and Management,* 27: pp 199-218.
8. Singh Arvind, Jha A. K. and Singh J. S., 1997. Influence of a Developing Tree Canopy on the Yield of Pennisetum pedicellatum Sown on a Mine Spoil, *Journal of Vegetation Science*, 8(4): pp 537-540.
9. Sundriyal R.C., Sharma E., Rai L.K. & Rai S.C., 1994. Tree structure, regeneration and woody biomass removal in a sub-tropical forest of Mamlay watershed in the Sikkim Himalaya, *Vegetatio* 113: pp 53—63.
10. Sundriyalss R.C and Sharma E., 1996**.** Anthropogenic pressure on tree structure and biomass in the temperate forest of Mamlay watershed in Sikkim, *Elsevier Forest Ecology and Management,* 81: pp 113-134.
11. Thapa B., Upadhaya M. P., Wallace D., and Sherpa S. L., 1989. Prediction of Biomass in a Semi-Natural Stand of Utis *(Alnus nepalensis)* at Pakhribas Agricultural Centre. Pakhribas Agricultural Centre, c/o BTCO, PO Box 106, Kathmandu, Nepal, PAC Technical Paper No. 115.
12. Tiwari A.K., 1992. Component – wise biomass models for trees: A non-Harvest technique, *Indian for*., 118: pp 405-410.

TABLE III: BIOMASS MODELS - TEMPERATE FOREST

EQUATIONS	REFERENCE
$Y=aDBH^b$ Where, y=Above-ground biomass of the model tree, DBH =Stem diameter at breast height (cm), *a* and *b* the parameter estimates.	Uri et al. (2007)
$AGB^{1/3} = -0.677+1.874 \times \ln(height)+ 0.014(crown\ closure)$ r^2=0.70, RMSE=33.7 t/ha	Hall et al. (2006)
$Volume^{1/3} = -3.252+3.089 \times \ln(height)+ 0.02(crown\ closure)$ r^2=0.71, RMSE=74.7 m^3/ha	Hall et al. (2006)
$Y= \exp\{-2.173+0.868 \ln(D^2 TH)+0.0939/2\}$ r^2=0.90 Where, Y=Total dry weight (kg), D=Diameter at breast height (cm), TH=Total height (m).	Cairns et al. (2003)
$\log_{10}$ biomass = a + b × ($\log_{10}(dia^c)$)	Jenkins et al. (2003)
biomass = a × (exp(b + (c × ln(dia)) + (d × dia)))	Jenkins et al. (2003)
biomass = a + ((b × (dia^c))/((dia^c) + d))	Jenkins et al. (2003)
ln biomass = a + b × dia + c × (ln(dia^d))	Jenkins et al. (2003)
ln biomass = a + b × ln(dia) + c × (d + (e × ln(dia)))	Jenkins et al. (2003)
biomass = a + b × dia + c × (dia^d)	Jenkins et al. (2003)
biomass = a + (b × dia) + c × (dia^2) + d × (dia^3)	Jenkins et al. (2003)
$\log_{100}$ biomass = a + (b × $\log_{10}$(dia))	Jenkins et al. (2003)
ln biomass = ln(a) + (b × ln(dia))	Jenkins et al. (2003)
$AB = 0.342+MCH^2+2.086 \times COVCHPX$ R^2=84%, P<0.0001 Where, AB=Above-ground biomass (Mg ha^{-1}), MCH^2= Mean canopy height (m) squared, COVCHPX =Product of mean cover and mean canopy height	Lefsky et al. (2002)

$AB = 0.378 \times MCH^2$ (R2=84%, P<0.0001) Where, AB=Above-ground biomass (Mg ha^{-1}), MCH^2= Mean canopy height (m) squared, COVCHPX =Product of mean cover and mean canopy height	Lefsky et al. (2002)
y = ba × 6.6 t dry weight m^{-2} Where, y=Total above ground biomass (t dry weight m^{-2}) and ba=Basal area over bark (m^2 ha^{-1}).	Snowdon (2000)
62. $AGBM=4.236+0.200\times CHP\_H\_X+13.325\times OLIGO+24.300\times CHP\_Q\_SD$ r^2=0.87, P<0.0001, RMSE=118.5 $Mgha^{-1}$ Where AGBM units are Mg ha^{-1}, CHP_H_X=Mean height of the forest canopy (m), OLIGO=Volume of shaded foliage and woody biomass in the canopy (m^3), CHP_Q_SD= standard deviation of the quadratic mean height of the canopy (m).	Lefsky et al. (1999) & Lefsky et al. (2005)
$BGBD=\exp\{-1.059+0.884\times Ln(AGBD)+0.284\}$ r^2=0.84, n=151 Where, BGBD=Belowground biomass density (fine and coarse roots), AGBD = Aboveground biomass density of the tree component (Mg ha^{-1})	Cairns et al. (1997)
For Tertiary Mediterranean ecosystems **$AGB=0.0551+DBH^{2.7157}$**	Fernandez-Palacios (1991)
For each arable crop: **$AGB=(Y+(Y\times E))\times D\times C\times(L/365)\times A$** AGB= Average annual above ground carbon stock ($tCha^{-1}$) Y=Crop yield (tha^{-1}) E=Expansion factor of yield to non-harvested biomass (residue/harvested crop) D=Proportion of dry matter C=Proportion of carbon content of *dry* matter L=Length of growing season A=Averaging coefficient for converting final standing biomass to average annual standing biomass (0.6 for crops, 0.75 for orchard crops).	Adger & Subak (1996)

REFERENCE:

1. Adger W. Neil and Subak Susan, 1996. Estimating Above-Ground Carbon Fluxes from UK Agricultural Land. The Geographical Journal, 162(2): pp 191-204.
2. Cairns M.A., Brown S., Helmer E.H. and Baumgardner G.A., 1997. Root biomass allocation in the world's upland forests. *Oecologia* 111, pp 1–11.
3. Cairns Michael A., Olmsted Ingrid, Granados Julian and Argaez Jorge, 2003. Composition and aboveground tree biomass of a dry semi-evergreen forest on Mexico's Yucatan Peninsula, *Forest Ecology and Management*, 186(1-3): pp 125-132.
4. Fernandez-Palacios J.M., Esteban J.J. Garcia, Lopez R.J. and Luzardo M.C., 1991. Aproximación a la estima de la biomasa y producción neta aéreas en una estación dela Laurisilva tinerfeña, *Vieraea,* 20: pp 11–20.
5. Hall R.J., Skakun R.S., Arsenault E.J. and Case B.S., 2006. Modeling forest stand structure attributes using Landsat ETM+ data: Application to mapping of aboveground biomass and stand volume, *Forest Ecology Management*, 225: pp 378-390.
6. Jenkins Jennifer C., Chojnacky David C., Heath Linda S. and Birdsey Richard A., 2003. Comprehensive Database of Diameter-based Biomass Regressions for North American Tree Species, United States Department of Agriculture Forest Service Northeastern Research Station, General Technical Report NE-319.
7. Lefsky M.A., Cohen W.B., Acker S.A., Spies T.A., Parker G.G. and Harding D., 1999. Lidar remote sensing of biophysical properties and canopy structure of forest of Douglas-fir and western hemlock, *Remote Sensing of Environment,* 70: pp 339–361.
8. Lefsky Michael A., Cohent Warren B., Harding David J. S., Parker Geoffrey G., Ackery Steven A. and Thomas Gower S., 2002. Lidar remote sensing of above-ground biomass in three biomes, Global *Ecology & Biogeography*, 11: pp 393-399,
9. Lefsky M.A., Hudak A.T., Cohen W.B. and Acker S.A., 2005. Geographic variability in lidar predictions of forest stands structure in the Pacific Northwest, *Remote Sensing of Environment,* 95: pp 532–548.
10. Snowdon P., Eamus D., Gibbons P., Khanna P. K., Keith H., Raison J., et al., 2000. Synthesis of Allometrics, Review of Root Biomass and Design of future woody Biomass Sampling Strategies. National Carbon Accounting System technical report no. 17. Australian Green house Office.
11. Uri Veiko, Vares Aivo, Tullus Hardi and Kanal Arno, 2007. Above-ground biomass production and nutrient accumulation in young stands of silver birch on abandoned agricultural land, *Biomass and bioenergy*, 31(4): pp 195-204.

TABLE IV: TEMPERATE FOREST (SPECIESWISE)

Species Name	**Biomass Equations**	**Reference**
1. For silver birch. (Haaslava plot)	$\mathbf{y = aDBH^b}$ a=160.61, b=2.046, r^2=0.993, S.E.=1.17, P<0.001 Where, y=Above-ground biomass of the model tree, DBH=Stem diameter at breast height (cm), a and b the parameter estimates.	Uri et al. (2007)

2. For silver birch (Valjakula plot)	$\mathbf{y = aDBH^b}$ a=152.32, b=2.246, r^2=0.987, S.E.=1.31, P<0.001 Where, y=Above-ground biomass of the model tree, DBH=Stem diameter at breast height (cm), a and b the parameter estimates.	Uri et al. (2007)
3. For silver birch (Lutsu plot)	$\mathbf{y = aDBH^b}$ a=160.93, b=2.046, r^2=0.992, S.E.=1.16, P<0.001 Where, y=Above-ground biomass of the model tree, DBH=Stem diameter at breast height (cm), a and b the parameter estimates.	Uri et al. (2007)
4. For silver birch (Puhatu plot)	$\mathbf{y = aDBH^b}$ a=180.19, b=2.079, r^2=0.983, S.E.=1.28, P<0.001 Where, y=Above-ground biomass of the model tree, DBH=Stem diameter at breast height (cm), a and b the parameter estimates.	Uri et al. (2007)
5. For silver birch (Kambja plot)	$\mathbf{y = aDBH^b}$ a=163.86, b=2.019, r^2=0.992, S.E.=1.14, P<0.001 Where, y=Above-ground biomass of the model tree, DBH=Stem diameter at breast height (cm), a and b the parameter estimates.	Uri et al. (2007)
6. Korean pine (*Pinus koraiensis Sieb*. et Zucc.) Total biomass Aboveground biomass Belowground biomass Stem biomass	 $\mathbf{Log_{10}B=2.033 + 2.469log_{10}DBH}$ r^2=0.972, P<0.001 $\mathbf{Log_{10}B=1.945 + 2.467log_{10}DBH}$ r^2=0.969, P<0.001 $\mathbf{Log_{10}B=2.033+ 2.469log_{10}DBH}$ r^2=0.972, P<0.001 $\mathbf{Log_{10}B=1.891 + 2.406log_{10}DBH}$	Wang (2006)

Total branch biomass Total foliage biomass	r^2=0.960, P<0.001 **$Log_{10}B=0.703 + 2.855log_{10}DBH$** r^2=0.903, P<0.001 **$Log_{10}B=0.855 + 2.135log_{10}DBH$** r^2=0.818, P<0.001 Where, B=Biomass (g), DBH=Diameter at breast height (cm)	
7. Dahurian larch (*Larix gmelinii Rupr.)* Total biomass Aboveground biomass Belowground biomass Stem biomass Total branch biomass Total foliage biomass	 **$Log_{10}B=2.033 + 2.469log_{10}DBH$** r^2=0.972, P<0.001 **$Log_{10}B=1.945 + 2.467log_{10}DBH$** r^2=0.969, P<0.001 **$Log_{10}B=2.033+ 2.469log_{10}DBH$** r^2=0.972, P<0.001 **$Log_{10}B=1.891 + 2.406log_{10}DBH$** r^2=0.960, P<0.001 **$Log_{10}B=0.703 + 2.855log_{10}DBH$** r^2=0.903, P<0.001 **$Log_{10}B=0.855 + 2.135log_{10}DBH$** r^2=0.818, P<0.001 Where, B=Biomass (g), DBH=Diameter at breast height (cm)	Wang (2006)
8. Mongolian oak (*Quercus mongolica* Fisch.) Total biomass Aboveground biomass	 **$Log_{10}B=2.033 + 2.469log_{10}DBH$** r^2=0.972, P<0.001 **$Log_{10}B=1.945 + 2.467log_{10}DBH$**	Wang (2006)

Belowground biomass Stem biomass Total branch biomass Total foliage biomass	r^2=0.969, P<0.001 **$Log_{10}B=2.033+ 2.469log_{10}DBH$** r^2=0.972, P<0.001 **$Log_{10}B=1.891 + 2.406log_{10}DBH$** r^2=0.960, P<0.001 **$Log_{10}B=0.703 + 2.855log_{10}DBH$** r^2=0.903, P<0.001 **$Log_{10}B=0.855 + 2.135log_{10}DBH$** r^2=0.818, P<0.001 Where, B=Biomass (g), DBH=Diameter at breast height (cm)	
9. White birch (*Betula platyphylla* Suk.) Total biomass Aboveground biomass Belowground biomass Stem biomass Total branch biomass Total foliage biomass	 **$Log_{10}B=2.033 + 2.469log_{10}DBH$** r^2=0.972, P<0.001 **$Log_{10}B=1.945 + 2.467log_{10}DBH$** r^2=0.969, P<0.001 **$Log_{10}B=2.033+ 2.469log_{10}DBH$** r^2=0.972, P<0.001 **$Log_{10}B=1.891 + 2.406log_{10}DBH$** r^2=0.960, P<0.001 **$Log_{10}B=0.703 + 2.855log_{10}DBH$** r^2=0.903, P<0.001 **$Log_{10}B=0.855 + 2.135log_{10}DBH$** r^2=0.818, P<0.001 Where, B=Biomass (g), DBH=Diameter at breast height (cm)	Wang (2006)
10. Amur cork-tree (*Phellodendron amurense* Rupr.)		Wang (2006)

Total biomass Aboveground biomass Belowground biomass Stem biomass Total branch biomass Total foliage biomass	**$Log_{10}B=2.033 + 2.469log_{10}DBH$** $r^2=0.972$, $P<0.001$ **$Log_{10}B=1.945 + 2.467log_{10}DBH$** $r^2=0.969$, $P<0.001$ **$Log_{10}B=2.033+ 2.469log_{10}DBH$** $r^2=0.972$, $P<0.001$ **$Log_{10}B=1.891 + 2.406log_{10}DBH$** $r^2=0.960$, $P<0.001$ **$Log_{10}B=0.703 + 2.855log_{10}DBH$** $r^2=0.903$, $P<0.001$ **$Log_{10}B=0.855 + 2.135log_{10}DBH$** $r^2=0.818$, $P<0.001$ Where, B=Biomass (g), DBH=Diameter at breast height (cm)	
11. Manchurian walnut (*Juglans mandshurica* Maxim.) Total biomass Aboveground biomass Belowground biomass Stem biomass Total branch biomass Total foliage biomass	 **$Log_{10}B=2.033 + 2.469log_{10}DBH$** $r^2=0.972$, $P<0.001$ **$Log_{10}B=1.945 + 2.467log_{10}DBH$** $r^2=0.969$, $P<0.001$ **$Log_{10}B=2.033+ 2.469log_{10}DBH$** $r^2=0.972$, $P<0.001$ **$Log_{10}B=1.891 + 2.406log_{10}DBH$** $r^2=0.960$, $P<0.001$ **$Log_{10}B=0.703 + 2.855log_{10}DBH$** $r^2=0.903$, $P<0.001$	Wang (2006)

	$Log_{10}B=0.855 + 2.135log_{10}DBH$ $r^2=0.818$, P<0.001 Where, B=Biomass (g), DBH=Diameter at breast height (cm)	
12. Manchurian ash (*Fraxinus mandshurica* Rupr.) Total biomass Aboveground biomass Belowground biomass Stem biomass total branch biomass total foliage biomass	**$Log_{10}B=2.033 + 2.469log_{10}DBH$** $r^2=0.972$, P<0.001 **$Log_{10}B=1.945 + 2.467log_{10}DBH$** $r^2=0.969$, P<0.001 **$Log_{10}B=2.033+ 2.469log_{10}DBH$** $r^2=0.972$, P<0.001 **$Log_{10}B=1.891 + 2.406log_{10}DBH$** $r^2=0.960$, P<0.001 **$Log_{10}B=0.703 + 2.855log_{10}DBH$** $r^2=0.903$, P<0.001 **$Log_{10}B=0.855 + 2.135log_{10}DBH$** $r^2=0.818$, P<0.001 B=Biomass (g), DBH=Diameter at breast height (cm)	Wang (2006)
13. Aspen (*Populous davidiana* Dode) Total biomass Aboveground biomass Belowground biomass Stem biomass	**$Log_{10}B=2.033 + 2.469log_{10}DBH$** $r^2=0.972$, P<0.001 **$Log_{10}B=1.945 + 2.467log_{10}DBH$** $r^2=0.969$, P<0.001 **$Log_{10}B=2.033+ 2.469log_{10}DBH$** $r^2=0.972$, P<0.001	Wang (2006)

Total branch biomass	**$Log_{10}B=1.891 + 2.406log_{10}DBH$** $r^2=0.960$, P<0.001	
Total foliage biomass	**$Log_{10}B=0.703 + 2.855log_{10}DBH$** $r^2=0.903$, P<0.001	
	$Log_{10}B=0.855 + 2.135log_{10}DBH$ $r^2=0.818$, P<0.001 Where, B=Biomass (g), DBH=Diameter at breast height (cm)	
14. Maple (*Acer mono* Maxim.)		Wang (2006)
Total biomass	**$Log_{10}B=2.033 + 2.469log_{10}DBH$** $r^2=0.972$, P<0.001	
Aboveground biomass	**$Log_{10}B=1.945 + 2.467log_{10}DBH$** $r^2=0.969$, P<0.001	
Belowground biomass	**$Log_{10}B=2.033+ 2.469log_{10}DBH$** $r^2=0.972$, P<0.001	
Stem biomass	**$Log_{10}B=1.891 + 2.406log_{10}DBH$** $r^2=0.960$, P<0.001	
Total branch biomass	**$Log_{10}B=0.703 + 2.855log_{10}DBH$** $r^2=0.903$, P<0.001	
Total foliage biomass	**$Log_{10}B=0.855 + 2.135log_{10}DBH$** $r^2=0.818$, P<0.001 Where, B=Biomass (g), DBH=Diameter at breast height (cm)	
15. Amur linden (*Tilia amurensis* Rupr.)		Wang (2006)
Total biomass	**$Log_{10}B=2.033 + 2.469log_{10}DBH$** $r^2=0.972$, P<0.001	
Aboveground biomass	**$Log_{10}B=1.945 + 2.467log_{10}DBH$**	

Belowground biomass Stem biomass Total branch biomass Total foliage biomass	r^2=0.969, P<0.001 **$Log_{10}B=2.033+ 2.469log_{10}DBH$** r^2=0.972, P<0.001 **$Log_{10}B=1.891 + 2.406log_{10}DBH$** r^2=0.960, P<0.001 **$Log_{10}B=0.703 + 2.855log_{10}DBH$** r^2=0.903, P<0.001 **$Log_{10}B=0.855 + 2.135log_{10}DBH$** r^2=0.818, P<0.001 Where, B=Biomass (g), DBH=Diameter at breast height (cm)	
16. For 10-year-old Scots pine trees (*P. sylvestris* L.) Stem Branch	Stem: **$Y = a DBH^b$** a(S.E.)=0.084 (0.019), b(S.E.)=1.985(0.107), R^2adj=0.986, RMSE=0.261, P<0.001 **$Y = a DBH^b H^c$** a(S.E.)=0.021(0.007), b(S.E.)=1.474(0.097), c(S.E.)=1.485(0.315), R^2adj=0.977, RMSE=0.315, P<0.001 Branch: **$Y = a DBH^b$** a(S.E.)=0.051 (0.011), b (S.E.)= 2.083 (0.102), R^2adj= 0.989, RMSE= 0.183, P < 0.001 **$Y = a DBH^b H^c$** a(S.E.)=0.010(0.004), b(S.E.)=1.483(0.104), c(S.E.)=1.758 (0.337), R^2adj= 0.976,	Xiao and Ceulemans (2004)

	RMSE=0.253, P<0.001 **$Y = a\ DBH^b\ CL^d$** a(S.E.)=0.034(0.008), b(S.E.)=1.7543(0.096), d(S.E.)=0.682(0.236), R^2adj=0.966, RMSE=0.297, P<0.001 **$Y = a\ DBH^b\ H^c\ CL^d$** a(S.E.)=0.005(0.002), b(S.E.)=1.441(0.099), c(S.E.)=3.221(0.587), d(S.E.)= -1.123(0.363), R^2adj=0.979, RMSE=0.234, P<0.001 **$Y = a\ BD^b$** a(S.E.)=31.41(2.07), b(S.E.)=2.15(0.04), R^2adj=0.936, RMSE=75.45, P<0.001 **$Y = a\ BD^b\ BL^c$** a(S.E.)=0.03(0.02)NS, b(S.E.)=1.31(0.07), c(S.E.)=1.51(0.15), R^2adj=0.967, RMSE=54.53, P<0.001 **$Y = BD^b\ BL^c$** b(S.E.)=1.67(0.04), c(S.E.)=0.76(0.01), R^2adj=0.960, RMSE=59.68, P<0.001 **$Y = a\ BD^b\ BL^c\ WP^d$** a(S.E.)=0.05(0.05)NS, b(S.E.)=1.41(0.10), c(S.E.)=1.31(0.21), d(S.E.)=0.21(0.11)NS R^2adj=0.967, RMSE=54.08, P<0.001 **$Y = BD^b\ BL^c\ WP^d$** b(S.E.)=1.73(0.04), c(S.E.)=0.64(0.03), d(S.E.)=0.42(0.09), R^2adj=0.964, RMSE=56.30, P<0.001 Needle:	

Needle	**$Y = a\ BD^b$** a(S.E.)=22.86(1.57), b(S.E.)=2.36(0.04), R^2adj=0.950, RMSE=68.78, P<0.001 **$Y = a\ BD^b\ BL^c$** a(S.E.)=0.22(0.19)NS, b(S.E.)=1.80(0.09), c(S.E.)=1.00(0.18), R^2adj=0.962, RMSE=60.18, P<0.001 **$Y = BD^b\ BL^c$** b(S.E.)=1.95(0.04), c(S.E.)=0.68(0.01), R^2adj=0.961, RMSE=60.81, P<0.001, **$Y = a\ BD^b\ BL^c\ WP^d$** a(S.E.)=0.02(0.02)NS, b(S.E.)=1.49(0.12), c(S.E.)=1.68(0.26), d(S.E.)= - 0.56(0.13)NS, R^2adj=0.966, RMSE=56.85, P<0.001 **$Y = BD^b\ BL^c\ WP^d$** b(S.E.)=1.93(0.04), c(S.E.)=0.73(0.03), d(S.E.)= - 0.17(0.08), R^2adj=0.962, RMSE=60.31, P<0.001 **$Y = a\ DBH^b$** a(S.E.)=0.032(0.007), b(S.E.)=2.249(0.102), R^2adj=0.991, RMSE=0.156, P<0.001 **$Y = a\ DBH^b\ H^c$** a(S.E.)=0.007(0.002), b(S.E.)=1.698(0.090), c(S.E.)=1.583(0.283), R^2adj=0.985, RMSE=0.192, P<0.001 **$Y = a\ DBH^b\ CL^d$** a(S.E.)=0.025(0.005), b(S.E.)=1.975(0.089), d(S.E.)=0.517(0.208), R^2adj=0.977,	

	RMSE=0.236, P<0.001 **$Y = a\ DBH^b\ H^c\ CL^d$** a(S.E.)=0.004(0.001), b(S.E.)=1.658(0.075), c(S.E.)=3.396(0.436), d(S.E.)= -1.398(0.271),	
Coarse root	R^2adj=0.990, RMSE=0.157, P<0.001 Coarse root: **$Y = a\ DBH^b$** a(S.E.)=0.007(0.003), b(S.E.)=2.897(0.193), R^2adj=0.983, RMSE=0.227, P<0.001 **$Y = a\ DBH^b\ H^c$** a(S.E.)=0.0001(0.00006), b(S.E.)=1.536(0.105), c(S.E.)=4.076(0.332), R^2adj=0.988,	
Small root	RMSE=0.185, P<0.001 Small root: **$Y = a\ DBH^b$** a(S.E.)=0.002(0.0006), b(S.E.)=2.222(0.129), R^2adj=0.985, RMSE=0.012, P<0.001 **$Y = a\ DBH^b\ H^c$** a(S.E.)=0.0001(0.00003), b(S.E.)=1.315(0.067), c(S.E.)=2.864(0.216), R^2adj=0.992,	
Total	RMSE=0.008, P<0.001 Total: **$Y = a\ DBH^b$** a(S.E.)=0.152(0.033), b(S.E.)=2.234(0.100), R^2adj=0.991, RMSE=0.705, P<0.001 **$Y = a\ DBH^b\ H^c$** a(S.E.)=0.02(0.007), b(S.E.)=1.53 (0.092), c(S.E.)=2.098(0.295), R^2adj=0.984,	

	RMSE=0.892, P<0.001 **$Y = a\ DBH^b\ CL^d$** a(S.E.)=0.092(0.022), b(S.E.)=1.85(0.095), d(S.E.)=0.820(0.227), R^2adj=0.972, RMSE=1.17, P<0.001 **$Y = a\ DBH^b\ H^c\ CL^d$** a(S.E.=0.01(0.004), b(S.E.)=1.49(0.081), c(S.E.)=3.741(0.469), d(S.E.)= -1.264(0.289) R^2adj=0.988, RMSE=0.768, P<0.001 Where, BD=Branch diameter (cm), BL=Branch length (cm), WP=Whorl position, NA=Non-significant(P>0.05), DBH=Diameter at breast height (cm), H=Tree height (m), CL=Crown length (m), SE=Standard error; R^2adj= Adjusted multiple coefficient of determination, RMSE=Root of mean squared error	
17. Sassafras	**Log 10 (bole + br)grams = 1.9566+2.3836 Log 10 (dbh cm)** Where, oven dry weight of biomass component of tree will be in kilograms and dbh in centimeters a and b are parameters and are different for every species	Xiao and Ceulemans (2004)
18. Sumac, Staghorn	**$M=0.0825\ dbh^{2.4680}$** Where, M=Oven dry weight of biomass component of tree in kilograms, D=dbh in centimeters, a and b are parameters and are different for every species	Xiao and Ceulemans (2004)
19. Witch Hazel	**Log 10 (bole + br)grams = 2.025 + 2.163 Log 10 (dbh cm)** Where, oven dry weight of biomass component of tree in kilograms and dbh in centimeters a and b are parameters and are different for every species	Xiao and Ceulemans (2004)
20. *Abies* spp (Fir)	**$CR=aD^b$** $a=5.2193.10^{-4}$, b=1.459 **$CR= a+bD^c$**	Broadmeadow & Matthews (2004)

	a=0.0060722, b=9.58.10^{-6}, c=2.5578 Where, CR=Crown biomass (in t), D=Diameter at breast height (in cm)	
21. *Picea spp.*	**AB= a.D^b.H^c** D (cm)=4.9-28.6,H (m)=4.8-15.4, n=56, r^2=0.965 a=0.1334, b=1.8716, c=0.4386 Where, AB=Total above ground biomass (kg), D=Diameter at breast height (cm), H=Height in (m) **CR= a.D^b.H^c** a=0.087, b=2.287, c= - 0.2897 D (cm)=4.9-28.6, H (m)=4.8-15.4, n=56, r^2=0.905 Where, CR=Crown biomass (t), D=Diameter at breast height(cm) **CR= a.D^b** a=5.2193.10^{-4}, b=1.459 Where, CR=Crown biomass (t), D=Diameter at breast height(cm) **CR= a+bD^c** a=0.0060722, b=9.58.10^{-6}, c=2.5578 Where, CR=Crown biomass (t), D=Diameter at breast height (cm) **ST= a.D^b.H^c** D (cm)=4.9-28.6,H (m)=4.8-15.4, n=56, r^2=0.981, a=0.0558, b=1.5953, c=0.9336 Where, ST=Total stem biomass (t), D=Diameter at breast height (cm)	Broadmeadow & Matthews (2004) Snorrason & Einarsson (2004)
22. *Acer pensylvanicum* L. and *Castenea dentate* (Marsh.) Borkh	For each sapling: **G = (ΔS + ΔB + ΔF) / ΔLA** Where, G=The mean annual production of above-ground biomass per unit leaf area**,** ΔB=Dry mass increment of all branches, ΔF=Total leaf biomass production, ΔS=Stem production, SLA=Specific surface area, which was determined from a sub sample of the current leaves for each sapling**,** ΔLA=Total leaf area (ΔLA = SLA × ΔF)	King (2003)
23. *Acer pensylvanicum* L. and *Castenea dentata* (Marsh.)Borkh	*ΔF=current leaf dry mass× (current leaf no.+ leaf scar no.) / current leaf no.* Where, ΔF=Total leaf biomass production	King (2003)
24. *Acer pensylvanicum* L. and	*ΔS= S×[I - ∑(A_f– A_i) / ∑A_f]+dry mass of stem extension increment*	King (2003)

Castenea dentata (Marsh.)Borkh	Where, ΔS=Stem production, S=Current stem dry mass after removal of the upper extension increment, $\sum A_f$=Stem cross-sectional area under the bark at harvest time, $\sum A_i$= stem cross-sectional area under the bark at initial time.	
25. *Quercus* spp. (Oak, Eiche)	**Ln(AB)=a+bln(D)** N=33, a= - 0.883, b=2.140 Where, AB=Total above ground biomass (kg),D=Diameter at breast height (cm) **Ln(ABW)=a+bln(D)** D (cm)=4.5-52, N=20, r^2=0.99, a= - 2.4232, b=2.4682 Where, ABW=Total above ground woody biomass (kg), D=Diameter at breast height (cm) **Ln(ABW)=a+bln(D)** D (cm)=4.3-35, N=16, r^2=0.99, a= - 2.3223, b=2.4029 Where, ABW=Total above ground woody biomass (kg), D=Diameter at breast height (cm) **Ln(ABW)=a+bln(D)** D (cm)=3.8-11, N=15, r^2=0.974, a= - 3.1404, b=2.8113 Where, ABW=Total above ground woody biomass (kg), D=Diameter at breast height (cm) **Ln(ABW)=a+bln(D)** D (cm)=5.7-33, N=18, r^2=0.995, a= - 3.1009, b=2.6996 Where, ABW=Total above ground woody biomass (kg), D=Diameter at breast height (cm) **$CR=a.D^b$** a= $2.1612.10^{-4}$ Where, CR=Crown biomass (t), D=Diameter at breast height (cm) **$CR=a.D^b.H^c$** a=$5.4224.10^{-4}$, b=2.35, c= - 1.022 Where, CR=Crown biomass (t), D=Diameter at breast height (cm), H=Height (m)	Hochbichler (2002) Bunce (1968) Bunce (1968) Bunce (1968) Bunce (1968) Broadmeadow & Matthews (2004) Broadmeadow & Matthews (2004)
26. Douglas-fir (*Pseudotsuga menziesii* (Mirbel)Franco)	Branch: **$Y=a+(b\times D_{10}^2)$** **$Y=a+(b\times D_{10})+(c\times D_{10}^2)$** **$Y=a\times D_{10}^2$**	Ponette et al. (2001)

	$Y=(a\times D_{10})+(b\times D_{10}^2)$ **$Y=a\times D_{10}^b$** Where, Y=Biomass or nutrient content at the branch level (needles, wood), D_{10} (mm)= Branch diameter 10 cm from the insertion on the stem	
27. Douglas-fir (*Pseudotsuga menziesii* (Mirbel)Franco)	Stem, crown: **$Y=a+(b\times DBH^2)$** **$Y=a+(b\times DBH)+(c\times DBH^2)$** **$Y=a\times DBH^2$** **$Y=(a\times DBH)+(b\times DBH^2)$** **$\ln Y=a+(b\times \ln DBH)$** **$Y=a\times DBH^b$** Where, Y=The biomass or nutrient content at the stem (wood, bark) or crown levels (needles, wood), DBH (cm)=Diameter at breast height	Ponette et al. (2001)
28. Ash, white	**$M= 0.1063\ dbh^{2.4798}$** Where, M=oven dry weight of biomass component of tree in kilograms, D=dbh in centimeters, a and b are parameters and are different for every species	Methods of Ecosystem Analysis Saltonstall Ridge, East Haven, CT. (1999) http://www.yale.edu/fes519b/saltonstall/index.htm
29. Basswood	**$M= 0.0617\ dbh^{2.5328}$** Where, M=oven dry weight of biomass component of tree in kilograms, D=dbh in centimeters, a and b are parameters and are different for every species	Methods of Ecosystem Analysis Saltonstall Ridge, East Haven, CT. (1999) http://www.yale.edu/fes519b/saltonstall/index.htm
30. Beech	**$M= 0.0842\ dbh^{2.5715}$** Where, M=oven dry weight of biomass component of tree in kilograms, D=dbh in centimeters, a and b are parameters and are different for every species	Methods of Ecosystem Analysis Saltonstall Ridge, East Haven, CT. (1999) http://www.yale.edu/fes519b/saltonstall/index.htm
31. Birch, black/sweet	**$M= 0.0629\ dbh^{2.6606}$** Where, M=oven dry weight of biomass component of tree in kilograms, D=dbh in centimeters, a and b are parameters and are different for every species	Methods of Ecosystem Analysis Saltonstall Ridge, East Haven, CT. (1999) http://www.yale.edu/fes519b/saltonstall/index.htm

32. Cedar, Red	**$M = 0.1019\ dbh^{2.3000}$** Where, M=oven dry weight of biomass component of tree in kilograms, D=dbh in centimeters, a and b are parameters and are different for every species	Methods of Ecosystem Analysis Saltonstall Ridge, East Haven, CT. (1999) http://www.yale.edu/fes519b/saltonstall/index.htm
33. Cherry, Black	**$M = 0.0716\ dbh^{2.6174}$** Where, M=oven dry weight of biomass component of tree in kilograms, D=dbh in centimeters, a and b are parameters and are different for every species	Methods of Ecosystem Analysis Saltonstall Ridge, East Haven, CT. (1999) http://www.yale.edu/fes519b/saltonstall/index.htm
34. Cherry, Sweet	**$M = 0.1556\ dbh^{2.1948}$** Where, M=oven dry weight of biomass component of tree in kilograms, D=dbh in centimeters, a and b are parameters and are different for every species	Methods of Ecosystem Analysis Saltonstall Ridge, East Haven, CT. (1999) http://www.yale.edu/fes519b/saltonstall/index.htm
35. Elm, American	**$M = 0.0629\ dbh^{2.6606}$** Where, M=oven dry weight of biomass component of tree in kilograms, D=dbh in centimeters, a and b are parameters and are different for every species	Methods of Ecosystem Analysis Saltonstall Ridge, East Haven, CT. (1999) http://www.yale.edu/fes519b/saltonstall/index.htm
36. Elm, slippery/red	**$M = 0.0629\ dbh^{2.6606}$** Where, M=oven dry weight of biomass component of tree in kilograms, D=dbh in centimeters, a and b are parameters and are different for every species	Methods of Ecosystem Analysis Saltonstall Ridge, East Haven, CT. (1999) http://www.yale.edu/fes519b/saltonstall/index.htm
37. Black Locust	**$M = 0.0792\ dbh^{2.6349}$** Where, M=oven dry weight of biomass component of tree in kilograms, D=dbh in centimeters, a and b are parameters and are different for every species	Methods of Ecosystem Analysis Saltonstall Ridge, East Haven, CT. (1999) http://www.yale.edu/fes519b/saltonstall/index.htm
38. Flowering dogwood	**$M = 0.0792\ dbh^{2.6349}$** Where, M=oven dry weight of biomass component of tree in kilograms, D=dbh in centimeters, a and b are parameters and are different for every species	Methods of Ecosystem Analysis Saltonstall Ridge, East Haven, CT. (1999) http://www.yale.edu/fes519b/saltonstall/index.htm
39. Hackberry	**$M = 0.0792\ dbh^{2.6349}$** Where, M=oven dry weight of biomass component	Methods of Ecosystem Analysis Saltonstall Ridge,

	of tree in kilograms, D=dbh in centimeters, a and b are parameters and are different for every species	East Haven, CT. (1999) http://www.yale.edu/fes519b/saltonstall/index.htm
40. Hemlock	**$M = 0.0622\ dbh^{2.4500}$** Where, M=oven dry weight of biomass component of tree in kilograms, D=dbh in centimeters, a and b are parameters and are different for every species	Methods of Ecosystem Analysis Saltonstall Ridge, East Haven, CT. (1999) http://www.yale.edu/fes519b/saltonstall/index.htm
41. Hickory, mocker nut	**$M = 0.0792\ dbh^{2.6349}$** Where, M=oven dry weight of biomass component of tree in kilograms, D=dbh in centimeters, a and b are parameters and are different for every species	Methods of Ecosystem Analysis Saltonstall Ridge, East Haven, CT. (1999) http://www.yale.edu/fes519b/saltonstall/index.htm
42. Hickory, pignut	**$M = 0.0792\ dbh^{2.6349}$** Where, M=oven dry weight of biomass component of tree in kilograms, D=dbh in centimeters, a and b are parameters and are different for every species	Methods of Ecosystem Analysis Saltonstall Ridge, East Haven, CT. (1999) http://www.yale.edu/fes519b/saltonstall/index.htm
43. Hickory, shagbark	**$M = 0.0792\ dbh^{2.6349}$** Where, M=oven dry weight of biomass component of tree in kilograms, D=dbh in centimeters, a and b are parameters and are different for every species	Methods of Ecosystem Analysis Saltonstall Ridge, East Haven, CT. (1999) http://www.yale.edu/fes519b/saltonstall/index.htm
44. Hop hornbeam	**$M = 0.0792\ dbh^{2.6349}$** Where, M=oven dry weight of biomass component of tree in kilograms, D=dbh in centimeters, a and b are parameters and are different for every species	Methods of Ecosystem Analysis Saltonstall Ridge, East Haven, CT. (1999) http://www.yale.edu/fes519b/saltonstall/index.htm
45. Hornbeam	**$M = 0.0792\ dbh^{2.6349}$** Where, M=oven dry weight of biomass component of tree in kilograms, D=dbh in centimeters, a and b are parameters and are different for every species	Methods of Ecosystem Analysis Saltonstall Ridge, East Haven, CT. (1999) http://www.yale.edu/fes519b/saltonstall/index.htm
46. Maple, Red	**$M = 0.0910\ dbh^{2.5080}$** Where, M=oven dry weight of biomass component of tree in kilograms, D=dbh in centimeters, a and b are parameters and are different for every species	Methods of Ecosystem Analysis Saltonstall Ridge, East Haven, CT. (1999) http://www.yale.edu/fes519b/saltonstall/index.htm

47. Maple, Sugar	**M= 0.2064 dbh** $^{2.5300}$ Where, M=oven dry weight of biomass component of tree in kilograms, D=dbh in centimeters, a and b are parameters and are different for every species	Methods of Ecosystem Analysis Saltonstall Ridge, East Haven, CT. (1999) http://www.yale.edu/fes519b/saltonstall/index.htm
48. Oak, black	**M= 0.0904 dbh** $^{2.5143}$ Where, M=oven dry weight of biomass component of tree in kilograms, D=dbh in centimeters, a and b are parameters and are different for every species	Methods of Ecosystem Analysis Saltonstall Ridge, East Haven, CT. (1999) http://www.yale.edu/fes519b/saltonstall/index.htm
49. Oak, chestnut	**M= 0.0554 dbh** $^{2.7276}$ Where, M=oven dry weight of biomass component of tree in kilograms, D=dbh in centimeters, a and b are parameters and are different for every species	Methods of Ecosystem Analysis Saltonstall Ridge, East Haven, CT. (1999) http://www.yale.edu/fes519b/saltonstall/index.htm
50. Oak, red	**M= 0.1130 dbh** $^{2.4572}$ Where, M=oven dry weight of biomass component of tree in kilograms, D=dbh in centimeters, a and b are parameters and are different for every species	Methods of Ecosystem Analysis Saltonstall Ridge, East Haven, CT. (1999) http://www.yale.edu/fes519b/saltonstall/index.htm
51. Oak, white	**M= 0.0579 dbh** $^{2.6887}$ Where, M=oven dry weight of biomass component of tree in kilograms, D=dbh in centimeters, a and b are parameters and are different for every species	Methods of Ecosystem Analysis Saltonstall Ridge, East Haven, CT. (1999) http://www.yale.edu/fes519b/saltonstall/index.htm
52. Olive	**Log 10 (bole + br)grams = 2.025 + 2.163 Log 10 (dbh cm)** Where, D=Dbh in centimeters, a and b are parameters and are different for every species	Methods of Ecosystem Analysis Saltonstall Ridge, East Haven, CT. (1999) http://www.yale.edu/fes519b/saltonstall/index.htm
53. Pine, White	**M= 0.1617dbh** $^{2.1420}$ Where, M=oven dry weight of biomass component of tree in kilograms, D=dbh in centimeters, a and b are parameters and are different for every species	Methods of Ecosystem Analysis Saltonstall Ridge, East Haven, CT. (1999) http://www.yale.edu/fes519b/saltonstall/index.htm

54. Norway spruce (*Picea abies*) Stem wood	**Ln(element or biomass, kg)** **$= \alpha + \beta \ln(DBH^2 \times H)$** α_{treat} and β_{treat} for treated plot and α_{cont} and $\beta_{cont\ for\ control}$ plot. **Biomass**: α= -3.24, β=0.88, R^2(n=20)=0.96, P (β=0&n=20)=0.00, P(β_{treat}= β_{cont}, N=20, n=5)= 0.84, P(α_{treat}= α_{cont}, N=20, n=5)=0.86 **N**: α= -9.62,β=0.83,R^2 (n=20)= 0.70, P (β=0&n=20)=0.00, P(β_{treat}= β_{cont}, N=20,n=5)= 0.21, P(α_{treat}= α_{cont},N=20, n=5)=0.66 **P**(CaMgPS): α= -9.51, β=0.52, R^2(n=20)= 0.37, P(β=0&n=20)= 0.00, P(β_{treat}= β_{cont}, N=20,n=5)= 0.02, P (α_{treat}= α_{cont},N=20, n=5)= 0.52 **K**: α= -8.81, β=0.66, R^2(n=20)= 0.59, P (β=0&n=20)=0.00, P(β_{treat}= β_{cont}, N=20,n=5)= 0.09, P(α_{treat}= α_{cont}, N=20,n=5)= 0.39 **Ca**: α= -9.21, β=0.73, R^2(n=20)= 0.74, P (β=0&n=20)=0.00, P(β_{treat}= β_{cont}, N=20,n=5)= 0.15, P(α_{treat}= α_{cont}, N=20, n=5)= 0.73 **Mg**: α= -8.98, β=0.53, R^2 (n=20)= 0.49, P (β=0&n=20)=0.00, P(β_{treat}= β_{cont}, N=20, n=5)= 0.09, P(α_{treat}= α_{cont}, N=20, n=5)=0.76. **S**: α= -11.70, β=0.75, R^2 (n=20)= 0.76, P (β=0&n=20)=0.00, P(β_{treat}= β_{cont}, N=20, n=5)= 0.01, P(α_{treat}= α_{cont}, N=20, n=5)= 0.58. **Biomass**: α= -5.51, β=0.88, R^2 (n=20)=0.84, P(β=0&n=20)=0.00, P(β_{treat}= β_{cont}, N=20, n=5)= 0.74, P(α_{treat}= α_{cont}, N=20, n=5)= 0.55. **N** (CaMgP. NPK): α= -10.93, β=0.90, R^2 (n=20)=0.72, P(β=0&n=20)=0.00, P(β_{treat}= β_{cont}, N=20, n=5)=0.02, P(α_{treat}= α_{cont}, N=20, n=5)= 0.52 **P** (CaMgPS", CaMgPS . NPK", and CaMgP. NPK"): α= -13.08, β=0.93, R^2 (n=20)= 0.65, P(β=0&n=20)=0.00, P(β_{treat}= β_{cont}, N=20, n=5)= 0.00, P(α_{treat}= α_{cont}, N=20, n=5)= 0.81. **K** (CaMgPS . NPK" and CaMgP . NPK): α= -10.70, β=0.81, R^2(n=20)= 0.77, P(β=0&n=20)= 0.00, P(β_{treat}= β_{cont}, N=20, n=5)=0.00, P(α_{treat}= α_{cont}, N=20,	Ingerslev and Hallbacken (1999)
Stem bark		

	n=5)= 0.57 **Ca**: α= -10.30, β=0.88, R^2(n=20)= 0.75, P(β=0&n=20)=0.00, P(β_{treat}= β_{cont}, N=20, n=5)= 0.25, P(α_{treat}= α_{cont}, N=20, n=5)=0.75. **Mg**: α= -10.52, β=0.68, R^2(n=20)= 0.61, P(β=0&n=20)=0.00, P(β_{treat}= β_{cont}, N=20, n=5)= 0.11, P(α_{treat}= α_{cont}, N=20, n=5)= 0.87. **S** (CaMgPS . NPK" and CaMgP. NPK): α= -13.36, β=0.92, R^2(n=20)=0.70, P (β=0&n=20)= 0.00,P(β_{treat}= β_{cont}, N=20, n=5)= 0.01, P(α_{treat}= α_{cont}, N=20, n=5)= 0.82. **Biomass**: α= -5.88, β=1.02, R^2(n=20)= 0.83, P(β=0&n=20)=0.00, P(β_{treat}= β_{cont}, N=20, n=5)= 0.45, P(α_{treat}= α_{cont}, N=20, n=5)= 0.45 **N**: α= -12.02, β=1.14, R^2 (n=20)= 0.85, P(β=0&n=20)=0.00, P (β_{treat}= β_{cont}, N=20, n=5)= 0.09, P(α_{treat}= α_{cont}, N=20, n=5)= 0.93. **P**: α= -15.03, β=1.24, R^2(n=20)= 0.85, P (β=0&n=20)=0.00, P (β_{treat}= β_{cont}, N=20, n=5)= 0.44, P(α_{treat}= α_{cont}, N=20, n=5)= 0.87. **K**: α= -13.35, β=1.16, R^2(n=20)= 0.87, P (β=0&n=20)=0.00, P(β_{treat}= β_{cont}, N=20, n=5)= 0.21, P (α_{treat}= α_{cont}, N=20, n=5)= 0.86 **C**a: α= -12.31, β=1.12, R^2(n=20)= 0.79, P (β=0&n=20)=0.00, P (β_{treat}= β_{cont}, N=20, n=5)= 0.51, P (α_{treat}= α_{cont}, N=20, n=5)= 0.79. **Mg**: α= -12.75, β=0.98, R^2(n=20)= 0.80, P (β=0&n=20)=0.00, P(β_{treat}= β_{cont}, N=20, n=5)= 0.17, P(α_{treat}= α_{cont}, N=20, n=5)= 0.97 **S**: α= -14.97, β=1.19, R^2(n=20)= 0.86, P (β=0&n=20)=0.00, P (β_{treat}= β_{cont}, N=20, n=5)= 0.29, P(α_{treat}= α_{cont}, N=20, n=5)= 0.95.	
Living branches	**Biomass**: α= -7.75, β=1.08, R^2 (n=20)= 0.58, P (β=0&n=20)=0.00, P (β_{treat}= β_{cont}, N=20, n=5)=0.08, P (α_{treat}= α_{cont}, N=20, n=5)=0.50 **N**: α= -11.81, β=0.98, R^2 (n=20)= 0.52,	

Dead branches	$P(\beta=0\&n=20)=0.00$, $P\beta_{treat}=\beta_{cont}$, N=20, n=5)= 0.07, $P(\alpha_{treat}=\alpha_{cont}$, N=20, n=5)= 0.76 **P**: α= -14.74, β=0.97, R^2 (n=20)= 0.47, $P(\beta=0\&n=20)=0.00$, $P(\beta_{treat}=\beta_{cont}$, N=20, n=5)= 0.18, P ($\alpha_{treat}=\alpha_{cont}$, N=20, n=5)= 0.74 **K** (CaMgPS, CaMgPS . NPK, and CaMgP . NPK): α= -14.44, β=0.98, R^2 (n=20)= 0.36, $P(\beta=0\&n=20)=0.00$, P ($\beta_{treat}=\beta_{cont}$, N=20, n=5)= 0.01, P ($\alpha_{treat}=\alpha_{cont}$, N=20, n=5)=0.35 **Ca**: α= -12.96, β=1.02, R^2 (n=20)= 0.48, P ($\beta=0\&n=20$)=0.00, P ($\beta_{treat}=\beta_{cont}$, N=20, n=5)= 0.34, P ($\alpha_{treat}=\alpha_{cont}$, N=20, n=5)= 0.14. **Mg**: α= -15.05, β=1.05, R^2 (n=20)= 0.59, P ($\beta=0\&n=20$)=0.00, P ($\beta_{treat}=\beta_{cont}$, N=20, n=5)= 0.26, P ($\alpha_{treat}=\alpha_{cont}$, N=20, n=5)= 0.40 **S**: α= -14.51, β=1.03, R^2 (n=20)= 0.54, P ($\beta=0\&n=20$)=0.00, P ($\beta_{treat}=\beta_{cont}$, N=20, n=5)= 0.09, P ($\alpha_{treat}=\alpha_{cont}$, N=20, n=5)= 0.94. **Biomass**: α= -4.24, β=0.67, R^2 (n=20)= 0.46 , P ($\beta=0\&n=20$)=0.01, $P(\beta_{treat}=\beta_{cont}$, N=20,n=5)= 0.17, P ($\alpha_{treat}=\alpha_{cont}$, N=20, n=5)= 0.21. **N** (CaMgPS . NPK and CaMgP . NPK): α= -9.00, β=0.73, R^2 (n=20)= 0.43, $P(\beta=0\&n=20)$= 0.00, P ($\beta_{treat}=\beta_{cont}$, N=20, n=5)=0.03, $P(\alpha_{treat}=\alpha_{cont}$, N=20, n=5)= 0.09 **P**(CaMgPS", CaMgPS . NPK",and CaMgP . NPK"): α= -14.49, β=1.14, R^2 (n=20)= 0.76, $P(\beta=0\&n=20)$= 0.01*, $P(\beta_{treat}=\beta_{cont}$, N=20, n=5)= 0.00*,$P(\alpha_{treat}=\alpha_{cont}$, N=20, n=5)= 0.09 **K** (CaMgPS. NPK" and CaMgP. NPK"): α= -10.37, β=0.81, R^2 (n=20)=0.48, $P(\beta=0\&n=20)$= 0.00, $P(\beta_{treat}=\beta_{cont}$, N=20, n=5)= 0.04, $P(\alpha_{treat}=\alpha_{cont}$, N=20, n=5)= 0.31. **Ca** (CaMgPS", CaMgPS. NPK",): α= -10.69, β=0.81, R^2 (n=20)=0.22, $P(\beta=0\&n=20)$=0.04, P ($\beta_{treat}=\beta_{cont}$, N=20, n=5)=0.04, $P(\alpha_{treat}=\alpha_{cont}$, N=20, n=5)=0.10 **Mg** (CaMgPS. NPK"): α= -10.16, β=0.60, R^2 (n=20)=0.30, P ($\beta=0\&n=20$)=0.01, $P(\beta_{treat}=\beta_{cont}$,	

Current year needles Older needles	N=20, n=5)=0.03, P (α_{treat}= α_{cont}, N=20, n=5)= 0.07. **S** (CaMgPS", CaMgPS. NPK" and CaMgP. NPK"): α= -11.30, β=0.70, R^2 (n=20)= 0.31, P (β=0&n=20)= 0.01, P(β_{treat}= β_{cont}, N=20, n=5)= 0.0, P(α_{treat}= α_{cont}, N=20, n=5)= 0.06 **Biomass**: α= -4.85, β=0.81, R^2 (n=20)=0.74, P (β=0&n=20)=0.00, P(β_{treat}= β_{cont}, N=20, n=5)= 0.62, P(α_{treat}= α_{cont}, N=20, n=5)= 0.37. **N**: α= -10.17, β=0.92, R^2 (n=20)= 0.73, P (β=0&n=20)=0.00, P(β_{treat}= β_{cont}, N=20, n=5)= 0.45, P (α_{treat}= α_{cont}, N=20, n=5)= 0.31. **P** (CaMgPS", CaMgPS. NPK" and CaMgP. NPK"): α= -12.23, β=0.93, R^2 (n=20)= 0.64, P (β=0&n=20)=0.00, P(β_{treat}= β_{cont}, N=20, n=5)= 0.04, P (α_{treat}= α_{cont}, N=20, n=5)= 0.65 **K**: α= -13.34, β=1.18, R^2 (n=20)= 0.86, P (β=0&n=20)=0.00, P(β_{treat}= β_{cont}, N=20, n=5)= 0.46, P (α_{treat}= α_{cont}, N=20, n=5)= 0.35 **Ca** (CaMgPS", and CaMgPS. NPK"): α= -12.08, β=1.09, R^2 (n=20)= 0.55, P (β=0&n=20)= 0.00, P (β_{treat}= β_{cont}, N=20, n=5)= 0.01, P(α_{treat}= α_{cont}, N=20, n=5)= 0.41 **Mg** (CaMgPS): α= -12.06, β=0.91, R^2 (n=20)= 0.64, P (β=0&n=20)=0.00, P (β_{treat}= β_{cont}, N=20, n=5)=0.01, P(α_{treat}= α_{cont}, N=20, n=5)= 0.64 **S**: α= -12.31, β=0.90, R^2 (n=20)= 0.67, P (β=0&n=20)=0.00, P (β_{treat}= β_{cont}, N=20, n=5)= 0.10, P (α_{treat}= α_{cont}, N=20, n=5)= 0.32	
55. Dominant loblolly pine (age 10 to 48) Bole Needle Branch	**log(B)=b0 + b1[log(D)]** $r^{2=}$0.98 **log(B)=b0 + b1[log(D)]** $r^{2=}$0.92	Naidu *et al.* (1998)

Total above ground	**log(B)=b0 + b1[log(D)]** $r^{2=}$0.92 **log(B)=b0 + b1[log(D)]** $r^{2=}$0.99	
56. Suppressed loblolly pine (age 10 to 48) Bole Needle Branch Total above ground	 **log(B)=b0 + b1[log(D)]** $r^{2=}$0.98 **log(B)=b0 + b1[log(D)]** $r^{2=}$0.85 **log(B)=b0 + b1[log(D)]** $r^{2=}$0.86 **log(B)=b0 + b1[log(D)]** $r^{2=}$0.98	Naidu *et al.* (1998)
57. *Picea* and *Abies*	**y = a v + b** a=0.4642, b=47.4990, n=13, r^2=0.98 Where, y=Stand biomass (Mg/ha), v=Stand volume (m^3/ha), a and b=Constants for a specific forest type.	Fang et al. (1998)
58. *Cunninghamia lanceolata*	**y = a v + b** a=0.3999, b=22.5410, n=56, r^2=0.95 Where, y=Stand biomass (Mg/ha), v=Stand volume (m^3/ha), a and b=Constants for a specific forest type.	Fang et al. (1998)
59. *Cypress*	**y = a v + b** a=0.6129, b=46.1451, n=11, r^2=0.96 Where, y=Stand biomass (Mg/ha), v=Stand volume (m^3/ha), a and b=Constants for a specific forest type.	Fang et al. (1998)
60. *Larix*	**y = a v + b** a=0.9671, b=5.7598, n=8, r^2=0.99 Where, y=Stand biomass (Mg/ha), v=Stand volume (m^3/ha), a and b=Constants for a specific forest type.	Fang et al. (1998)

61. *Pinus koraiensis*	**y = a v + b** a=0.5185, b=18.2200, n=17, r^2=0.90 Where, y=Stand biomass (Mg/ha), v=Stand volume (m^3/ha), a and b=Constants for a specific forest type.	Fang et al. (1998)
62. *Pinus armandii*	**y = a v + b** a=0.5856, b=18.7435, n=9, r^2=0.91 Where, y=Stand biomass (Mg/ha), v=Stand volume (m^3/ha), a and b=Constants for a specific forest type.	Fang et al. (1998)
63. *Pinus massoniana, Pinus yunnanesis*	**y = a v + b** a=0.5101, b=1.0451, n=12, r^2=0.92 Where, y=Stand biomass (Mg/ha), v=Stand volume (m^3/ha), a and b=Constants for a specific forest type.	Fang et al. (1998)
64. *Pinus sylvestris* var. *mongolica*	**y = a v + b** a=1.0945, b=2.0040, n=11, r^2=0.98 Where, y=Stand biomass (Mg/ha), v=Stand volume (m^3/ha), a and b=Constants for a specific forest type.	Fang et al. (1998)
65. *Pinus tabulaefomis*	**y = a v + b** a=0.7554, b=5.0928, n=82, r^2=0.96 Where, y=Stand biomass (Mg/ha), v=Stand volume (m^3/ha), a and b=Constants for a specific forest type.	Fang et al. (1998)
66. Other pines and conifer forests	**y = a v + b** a=0.5168, b=33.2378, n=16, r^2=0.94 Where, y=Stand biomass (Mg/ha), v=Stand volume (m^3/ha), a and b=Constants for a specific forest type.	Fang et al. (1998)
67. *Tsugn, Cryptomeria, Keteleeria*	**y = a v + b** a=0.4158, b=41.3318, n=21, r^2=0.89 Where, y=Stand biomass (Mg/ha), v=Stand volume (m^3/ha), a and b=Constants for a specific forest type.	Fang et al. (1998)
68. Mixed conifer and deciduous forests	**y = a v + b** a=0.8019, b=12.2799, n=9, r^2=0.99 Where, y=Stand biomass (Mg/ha), v=Stand volume	Fang et al. (1998)

	(m^3/ha), a and b=Constants for a specific forest type.	
69. *Betula*	**y = a v + b** a=0.9644, b=0.8485, n=4, r^2=0.96 Where, y=Stand biomass (Mg/ha), v=Stand volume (m^3/ha), a and b=Constants for a specific forest type.	Fang et al. (1998)
70. *Casuarina*	**y = a v + b** a=0.9505, b=8.5648, n=3, r^2=1.00 Where, y=Stand biomass (Mg/ha), v=Stand volume (m^3/ha), a and b=Constants for a specific forest type.	Fang et al. (1998)
71. Deciduous oaks	**y = a v + b** a=1.3288, b= - 3.8999, n=3, r^2=0.99 Where, y=Stand biomass (Mg/ha), v=Stand volume (m^3/ha), a and b=Constants for a specific forest type.	Fang et al. (1998)
72. *Eucalyptus*	**y = a v + b** a=0.7893, b=6.9306, n=4, r^2=0.99 Where, y=Stand biomass (Mg/ha), v=Stand volume (m^3/ha), a and b=Constants for a specific forest type.	Fang et al. (1998)
73. Lucidophyllous forests	**y = a v + b** a=1.0357,b=8.0591, n=17 ,r^2=0.89 Where, y=Stand biomass (Mg/ha), v=Stand volume (m^3/ha), a and b=Constants for a specific forest type.	Fang et al. (1998)
74. Mixed deciduous and *Sassafras*	**y = a v + b** a=0.6255, b=91.0013, n=19, r^2=0.86 Where, y=Stand biomass (Mg/ha), v=Stand volume (m^3/ha), a and b=Constants for a specific forest type.	Fang et al. (1998)
75. Nonmerchantable woods	**y = a v + b** a=0.7564, b=8.3103, n=11, r^2=0.98 Where, y=Stand biomass (Mg/ha), v=Stand volume (m^3/ha), a and b=Constants for a specific forest type.	Fang et al. (1998)
76. *Populus*	**y = a v + b** a=0.4754, b=30.6034, n=10, r^2=0.87	Fang et al. (1998)

	Where, y=Stand biomass (Mg/ha), v=Stand volume (m^3/ha), a and b=Constants for a specific forest type.	
77. Tropical forests	**y = a v + b** a=0.9505, b=8.5648, n=3, r^2=0.99 Where, y=Stand biomass (Mg/ha), v=Stand volume (m^3/ha), a and b=Constants for a specific forest type.	Fang et al. (1998)
78. Loblolly pine (age 9 to 41) Branch New foliage Old foliage	**ln(B)=b0 +b1[ln(D)]+b2[ln(L)]+b3[ln(R)]** $r^{2=}$0.93 **ln(B)=b0 +b1[ln(D)]+b2[ln(L)]+b3[ln(R)]** $r^{2=}$0.88 **ln(B)=b0 + b1[ln(D)]+b2[ln(R)]** $r^{2=}$0.88	 Baldwin *et al.* (1997) Baldwin *et al.* (1997) Baldwin *et al.* (1997)
79. Hardwoods (Based on tree diameter < 85 cm)	**Biomass=** **(0. 5+25 000 $dbh^{2.5}$) / ($dbh^{2.5}$+246872)** r^2=0.99 Where, biomass is in units of kg per tree and diameter (dbh) is in cm.	Schroeder et al. (1997)
80. Conifers (Based on tree diameter < 72 cm)	**Biomass=** **(0. 5 + 15 000$dbh^{2.7}$) / ($dbh^{2.7}$ + 364946)** r^2=0.98 Where, biomass is in units of kg per tree and diameter (dbh) is in cm.	Schroeder et al. (1997)
81. Douglas-fir (*Pseudotsuga menziesii* (Mirbel)Franco)	Branch: **Y=(a×$D10^2$)+b($D10^2$×HREL(1-HREL))** Where, Y=Biomass or nutrient content at the branch level (needles, wood), D10 (mm)= Branch diameter 10 cm from the insertion on the stem, HREL=Height above the base of the crown divided by the length of the crown, i.e. (1 - (DINC/CL)), CL (m)=Crown length, DINC (m)=Depth into crown or tree height minus branch	Bartelink (1996)

	height.	
82. Douglas-fir (*Pseudotsuga menziesii* (Mirbel)Franco)	Branch: **Ln Y=a+(b × lnD10)** **Ln Y=a+(b×lnD10)+(c×ln DINC)** **LnY=a+(b×lnD10)+(c×lnDINC)+** **(d×lnRelHACB)** Where, Y=Biomass or nutrient content either at the branch level (needles, wood),D10 (mm)= Branch diameter 10 cm from the insertion on the stem, HREL=Height above the base of the crown divided by the length of the crown, i.e. (1 - (DINC/CL)), CL (m)=Crown length, DINC (m)=Depth into crown or tree height minus branch height, RelHACB=Relative height above crown base, i.e. (1.1 - (DINC/CL)).RelHACB is similar to HREL except it is based on a maximum ratio of 1.1 to avoid computational problems in Ln-transformed regressions.	Kershaw & Maguire (1995)
83. *Eucalyptus* spp. (Eucalypt)	**Ln (AB)= a+ b. ln(D)** D(cm)=4-25, n=22, r^2=0.99, a= -1.762, b=2.2644 Where, AB=Total above ground biomass (kg), D=Diameter at breast height (cm)	Menguzzato (1988)
84. Loblolly pine (age 25) Foliage Live branch Dead branch Stem bark Stem wood	**ln(B)= b0 + b1[ln(D)]** r^2=0.83 **ln(B)= b0 + b1[ln(D)]** r^2=0.91 **B = b0 + b1(D^2)** r^2=0.62 **B = b0 + b1(D^2)** r^2=0.88 **B = b0 + b1(D^2)** r^2=0.99	Pehl *et al.* (1984)

	Where, B=Biomass, D=Diameter	
85. Loblolly pine (age 41) Total stem (5cm top) Branches Foliage Total above Ground	**ln(B)=b0 + b1[log(D)]** r^2=0.985 **ln(B)=b0 + b1[log(D)]** r^2=0.953 **ln(B)=b0 + b1[log(D)]** r^2=0.937 **ln(B)=b0 + b1[log(D)]** r^2=0.985 Where, B=Biomass, D=Diameter	Van Lear *et al.* (1984)
86. Loblolly pine (age 2 to 8) Total above ground	**log(B)=b0 + b1[log(D^2H)]** r^2=0.99 Where, B=Biomass, D=Diameter, H=Tree height	Edwards & McNab (1979)
87. Non-plantation loblolly pine (age 37 to 47**)** Total above ground	**log(B)=b0 + b1[log(D^2H)]** $r^{2=}$0.99 Where, B=Biomass, D=Diameter, H=Tree height	Clark (III) & Taras (1976)
88. Slash pine (age 4 to 8) and loblolly pine (age 4 to 12) Main stem Total branch	**ln(B)=b0 +b1[ln(D+1)]+b2[ln(D+1)]^2+** **b3[ln(H)]** r^2=0.991	Nemeth (1973)

	$ln(B)=b0+b1[ln(D+1)]+b2[ln(D+1)]^2+$ **$b3[ln(L)]+b4[ln(H)]+b5[ln(H)]^2$** $r^2=0.947$ Where, B=Biomass, D=Diameter, H=Tree height	

REFERENCE:

1. Baldwin (Jr.) V. C., Peterson K. D., Burkhart H. E., Amateis R. L., and Dougherty P. M., 1997. Equations for estimating loblolly pine branch and foliage weight and surface area distributions, *Canadian Journal of Forest Research*, 27: pp 918-927.
2. Bartelink, H.H. 1996. Allometric relationships on biomass and needle area of Douglas-fir. *Forest Ecology and Management,* 86: pp 193–203.
3. Broadmeadow, M. & Matthews, R. 2004. Survey methods for Kyoto Protocol monitoring and verification of UK forest carbon stocks. UK Emissions by Sources and Removals by Sinks due to land Use, Use change and Forestry Activities, Report. CEH, Edinburgh (June 2004).
4. Bunce R.G.H. 1968. Biomass and production of trees in mixed deciduoud woodland. I. Girth and height as parameters for the estimation of tree dry weight. *Journal of Ecology* 56: pp 759–775.
5. Clark (III) A. and Taras M. A., 1976. Comparison of aboveground biomass of the four major southern pines. *Forest Products Journal*, 26(10): pp 25-29.
6. Edwards M. B. and McNab W. H., 1979. Biomass prediction for young southern pines. *Journal of Forestry,* 77: pp 291-292.
7. Fang Jing-yun, Wang G.Geoff, Liu Gew-Hua, Xu Song-Ling, 1988. Forest biomass of china: an estimate based on the biomass-volume relationship, *Ecological Applicntioris,* 8(4): pp 1084-1091.
8. Hochbichler, E. 2002. Vorläufige Ergebnisse von Biomasseninventuren in Buchen und Mittelwaldbeständen. In: Dietrich, H.-P., Raspe, S. & Preuhsler, T. (eds.): Inventur von Biomasse- und Nährstoffvorräten in Waldbeständen. Forstliche Forschungsberichte, München, 186: pp 37–46.
9. Ingerslev Morten and Hallbacken Leif, 1999. Above ground biomass and nutrient distribution in a limed and fertilized Norway spruce (*Picea abies*) plantation Part II. Accumulation of biomass and nutrients, *Forest Ecology and Management,* 119, pp 21-38.
10. Kershaw Jr. J.A., Maguire D.A., 1995. Crown structure in western hemlock, Douglas-fir, and grand fir in western Washington: trends in branch-level mass and leaf area. *Can. J. For. Res*. 25: pp 1897-1912.
11. King D. A, 2003. Allocation of above-ground growth is related to light in temperate deciduous saplings, *Functional Ecology,* 17: pp 482-488.
12. Menguzzato, G. 1988. Modelli di previsione del peso fresco, della biomassa e del volume per pino insigne ed eucalitti nell'Azienda Massanova (Salerno). Ann. Ist. Sper. Selvicoltura 19: pp 323–354.
13. Methods of Ecosystem Analysis Saltonstall Ridge, East Haven, CT.1999.
14. .http://www.yale.edu/fes519b/saltonstall/index.htm

15. Naidu S. L., DeLucia E. H., and Thomas R. B., 1998. Contrasting patterns of biomass allocation in dominant and suppressed loblolly pine. *Canadian Journal of Forest Research*, 28: pp 1116 - 1124.
16. Nemeth, J. C., 1973. Dry matter production in young loblolly (*Pinus taeda L.*) and slash pine (*Pinus Elliotti Engelm.*) plantations. Ecological Monographs 43: pp 21-41.
17. Pehl C. E., Tuttle C. L., Houser J. N., and Moehring D. M., 1984. Total biomass and nutrients of 25-year-old loblolly pines (*Pinus taeda L.*). *Forest Ecology and Management,* 9: pp 155-160.
18. Ponette Quentin, Ranger Jacques, Ottorini Jean-Marc, Ulrich Erwin, 2001. Aboveground biomass and nutrient content of five Douglas-fir stands in France, *Forest Ecology and Management,* 142: pp 109-127.
19. Schroeder P.E., Brown S., MO. J., Birdsey R. and Cieszewski C., 1997. Biomass estimation for temperate broadleaf forests of the U.S. using inventory data. For. Sci., in press.
20. Snorrason, A. & Einarsson, S.F. 2004. Single-tree biomass and stem volume functions for eleven tree species used in Icelandic forestry. Submitted manuscript.
21. Uri Veiko, Vares Aivo, Tullus Hardi, Kanal Arno, 2007. Above-ground biomass production and nutrient accumulation in young stands of silver birch on abandoned agricultural land, *Biomass and Bioenergy*, 31: pp 195–204.
22. Van Lear, D. H., Wade J. B., and Teuke M. J., 1984. Biomass and nutrient content of a 41-yearold loblolly pine (*Pinus taeda L.*) Plantation on a poor site in South Carolina. *Forest Science*, 30: pp 395-404.
23. Wang Chuankuan, Biomass allometric equations for 10 co-occurring tree species in Chinese temperate forests, *Forest Ecology and Management,* 222: pp 9–16.
24. Xiao Chun-Wang, Ceulemans R., 2004. Allometric relationships for below- and aboveground biomass of young Scots pines, *Forest Ecology and Management*, 203: pp 177–186.

TABLE V: TROPICAL FOREST

EQUATIONS	REFERENCE
63. *For gbh 30–50 cm* **Volume of tree = - 0.191+0.004936×□GBH+0.01222×□length**. r^2=0.79	Ramachandran et al. (2007)
64. *For gbh 51–100 cm* **Volume = - 0.609+0.008246×□GBH+0.0409×□length.** r^2=0.83	Ramachandran et al. (2007)
65. *For gbh 101–150 cm* **Volume = - 2.328+0.01902×□GBH+0.103×□length**. r^2=0.80	Ramachandran et al. (2007)
66. *For gbh 151–200 cm* **Volume = - 4.771+0.02683×□GBH+0.211×□length**. r^2=0.83	Ramachandran et al. (2007)
67. *For gbh > 201 cm* **Volume = - 13.194+0.05515×□GBH+0.368×□length**. r^2=0.96	Ramachandran et al. (2007)
68. $W_{leaf}=b_1 (D_{BH})^{b2}$ $W_{woody}=b_1 (D_{BH}^2 H_T)^{b2}$ $W_{total}= b_1 (D_{BH}^2 H_T)^{b2}$ *N=26.* *Where, W=Oven-dry biomass (kg), D_{BH}=Diameter at 1.37m, H_T=Total height*	Brandeis et al. (2006)
69. $\ln W_{leaf}=b'_1 + b_2 \ln D_{BH}$ $\ln W_{woody}=b'_1 + b_2 \ln (D_{BH}^2 H_T)$ $\ln W_{total}=b'_1 + b_2 \ln (D_{BH}^2 H_T)$ Where ln=Natural logarithm, W=Oven-dry biomass (kg), D_{BH}=Diameter at 1.37 m, H_T=Total height, b'_1= ln b_1.	Brandeis et al. (2006)
70. $V_{stem}=b_1 + b_2 (D_{BH}^2 H_T)$ $V_{stem}=b_1 + b_2 (D_{BH}) + b_3 (D_{BH})^2$ Where, V_{stem}=The stem volume in cubic meters, DBH the diameter at 1.37 m and HT=The total height.	Brandeis et al. (2006)

71. *From Permanent Growth Sample plot in BioSTRUCT (Biomass estimation from stand STRUCTure)method:* $AGB^{1/3}$= - 0.677+1.874×ln(height)+0.014(crown closure) R^2=0.70, RMSE=33.7tonnes/ha $AGB^{1/3}$= - 0.677+1.874×ln(height)+0.014(crown closure) R^2=0.71, RMSE=74.7m^3/ha	Hall et al. (2006)
72. *For tropical fallows:* $ALB_{age}= a / 1+b\ exp(c \times age)$ Where, ALB=The above-ground life biomass ($MgDMha^{-1}$), age=Years since abandonment (0<age<15), a=57.154, b=844.654, c=2.006.	Jepsen (2006)
73. *For tropical fallows:* $y'_{(age)} = ((-abc) / (1+b(-c \times age))^2)exp(-c \times age)$ a=57.154, b=844.654, c=2.006. Where, age=Years since abandonment (0<age<15), $y'_{(age)}$=Biomass accumulation rates (in $MgDMha^{-1}annum^{-1}$)	Jepsen (2006)
74. *In forest DNDC(DeNitrification-DeComposition) model:* *GDDWoodEff = (2.233×air_temp) /* **((GDDWoodEnd −GDDWoodStart)×day water_stress)** Where, day_WoodProdC=WoodC × GDDWoodEff, GDDWoodEff=Wood production efficiency (It is the fraction of the total forest C storage available for wood growth), air_temp=Air temperature, GDDWoodStart=Accumulative temperature for wood growth to start, GDDWoodEnd= Accumulative temperature for wood growth to cease, day water_stress=The daily water stress factor, WoodC=Forest C storage available for wood growth and day_WoodProdC=The daily wood production.	Miehle et al. (2006)
75. $ln(AGB)=\alpha + \beta_1 ln(D) + \beta_2 ln(H) + \beta_3 ln(\rho)$ ***Dry forest***: α= - 2.680, β_1=1.805, β_2=1.038, β_3=0.377, df=312 **Moist forest**: α= - 2.994, β_1=2.135, β_2=0.824, β_3=0.809, df=1344, RSE=0.302, r^2=0.996 ***Wet forest***: α= - 2.408, β_1=2.040, β_2=0.659, β_3=0.746,df=139 **All types forest**: α= - 2.801, β_1=2.115, β_2=0.780, β_3=0.809, df=1804, RSE=0.316, r^2=0.969	Chave et al. (2005)

Where, D=Trunk diameter at 130cm above ground (cm), H=Total tree height (m), ρ=Wood specific gravity (g/cm^3), RSE=Residual Standard Error.	
76. $ln(AGB)=\alpha + \beta_2 ln(D^2H\rho)$ ***Dry forest***: $\alpha= - 2.235$, $\beta_2=0.916$, $df=314$ ***Moist forest***: $\alpha= - 3.080$, $\beta_2=1.007$, $df=1346$, $RSE=0.311$, $r^2=0.996$ ***Wet forest***: $\alpha= - 2.605$, $\beta_2=0.940$, $df=141$ ***All types forest***: $\alpha= - 2.922$, $\beta_2=0.990$, $df=1806$, $RSE=0.323$, $r^2=0.967$ Where, D=Trunk diameter at 130cm above ground (cm), H=Total tree height (m), ρ=Wood specific gravity (g/cm^3), RSE=Residual Standard Error.	Chave et al. (2005)
77. $ln(AGB)=\alpha + ln(D^2H\rho)$ ***Dry forest***: $\alpha= - 2.843$, $df=316$ ***Moist forest***: $\alpha= - 3.027$, $df=1349$, $RSE=0.316$, $r^2=0.989$ ***Wet forest***: $\alpha= - 3.024$, $df=143$ ***All types forest***: $\alpha= - 2.994$, $df=1808$, $RSE=0.324$ Where, D=Trunk diameter at 130cm above ground (cm), H=Total tree height (m), ρ=Wood specific gravity (g/cm^3), RSE=Residual Standard Error.	Chave et al. (2005)
78. $ln(AGB)=a + bln(D) + c(ln(D))^2 + d(ln(\rho))^3 + \beta_3 ln(\rho)$ ***Dry***: $a= - 1.023$, $b=1.821$, $c=0.198$, $d= - 0.0272$, $\beta_3=0.388$, $df=401$ ***Moist***: $a= - 1.576$, $b=2.179$, $\beta_3=1.036$, $df=1501$, $RSE=0.353$, $r^2=0.995$ ***Wet***: $a= - 1.362$, $b=2.013$, $\beta_3=0.956$, $df=415$ ***Mangrove***: $a= - 1.265$, $b=2.009$, $\beta_3=1.700$, $df=81$ ***All types***: $a= - 1.602$, $b=2.266$, $c=0.136$, $d= - 0.0206$, $\beta_3=0.809$, $df=2405$, $RSE=0.377$, $r^2=0.958$ Where, D=Trunk diameter at 130cm above ground (cm), H=Total tree height (m), ρ=Wood specific gravity (g/cm^3), RSE=Residual Standard Error.	Chave et al. (2005)
79. $ln(AGB)=a + bln(D) + c(ln(D))^2 + d(ln(\rho))^3 + ln(\rho)$ ***Dry***: $a= - 0.730$, $b=1.784$, $c=0.207$, $d= - 0.0281$, $df=402$ ***Moist***: $a= - 1.562$, $b=2.148$, $df=1502$, $RSE=0.356$, $r^2=0.996$ ***Wet***: $a= - 1.302$, $b=1.980$, $df=416$ ***Mangrove***: $a= - 1.412$, $b=1.980$, $df=82$ ***All types***: $a= - 1.589$, $b=2.284$, $c=0.129$, $d= - 0.0197$, $df=2408$, $RSE=0.377$, $r^2=0.958$ *Where, D=Trunk diameter at 130cm above ground (cm), H=Total tree height (m), ρ=Wood specific gravity (g/cm^3), RSE=Residual Standard Error.*	Chave et al. (2005)

80. *ln(AGB)=a + bln(D) + ln(ρ)* ***Dry**: a= - 1.083, b=2.266, df=402* ***Moist**: a= - 1.864, b=2.608, df=1502, RSE=0.357, r^2=0.996* ***Wet**: a= - 1.554, b=2.420, df=416* ***Mangrove**: a= - 1.786, b=2.471, df=82* ***All types**: a= - 1.667, b=2.510, df=2408, RSE=0.378, r^2=0.957* *Where, D=Trunk diameter at 130cm above ground (cm), H=Total tree height (m), ρ=Wood specific gravity (g/cm^3), RSE=Residual Standard Error.*	Chave et al. (2005)
81. *For dry forest stands (diameter range 5 to 63.4cm)* W_{total}= 0.0112×($pD_{BH}^2H_T$) *N=404* *Where, W_{total}=Total tree aboveground biomass in oven-dry kg, D_{BH}=Diameter at breast height outside bark,* **82.** *HT=Total tree height (in m), p=wood specific gravity(in g/cm^3)*	Chave et al. (2005)
83. *For Dry forest stands* **<AGB>est = exp(-2.187+0.916×ln(ρD^{2}H))** **≡0.112×(ρD^{2}H)$^{0.916}$** **<AGB>est = ρ × exp(-0.667+1.784ln(D)+** **0.207(ln(D))^2 - 0.0281(ln(D))^3)** Where, D=Trunk diameter at 130cm above ground (cm), H=Total tree height (m), ρ=Wood specific gravity (g/cm^3).	Chave et al. (2005)
84. *For Moist forest stands:* **<AGB>est = exp(-2.977 + ln(ρD^{2}H))** **≡0.0509 × ρD^{2}H** **<AGB>est = ρ × exp(-1.499 + 2.148ln(D) +** **0.207(ln(D))^2 - 0.0281(ln(D))^3)** Where, D=Trunk diameter at 130cm above ground (cm), H=Total tree height (m), ρ=Wood specific gravity (g/cm^3).	Chave et al. (2005)
85. *For Moist mangrove forest stands:* **<AGB>est = exp (-2.977 + ln(ρD^{2}H))** **≡0.0509 × ρD^{2}H** **<AGB>est = ρ × exp (-1.349 + 1.980ln(D) +** **0.207(ln(D))^2 - 0.0281(ln(D))^3)** Where, D=Trunk diameter at 130cm above ground (cm), H=Total	Chave et al. (2005)

tree height (m), ρ=Wood specific gravity (g/cm^3).	
86. *For Wet forest stands:* **<AGB>est = exp (-2.557 + 0.940 × ln(ρD^{2}H))** **≡ 0.0776 × ρ(D^{2}H)$^{0.916}$** **<AGB>est = ρ × exp(-1.239 + 1.980ln(D) +** **0.207(ln(D))^2 - 0.0281(ln(D))^3)** Where, D=Trunk diameter at 130cm above ground (cm), H=Total tree height (m), ρ=Wood specific gravity (g/cm^3).	Chave et al. (2005)
87. *ln(Y)= a + b ln(DBH)* Where, ln=Natural logarithm, Y=Tree biomass (in kg), DBH=Diameter at breast height (in cm), H=Total height (in m), a, b, and c=Constant values.	Montero and Montagnini (2005)
88. *ln(Y) = a + b ln(DBH) + c ln(H)* Where, ln=Natural logarithm, Y=Tree biomass (in kg), DBH=Diameter at breast height (in cm), H=Total height (in m), a, b, and c=Constant values.	Montero and Montagnini (2005)
89. *Deciduous (n=11)* **Y= C+m. basal area** - 73.55+10.73(r^2= 0.82, % error=48) **Y=C+m. Ln(basal area)** - 1168.66+429.63(r^2=0.87, % error=24.98) Where, Y=biomass (in t/ha) and basal area is (in m^2/ha)	Murali et al. (2005)
90. *Deciduous (n=10)* **Y=C+m (basal area)+ m ln(height)** 11.27+6.03+1.83 (r^2=0.94, % error=49) **Y=C+m ln(basal area)+ m ln(height)** –766+452.19–166.66 (r^2=0.94, % error=28.94) Where, Y=biomass(in t/ha) and basal area is (in m^2/ha)	Murali et al. (2005)
91. *Deciduous (n=10)* **Y=C+m (density)+ m (basal area)** –160.64–0.025+15.4(r^2=0.92, % error=19.5) **Y=C+ m ln(density)+m ln(basal area)**	Murali et al. (2005)

–957.1–44.07+460.63(r^2=0.91, % error=31) Where, Y=biomass(in t/ha) and basal area is (in m^2/ha)	
92. *Deciduous (n=10)* **Y=C+m (density)+m (height)** 227.2+0.03–3.54(r^2=0.46, % error=123) **Y=C+m ln(density)+ m ln(height)** –439.2+40.3–134.17(r^2=0.14, % error=129) Where, Y=biomass(in t/ha) and basal area is (in m^2/ha)	Murali et al. (2005)
93. *Deciduous (n=10)* **Y=C+m(basal area)+m(height)+ m(density)** –56.8–0.015+13.6–4.21(r^2=0.92, % error=27.8) **Y=C+m ln(basal area)+ m ln(height)+ m ln(density)** –760.94–6.4+455.05–155.82(r^2=0.94, % error=26.62) Where, Y=biomass(in t/ha) and basal area is (in m^2/ha)	Murali et al. (2005)
94. *For all trees (dbh≥10 cm) and for palms:* $AGB=\sum_{1}^{n} \rho i/0.58\{\exp[2.42(\ln Di)-2.00]\}$ Where, $BA=\sum_{1}^{n} \Pi (Di/2)^2$ Di=Diameter of tree i, ρi=Wood density of tree i, n=Number of stems per plot, BA=Plot basal area, AGB=Stand above-ground biomass (kg dry weight/ha)	Baker et al. (2004)
95. *For all trees (dbh≥10 cm) and for palms:* $AGB=\sum_{1}^{n} \rho i/0.67\{\exp[0.33(\ln Di)+0.933 \ln(Di)^2 - 0.122(\ln Di)^3 - 0.371]\}$	Baker et al. (2004)

n Where BA= $\sum \Pi (Di/2)^2$ Di=Diameter of tree i, ρi=Wood density of tree i, n=Number of stems per plot, BA=Plot basal area, AGB=Stand above-ground biomass (kg dry weight/ha)	
96. *For Primary forest* **1/H = 1/(1.5D) + 1/61** n=3224, r^2=0.736, P<0.0001, Standard error=0.007 **ln(TAGB) = - 2.372 + 1.441 ln(MCH)** r^2=0.326, P<0.0001 Where, D=DBH, H=Tree height, TAGB=Total above ground biomass, MCH=Mean canopy height.	Okuda et al. (2004)
97. *For logged forest* **1/H = 1/(2.2D) + 1/47** n=819, r^2=0.703, P<0.0001, Standard error=0.011 **ln(TAGB) = - 1.983 + 1.348 ln(MCH)** r^2=0.439, P<0.0001 Where, D=DBH, H=Tree height, TAGB=Total above ground biomass, MCH=Mean canopy height.	Okuda et al. (2004)
98. *$y = - 6.386849 + 0.006265x + (- 137.02487 / x^2)$* Where, y=Backscatter from P-band image (HH polarization) or P_{HH} images, x=Biomass (t/ha)	Santos et al. (2003)
99. $AGB = \left(\sum_{i=1}^{m} DW1_i + \sum_{j=1}^{n} DW2_j \right)/AP + \left(\sum_{k=1}^{s} DW1_k\right)/AS$ Where, D=Diameter at breast height (in cm), H=Total height (in m), DW1=Individual tree or sapling biomass (in kg) when DBH is less than 25cm, DW2=Individual tree biomass (in kg) when DBH is greater than or equal to 25cm, m=Total tree number in a plot when DBH is between 10 and 25 cm, n=Total tree number in a plot when DBH is greater than or equal to 25 cm, s=Total sapling number in a subplot area when DBH is between 2 and 10 cm, AP=Plot area (in m^2), AS=Subplot area (in m^2) and AGB=Above ground biomass (in kg/ m^2), DW1was calculated by using Nelson et al. (1999), DW1	Lu et al. (2002)

was calculated by using Overman et al. (1994)	
100. $Biomass = 122.288 - 1.078 \times KT1 - 128.913 \times VARtm2\_9$ R=0.878, Beta value= - 0.28(sp), - 0.72(txt) Where, KT=Tasseled cap, VARtm2_9=Variance combined with TM2 and 9 ×9 window size, Sp=Spectral variables, Txt=texture variables	Lu et al. (2002)
101. $Biomass = 64.037 - 1.651 \times TM4 + 1.405 \times SKtm4\_9$ R=0.883, Beta value= - 0.76(sp), 0.29(txt) Where, TM=Thematic mapper, SKtm4_9=Skewness combined with TM4 and 9×9window size, Sp=Spectral variables, Txt=texture variables	Lu et al. (2002)
102. $y_{leaf} = -3.39 - 0.3170H + 0.00033N - 0.11290S + 1.2015ln(D^2H)$ Where, y_{leaf}=Aerial biomass of leaf per hectare, N=Stand density, H=Average top height, S=Species richness, BA=Basal area, D=Diameter at breast height	Navar et al. (2002)
103. $y_{branch} = 1.46 + 0.00403N - 1.39287S + 0.08707 D^2H$ Where, y_{branch} =Aerial biomass of branch per hectare, N=Stand density, H=Average top height, S=Species richness, BA=Basal area, D=Diameter at breast height	Navar et al. (2002)
104. $y_{stem} = 246.99 + 11.9170H - 32.8904ln(D^2H)$ - 25.2786ln (N) + 37.7530ln (BA). Where, y_{stem}=Aerial biomass of steam per hectare, N=Stand density, H=Average top height, S=Species richness, BA=Basal area, D=Diameter at breast height	Navar et al. (2002)
105. $RB = 2.93 + 0.56BT$ r^2=0.64, n=34, S_x=5.4 $Mgha^{-1}$ Where, RB=Root Biomass ($Mgha^{-1}$), BT=Total aboveground biomass ($Mgha^{-1}$)	Navar et al. (2002)
106. $y_{total} = 245.06 + 11.6H + 0.00436N - 1.50577S$ - 31.6889ln(D^2H) + 0.08707D^2H - 25.2786 ln(N) +37.7530 ln(BA) Where, y_{total}=Total above ground biomass per hectare, N=Stand density, H=Average top height, S=Species richness, BA=Basal area, D=Diameter at breast height	Navar et al. (2002)

107. *Height trees<20 cm DBH (m)* **Agb=[(exp(0.6387+0.7988 ×ln(D))]× 1.0438** R^2=0.85, N=40 Where, D=DBH (cm), Agb=Above ground biomass (in Mg on a dry basis).	Cummings et al. (2002)
108. *Height trees>20 cm DBH(m)* **Agb=[- 19.5873+13.2823×ln(D)]× 0.9999** R^2=0.64, N=89 Where, D=DBH (cm), Agb=Above ground biomass (in Mg on a dry basis).	Cummings et al. (2002)
109. *BIO1 = 698TM2 - 1158TM1 - 11393TM3 +3523TM7 -* **5733WI - 45VI5 - 632952TSAVI- 10085DVI - 8403PC2** **+10983PC3 + 2214PC4 + 4067PC5 - 5IM + 11PA - 55T0 +** **19513TA + 558382NDVI - 3991 RVI** **- 14DEM- 63682**. Relation coefficient= 0.673 BIO1=Biomass of sample plot 30×30 m^2, WI=Wetness index, VI5=Vegetation index, TSAVI=Transformed soil adjusted vegetation index, DVI=Difference vegetation index, NDVI=Normalized difference vegetation index, RVI=Ratio vegetation index, PC2=Second principle component, PC3=Third principle component, PC4=Fourth principle component, PC5=Fifth principle component.	Yang et al. (2001)
110. *BIO2 = 1251266 –7314TM3 + 923TM4 – 11219TM7–* **7348WI–262VI5 +132147TSAVI –68242SARVI –3332 PC2** **+7358 PC4 –11697 PC5 –10IM + 19PA–9T0 +3355TA** **+53ASP.** Relation coefficient= 0.725 BIO2=Biomass of sample plot 30×30 m^2, WI=Wetness index, VI5=Vegetation index, TSAVI=Transformed soil adjusted vegetation index, SARVI=Soil adjusted ratio vegetation index, DVI=Difference vegetation index, NDVI=Normalized difference vegetation index, RVI=Ratio vegetation index, PC2=Second principle component, PC4=Fourth principle component, PC5=Fifth principle component.	Yang et al. (2001)

111. *BIO3 = 1689804 + 15920TM1+10578TM2+4722TM-11072* **TM7 + 86VI5+851185TSAVI-7632DVI-807PC1+ 3146PC2 +12261PC3-13766PC4-21048PC5-9IM+14PA+10T0- 2956TA-776122NDVI-42127RVI-107ASP +35DEM.** Relation coefficient= 0.733 BIO3=Biomass of sample plot 30×30 m^2, WI=Wetness index, VI5=Vegetation index, TSAVI=Transformed soil adjusted vegetation index, DVI=Difference vegetation index, NDVI=Normalized difference vegetation index, RVI=Ratio vegetation index, PC1=First principle component, PC2=Second principle component, PC3=Third principle component, PC4=Fourth principle component	Yang et al. (2001)
112. $B=r\rho D^{2+c}$ For Sepunggur r = 0.11, c and ρ are parameters , If we use the value of k from $H=kD^c=2.54D^{0.62}$ then equation become **$B=0.042\rho D^2H$** This equations are used for trees (7.6<D<48.1cm)in mixed Secondary forest in Sepunggur and for tree in secondary forest of Sumatra for D=8-48 cm, B **(kg per tree)=$0.066D^{2.59}$** ρ=Average wood density for the site and a=rρ is hypothesized and a and r are parameters, H=Height, D=Diameter b=2+c	Ketterings et al. (2001)
113. *If minimum dbh is 10 cm* **AGB = exp[- 2.00 + 2.42 ln(D)]** Where, D=Diameter measured at 1.30 m above ground, below irregularities, or above buttresses (in cm), AGB=Above ground biomass (in kg $tree^{-1}$)	Chave et al. (2001)
114. *If minimum dbh is 5 cm* **AGB = exp[- 0.37+0.333ln(D)+0.933ln(D)2 - 0.122 $ln(D)^3$]** Where, D=Diameter measured at 1.30 above ground, below irregularities, or above buttresses (in cm), AGB=Above ground	Chambers et al. (2001)

biomass (in kg tree^{-1})	
115. *For primary forest:* *ln (biomass) = - 0.370+0.333ln(DBH)+* **0.933[ln(DBH)]^2 - 0.122 [ln (DBH)]^3** Where, DBH=Diameter at breast height.	Chambers et al. (2001)
116. *For all trees (dbh≥10 cm), including palms:* **n** **AGB=∑exp[0.33(ln Di)+0.933(ln Di)^2 - 0.122(lnDi)^3 -0.37]** **i** n Where BA= ∑ Π (Di/2)^2, Di=Diameter of tree i, ρi=Wood density of tree i, n=Number of stems per plot, BA=Plot basal area.	Chambers et al. (2001)
117. *For all trees (dbh≥10 cm), including palms:* **n** **AGB=∑exp[2.42(ln Di)-2.00]** **i** n Where BA= ∑ Π (Di/2)^2 Di=Diameter of tree i, ρi=Wood density of tree i, n=Number of stems per plot, BA=Plot basal area.	Chave et al. (2001)
118. *For stands younger than 10 years* **Y = 53/(1 + exp(1.86 ─ 0.36t))** Where, t=Since Abandonment	Hashimotio et al. (2000)
119. $Y = aX_1^b \epsilon$ Where, Y=Total aboveground biomass (AB), commercial biomass (CB) or leaf area (LA). Commercial biomass was defined as the biomass of stem sections up to 20 cm top diameter. X_1=Stem DBH, a and b=Model parameters, Є=Error term	Ares & Fownes (2000)
120. $Y = aX_1^b X_2^c \epsilon$ Where, Y=Total aboveground biomass (AB), X_1=Stem DBH, X_2=Total height, a and b=Model parameters, and Є = Error term	Ares & Fownes (2000)
121. *Ln(DW1)= - 2.5202+ 2.14ln(D) +0.4644 ln(H)* Where, D=Diameter at breast height (cm), H=Total height (m),	Niklas et al. (1999)

DW1=Individual tree or sapling biomass (kg) when DBH is less than 25cm., DW2=Individual tree biomass (kg) when DBH is greater than or equal to 25cm.,m=Total tree number in a plot when DBH is between 10 and 25 cm, n=Total tree number in a plot when DBH is greater than or equal to 25 cm, s=Total sapling number in a subplot area when DBH is between 2 and 10 cm, AP=Plot area (m^2), AS=Subplot area (m^2) and AGB=Above ground biomass (kg/ m^2)	
122. *Standing dead trees (Trees<10cm DBH)* **$Agb = [(\exp(1.1788 \times \ln(D^2)+4.4189)) \times 1.0819] / 10^6$** R^2=0.96, N=66, Where, D=DBH (cm), Biomass is expressed in Mg on a dry basis.	Hughes et al. (1999)
123. *Saplings (minimum dbh is 1 cm)* **$AGB = \rho/\rho_{av} \exp[-1.839 + 2.116 \ln(D)]$** Where, D=Diameter measured at 1.30 above ground, below irregularities or above buttresses (in cm), ρ=oven-dry wood specific gravity (in g cm-'), ρ_{av} =Mean wood specific gravity of the plot (0.54 g cm^{-3}), H=Total tree height (in m) and AGB =Above ground biomass (in kg $tree^{-1}$)	Hughes et al. (1999)
124. *Tree<5 cm DBH* **$Agb=[(\exp(1.0583 \times \ln(D^2)+4.9375)) \times 1.143] / 10^6$** R^2=0.94, N=244 Where, D=DBH (cm), Biomass is expressed in Mg on a dry basis.	Hughes et al. (1999)
125. *For secondary succession:* *ln (biomass) = - 1.9968 + 2.1428 ln (DBH)* Where, Biomass is the above ground biomass.	Nelson et al. (1999)
126. $DW = a + b(D^2H)$ Where, DW=Above-ground biomass dry weight of tree, DBH=Diameter at breast height measured 1.3 m above-ground, H=Tree height	FAO (1999)
127. $sqrt\ (DW) = a + b(DBH)$ Where, DW=Above-ground biomass dry weight of tree, DBH=Diameter at breast height measured 1.3 m above-ground, H=Tree height	FAO (1999)
128. $DW_f = FV_f \times DW_s / FV_s$ Where, DW_f =Dry weight of the stump, FV_f =Fresh volume of stump, DW_s=Dry weight of the subsample of the stem and FV_s=Fresh volume of the subsample of the stem	Jarayaman (1999)
129. $DW_f = FW_f \times DW_s / FW_s$ Where, DW_f=Dry weight of the faction, FW_f=Fresh weight of the	Jarayaman (1999)

faction, DW_s=Dry weight of the subsample of the faction, FW_s=Fresh weight of the subsample of the faction	
130. *Trees 5-20 cm DBH* **Agb = [(exp(−1.754+2.665×ln(D)))×0.604] / 10^3** R^2=0.92, N=244 Where, D=DBH (cm), Biomass is expressed in Mg on a dry basis.	Higuchi et al. (1998)
131. *For all trees (dbh≥10 cm), including palms:* *AGB=0.6 ×[66.92+(16.85×BA)]* **n** Where **BA=** $\sum$ **Π (Di/2)^2** Di=Diameter of tree i, ρi=Wood density of tree i, n=Number of stems per plot, BA=Plot basal area.	Philips et al. (1998)
132. *Trees>20 cm DBH* **Agb = [(exp(-0.151+2.17×ln(D)))×0.604] / 10^3** R^2=0.90, N=244 Where, D=DBH (cm), Biomass is expressed in Mg on a dry basis.	Higuchi et al. (1998)
133. *For moist and precipitation 1500-4000 mm:* **Y = exp(- 2.134 + 2.530 ln(D))** Where, ln is the natural logarithm, Y=Total tree aboveground biomass in oven-dry kg, D=Diameter at breast height outside bark.	Brown (1997)
134. *lnW_{total}= - 1.990+2.32 ln (D^2_{BH})* Where ln is the natural logarithm, W_{total}=Total tree aboveground biomass in oven-dry kg, D_{BH}=Diameter at breast height outside bark.	Brown (1997)
135. *For humid tropical forests* **W = 0.118 D $^{2.53}$**	Brown (1997)
136. *For hardwood* **Biomass= 0.5+25000 dbh $^{2.5}$ /dbh $^{2.5}$ + 246872** R^2=0.99	Schroeder et al. (1997)
137. *For conifers* **Biomass=0.5+15000 dbh $^{2.7}$ /dbh $^{2.7}$ + 364946** R^2=0.98	Schroeder et al. (1997)
138. *For tree fresh dry biomass of Amazonian tree species:* For trees < 20 cm dbh:	Higuchi et al. (1997)

ln (mass) =□ 1.754 □□+ 2.665 ln (dbh) For trees > 20 cm dbh: **ln (mass) =□□ - 0.151 + □□2.170 ln (dbh)** Dry biomass was calculated by multiplying fresh biomass by the mean dry mass: fresh mass ratio of 0.603.	
139. *BGBD=exp{−1.059+0.884×ln(AGBD)+0.284}* r^2=0.84, n=151 Where, BGBD=Belowground biomass density and AGBD=Above ground biomass density	Cairns et al. (1997)
140. *AGBM=(exp(3.323+(2.546×(ln(DBH/100)))))× 600* Where, AGBM=Above ground biomass, DBH=Diameter at breast height	Santosh (1996)
141. *$B= 0.062\rho(0.1(\pi/4)D^2H) = 0.049\rho D^2H$* *Where, D=Diameter measured at 1.30 above ground, below irregularities or above buttresses (in cm), ρ=oven-dry wood specific gravity (in g cm^{-1}), H=Total tree height (in m)*	Brown et al. (1995)
142. *For trees (DBH≥25 cm)* *$Ln(DW2)= - 3.843+ 1.035ln(D^2 H)$* Where, D=Diameter at breast height (cm), H=Total height (m), DW2=Individual tree biomass (kg) when DBH is greater than or equal to 25cm.,	Overman et al. (1994)
143. *$DW = \alpha(DBH)^{\beta}$* For all trees: R^2=0.90, δB (%)=39.4, P<0.0001, α=0.465, Standard error=0.307 β=2.202, Standard error=0.151 For trees with DBH≤45 cm: R^2=0.81, δB(%)=42.8, P<0.0001, n=33 α=0.749, Standard error=0.552 β=2.011, Standard error=0.204	Overman et al. (1994)

Where, DW=Aerial dry weight of the tree (kg), DBH= Diameter at breast height 1.30 m above ground level (cm) h=Height of the tree (m), d=Wood density (gcm^{-3}) δB(%)=Percentage deviation	
144. $DW = \alpha(DBH)^2$ For all trees: R^2=0.94, δB(%)=62.8, P<0.0001, α=1.120, Standard error=0.040 For trees with DBH≤45 cm: R^2=0.93, δB(%)=43.5, P<0.0001, n=33 α=0.780, Standard error=0.039	Overman et al. (1994)
145. $ln(DW)=C+\alpha\, ln(DBH^2 \times h \times d)$ For all trees: R^2=0.97, δB(%)=25.6, P<0.0001, α=1.242, Standard error=0.032 C= - 1.966, Standard error=0.235 For trees with DBH≤45 cm: R^2=0.93, δB(%)=27.5, P<0.0001, n=33 α=1.256, Standard error=0.061 C= - 2.059, Standard error=0.061	Overman et al. (1994)
146. $ln(DW)=C+\alpha\, ln(DBH^2 \times d)$ For all trees: R^2=0.99, δB(%)=11.2, P<0.0001, α=0.993, Standard error=0.012 C= - 2.904, Standard error=0.120 For trees with DBH≤45 cm: R^2=0.98, δB(%)=12.9, P<0.0001, n=33 α=0.990, Standard error=0.024 C= - 2.885, Standard error=0.024	Overman et al. (1994)

147. $ln(DW)=C+\alpha\ ln(DBH^2\times h)$ For all trees: R^2=0.99, δB(%)=14.8, P<0.0001, α=1.177, Standard error=0.018 C= - 0.906, Standard error=0.125 For trees with DBH≤45 cm: R^2=0.98, δB(%)=15.6, P<0.0001, n=33 α=1.229, Standard error=0.035 C= - 1.192, Standard error=0.206	Overman et al. (1994)
148. $ln(DW)=C+\alpha\ ln(DBH^2)$ For all trees: R^2=0.97, δB(%)=24.3, P<0.0001, α=1.035,Standard error=0.025 C= - 3.843, Standard error=0.259 For trees with DBH≤45 cm: R^2=0.94, δB(%)=26.3, P<0.0001, n=33 α=1.002, Standard error=0.045 C= - 3.555, Standard error=0.428	Overman et al. (1994)
149. $ln(DW)=C+\alpha\ ln(DBH^2)+\beta ln(d)$ For all trees: R^2=0.99, δB(%)=14.7, P<0.0001, C= - 1.020, Standard error=0.175 β=1.185, Standard error=0.021 α=1.071, Standard error=0.114 For trees with DBH≤45 cm: R^2=0.98, δB(%)=15.0, P<0.0001, n=33 C= - 1.322, Standard error=0.256 β=1.239, Standard error=0.037 α=1.106, Standard error=0.148	Overman et al. (1994)

150. $B=aD^bH$ If $H=kD^c$ then **, $B=akD^{b+c}$** Where, H=height and D=Diameter, B=Above ground biomass.	Niklas (1994)
151. $DW = a(DBH)^b \times Є$ **$\ln(DW) = \ln(a) + b \times \ln(DBH) + \ln(Є)$** Where, DW=Above-ground biomass dry weight of tree, DBH=Diameter at breast height measured 1.3 m above-ground, Є=Standard error	Overman et al. (1994), Brown. (1997), Ketterings et al. (2001)
152. $W_{total} = - 0.5352+log_{10}(BA)$ Where, W_{total}=Total tree aboveground biomass in oven-dry kg, BA=Basal area.	Martinez-Yrizar et al. (1992)
153. $AGB = exp\{- 3.1141 + 0.9719 \log(d^2_{1.3}h)\}$ n =168, r^2=0.97 Where, $d_{1.3}$=Diameter at breast height1.3m (cm), h=Total tree height (m), AGB=Total above-ground biomass (kg per tree), n=Number of sample and r^2=Regression coefficient	Brown et al. (1989)
154. *For fallows aged 7–10 years precipitation 4000 mm year^{-1}* **$Y = 17.376 - 6.042x + 0.72x^2 - 0.0084x^3$** x = Time since abandonment	Halenda (1989)
155. $y= 34.4703 - 8.0671\ dbh + 0.6589\ dbh^2$ *y=Total above ground biomass, dbh=Diameter at breast height 1.3m (cm)*	Brown et al. (1989)
156. *For primary forest:* $biomass = 0.044 \times (DBH^2 \times height)^{0.9719}$ *Where, biomass=Above ground biomass.*	Brown et al. (1989)
157. *If minimum dbh is 5 cm* **$y= \exp[- 3.1141+0.9719 \ln(dbh^2H)]$** Where, dbh=Diameter measured at 1.30 above ground, below irregularities or above buttresses (in cm), ρ=oven-dry wood specific gravity (in g cm^{-1}), H=Total tree height (in m), y=Above ground biomass (in kg $tree^{-1}$)	Brown et al. (1989)
158. $AGB=F\times(\rho\times(\Pi D^2/4)\times H)^{\beta}$ β<1 may actually be a better model. Where, D=Diameter measured at 1.30 above ground, below irregularities or above buttresses (in cm), ρ=oven-dry wood specific gravity (in g cm^{-1}), H=Total tree height (in m), AGB =Above ground	Brown et al. (1989)

biomass (in kg tree^{-1})	
159. *For secondary succession:* **ln Y = - 2.17 + 1.02 ln(DBH)^2 + 0.39 ln(H)** Where, Y=Above ground biomass, SG=Specific gravity, H=Height and DBH=Diameter at breast height	Uhl et al. (1988)
For DBH>10cm in forest. Precipitation:1750 mm year^{-1} **ln Y = 0.991 ln((DBH)^2 × H × SG) - 2.968** Where, Y=Above ground biomass, SG=Specific gravity, H=Height, DBH=diameter at breast height	Uhl et al. (1988)
160. $Ws = 0.02903(DBH^2H)^{0.9813}$ Where, Ws=Stem biomass, DBH=Diameter at breast height, H=Height of the tree	Yamakura et al. (1986)
161. $Wb = 0.1192Ws^{1.059}$ Where, Wb=Branch biomass, Ws=Stem biomass, DBH= Diameter at breast height	Yamakura et al. (1986)
162. $Wl = 0.09146(Ws + Wb)^{0.7266}$ Where, Wl=Leave biomass, Ws=Stem biomass, Wb=Branch biomass, DBH=Diameter at breast height	Yamakura et al. (1986)
163. $B = \sum_{i=0}^{m} a_i \times (DBH)^i + \epsilon$	Cunia (1986a), Brown (1997), De Gier (2003)
164. $DW = a + b(DBH)^2 + c(DBH)^3$ Where, DW=Above-ground biomass dry weight of tree, DBH=Diameter at breast height, measured 1.3 m above-ground	Cunia (1986) and Brown (1997)
165. $Y = 0.0921 \times (dbh)^{2.5899}$ r^2=0.991 Where, Y=Above ground biomass, dbh=Diameter at breast height.	Lim (1986) and Lim (1988)
166. *Palm>10cm dbh* **AGB =(4.5+(7.7(stem H))/ 10^3** r^2=0.90, N=25	Frangi and Lugo (1985)

167. $WT = F(HG)\ D$ Where, WT=Aboveground woody biomass, F=Stand form factor, H=Mean tree height, G=Stand, over bark, basal area at breast height	Cannell (1984)
168. $log\ y = log\ a + b\ log\ x$ Where, x=Stem diameter and y=Biomass or productivity of some tissue.	Sprugel (1983)
169. $W_s = 0.0313(D^2H)^{0.9733}$ Where, H=Tree's height (in m), D=DBH (in cm), W_s=Weights (in kg) of the main stem.	Kato et al. (1978)
170. $W_b = 0.039(D^2H)^{1.041}$ Where, H=Tree's height (in m), D=DBH (in cm), W_b=Weights (in kg) of the branches.	Kato et al. (1978)
171. $1 / W_l = 1 / 0.124W_s^{0.794} + 1 / 125$ Where, H=Tree's height (in m), D=DBH (in cm), W_s=Weights (in kg) of the main stem, W_l=Weights (in kg) of the leaves.	Kato et al. (1978)
172. *For all trees with DBH ≥5 cm.* **TAGB= W_s +W_b + W_l** Where, W_s=Weights (in kg) of the main stem, W_b=Weights (in kg) of the branches, W_l=Weights (in kg) of the leaves, TAGB=Total aboveground biomass for all trees with DBH ≥5 cm.	Kato et al. (1978)
173. $AGB = c\rho D^{2+B}$ Where, AGB=Above ground biomass (in kg), D=Diameter of tree (in cm), c=Measure the taper of a mean tree, ρ=Oven-dry wood over green volume (g/cm^3), B=Can be derived from engineering considerations.	Mc Mahon and kronauer (1976) Taken from Chave 2005
174. $TB = 0.5 \times BABH \times TH$ Where TB=Total biomass of tree, TH=Total height, BABH=Basal area at breast height	Whittaker and Marks (1975)
175. *Wood debris >76 cm dbh* **AGB =Sg×((Π^2×∑D^2×s×Cs×d^2)/8L) ×10^2** Sg sound=482 g cm^{-3} Sg rotten=0.342 g cm^{-3} Sg palm=0.327 g cm^{-3}	Van Wagner (1968), Brown and Roussopoulos (1974)

Where, D=dbh (cm), H=height (m), BA=Basal area (cm^2) Sg=specific gravity of wood (g cm^{-3}), d^2=quadratic mean diameter of wood particles, L=Transect length (cm), S=Secant of wood particles, N=Number of intercepted wood particles, $\sum D^2$=Sum of wood particles diameter squared, r=radius (m), Cs=Slope correction factor ($\sqrt{1+(\%slope/100)^2}$)	
176. *Wood debris 2.5 to 7.60 cm dbh* **AGB =Sg×((Π²×N×s×Cs×d²)/8L) ×10²** Sg=0.413 g cm^{-3} Where, D=dbh (cm), H=Height (m), BA=Basal area (cm^2), Sg=Specific gravity of wood (g cm^{-3}), d^2=Quadratic mean diameter of wood particles, L=Transect length (cm), =Secant of wood particles, N=Number of intercepted wood particles, $\sum D^2$=Sum of wood particles diameter squared, r=Radius (m) Cs=Slope correction factor ($1+(\%slope/100)^2$)	Van Wagner (1968), Brown and Roussopoulos (1974)
177. $AGB=F\times\rho\times(\Pi D^2/4)\times H$ AGB=Above ground biomass (in kg) of a tree, D=Diameter, ρ=Wood specific gravity, BA=trunk basal area ($\Pi D^2/4$), H=Total tree height.	Dawkins (1961)
178. $ln\ AGB = \alpha + \beta_1 ln\ (D) + \beta_2 ln\ (H) + \beta_3 ln\ (\rho)$ AGB=Above ground biomass, D=Trunk diameter (in cm), H=Height of tree (in m), ρ=Wood specific gravity (in g/cm^3), α, β_1, β_2 and β_3=Parameters	Schumacher and Hall (1933)

References

1. Ares Adrian and Fownes James H., 2000. Comparisons between generalized and specific tree biomass functions as applied to tropical ash (*Fraxinus uhdei*). *New Forests*, 20: pp 277–286.
2. Baker T. R. (and 16 others), 2004. Variation in wood density determines spatial patterns in Amazonian forest biomass. *Global Change Biol,* (In the press.)
3. Brandeis Thomas J., Delaney Matthew, Bernard R. Royer, Parresoland Larry, 2006. Development of equations for predicting Puerto Rican subtropical dry forest biomass and volume. *Forest Ecology and Management*, 233(1): pp 133-142.
4. Brown J.K. and Roussopoulos P.J., 1974. Estimating biases in the planar intersect method for estimating volumes of small fuels. *For. Sci*., 20: pp 350-356.
5. Brown S., Gillespie A.J.R. and Lugo A.E., 1989. Biomass estimation methods for tropical forest with applications to forest inventory data. *For. Sci.* 35: pp 881–902.
6. Brown I.F., Martinelli L.A., Thomas W.W., Moreira M.Z., Ferreira C.A.C. and Victoria R.A., 1995. Uncertainty in the biomass of Amazonian forests: an example from Rondonia, Brazil. *For. Ecol. Mgmt.*, 7**5:** pp 175–189.
7. Brown S., 1997. Estimating Biomass and Biomass Change of Tropical Forests: a Primer (FAO Forestry Paper-134), FAO, United Nations, Rome.

8. Cairns M.A., Brown S., Helmer E.H., Baumgardner G.A., 1997. Root biomass allocation in the world's upland forests. *Oecologia* 111: pp 1-11.
9. Cannell M.G.R., 1984. Woody biomass of forest stands. *Forest Ecology and Management*, 8: pp 299–312.
10. Chambers J.Q., Santos J., Ribeiro R.J. and Higuchi N., 2001. Tree damage, allometric relationships, and above-ground net primary production in central Amazon forest. *Forest Ecology and Management*, 152: pp 73-84.
11. Czapowskyj M. M., Robison D. J., Briggs R. D. and White E. H., 1985. Component biomass equations for black spruce in Maine, Res. Pap. NE-564.
12. Chave J., Andalo C., Brown S.L., Cairns M.A., Chambers J.Q., Eamus D., Folster H., Fromard F., Higuchi N., Kira T., Lescure J.P., Nelson B.W., Ogawa H., Puig H., Riera B. and Yamakura T.,2005. Tree allometry and improved estimation of carbon stocks and balance in tropical forests. *Oecologia,* 145, pp 87–99.
13. Chave J., Riera B. and Dubois M. A., 2001. Estimation of biomass in a neotropical forest of French Guiana: spatial and temporal variability. *J. Trop. Ecol.,* 17: pp79–96.
14. Chambers J. Q., Santos J., Ribeiro R. J. and Higuchi N., 2001. Tree damage, allometric relationships and aboveground net primary production in a tropical forest. *Forest Ecol. Mngmt.,* 152: pp 73–84.
15. Cummings D. L, Kauffman J. Boone, Perry David A. and Hughes R. Flint, 2002. Above ground biomass and structure of rainforests in the southwestern Brazilian Amazon. *Forest Ecology & Management*, 163: pp 293-307.
16. Cunia T., 1986a. Construction of tree biomass tables by linear regression technique. In: E.H. Wharton and T. Cunia (ed.), *Estimating* tree *biomass and their error*. USDA, Northeastern Forest Experimental Station, Broomall, Pennsylvania.
17. Dawkins H. C., 1961. Estimating total volume of some Caribbean trees. *Caribb For*, 22: pp 62–63.
18. De Gier A., 2003. A new approach to woody biomass assessment in woodlands and shrublands. In: P. Roy (Ed), *Geoinformatics for Tropical Ecosystems*, India, pp 161-198.
19. Frangi J.L., Lugo A.E., 1985. Ecosystem dynamics of a subtropical floodplain forest. *Ecol. Monographs*, 55: pp 351-369.
20. Halenda C.J., 1989. The Ecology of a Fallow Forest After Shifting Cultivation in Niah Forest Reserve. Report. Forest Department, Sarawak, Malaysia. *Forest Ecology*.
21. Hall R.J., Skakun R.S., Arsenault E.J. and Case B.S., 2006. Modelling forest stand structure attributes using Landsat ETM+ data: Application to mapping of aboveground biomass and stand volume. *Forest ecology and management*, 225(1-3): pp 378-390.
22. Hashimotio T., Kojima K., Tange T. and Sasaki S., 2000. Changes in carbon storage in fallow forests in the tropical lowlands of Borneo. *Forest Ecol. Manage.*, 126: pp 331–337.
23. Higuchi N., Santos J. D., Ribeiro R. J., Minette L. and Biot Y., 1997. Biomassa da parte aerea de vegetacao daoresta tropical umida de terrarme da Amazonia Brasileira. Pp. 47-64 in *Biomassa e nutrientes orestais*. Projeto Bionte. INPA, Manaus.
24. Higuchi N., Dos Santos J., Ribeiro R. J., Minette L. and Biot Y., 1998. Biomass da Parte Aerea da vegetacao da Floresta tropical Umida de Terra- firmed a Amazonia Brasileira.Acta Amazonica. 28(2): pp 153-165.
25. Hughes R. F., Kauffnlan J. B. and Jaramillo V. J., 1999. Biomass carbon and nutrient dynamics of secondary forests in a humid tropical region of Mexico. *Ecology,* 80: pp 1897-1907.
26. Jensen Martin Rudbeck, 2006. Above-ground carbon stocks in tropical fallows, Sarawak, Malaysia. *Forest Ecology and Management,* 225: pp 287–295.
27. Jarayaman K., 2000. Statistical Manual for Forestry Research, *FORSPA / FAO*.[Online]
28. http://www.fao.org/docrep/003/x6831e/x6831e00.htm (Accessed on December 5, 2006).

29. Kato R., Tadaki Y. and Ogawa H., 1978. Plant biomass and growth increment studies in Pasoh Forest. *Malay. Nat. J.*, 30: pp 211–224.

30. Ketterings Quirine M., Coe Richard, Noordwijk Meine van, Ambagau Yakub and Palm Cheryl A., 2001. Reducing uncertainty in the use of allometric biomass equations for predicting above-ground tree biomass in mixed secondary forests. *Forest Ecology and Management*, 146(1-3): pp 199-209.
31. Lefsky Michael A., Cohent Warren B., Harding David J. S, Parker Geoffrey G., Ackery Steven A. and Thomas Gower S., 2002. Lidar remote sensing of above-ground biomass in three biomes. Global *Ecology & Biogeography*, 11: pp 393-399.
32. Lim M.T., 1986. Biomass and productivity of 4.5 year-old *Acacia mangium* in Sarawak. *Pertanika,* 9(1): pp 81-87.
33. Lim M.T., 1988. Studies on *Acacia mangium* in Kemasul Forest, Malaysia. I. Biomass and productivity. *Journal of Tropical Ecology*, 4: pp 293 –302.
34. Lu Dengsheng, Mausel Paul, Brondizio Eduardo and Moran Emilio, 2002. Above ground biomass estimation of successional and mature forests using TM images in the Amazon Basin, Symposium on geospatial theory, Processing and applications, Symposium sur la theorie, les traitements et les applications des donnees Geospatiales, Ottawa.
35. Martinez-Yrizar A., Sarukhan J., Perez-Jimenez A., Rincon E., Maass M., Solis-Magallanes A. and Cervantes L., 1992. Above-ground phytomass of a tropical deciduous forest on the coast of Jalisco, México. *J. Trop. Ecol.*, 8: pp 87–96.
36. McMahon T. A. and Kronauer R. E., 1976. Tree structures: deducing the principles of mechanical design. *J theor Biol*, 59: pp 443–466.
37. Miehle P., Livesley S.J., Feikema P.M., Li C. and Arndt S.K., 2006. Assessing productivity and carbon sequestration capacity of *Eucalyptus globulus* plantations using the process model Forest-DNDC: Calibration and validation. *Ecological Modelling*, 192: pp 83–94.
38. Montero M. and Montagnini F., 2005. Modelos alometricos para la estimacion de biomasa de diez especies nativas en plantaciones en la region Atlantica de Costa Rica. *Recur. Nat. y Ambiente,* 45: pp 118–125.
39. Murali K.S., Bhat D.M. and Ravindranath N.H, 2005. Biomass estimation equation for tropical deciduous and evergreen forests. *International Journal of Agricultural Resources, Governance and Ecology*, 4: pp 81–92.
40. Navar Jose, Mendez Eduardo and Dale Virginia, 2002. Estimating stand biomass in the Tamaulipan thornscrub of northeastern Mexico. *Ann. For. Sci.*, 59: pp 813-821.
41. Nelson B.W., Mesquita R. Pereira, J.L.G., Souza S.G.A., Batista G.T. and Couto L.B., 1999. Allometric regressions for improved estimate of secondary biomass in central Amazon. *Forest Ecology and Management*, 117: pp 149-167.
42. Nikolas K. J., 1994. Plant Allometry, the scaling of form and process. University of Chicago Press, Chicago, pp 365.
43. Okuda Toshinori, Suzuki Mariko, Numata Sinya, Yoshida Keiichiro, Nishimura Sen, Adachi Naoki, Niiyama Kaoru, Manokaran N. and Hashim Mazlan, 2004. Estimation of above ground biomass in logged and primary lowland rainforests using 3-D photogrammetric analysis. *Forest Ecology and Management*, 203: pp 63-75.
44. Overman J. P. M., Witte H. J. L. and Saldarriaga J. G., 1994. Evaluation of regression models for above-ground biomass determination in Amazon rainforest. Journal of Tropical ecology, 10: pp 207-218.
45. Phillips O. L. (and 10 others), 1998. Changes in the carbon balance of tropical forests: evidence from long-term plots. *Science,* 282: pp 439–442.

46. Ramachandran A., Jayakumar S., Haroon R. M., Bhaskaran A. and Arockiasamy D. I., 2007. Carbon sequestration: estimation of carbon stock in natural forests using geospatial technology in the Eastern Ghats of Tamil Nadu, India, Current Science, 92 (3).
47. Santosh J., 1996. Analise de modelos de regressao para estimar a fitomassa de floresta tropical umida de terra-firme da Amazonia Central. Ph.D. thesis, Universidade Federal de Vicosa, Minas Gerais, Brazil.
48. Santos J.R., Araujo L.S., Freitas C.C., Dutra L.V., Sant Anna S.J.S., Kuplich T.M. and Gama F.F., 2003. Allometric equations for tropical forest estimation and its relationship with P-band SAR data. Geoscience and Remote sensing Symposium, 3: pp 1948-1950.
49. Schroeder P., Brown S., Mo J., Birdsey R. and Cieszewski C., 1997. Biomass estimation for temperate broadleaf forests of the United States using inventory data. Forest Science, 43: pp 424-434.
50. Schumacher F. X. and Hall F. S., 1933. Logarithmic expression of timber tree volume. *J Agric Res*, 47: pp 719–734.
51. Sprugel D. *G.*, 1983. Correctiivg for bias iiv log-tra nsformed allometric equa tioivs, *Ecology*, 64(1): pp 209-210.
52. Van Wagner C.E., 1968. The lines intersect method in forest fuel sampling. *For. Sci.*, 14: pp 20-26.
53. Uhl C., Buschbacher R. and Serrao E. A. S., 1988. Abandonned pastures in eastern Amazonia, I: patterns of plant sucession. *Journal of Ecology,* 76, pp 663-681.
54. Whittaker R. H. and Marks P. L., 1975. Methods of assessing primary productivity. Ch. 4 *ill* H. Leith and R. H. Whittaker, editors. Primary productivity of the biosphere. Springer-Verlag. New York.USA.
55. Yamakura T., Hagihara A., Sukardjo S. and Ogawa H., 1986. Aboveground biomass of tropical rain forest stands in Indonesian Borneo, *Vegetatio,* 68**:** pp 71–82.
56. Yang Cunjian, Liu Jiyuan, Zhang Zengxiang and Zhang Zongke, 2001. Estimation of the carbon stock of tropical forest vegetation by using Remote Sensing and GIS. *IEEE*, 0-7803-7031-7/01: pp 1672-1674.

TABLE VI: TROPICAL FORESTS (SPECIESWISE)

SPECIES	MODEL	REFERENCES
1. Aboveground tree biomass in primary forests (D ≥ 1 cm)	**ln (AB-T) = - 2.286 + 2.471 ln (D)** Range in D (cm)=0.5–198, n=140, CF=0.091, r^2(%)=97.90 Where, AB-T=Above ground biomass of tree, D=Diameter, H=Height	Sierra et al. (2007)
2. Aboveground tree biomass in secondary forests (D ≥ 1 cm)	**ln (AB-T) = - 2.232 + 2.422 ln (D)** Range in D (cm)=0.9–40, n=152, CF=0.083, r^2(%)=97.47 Where, AB-T=Above ground biomass of tree, D=Diameter, H=Height	Sierra et al. (2007)
3. Coarse root biomass (primary and secondary forest)	**ln (CRB) = - 4.394 + 2.693 ln (D)** Range in D (cm)=1.7–64, n=649, CF=0.316, r^2(%)=91.79 Where, CRB=Coarse root biomass, D=Diameter, H=Height	Sierra et al. (2007)
4. Aboveground biomass for *Oenocarpus bataua*	**AB-Ob = 139.48 + 7.308H $^{1.133}$** Range in H (cm)=50–250, n=83, r^2(%) =82.95 Where, AB-Ob=Above ground biomass for *Oenocarpus bataua*, D=Diameter, H=Height	Sierra et al. (2007)
5. Aboveground biomass for other palms	**ln (AB-OP) = 0.360 + 1.218 ln (H)** Range in H (cm)=100-150, n=37, CF=0.325, r^2(%)=65.28 Where, AB-OP=Above ground biomass for other palms, D=Diameter, H=Height	Sierra et al. (2007)

6. Aboveground biomass for lianas	**ln (AB-L) = 0.028 + 1.841 ln (D)** Range in D (cm)=1-11, n=33, CF=0.133, r^2(%)=87.44 Where, AB-L=Above ground biomass for lianas, D=Diameter, H=Height	Sierra et al. (2007)
7. *Diptychandra aurantiaca* Total biomass(L) Volume(L) Trunk(L) Branches(L) Leaves(L)	**ln Y = ln a + b ln D** **Or** **$Y = aD^b$** Where, Y=Dry weight or wood volume, D= Diameter at breast height, R^2=Square of the correlation coefficient, E=Estimated standard error, CF=Correction factor, L=Linear equation, NL=Non linear equation D=5-35 cm, n=10, ln a= -2.119, b=2.380, r^2=0.986, E=0.167, CF=1.0140 D=5-35 cm, n=10, ln a= -2.119, b=2.380, r^2=0.986, E=0.167, CF=1.0140 D=5-35 cm, n=10, ln a= -2.781, b=2.382, r^2=0.988, E=0.151, CF=1.0115 D=5-35 cm, n=10, ln a= -3.314, b=2.508, r^2=0.952, E=0.329, CF=1.0556 D=5-35 cm, n=10, ln a= -3.289, b=1.575, r^2=0.795, E=0.469, CF=1.1101	Salis et al. (2006)
8. *Protium heptaphyllum* Total biomass(L) Volume(L)	D=8-36 cm, n=10, ln a= -2.083, b=2.536, r^2=0.971, E=0.250 D=8-36 cm, n=10, ln a= -8.914, b=2.266, r^2=0.974, E=0.212, CF=1.0227	Salis et al. (2006)

Trunk(L) Branches(L) Leaves(L)	D=8-36 cm, n=10, ln a= -2.065, b=2.150, r^2=0.976, E=0.191, CF=1.0184 D=8-36 cm, n=10, ln a= -3.554, b=2.868, r^2=0.911, E=0.510 D=8-36 cm, n=10, ln a= -4.319, b=2.076, r^2=0.912, E=0.367, CF=1.0697	
9. *Magonia pubescens* Total biomass(L) Volume(L) Trunk(L) Branches(L) Leaves(L)	 D=7-35 cm, n=10 ln a= -2.888, b=2.795, r^2=0.994, E=0.123 D=7-35 cm, n=10, ln a= -8.730, b=2.269, r^2=0.994, E=0.100 D=7-35 cm, n=10, ln a= -2.525, b=2.411, r^2=0.984, E=0.172 D=7-35 cm, n=10, ln a= -3.972, b=2.937, r^2=0.987, E=0.163 D=7-35 cm, n=10, ln a= -4.998, b=2.342, r^2=0.881, E=0.490	Salis et al. (2006)
10. *Terminalia argentea* Total biomass(L) Volume(L) Trunk(L) Branches(L) Leaves(L)	 D=6–31 cm, n=10, ln a= -1.915, b=2.409, r^2=0.987, E=0.172, C.F.=1.0149 D=6–31 cm, n =10, ln a= -8.285, b=2.113, r^2=0.949, E=0.300, C.F.=1.0460 D=6–31 cm, n=10, ln a= -1.380, b=1.984, r^2=0.950, E=0.281 D=6–31 cm, n=10, ln a= -5.161, b=3.195, r^2=0.920, E=0.581, C.F.= 1.1839 D=6–31 cm, n=10, ln a= -4.074, b=1.967, r^2=0.807, E=0.592, C.F.= 1.1915	Salis et al. (2006)
11. *Licania minutiflora* Total biomass(L) Volume(L)	 D=10–36 cm, n=10, ln a= -2.265, b=2.386, r^2=0.912, E=0.322	Salis et al. (2006)

Trunk(NL) Branches(NL) Leaves(NL)	D=10–36 cm, n=10, ln a= -9.376, b=2.439, r^2=0.975, E=0.176 D=10-36 cm, n=10, ln a=0.031, b=2.556, r^2=0.926 D=10-36 cm, n=10, ln a=0.140, b=2.076, r^2= 0.948 D=10-36 cm, n=10, ln a=0.030, b=1.532, r^2= 0.898	
12. Group of 11 species Total biomass(L) Volume(NL) Trunk(NL) Branches(NL) Leaves(NL)	 D=6–27 cm, n=11, ln a= - 2.566, b= 2.533, r^2=0.906, E= 0.451 D=6–27 cm, n=11, ln a=0.0005, b=1.899, r^2=0.973 D=6–27 cm, n=11, ln a=0.339, b= 1.836, r^2=0.950 D=6–27 cm, n=11, ln a=0.011, b=2.905, r^2=0.868 D=6–27 cm, n=11, ln a=0.0001, b=3.756, r^2=0.903	Salis et al. (2006)
13. Mixed species	**$\ln W_{leaf} = b'_1 + b_2 \ln D_{BH}$** **$\ln W_{woody} = b'_1 + b_2 \ln (D_{BH}^2 H_T)$** **$\ln W_{total} = b'_1 + b_2 \ln (D_{BH}^2 H_T)$** Where, ln=Natural logarithm, ln W=Biomass in oven-dry kg, DBH=Diameter at 1.37 m and H_T =Total height, $b'_1 = \ln b_1$. Leaf : n=26, b_1= - 1.75242, b_2= 1.71833, M.S.E=0.57199, r^2=0.75980 Woody: n=26, b_1= - 2.87503, b_2=0.92900, M.S.E=0.27738, r^2=0.92500 Total: n=26, b_1= - 1.94371, b_2=0.84134, M.S.E=0.25252, r^2=0.91750	Brandeis et al. (2006)

Bucida buceras Leaf: n=11, b_1= - 1.47983, b_2=1.83142, M.S.E=0.19500, r^2=0.92300 Woody: n=11 , b_1= - 2.68937, b_2=0.94081, M.S.E.=0.07125, r^2=0.98060 Total: n=11, b_1= - 1.76887, b_2=0.86389, M.S.E=0.03091, r^2=0.98990		
14. Mixed species Total volume (Inside bark portion of the tree's stem between a 30 cm tall stump and the tip of the tree's stem without a minimum upper diameter merchantability limit.) Merchantable volume (Inside bark portion of the tree's stem between a 30 cm tall stump and a 10 cm upper stem diameter.) *Bucida buceras* Total volume (Inside bark portion of the tree's stem between a 30 cm tall stump and the tip of the tree's stem without a minimum upper diameter merchantability limit.) Merchantable volume (Inside bark portion of the tree's stem between a 30 cm tall stump and a 10 cm upper stem diameter.)	$\mathbf{V_{stem} = b_1 + b_2 \ln(D_{BH}^2 H_T)}$ Total volume for Mixed species: Inside bark: n=17, b_1= - 0.0173, b_2=0.000047, M.S.E=0.0011, r^2=0.9906 Outside bark: n=17, b_1= - 0.0114, b_2= 0.000046, M.S.E=0.0010, r^2=0.9916 Merchantable volume for Mixed species: Inside bark: n=17, b_1= - 0.0593, b_2=0.000046, M.S.E=0.0020, r^2=0.9826 Outside bark: n=17, b_1= - 0.0576, b_2=0.000045, M.S.E=0.0019, r^2=0.9828 Total volume for *Bucida buceras*: Inside bark: n=9, b_1=0.0001, b_2=0.000047, M.S.E=0.0010, r^2=0.9952 Outside bark: n=9 , b_1=0.0002, b_2=0.000046, M.S.E=0.0010, r^2=0.9950	Brandeis et al. (2006)

Bursera simaruba Total volume (Inside bark portion of the tree's stem between a 30 cm tall stump and the tip of the tree's stem without a minimum upper diameter merchantability limit.)	Merchantable volume for *Bucida buceras*: Inside bark: n=9 , b_1= - 0.0697, b_2=0.000046, M.S.E=0.0024, r^2=0.9888 Outside bark: n=9 , b_1= - 0.0688, b_2=0.000046, M.S.E=0.0023, r^2=0.9890	
Merchantable volume (Inside bark portion of the tree's stem between a 30 cm tall stump and a 10 cm upper stem diameter.)	Total volume for *Bursera simaruba* Inside bark: n=8, b_1= 0.0370, b_2= 0.000028, M.S.E.=0.0003, r^2= 0.8536 Outside bark: n=8 , b_1= 0.0354, b_2= 0.000030, M.S.E.=0.0004, r^2= 0.8312	
Mixed species Total volume (Inside bark portion of the tree's stem between a 30 cm tall stump and the tip of the tree's stem without minimum upper diameter merchantability limit.) Merchantable volume (Inside bark portion of the tree's stem between a 30 cm tall stump and a 10 cm upper	Merchantable volume for *Bursera simaruba* Inside bark: n=8 , b_1= 0.2890, b_2= 0.000025, M.S.E.=0.0009, r^2= 0.5553 Outside bark: n=8 , b_1= 0.0285, b_2= 0.000023, M.S.E.=0.0009, r^2= 0.5620 $V_{stem} = b_1 + b_2 (D_{BH}) + b_3 \ln (D_{BH})^2$ Where, V_{stem} = the stem volume in cubic meters, D_{BH} the diameter at 1.37 m and H_T = the total height	

stem diameter.)	Total volume for Mixed species:	
Bucida buceras Total volume (Inside bark portion of the tree's stem between a 30 cm tall stump and the tip of the tree's stem without minimum upper diameter merchantability limit.)	Inside bark: n=17, b_1= 0.1810, b_2= 0.0234, b_3= 0.0012, M.S.E.=0.0044, r^2= 0.9662 Outside bark: n=17 , b_1= 0.1726, b_2= - 0.0222, b_3=0.0012 M.S.E.=0.0036, r^2= 0.9708	
Merchantable volume (Inside bark portion of the tree's stem between a 30 cm tall stump and a 10 cm upper stem diameter.)	Merchantable volume for Mixed species: Inside bark: n=17 , b_1= 0.0744, b_2= 0.0182, b_3= 0.0011, M.S.E.=0.0028, r^2= 0.9771 Outside bark: n=17 , b_1= 0.0729, b_2= - 0.0179, b_3=0.0011, M.S.E.=0.0027, r^2= 0.9780	
Bursera simaruba Total volume (Inside bark portion of the tree's stem between a 30 cm tall stump and the tip of the tree's stem without minimum upper diameter merchantability limit.)	Total volume for *Bucida buceras:* Inside bark: n=9, b_1= - 0.0182, b_2= - 0.0018, b_3= 0.0008, M.S.E.=0.0012, r^2= 0.9951 Outside bark: n=9 , b_1= 0.0007, b_2= - 0.0034, b_3=0.0008, M.S.E.=0.0012, r^2= 0.9950	
Merchantable volume (Inside bark portion of the tree's stem between a 30 cm tall stump and a 10 cm upper stem diameter.)	Merchantable volume for *Bucida buceras:* Inside bark: n=9 , b_1= - 0.0991, b_2= - 0.0009, b_3= 0.0008, M.S.E.=0.0025, r^2= 0.9897 Outside bark: n=9 , b_1= - 0.0949, b_2= - 0.0011, b_3=0.0008, M.S.E.=0.0025, r^2= 0.98990 Total volume for *Bursera simaruba*	

	Inside bark: n=8, b_1= - 0.2921, b_2= 0.0340, b_3= - 0.0006, M.S.E.=0.0004, r^2= 0.8255 Outside bark: n=8 , b_1= - 0.2388, b_2= 0.0273, b_3= - 0.0004, M.S.E.=0.0006, r^2= 0.8091 Merchantable volume for *Bursera simaruba* Inside bark: n=8 , b_1= 0.0807, b_2= - 0.0126, b_3= 0.0007, M.S.E.=0.0000672, r^2= 0.9708 Outside bark: n=8 , b_1= 0.0877, b_2= - 0.0135, b_3=0.0007, M.S.E.=0.000065, r^2= 0.9727	
15. Dry forest stands	$\mathbf{(AGB)_{est} = Exp(-2.187+0.916 \times \ln(\rho D^2 H))}$ $\mathbf{\equiv 0.112 \times \rho (D^2 H)\ 0.916}$ $\mathbf{(AGB)_{est} =}$ $\mathbf{\rho \times Exp(0.667+1.784 \times \ln(D)+0.207(\ln(D))^2 - 0.0281(\ln(D))^3)}$ Where, H=Total tree height, AGB=Total aboveground biomass (in kg) of a tree, D=Diameter of tree, ρ=Wood specific gravity	Chave et al. (2005)
16. Moist forest stands	$\mathbf{(AGB)_{est} = Exp(-2.977+\ln(\rho D^2 H))}$ $\mathbf{\equiv 0.0509 \times \rho (D^2 H)}$ $\mathbf{(AGB)_{est} =}$ $\mathbf{\rho \times Exp(-1.499+2.148 \times \ln(D)+2.07(\ln(D))^2 - 0.0281(\ln(D))^3)}$ Where, H=Total tree height, AGB=Total aboveground biomass (in kg) of a tree, D=Diameter of tree, ρ=Wood specific gravity	Chave et al. (2005)
17. Moist mangrove forest stands	$\mathbf{(AGB)_{est} = Exp(-2.977+\ln(\rho D^2 H))}$ $\mathbf{\equiv 0.0509 \times \rho (D^2 H)}$ $\mathbf{(AGB)_{est} =}$ $\mathbf{\rho \times Exp(-1.349+1.980\ln(D)+0.207(\ln(D))^2 -}$	Chave et al. (2005)

	$0.0281(\ln(D))^3$) Where, H=Total tree height, AGB=Total aboveground biomass (in kg) of a tree, D=Diameter of tree, ρ=Wood specific gravity	
18. Wet forest stands:	**$(AGB)_{est} = Exp(-2.557+0.940\times\ln(\rho D^2H))$** **$\equiv 0.0776\times \rho(D^2H)^{0.940}$** **$(AGB)_{est} =$** **$\rho \times Exp(-1.239+1.980\ln(D)+0.207(\ln(D))^2 - 0.0281(\ln(D))^3)$** Where, H=Total tree height, AGB=Total aboveground biomass (in kg) of a tree, D=Diameter of tree, ρ=Wood specific gravity	Chave et al. (2005)
19. *Erica arborea*	**Ln AGB= a+bln DBH** a=0.570, b=0.506, r^2=0.97, P<0.001	Aboal et al. (2005)
20. *Ilex canariensis*	**Ln AGB= a+bln DBH** a=0.478, b=0.477, r^2=0.97, P<0.001	Aboal et al. (2005)
21. *Laurus azorica*	**Ln AGB= a+bln DBH** a=1.783, b=0.202, r^2=0.99, P<0.001	Aboal et al. (2005)
22. *Myrica faya*	**Ln AGB= a+bln DBH** a=0.570, b=0.506, r^2=0.99, P<0.001	Aboal et al. (2005)
23. *Persea indica*	**Ln AGB= a+bln DBH** a=0.570, b=0.506, r^2=0.98, P<0.001	Aboal et al. (2005)
24. *Casuarina glauca* Stem Branch Leaf Total yield	**$Y = a + b \cdot h$** Where, Y=Biomass (in kg), h=Plant height , FW=Fresh weight, DW=Dry weight, sb=Error of regression coefficient, F-value is Significant at 1% level Stem FW: a= - 20.64, b=0.480, sb=0.053, r^2=0.460, n=98, F-value=83.11 DW: a= - 10.40, b=0.244, sb=0.020 Branch	Goel and Behl (2005)

Stem Branch Leaf Total yield	FW: a= - 3.10, b=0.083, sb=0.010, r^2=0.409, n=98, F-value=66.67 DW: a= - 1.370, b=0.036, sb=0.004 Leaf FW : a= - 0.696, b=0.036, sb=0.006, r^2=0.245, n= 98, F-value=31.15 DW : a= - 0.302, b=0.015, sb=0.002 Total yield FW: a= - 24.44, b=0.604, sb=0.067, r^2=0.456, n= 98, F-value=80.59 DW : a = - 12.07, b=0.296, sb=0.033 (ii)**$Y = a + b \cdot d^2$(dbh)** Where, Y=Biomass (in kg), d^2=Diameter, FW=Fresh weight, DW=Dry weight, sb=Error of regression coefficient, F-value is Significant at 1% level Stem FW: a=0.751, b=39.99, sb=2.03, r^2=0.80, n=98, F-value=385.06 DW: a=0.378, b=20.15, sb=1.027 Branch FW: a=0.741, b=6.25, sb=0.532, r^2=0.58, n=98, F-value=137.59 DW: a=0.327, b=2.750, sb=0.234 Leaf FW: a=0.768, b=3.41, sb=0.314, r^2=0.55, n=98, F-value=118.0 DW: a=0.332, b=1.471, sb=0.135 Total yield FW: a=2.261, b=49.65, sb=2.677, r^2= 0.78, n=98 F-value=344.0 DW: a=1.037, b=24.38, sb=1.307	

Stem Branch Leaf Total yield	(iii)$\mathbf{Y = a + b \cdot d^2h}$ Where, Y=Biomass (in kg), h=Plant height , d^2=diameter, FW=Fresh weight, DW=Dry weight, sb=Error of regression coefficient Stem, F-value is Significant at 1% level FW: a=2.56, b=0.46, sb=0.021, r^2=0.828, n=98, F-value=465.09 DW: a=1.290, b=0.231, sb=0.010 Branch FW: a=1.02, b=0.072, sb=0.005, r^2=0.611, n=98, F-value=151.28 DW: a=0.450, b=0.031, sb=0.002 Leaf FW: a=0.925, b=0.039, sb=0.003, r^2=0.568, n=98, F-value=126.58 DW: a=0.399, b=0.016, sb=0.001 Total yield FW: a=4.51, b=0.571, sb=0.028, r^2= 0.809, n=98, F-value=408.45 DW: a=2.140, b=0.280, sb=0.010	
25. *Byrsonima lucida*	Fuel type: T (Total shrub or tree biomass i.e. plant parts of all sizes) $\mathbf{B = a + b(CA) + c(CA^2)}$ P<0.001, r^2=0.97, N=8, a or a'=0.310, b=0.672, c=0.035, FI=0.97, S.E.E.=0.297 Fuel type: F (Fine fuel shrub or tree biomass i.e. leaves) $\mathbf{B = a + b(CA) + c(CA^2)}$ P<0.001, r^2=0.97, N=8, a or a'=0.280 , b=0.272, c=0.036, FI=0.97, S.E.E.=0.175 CF (Correction factor)=exp ($S_{y,x}^2$/2), FI (Fit Index)=1-($S(Y_i- \hat{Y}_i)^2$) / $\Sigma(Y_i- \hat{Y}_i)^2$ Where, Y_i is the ith observed value, $\hat{Y}_i$ is the ith	Sah et al. (2004)

	predicted value for Y_i, and $\hat{Y}$ is the mean observed value of Y_i.(for comparison we use this factor) CA=Crown area in square meters, HT=Plant height in meters. Assuming an elliptical crown shape, crown area was calculated as CA = π (C_L/2) (C_W/2), where C_L is the crown length at its widest point and C_W the perpendicular crown extent at the same height.	
26. *Conocarpus erectus*	Fuel type: T(Total shrub or tree biomass i.e. plant parts of all sizes) **$B = a'CA^b HT^c$** P<0.001, r^2=0.86, N=12, a or a'=0.323 , b=0.360, c=1.824, CF=1.07, FI=0.77, S.E.E.=0.816 Fuel type: F(Fine fuel shrub or tree biomass i.e. leaves) **$B = a'CA^b HT^c$** P<0.001, r^2=0.82, N=12, a or a'=0.169, b=0.246, c=1.512, CF=1.06, FI=0.79, S.E.E.=0.195 CF (Correction factor)=exp ($S_{y,x}^2$/2), FI (Fit Index)=1-($S(Y_i- \hat{Y}_i)^2$) / $\Sigma(Y_i- \hat{Y}_i)^2$ Where, Y_i is the ith observed value, $\hat{Y}_i$ is the ith predicted value for Y_i, and $\hat{Y}$ is the mean observed value of Y_i.(for comparison we use this factor) CA=Crown area in square meters, HT=Plant height in meters. Assuming an elliptical crown shape, crown area was calculated as CA = π (C_L/2) (C_W/2), where C_L is the crown length at its widest point and C_W the perpendicular crown extent at the same height.	Sah et al. (2004)
27. *Croton linearis*	Fuel type: T(Total shrub or tree biomass i.e. plant parts of all sizes) **$B = a + b(CA) + c(CA^2)$** P<0.001, r^2=0.99, N=10, a or a'=0.077, b= - 0.086, c=0.175, FI=0.99, S.E.E.=0.045 Fuel type: F(Fine fuel shrub or tree biomass i.e.	Sah et al. (2004)

	leaves) **$B = a + b(CA) + c(CA^2)$** $P<0.001$, $r^2=0.99$, N=10, a or a'=0.057, b= - 0.049, c=0.111, FI=0.99, S.E.E.=0.034 CF (Correction factor)=exp ($S_{y,x}^2/2$), FI (Fit Index)=1-($S(Y_i- \hat{Y}_i)^2$) / $\Sigma(Y_i- \hat{Y}_i)^2$ Where, Y_i is the ith observed value, $\hat{Y}_i$ is the ith predicted value for Y_i, and $\hat{Y}$ is the mean observed value of Y_i.(for comparison we use this factor) CA=Crown area in square meters, HT=Plant height in meters. Assuming an elliptical crown shape, crown area was calculated as $CA = \pi (C_L/2) (C_W/2)$, where C_L is the crown length at its widest point and C_W the perpendicular crown extent at the same height.	
28. *Guettarda scabra*	Fuel type: T(Total shrub or tree biomass i.e. plant parts of all sizes) **$B = a'CA^b HT^c$** $P<0.001$, $r^2=0.96$, N=13, a or a'=0.119 , b=0.419, c=2.159, FI=0.94, S.E.E.=0.417 Fuel type: F(Fine fuel shrub or tree biomass i.e. leaves) **$B = a'CA^b HT^c$** $P<0.001$, $r^2=0.90$, N=13, a or a'=0.041, b=0.332, c=1.788, CF=1.12, FI=0.92, S.E.E.=0.089 CF (Correction factor)=exp ($S_{y,x}^2/2$), FI (Fit Index)=1-($S(Y_i- \hat{Y}_i)^2$) / $\Sigma(Y_i- \hat{Y}_i)^2$ Where, Y_i is the ith observed value, $\hat{Y}_i$ is the ith predicted value for Y_i, and $\hat{Y}$ is the mean observed value of Y_i.(for comparison we use this factor) CA=Crown area in square meters, HT=Plant	Sah et al. (2004)

	height in meters. Assuming an elliptical crown shape, crown area was calculated as CA = π (C_L/2) (C_W/2), where C_L is the crown length at its widest point and C_W the perpendicular crown extent at the same height.	
29. *Myrica cerifera*	Fuel type: T(Total shrub or tree biomass i.e. plant parts of all sizes) **$B = a'CA^b HT^c$** P<0.001, r^2=0.93, N=15, a or a'=0.341, b=0.977, c=1.363, CF=1.09, FI=0.80, S.E.E.=0.701 Fuel type: F(Fine fuel shrub or tree biomass i.e. leaves) **$B = a'CA^b HT^c$** P<0.001, r^2=0.89, N=15, a or a'=0.306, b=1.028, c=0.649, CF=1.12, FI=0.74, S.E.E.=0.354 CF (Correction factor)=exp ($S_{y,x}^2$/2), FI (Fit Index)=1-($S(Y_i- \hat{Y}_i)^2$) / $\Sigma(Y_i- \hat{Y}_i)^2$ Where, Y_i is the ith observed value, $\hat{Y}_i$ is the ith predicted value for Y_i, and $\hat{Y}$ is the mean observed value of Y_i.(for comparison we use this factor) CA=Crown area (in m^2), HT=Plant height (in m). Assuming an elliptical crown shape, crown area was calculated as CA = π (C_L/2) (C_W/2), where C_L is the crown length at its widest point and C_W the perpendicular crown extent at the same height.	Sah et al. (2004)
30. *Myrsine floridana*	Fuel type: T(Total shrub or tree biomass i.e. plant parts of all sizes) **$B = a + b(DBH)^2 + c(HT)$** P<0.001, r^2=0.86, N=19, a or a'= -0.258, b=0.124, c=0.003, FI=0.86, S.E.E.=0.167 Fuel type: F(Fine fuel shrub or tree biomass i.e. leaves) **$B = a + b(DBH)^2 + c(HT)$** P<0.001, r^2=0.79, N=19, a or a'= - 0.043,	Sah et al. (2004)

	b=0.179, c=0.000, FI=0.84, S.E.E.=-0.062 CF (Correction factor)=exp ($S_{y,x}^2/2$), FI (Fit Index)=1-($S(Y_i- \hat{Y}_i)^2$) / $\Sigma(Y_i- \hat{Y}_i)^2$ Where, Y_i is the ith observed value, $\hat{Y}_i$ is the ith predicted value for Y_i, and $\hat{Y}$ is the mean observed value of Y_i.(for comparison we use this factor) CA=Crown area in square meters, HT=Plant height in meters. Assuming an elliptical crown shape, crown area was calculated as CA = π ($C_L/2$) ($C_W/2$), where C_L is the crown length at its widest point and C_W the perpendicular crown extent at the same height.	
31. *Pisonia rotundata*	Fuel type: T(Total shrub or tree biomass i.e. plant parts of all sizes) **$B = a'CA^b HT^c$** P=0.001, r^2=0.79, N=12, a or a'= -0.379, b=0.510, c=0.983, CF=1.06, FI=0.90, S.E.E.=0.127 Fuel type: F(Fine fuel shrub or tree biomass i.e. leaves) **$B = a'CA^b HT^c$** P<0.001, r^2=0.90, N=12, a or a'= -0.159 , b=0.616, c=0.813, CF=1.03, FI=0.88, S.E.E.=0.061 CF (Correction factor)=exp ($S_{y,x}^2/2$), FI (Fit Index)=1-($S(Y_i- \hat{Y}_i)^2$) / $\Sigma(Y_i- \hat{Y}_i)^2$ Where, Y_i is the ith observed value, $\hat{Y}_i$ is the ith predicted value for Y_i, and $\hat{Y}$ is the mean observed value of Y_i.(for comparison we use this factor) CA=Crown area in square meters, HT=Plant height in meters. Assuming an elliptical crown shape, crown area was calculated as CA = π ($C_L/2$) ($C_W/2$), where C_L is the crown length at its widest point and C_W the perpendicular crown extent at the same height.	Sah et al. (2004)

32. *Pithecellobium guadalupense*	Fuel type: T(Total shrub or tree biomass i.e. plant parts of all sizes) **$B = a + b(CA) + c(CA^2)$** $P<0.001$, $r^2=0.99$, N=12, a or a'= -0.373 , b=0.258, c=0.182, FI=0.99, S.E.E.=0.446 Fuel type: F(Fine fuel shrub or tree biomass i.e. leaves) **$B = a + b(CA) + c(CA^2)$** $P<0.001$, $r^2=0.99$, N=12, a or a'=0.373, b=0.142, c=0.043, FI=0.99, S.E.E=0.158 CF (Correction factor)=exp ($S_{y,x}^2/2$), FI (Fit Index)=1-($S(Y_i- \hat{Y}_i)^2$) / $\Sigma(Y_i- \hat{Y}_i)^2$ Where, Y_i is the ith observed value, $\hat{Y}_i$ is the ith predicted value for Y_i, and $\hat{Y}$ is the mean observed value of Y_i.(for comparison we use this factor) CA=Crown area in square meters, HT=Plant height in meters. Assuming an elliptical crown shape, crown area was calculated as $CA = \pi (C_L/2) (C_W/2)$, where C_L is the crown length at its widest point and C_W the perpendicular crown extent at the same height.	Sah et al. (2004)
33. *Psidium longipes*	Fuel type: T(Total shrub or tree biomass i.e. plant parts of all sizes) **$B = a'CA^b HT^c$** P=0.002, $r^2=0.76$, N=12, a or a=0.672, b=0.956, c=0.872, CF=1.16, FI=0.67, S.E.E.=1.591 Fuel type: F(Fine fuel shrub or tree biomass i.e. leaves) **$B = a'CA^b HT^c$** P=0.006, $r^2=0.68$, N=12, a or	Sah et al. (2004)

	a=0.270, b=0.995, c=0.503, CF=1.16, FI=0.64, S.E.E.=0.505 CF (Correction factor)=exp ($S_{y,x}^2/2$), FI (Fit Index)=1-($S(Y_i- \hat{Y}_i)^2$) / $\Sigma(Y_i- \hat{Y}_i)^2$ Where, Y_i is the ith observed value, $\hat{Y}_i$ is the ith predicted value for Y_i, and $\hat{Y}$ is the mean observed value of Y_i.(for comparison we use this factor) CA=Crown area in square meters, HT=Plant height in meters. Assuming an elliptical crown shape, crown area was calculated as CA = π ($C_L/2$) ($C_W/2$), where C_L is the crown length at its widest point and C_W the perpendicular crown extent at the same height.	
34. *Randia aculeate*	Fuel type: T(Total shrub or tree biomass i.e. plant parts of all sizes) **$B = a'CA^b HT^c$** P=0.004, r^2=0.79, N=12, a or a'=0.017, b=0.121, c=3.222, CF=1.25, FI=0.70, S.E.E=0.117 Fuel type: F(Fine fuel shrub or tree biomass i.e. leaves) **$B = a'CA^b HT^c$** r^2=0.79, N=12, a or a=0.022, b=0.138, c=1.980, CF=1.12, FI=0.79, S.E.E=0.032 CF (Correction factor)=exp ($S_{y,x}^2/2$), FI (Fit Index)=1-($S(Y_i- \hat{Y}_i)^2$) / $\Sigma(Y_i- \hat{Y}_i)^2$ Where, Y_i is the ith observed value, $\hat{Y}_i$ is the ith predicted value for Y_i, and $\hat{Y}$ is the mean observed value of Y_i.(for comparison we use this factor) CA=Crown area in square meters, HT=Plant height in meters. Assuming an elliptical crown shape, crown area was calculated as	Sah et al. (2004)

	CA = π (C_L/2) (C_W/2), where C_L is the crown length at its widest point and C_W the perpendicular crown extent at the same height.	
35. Mixed-species (shrub-like)	Fuel type: T(Total shrub or tree biomass i.e. plant parts of all sizes) **$B = a'CA^b HT^c$** P<0.001, r^2=0.87, a or a=0.446, b=0.869, c=1.112, CF=1.15, FI=0.72, S.E.E=0.911 Fuel type: F(Fine fuel shrub or tree biomass i.e. leaves) **$B = a'CA^b HT^c$** P<0.001, r^2=0.82, a or a=0.269, b=0.855, c=0.609, CF=1.18, FI=0.58, S.E.E=0.387 CF (Correction factor)=exp ($S_{y,x}^2$/2), FI (Fit Index)=1-($S(Y_i- \hat{Y}_i)^2$) / $\Sigma(Y_i- \hat{Y}_i)^2$ Where, Y_i is the ith observed value, $\hat{Y}_i$ is the ith predicted value for Y_i, and $\hat{Y}$ is the mean observed value of Y_i.(for comparison we use this factor) CA=Crown area in square meters, HT=Plant height in meters. Assuming an elliptical crown shape, crown area was calculated as CA = π (C_L/2) (C_W/2), where C_L is the crown length at its widest point and C_W the perpendicular crown extent at the same height.	Sah et al. (2004)
36. Mixed-species (tree-like)	Fuel type: T(Total shrub or tree biomass i.e. plant parts of all sizes) **$B = a + b(DBH)^2 + c(HT)$** P<0.001, r^2=0.57, a or a=0.060, b=0.227, c=0.002, FI=0.57, S.E.E=0.437 Fuel type: F(Fine fuel shrub or tree biomass i.e. leaves) **$B = a + b(DBH)^2 + c(HT)$** P<0.001, r^2=0.58, a or a=0.184, b=0.067,	Sah et al. (2004)

	c=0.002, FI=0.58, S.E.E=0.136 CF (Correction factor)=exp ($S_{y,x}^2$/2), FI (Fit Index)=1-($S(Y_i- \hat{Y}_i)^2$) / $\Sigma(Y_i- \hat{Y}_i)^2$ Where, Y_i is the ith observed value, $\hat{Y}_i$ is the ith predicted value for Y_i, and $\hat{Y}$ is the mean observed value of Y_i.(for comparison we use this factor) CA=Crown area in square meters, HT=Plant height in meters. Assuming an elliptical crown shape, crown area was calculated as CA = π (C_L/2) (C_W/2), where C_L is the crown length at its widest point and C_W the perpendicular crown extent at the same height.	
37. *Bauhinia racemosa*	**Y = a + b × X** (X = cbh^2 × height) N=19, a=0.0431, b=0.0025, r^2=0.97, SE=3.17 Y=Above ground biomass, cbh=Circumference at breast height	Kale et al. (2004)
38. *Ziziphus xylopyra*	**Log10 Y = a + b × log X** (X = cbh) N=15, a= -3.20, b=2.87, r^2=0.94, SE=0.12 Y=Above ground biomass, cbh=Circumference at breast height	Kale et al. (2004)
39. *Tectona grandis*	**log *Y* = *a* + *b* × log *X*** (*X* = cbh) N=15, a= -2.85, b=2.655 , r^2=0.98, SE=0.075 Y=Above ground biomass, cbh=Circumference at breast height	Kale et al. (2004)
40. *Lannea coromandelica*	***Y* = *a* + *b* × *X*** (*X* = cbh^2 × height) N=15, a= -1.84, b=0.002, r^2=0.98, SE=14.49 Y=Above ground biomass, cbh=Circumference at breast height	Kale et al. (2004)

41. *Miliusa tomentosa.*	$\boldsymbol{Y = a + b \times X}$ (X = cbh^2 * height) N=17, a= -0.68, b=0.0024, r^2=0.99, SE=1.33 Y=Above ground biomass, cbh=Circumference at breast height	Kale et al. (2004)
42. *Prosopis pallida* (H. & B. ex. Willd.)	*For fresh above ground woody biomass:* $\mathbf{y = (a + b \times x)^2}$ r=0.9700, r^2=0.9410, P=0.000, a=2.79320, b=0.82300, S.E.=2.3470 Where, y=Fresh above ground woody biomass, x=Diameter at the base $\mathbf{y = a \times x^b}$ r=0.9648, r^2=0.9308, P=0.000, a=0.11320, b=1.11320, S.E.=0.2857 r=0.9573, r^2=0.9164, P=0.000, a= - 0.3616, b=2.10750, S.E.=0.2730 r=0.9573, r^2=0.9164, P=0.000, a=0.36257, b=1.05372, S.E.=0.2725 **y= a + b × x** r=0.9602, r^2=0.9220, P=0.000, a=41.9637, b=0.59540, S.E.=120.68 r=0.9530, r^2= 0.9082, P=0.000, a= - 41.963, b=0.59540, S.E.=105.96 y= Fresh above ground woody biomass x=Diameter at the base **y= a + b × diameter at the base + c × crown height** r^2=0.9198, P=0.000, a= - 868.69, b=41.41, c=67.955, S.E.=145.298, MAE=105.447 $\mathbf{y = a + b \times x^{1/2}}$ r=0.9656, r^2=0.9325, P=0.000, a= -132.588, b=3.03678, S.E.=3.03678 Where, y=Fresh above ground woody, x=(Diameter at the base)^2 total height ×greatest	Padron and Navarro (2004)

	crown diameter **$y= a+ b \times x^{1/2}$** r=0.9721, r^2=0.9450, P=0.000, a= - 448.817, b=16.6861, S.E.=124.164 Where, y=Fresh above ground woody, x=(Diameter at the base)^2 ×crown height **$y= a+ b \times x^{1/2}$** r=0.9509, r^2=0.9041, P=0.000, a= - 283.119, b=5.15510, S.E.=163.977 Where, y=Fresh above ground woody, x=(Diameter at the base)^2×total height×crown height **$y= a + b \times x$** r=0.9800, r^2=0.9509, P=0.000, a=75.1691, b=0.08732, S.E.=117.335 Where, y=Fresh above ground woody, x=(Diameter at the base)^2×total height **$y= a + b \times x$** r=0.9605, r^2=0.9225 ,P=0.000, a=302.500, b=4.73740, S.E.=147.436 Where, y=Fresh above ground woody, x=(Diameter at the base) × total height	
43. *Prosopis pallida* (H. & B. ex. Willd.)	**179.** *For woody dry biomass:* **$y= a \times x^b$** r= - 0.9684, r^2=0.9379, P=0.000, a=2972.51, b=2587.65, S.E.=0.2708 r=0.9643, r^2=0.9300, P=0.000, a= - 2972.5, b=2587.65, S.E.= 0.2494 Where, y=Woody dry biomass, x=Diameter at the base **y= a + b × diameter at the base + c × crown height** r^2=0.9137, P=0.000, a= - 868.69, b=41.41,	Padron and Navarro (2004)

	c=67.955, S.E.= 122.854, MAE=90.4698 Where, y=Woody dry biomass, x=Diameter at the base **y= a + b × x** r=0.9698, r^2=0.9405, P=0.000, a= - 186.817, b=3.15880, S.E.=85.3203 Where, y=Woody dry biomass, x=(Diameter at the base)×total height **$y= a+ b \times x^{1/2}$** r=0.9619, r^2=0.9252, P=0.000, a= - 174.938, b=3.44379, S.E.=95.6336 Where, y=Woody dry biomass, x=$(\text{Diameter at the base})^2$ total height×crown height **y= a + b × x** r=0.9801, r^2=0.9607, P=0.000, a=66.5541, b=0.05796, S.E.=69.3366 Where, y=Woody dry biomass, x=$(\text{Diameter at the base})^2$×total height **$y= a+ b \times x^{1/2}$** r=0.9806, r^2=0.9616, P=0.000, a=283.686, b=11.1153, S.E.=68.5285 Where, y=Woody dry biomass, x=$(\text{Diameter at the base})^2$ ×crown height	
44. *Prosopis pallida* (H. & B. ex. Willd.)	*Fresh biomass* *(35cm<diameter at the base≤45cm)* **y=a + b ×x** r=0.9954, r^2=0.9907, P=0.000, a=60.6685, b=0.054867, S.E.=31.3628 Where, y=Woody dry biomass, x=$(\text{Diameter at the base})^2$×total height	Padron and Navarro (2004)

45. *Prosopis pallida* (H. & B. ex. Willd.)	*Fresh biomass (15cm<diameter at the base≤35cm)* $\mathbf{Y = a \times x^{b}}$ r=0.9448, r^2=0.8927, P=0.000, a=0.38530, b=0.72270, S.E.=0.24490 Where, y=Woody dry biomass, x=(Diameter at the base)^2×crown height	Padron and Navarro (2004)
46. *Elaeis guineensis* (Oil palm)	*Wet Weight (kg/tree)=1.5729×Palm stem height (cm)-8.2835* *r^2=0.9746* *Dry Weight (kg/tree)=0.3747×Palm stem height (cm)+3.6334* *r^2=0.9804* *The total weights for each tree were summed from individual components that included above ground core, leaf (dead and live), rachis (dead and live), flower, and palm nut.*	Thenkabail et al. (2004)
47. *Elaeis guineensis* (Oil palm)	Biomass based on reflectivity in IKONOS bands: *Dry biomass (kg/m^2)=0.0046 $e^{10.814\times NDVI43}$* *Dry biomass (kg/m^2) =1499.3 $e^{(-66.64\times band\ 3\ reflectance)}$* *Dry biomass (kg/m^2) =1595 $e^{(-0.0338\times band\ 3\ digital\ number)}$*	Thenkabail et al. (2004)
48. *Anacardium excelsum* (2.4-18.6 cm DBH)	Four different methods to determine the *carbon content of each tree sampled* ***Method 1**:* *Ln (C)= c+α ln (DBH)* c= - 3.4931, S.E.=0.0983, r^2=0.9957, Avg unsigned deviation (%)=8.9, t-value=0.0000 α=2.4843, S.E.=0.0470, r^2=0.9957, Avg unsigned deviation (%)=8.9, t-value=0.0000 *Ln (C)= c+α ln (DBH)+β ln(H)* *c= - 3.7179, S.E.=0.2227, r^2=0.9962, Avg unsigned deviation (%)=8.6, t-value=0.0000* *α=2.1936, S.E.=0.2633, t-value=0.0000* *β=0.4132, S.E.=0.3684, t-value=0.28 (NS)* **Method 2:**	Losi et al. (2003)

	Ln (C)= c+α ln (DBH) *c= - 3.4577, S.E.=0.1007, r^2=0.9955, Avg unsigned deviation (%)=9.2, t-value=0.0000* *α=2.4889, S.E.=0.0482, t-value=0.0000* **Method 3:** **Ln (C)= c+α ln (DBH)** *c= - 3.4278, S.E.=0.1007, r^2=0.9955, Avg unsigned deviation (%)=9.2, t-value=0.0000* *α=2.4830, S.E.=0.0482, t-value=0.0000* **Method 4:** **Ln (C)= c+α ln (DBH)** *c= - 3.4877, S.E.=0.1075, r^2=0.9950, Avg unsigned deviation (%)=9.7, t-value=0.0000* *α=2.5143, S.E.=0.0515, t-value=0.0000* *c, α, β=Coefficients, DBH=Diameter at breast height (in cm), H=Height (in m), C=Total above ground carbon content (in kg)*	
49. *Dipteryx panamensis* (1.8-11.2 cm DBH)	**Method 1:** **Ln (C)= c+ α ln (DBH)** c= - 2.6344, S.E.=0.0666, r^2=0.9975, Avg unsigned deviation (%)=7.1, t-value=0.0000 α=2.5170, S.E.=0.0363, t-value=0.0000 *Ln (C)= c+α ln (DBH)+β ln(H)* *c= - 2.8313, S.E.=0.1010, r^2=0.9983, Avg unsigned deviation (%)=5.7, t-value=0.0000* *α=2.1850, S.E.=0.1442, t-value=0.0000* *β=0.4128, S.E.=0.1752, t-value=0.0380* **Method 2:** **Ln (C)= c+ α ln (DBH)** c= - 2.6362, S.E.=0.0696, r^2=0.9973, Avg unsigned deviation (%)=7.5, t-value=0.0000 α=2.5339, S.E.=0.0379, t-value=0.0000 For trees 8.4- 11.2 cm	Losi et al. (2003)

	Ln (C)= c+ α ln (DBH) c= - 2.2433, S.E.=0.9620, r^2=0.8877, Avg unsigned deviation (%)=5.5, t-value=0.0801 α=2.3661, S.E.=0.4208, t-value=0.0049 **Method 3:** **Ln (C)= c+ α ln (DBH)** c= - 2.6203, S.E.=0.0699, r^2=0.9973, Avg unsigned deviation (%)=7.5, t-value=0.0000 α=2.5327, S.E.=0.0380, t-value=0.0000 **Method 4:** **Ln (C)= c+ α ln (DBH)** c= - 3.3814, S.E.=0.1213, r^2=0.9937, Avg unsigned deviation (%)=12.8, t-value=0.0000 *α=2.8643, S.E.=0.0660, t-value=0.0000* **180.** *c, α, β=Coefficients, DBH=Diameter at breast height (in cm), H=Height (in m), C=Total above ground carbon content (in kg)*	
50. *Acer rubrum*	**Dry mass (g) = *a* + b(DBH (cm))** Where, DBH is diameter at breast height (3.7 m above ground). **Log_{10} (branch biomass) =1.21264 + 2.57934 (Log_{10} DBH)** N=12, r^2=0.91, MSE=0.01678, P=0.0001 **Log_{10} (stem biomass) =2.04101 + 2.32487 (Log_{10} DBH)** N=12, r^2=0.97, MSE=0.00392, P=0.0001	Elliott et al. (2002)
51. *Liriodendron tulipifera*	**Dry mass (g) = *a* + b(DBH (cm))** Where, DBH is diameter at breast height (3.7 m above ground). **Log_{10} (branch biomass) =0.71955 + 2.70444 (Log_{10} DBH)** N=16, r^2=0.93, MSE=0.046 58, P=0.0001 **Log_{10} (stem biomass) =1.90272 + 2.33725 (Log_{10}**	Elliott et al. (2002)

	DBH) N=16, r^2=0.98, MSE=0.010 00, P=0.0001	
52. *Quercus prinus*	**Dry mass (g) = *a* + b(DBH (cm))** Where, DBH is diameter at breast height (3.7 m above ground). **Log_{10} (branch biomass) =0.46597 + 3.30505 (Log_{10} DBH)** N=13, r^2=0.86, MSE=0.01656, P=0.0001 **Log_{10} (stem biomass) =1.73250 + 2.59378 (Log_{10} DBH)** N=13, r^2=0.93, MSE=0.00499, P=0.0001	Elliott et al. (2002)
53. *Robinia pseudoacacia*	**Dry mass (g) = *a* + b(DBH (cm))** Where, DBH is diameter at breast height (3.7 m above ground). **Log_{10} (branch biomass) =1.07682 + 2.53262 (Log_{10} DBH)** N=23, r^2=0.87, MSE=0.05386, P=0.0001 **Log_{10} (stem biomass) =1.75911 + 2.60392 (Log_{10} DBH)** N=23, r^2=0.98, MSE=0.00875, P=0.0001	Elliott et al. (2002)
54. *Quercus rubra*	**Dry mass (g) = *a* + b(DBH (cm))** Where, DBH is diameter at breast height (3.7 m above ground). **Log_{10} (branch biomass) =0.20948 + 3.70107 (Log_{10} DBH)** N=12, r^2=0.95, MSE=0.01380, P=0.0001 **Log_{10} (stem biomass) =2.00703 + 2.35049 (Log_{10} DBH)** N=12, r^2=0.94, MSE=0.00744, P=0.0001	Elliott et al. (2002)
55. All oaks	**Dry mass (g) = *a* + b(DBH (cm))** Where, DBH is diameter at breast height (3.7 m above ground).	Elliott et al. (2002)

	Log_{10} (branch biomass) =0.54101 + 3.28005 (Log_{10} DBH) N=27, r^2=0.94, MSE=0.01758, P=0.0001 **Log_{10} (stem biomass) =2.009 99 + 2.338 66 (Log_{10} DBH)** N=27, r^2=0.96, MSE=0.00577, P=0.0001	
56. All tree species	**Dry mass (g) = *a* + b(DBH (cm))** Where, DBH is diameter at breast height (3.7 m above ground). **Log_{10} (branch biomass) =1.58238 + 2.11319 (Log_{10} DBH)** N=43, r^2=0.77, MSE=0.08866, *P*=0.0001 **Log_{10} (stem biomass) =1.90443 + 2.37735 (Log_{10} DBH)** N=43, r^2=0.96, MSE=0.01754, P=0.0001	Elliott et al. (2002)
57. *Bombacopsis quinata* Type 1	**Log $_{10}$Y=a+b log $_{10}$ DBH**(cm) Y=Foliage dry biomass (kg): a= -2.148±0.549, b=2.047±0.395, r^2=0.64, RMSE=0.201. Y=Branch dry biomass (kg): a= -2.665±0.432, b=3.138±0.311, r^2=0.87, RMSE=0.158. Y=Stem dry biomass (kg): a= -2.143±0.186, b=2.95±0.133, r^2=0.97, RMSE=0.068. Y=Total tree dry biomass (kg): a= -1.988±0.192, b=2.993±0.138, r^2=0.97, RMSE=0.070. Y=Crown diameter(m): a=-0.177±0.208, b=0.689±0.149, r^2=0.59, RMSE=0.076.	Cordero & Kanninen (2002)

58. *Bombacopsis quinata* Type 2	**Log $_{10}$Y=a+b log $_{10}$ crown diameter**(m) Y=Foliage dry biomass (kg): a= -1.292±0.256, b=2.544±0.326, r^2=0.80, RMSE=0.149	Cordero & Kanninen (2002)
59. *Bombacopsis quinata* Type 3	**Log $_{10}$Y=a+b log $_{10}$ branch dry biomass**(kg) Y=Foliage dry biomass (kg): a= -0.280±0.223, b=0.575±0.128, r^2=0.57, RMSE=0.219.	Cordero & Kanninen (2002)
60. *Bombacopsis quinata* Type 4	**Log $_{10}$Y=a+b log $_{10}$ DBH**(cm)+**c log $_{10}$ H**(m) Y=Foliage dry biomass (kg): a= -1.468±0.373, b= -1.468±0.373, c= -3.148±0.646, r^2=0.87, RMSE=0.122. Y=Crown diameter(m): a=0.041±0.171, b=1.405±0.239, c= -1.011±0.296, r^2=0.78, RMSE=0.056.	Cordero & Kanninen (2002)
61. Coffee root	**$W=0.0074\ D_{prox}^{3.14}$** r^2=0.95 Where, W=Root Biomass(kg tree^{-1}), D=Stem diameter at 1.35m (cm)	Noordwijk et al. (2002)
62. Fern Tree (*Cyathea* spp.)	**$y= a / 1+be^{-cx}$** r^2=0.88, y=Biomass, x=Height, a= - 4.266348 e+009, b= -2792284, c=0.31367768	Tiepolo et al. (2002)
63. *Palm< 10 cm dbh*	**Agb=** **$[[(\exp(0.9285\times \ln(D^2))+5.7236]\times 1.050]/10^6$** R^2=0.39, N=15 Where, D=DBH (cm), Agb=Above ground biomass (in Mg on a dry basis).	Cummings et al. (2002)
64. *Stem less palm*	**Agb=(leaves × 296.54)/ 10^6** Where, Agb=Above ground biomass (in Mg on a dry basis).	Cummings et al. (2002)

65. *Dicot seedlings*	**Agb=Seedling Count × Mean wt.(determined from sub- sample)/ 10^6** Where, Agb=Above ground biomass (in Mg on a dry basis), Wt=Weight (in gram)	Cummings et al. (2002)
66. *Forest floor*	**Agb=Wet wt. ×%dry wt./100(determined from sub sample)/ 10^6** Where, Agb=Above ground biomass (in Mg on a dry basis), Wt=Weight (in gram)	Cummings et al. (2002)
67. *Palm <10 cm dbh*	**Agb=[(exp(1.5321×ln(D^2)+3.2758)) ×1.0931]/ 10^6** R^2=0.34, N=15 Where, D=DBH (cm), Agb=Above ground biomass (in Mg on a dry basis).	Cummings et al. (2002)
68. *Palm>10 cm dbh*	**Agb=((Π r^2×H) ×sg)/ 10^6** sg=0.327g cm^{-3} Where, D=dbh (in cm), H=Height (in m), BA=Basal area (in cm^2), sg=Specific gravity of wood (in g cm^{-3}), r=Radius (in m), Wt=Weight (in gram)	Cummings et al. (2002)
69. *Dipteryx panamensis* (8.4-11.2 cm DBH)	**Ln (C)= c+ α ln (DBH)** c= - 2.0619, S.E.=0.6700, r^2=0.9544, Avg unsigned deviation (%)=4.8, t-value=0.0543 α=2.3088, S.E.=0.2914, t-value=0.0042 **Ln (C)= c+ α ln (DBH)** c= - 2.7450, S.E.=0.5720, r^2=0.9385, Avg unsigned deviation (%)=9.4, t-value=0.0004 α=2.6244, S.E.=0.2125, t-value=0.0000 c, α, β=Coefficients, DBH=Diameter at breast height (in cm), H=Height (in m), C=Total above ground carbon content (in kg)	Shepherd & Montagnini (2001)
70. Bamboo	**$Y=0.131\ x^{2.278}$** r^2=0.95, Y=Biomass (kg $tree^{-1}$), x=Stem diameter at 1.35m (cm) **$Y=1.45x^{0.96}$** r^2=0.98, Y=Tree height (m), x=Stem diameter at	Hairiah et al. (2001)

	1.35m (cm)	
71. Banana	**$Y=0.030\ x^{2.13}$** r^2=0.99, Y=Biomass (kg $tree^{-1}$), x=Stem diameter at 1.35m (cm) **$Y=0.707x^{0.6835}$** r^2=0.81, Y=Tree height (m), x=Stem diameter at 1.35m (cm)	Hairiah et al. (2001)
72. Pruned Coffee	**$Y=0.2811\ x^{2.06357}$** r^2=0.95, Y=Biomass (kg $tree^{-1}$), x=Stem diameter at 1.35m (cm) **$Y=1.79x^{0.0797}$** r^2=0.84, Y=Tree height (m), x=Stem diameter at 1.35m (cm)	Hairiah et al. (2001)
73. Palms	**Y=0.3999+7.907× height** r^2=0.75, Dbh and height range=1-33m	Brown et al. (2000)
74. Cecropia	**$Y = (-0.48367+1.13488\times (Sqr(dbh)) \times Log(dbh))^2$** r^2=0.62, Dbh and height Range=1-11m	Brown et al. (2000)
75. Lianas	**$Y=563.56\times(dbh)^{2.6277}$** r^2=0.89, Dbh and height range=0.3-2.5cm	Brown et al. (2000)
76. *Fraxinus uhdei*	**$0.0466D^{2.70184}$** r^2 =0.99, Mean squared error=0.011,DBH range=8-44(cm) Where, D = Tree DBH (in cm).	Ares & Fownes (2000)
77. Liana	**Log(leaf mass)=0.81 log(basal area) - 0.57** r^2=0.84, n=19, P<0.001 **Log(mass)=0.07+2.17log(dbh)** r^2=0.95, n=19, P<0.001 mass=Dry mass	Gerwing & Farias (2000)

78. All *Acacias*	**Dry weight = 0.0864 x (BA) $^{1.36}$** N=23, r^2=0.96, P<0.01 **Dry weight = 0.0067 (C1 + C2 + H)$^{3.05}$** N=23, r^2=0.96, P<0.01 Where, BA=Basal area (cm^2), C=Crown diameter (m), H=Height (m)	Gerwing & Farias (2000)
79. *Balanites aegyptica*	**Dry weight = 0.0111 x (BA)$^{1.64}$** N=5, r^2=0.97, P<0.01 **Dry weight = 0.0007 (C1 + C2 + H)$^{5.54}$** N=5, r^2=0.96, P<0.01 Where, BA=Basal area (cm^2), C=Crown diameter (m), H=Height (m)	Gerwing & Farias (2000)
80. *Cordia sinensis*	**Dry weight = 0.0436 x (BA) $^{1.24}$** N=25, r^2=0.92, P<0.01 **Dry weight = 0.0062 (C1 + C2 + H)$^{3.10}$** N=25, r^2=0.92, P<0.01 Where, BA=Basal area (cm^2), C=Crown diameter (m), H=Height (m)	Gerwing & Farias (2000)
81. *Prosopis chilensis*	**Dry weight = 0.0550 x (BA)$^{1.34}$** N=25, r^2=0.96, P<0.01 **Dry weight = 0.0018 (C1 + C2 + H)$^{3.46}$** N=25, r^2=0.95, P<0.01 Where, BA=Basal area (cm^2), C=Crown diameter (m), H=Height (m)	Gerwing & Farias (2000)
82. All species combined	**Dry weight = 0.0513 x (BA)$^{1.35}$** N=78, r^2=0.90, P<0.01 **Dry weight = 0.0073 (C1 + C2 + H)$^{2.98}$** N=78, r^2=0.94, P<0.01 Where, BA=Basal area (cm^2), C=Crown diameter (m), H=Height (m)	Gerwing & Farias (2000)

83. All species combined	**Fresh weight = 0.0799 x $(BA)^{1.35}$** N=78, r^2=0.91, P<0.01 **Fresh weight = 0.0109 $(C1 + C2 + H)^{2.98}$** N=78, r^2=0.94, P<0.01 Where, BA=Basal area (cm^2), C=Crown diameter (m), H=Height (m)	Gerwing & Farias (2000)
84. All species combined	Canopy volume **Dry weight = 0.2555 $(CA \times H)^{1.0}$** N=78, r^2=0.94, P<0.01 Canopy area **Dry weight = 0.3102 $(CA \times H)^{1.35}$** N=78, r^2= 0.90, P<0.01	Gerwing & Farias (2000)
85. Eucalypt plantations	**y = ba × 6.6** Where, y=Total above ground biomass (t dry weight m^{-2}), ba=The basal area over bark (m^2 ha^{-1})	Snowdon et al. (2000)
86. Savanna (480 to 870 mm) Tree > 4m height Shrub < 4m height	**DW(kg) = 0.0752 x sum BA $(cm^2)^{1.20}$** r^2=0.94 **DW(kg) = 0.0943 x sum BA$(cm^2)^{1.16}$** r^2=0.94 Where, DW=Dry weight, BA=Basal area	Shackleton (1997)
87. Temperate broadleaf forests	**Total AGB=0.5+25000$D^{2.5}$/$D^{2.5}$+ 246872** r^2=0.99, DBH range=1-85 (cm) Where, Total AGB=Total above ground biomass (in kg), D=Tree DBH (in cm)	Schroeder et al. (1997)
88. *Pennisetun pedicellaturm*	**log Y = 1.515 + 0.822 log X** r^2=0.777, P=0.000 Where, Y=Shoot biomass, X=Percentage of full	Singh et al. (1997)

	Sunlight	
89. *Pennisetun pedicellaturm*	**log Y = 0.712+0.838 log X** r^2= 0.826, P = 0.000. Where, Y=Root biomass, X=Percentage of full Sunlight **logY=0.834+0.969logX** r^2=0.918, P=0.000 Where, Y=Grass shoot weight, X=Grass root weight	Singh et al. (1997)
90. *Pennisetum pedicellatum*	$\boldsymbol{Y = aX^h}$ Where, Y=Shoot or root weights, X= Percentage of full sunlight (estimated with the help of digital light meter)	Singh et al. (1997)
91. *Pennisetum pedicellatum*	**log Y = 1.58+0.82 log X** r^2= 0.792, P= 0.000 Where, Y=Total plant biomass in (g/m^2), X=Percentage of full sunlight (estimated with the help of digital light meter)	Singh et al. (1997)
92. *Fraxinus americana*	**Total AGB=0.1634 D $^{2.3480}$** DBH range=4-32 (cm) Where, Total AGB=Total above ground biomass (in kg), D=Tree DBH (in cm)	Perala & Alban (1994)
93. Savanna (Precipitation: 280 to 350 mm) *A. zanzibarica* *A. reficiens* Other species	**FW (kg) = 0.153 x sum stem diameter (cm)$^{2.48}$** **FW (kg) = 0.158 x sum stem diameter (cm)$^{2.44}$** **FW (kg) = 0.160 x sum stem diameter (cm)$^{2.45}$**	Johansson & Kaarakka (1992)
94. Savanna (Precipitation:1250 mm)		Tietema (1992)

Acacia erubescens *Acacia karoo* *Acacia tortilis* *Acacia melifera* *Dichrostachys cinerea* *Ziziphus murcronata*	**FW (kg) = 0.0137 x canopy sum (m)$^{3.86}$** N=38, r^2= 0.91 **FW (kg) = 0.0079 x canopy sum (m)$^{3.19}$** N= 41, r^2= 0.91 **FW (kg) = 0.0096 x canopy sum (m)$^{3.30}$** N=50, r^2= 0.90 **FW (kg) = 0.0548 x canopy sum (m)$^{2.58}$** N=27, r^2= 0.90 **FW (kg) = 0.0029 x canopy sum (m)$^{3.74}$** N=33, r^2= 0.94 **FW (kg) = 0.0130 x canopy sum (m)$^{2.86}$** N=17, r^2= 0.96 FW = fresh weight	
95. Savanna (Precipitation:790 mm) Lesihwa (*T. camohoratus)*	**FW = (0.552 stem diameter - 0.25)^2** FW = Fresh weight	Young & Francombe (1991)
96. Savanna (Precipitation:1200 mm) Small diameter breast height < 5cm Large diameter breast height > 5cm	For Small diameter breast height < 5cm: **Leaf biomass = 0.15 stem basal diameter - 0.17** N=7, r^2=0.99 For Large diameter breast height > 5cm: **Wood biomass=1.60 stem basal diameter - 4.00** N=7, r^2=0.94 **Leaf biomass = 0.51 DBH – 2.11** N=14, r^2=0.98	Chidumayo (1990)

	Twig wood = 0.94 DBH – 3.34 N=20, r^2=0.98 **Cord wood = 22.40 DBH – 215** N=20, r^2=0.91 Where, DBH=Diameter breast height	
97. Savanna (Precipitation:150 to 800 mm) *Acacia reficiens* *Acacia tortilis* Diam. > 1.57 cm *Acacia tortilis* Diam. < 1.57 cm Combi basal diameter >1.57 cm	**DW(g) =** **0.46 × sum stem diameter (mm)$^{2.56}$** N=27, r^2=0.96 **DW (g) =** **0.10 × sum stem diameter (mm)$^{2.95}$** N=100, r^2=0.98 **DW (g) =** **5.49 × sum stem diameter (mm)$^{3.98}$** N=14, r^2=0.98 **DW (g) =** **0.2089 × sum stem diameter (mm)$^{2.66}$** N=127, r^2=0.98 Where, DW=Dry weight	Coughenour et al. (1990)
98. Dry tropical forests	**Total AGB=34.4703 - 8.0671 D + 0.6589 D^2** r^2=0.67, Mean Squared Error=0.022 Where, Total AGB=Total above ground of tree (in kg), D=Tree DBH (in cm)	Brown et al. (1989)
99. Moist tropical forests	**Total AGB=38.4908 - 11.7883 D + 1.1926 D^2** r^2=0.78, Mean Squared Error=0.062 Where, Total AGB=Total above ground of tree (in kg), D=Tree DBH (in cm)	Brown et al. (1989)

100. Wet tropical forests	**Total AGB=13.2579 - 4.8945 D + 0.6713 D^2** r^2=0.90, Mean Squared Error=0.022 Where, Total AGB=Total above ground of tree (in kg), D=Tree DBH (in cm)	Brown et al. (1989)
101. Black spruce trees (Diameter 1-3cm, at 15cm. height) Needle Branch Bole wood Bole bark Aboveground Stump and root Complete tree	**$y = b_0 + b_1 d$** b_0= - 0.1627, b_1=0.1583, r^2=0.86, $S^2y.x$=0.00143, n=25 b_0= - 0.1655, b_1=0.1530 , r^2=0.88, $S^2y.x$=0.00114 , n=25 b_0= - 0.1231, b_1=0.1194, r^2=0.93, $S^2y.x$=0.00037, n=25 b_0= - 0.0356, b_1= 0.0362, r^2=0.94, $S^2y.x$=0.0003, n=25 b_0= - 0.4869, b_1=0.4669, r^2=0.92, $S^2y.x$=0.00700, n=25 b_0= - 0.1231, b_1=0.1227, r^2=0.87, $S^2y.x$=0.00082, n=25 b_0= - 0.6100, b_1=0.5397, r^2=0.92, $S^2y.x$=0.01149, n=25 where y=Component oven-dry biomass (kg) d=Diameter outside bark at 15cm height (cm)	Czapowskyj et al. (1985)
102. *Attalea sp.palm* >1.78m height	**Above ground biomass={[(46.1×StemH)-82.1]+[0.375×[(46.1×StemH)-82.1]]}/10^3** r^2=0.99, N=7 Where, StemH= Stem height	Anderson (1983)
103. Savanna (Precipitation:650mm) *Prosopis*	**DW (kg) = 0.0667 × sum BA (cm^2)$^{1.28}$** N=63	Felker et al. (1982)

	Where, BA=Basal area, DW=Dry weight	
104. *Prosopis glandulosa*	**$Log_e y = log_e a + b\ log_e x$** **For Branch total Dry weight** y=Branch total Dry weight, x=Diameter, All: n=73, Range(cm)=0.81-7.48, a=74.888, b=2.519, r=0.944, SEE=0.43 Tree: n=45, Range(cm)=0.81-5.62, a=66.134, b=2.676, r=0.982, SEE=0.26 Shrub: n=27, Range(cm)=1.01-7.48, a=69.205, b=2.455, r=0.970, SEE=0.30 **For Leaf total Dry weight** y=Leaf total Dry weight, x=Diam, Tree: n=45, Range(cm)=0.81-5.62, a=15.265, b=2.301, r=0.967, SEE=0.31 Shrub: n=28, Range(cm)=1.01-7.48, a=13.371, b=2.234, r=0.920, SEE=0.44 **For Inflorescence Dry weight** y=Inflorescence Dry weight, x=Diam , All: n= 22, Range(cm)=0.81-3.81, a=3.641, b=1.713, r=0.814, SEE=0.62 Tree: n=16, Range(cm)=0.81-3.81, a=2.994, b=1.671, r=0.798, SEE=0.74 **For Pod total Dry weight** y=Pod total Dry weight, x=Diam All: n= 21, Range(cm)=1.38-5.62, a=12.43, b=2.283, r=0.739, SEE=0.830 Tree: n=15, Range(cm)=1.38-5.62, a=13.65, b=2.380, r=0.777, SEE=0.830 **For Juvenile twig Dry weight**	Sharifi et al. (1982)

	y=Juvenile twig Dry weight, x=Length, All: n=48, Range(cm)=12.5-51.5, a=0.004, b=1.740, r=0.899, SEE=0.337 Shrub: n=35, Range(cm)=10.4-40.4, a=0.011, b=1.534, r=0.914, SEE=0.24 **For Juvenile leaf Dry weight** y=Juvenile leaf Dry weight, x=Length, Tree: n=50, Range(cm)=8.0-40.5, a=0.018, b=1.166, r=0.741, SEE=0.425 Shrub: n=37, Range(cm)=8.0-40, a=0.182, b=0.060, r=0.844, SEE=0.303 **For Bare twig Dry weight** y=Juvenile leaf Dry weight, x=Length, Tree: n=75, Range (cm)=8-51.5, a=0.001, b=2.130, r=0.938, SEE=0.333 Shrub: n=35, Range (cm)=8-40, a=0.002, b=1.840, r=0.933, SEE=0.284	
105. Savanna	**FW (kg) = 0.1638 x sum BA (cm^2)$^{1.26}$** Where, FW=Fresh weight and BA=Basal area	Guy (1981)
106. *Fraxinus americana*	**Total AGB=0.1535 D $^{2.3213}$** r^2=0.99, DBH range=1-28 (cm) Where, Total AGB=Total above ground biomass (in kg), D=Tree DBH (in cm)	Ker (1980)
107. *Prosopis flexuosa*	**dry weight = 0.232995 × volume $^{1.035294}$**	Braun et al. (1979)
108. *Fraxinus americana*	**Total AGB=0.1063 D $^{2.4798}$** r^2 =0.99, DBH range=5-50 (cm) Where, Total AGB=Total above ground biomass(in kg), D=Tree DBH (in cm)	Brenneman et al. (1978)

References

1. Aboal Jesus Ramon, Arevalo Jose Ramon, Fernandez Angel, 2005. Allometric relationships of different tree species and stand above ground biomass in the Gomera laurel forest (Canary Islands). *Flora*, 200: pp 264–274.
2. Anderson A.B., 1983. The biology of Orbignya martiana (Palmae), a tropical dry forest dominant in Brazil. Dissertation, University of Florida, Gainesville. Florida, USA.
3. Ares Adrian and Fownes James H., 2000. Comparisons between generalized and specific tree biomass functions as applied to tropical ash (*Fraxinus uhdei*). *New Forests,* 20: pp 277–286.
4. Braun, R.H., Candia R.J., Leiva R., Paez M.N., Stassi C.R. and Wuilloud C.F., 1979. Productividad primaria aera neta del algarrobal de Nacunan (Mendoza). In: Deserta 5, Instituto Argentino de Investigaciones de las Zonas Aridas {IADIZA), Mendoza, Argentina, pp 7-43.
5. Brown S., Burnham M., Delaney M., Vacca R., Powell M. and Moreno A., 2000. Issues and challenges for forest-based carbon-offset projects: a case study of the Noel Kempff Climate Action Project in Bolivia, Mitigat. Adapt. Strategies Global Change, 5: pp 99-121.
6. Brown S., Gillespie A.J.R. and Lugo A.E., 1989. Biomass estimation methods for tropical forests with application to forest inventory data. *For. Sci*., 35: pp 881–902.
7. Chave J., Andalo C., Brown S., Cairns M. A., Chambers J. Q., Eamus D., Folster H., Fromard F., Higuchi N., Kira T., Lescure J. P., Nelson B. W., Ogawa H., Puig H., Riera B. and Yamakura T., 2005. Tree allometry and improved estimation of carbon stocks and balance in tropical forests. *Oecologia*, DOI 10.1007/s00442-005-0100.
8. Chidumayo E. N., 1990. Aboveground woody biomass structure and productivity in Zambezian woodland. *Forest Ecology and Management,* 36: pp 33-46.
9. Cordero Luis Diego Perez and Kanninen Markku, 2002, Wood specific gravity and aboveground biomass of *Bombacopsis quinata* plantations in Costa Rica. *Forest Ecology and Management,* 165(1-3): pp 1-9.
10. Coughenour M. B., Ellis J. E. and Popp R. G., 1990. Morphometric relationships and development patterns of *Acacia tortilis* and *Acacia reficiens* in Southern Turkana, Kenya. *Bulletin of the Torrey Botanical Club,* 117: pp 8-17.
11. Cummings D. L, Kauffman J. Boone, Perry David A. and Hughes R. Flint, 2002. Above ground biomass and structure of rainforests in the southwestern Brazilian Amazon. *Forest Ecology & Management*, 163: pp 293-307.
12. Czapowskyj M. M., Robison D. J., Briggs R. D. and White E. H., 1985. Component biomass equations for black spruce in Maine**.** Res. Pap. NE-564. Broomall, PA: U.S. Department of Agriculture, Forest Service, Northeastern Forest Experiment Station, 7p.
13. Elliott Katherine J., Boring Lindsay R. and Swank Wayne T., 2002. Aboveground biomass and nutrient accumulation 20 years after clear-cutting a southern Appalachian watershed. *Can. J. For. Res*., 32: pp 667-683.
14. Felker P, Clark P. R., Osborn J.F. and Cannell G.H., 1982. Biomass estimation in a young stand of mesquite (*Prosopis* spp), ironwood (*Olneya-tesota*), palo verde (*Cercidium-floridium*, and *Parkinsonia-aculeata*), and leucaena (*Leucaena-leucocephala)*. *Journal Of Range Management,* 35: pp 87-89.
15. Gerwing Jeffrey John and Farias Damiaäo Lopes, 2000. Integrating liana abundance and forest stature into an estimate of total aboveground biomass for an eastern Amazonian forest. *Journal of Tropical Ecology,* 16: pp 327-335.
16. Goel V. L. and Behl H. M., 2005. Growth and productivity assessment of Casuarina glauca Sieb. ex. Spreng on sodic soil sites. *Bioresource Technology*, 96: pp 1399–1404.
17. Guy P. R., 1981. The estimation of the above-ground biomass of the trees and shrubs in the Sengwa Wildlife Research Area, Zimbabwe. *South African Journal Of Wildlife Research,* 11: pp 135-142.

18. Hairiah K., Sitompul S. M., Van Noordwijk, M. et al., 2001. Methods for sampling carbon stocks above and below ground, ASB Lecture Note 4B, International Centre for Research in Agroforestry (ICRAF), Bogor.
19. Johansson S. G. and Kaarakka V. J., 1992. Regeneration of cleared *Acacia zanzibarica* bushland in Kenya. *Journal of Vegetation Science,* **3: pp** 401-406.
20. Kale Manish, Singh Sarnam, Roy P. S., Deosthali Vrishali and Ghole V. S., 2004. Biomass equations of dominant species of dry deciduous forest in Shivpuri district Madhya Pradesh. *Current science*, 87(5).
21. Ker M.F., 1984. Tree biomass equations for ten major species in Cumberland Country, Nova Scotia. Can For. Serv. Marit. For. Res. Cent. Inf. Rep. M-X-108.
22. Losi Christopher J., Siccama Thomas G., Condit Richard, Morales Juan E., 2003. Analysis of alternative methods for estimating carbon stock in young tropical plantations, *Forest Ecology and Management*, 184: pp 355–368.
23. Noordwijk Meine van, Rahayu Subekti, Hairiah Kurniatun, Wulan Y. C.,
24. Farida A. & Verbist Bruno, 2002. Carbon stock assessment for a forest-to-coffee conversion landscape in Sumber-Jaya (Lampung, Indonesia): from allometric equations to land use change analysis. *Science in China* (Series C), 45.
25. Padron Eva and Navarro Rafael M., 2004. Estimation of above-ground biomass in naturally occurring populations of *Prosopis pallida* (H. & B. ex. Willd.) H.B.K. in the north of Peru. *Journal of Arid Environments*, 56(2): pp 283-292.
26. Perala D. and Alban D.H., 1994. Allometric biomass estimates for aspen-dominated ecosystems in the upper Great Lakes. USDA Forest Serv., NC Forest Exp. Sta., St. Paul, MN. Res. Paper NC-314.
27. Putz F.E., 1983. Liana biomass and leaf area of a tierra firme forest in the Rio Negro Basin, Venezuela. *Biotropica*, 15: pp 185-189.
28. Sah J.P, Ross M.S, Kaptur S. and Snyder J.R., 2004. Estimating aboveground biomass of broadleaved woody plants in the under story of Florida Keys pine forests. *Forest Ecology and management,* 203(1-3): pp 319-329.
29. Salis Suzana M., Assis Marco A., Mattos Patricia P. and PiaoAntonio C.S., 2006. Estimating the aboveground biomass and wood volume of savannawoodlands in Brazil's Pantanal wetlands based on allometric correlations. *Forest Ecology and Management*, 228: pp 61–68.
30. Schroeder P., Brown S., Mo J., Birdsey R. and Cieszewski C., 1997. Biomass estimation for temperate broadleaf forests of the United States using inventory data. *For. Sci*., 43: pp 424–434.
31. Shackleton C. M., 1997. The Prediction of Woody Productivity in the Savanna Biome, South Africa. PhD thesis, Faculty of Science, University of Witwatersrand, Johannesburg, South Africa, pp 208.
32. Sharifi .M. Rasoul, Nilsen Erik T. and Rundel Philip W., 1982. Biomass and net primary production of *prosopis glandulosa* (fabaceae) in the sonoran desert of California. *Amer. J. Bot.*, 69(5): pp 760-767.
33. Sierra Carlos A., Valle Jorge I. del, Orrego Sergio A., Moreno Flavio H., Harmon Mark E., Zapata Mauricio, Colorado Gabriel J., Herrera Marı´a A., Lara Wilson, Restrep David E. o, Berrouet Lina M, Loaiza Lina M., Benjumea John F., 2007. Total carbon stocks in a tropical forest landscape of the Porce region, Colombia. *Forest Ecology and Management*, 243: pp 299-309.
34. Singh Arvind, Jha A.K. and Singh J.S., 1997. Influence of a developing tree canopy on the yield of *Pennisetum pedicellatum* sown on a mine spoil. *Journal of Vegetation Science*, 8: pp 537-540.
35. Snowdon P., Eamus D., Gibbons P., Khanna P. K., Keith H., Raison J., et al., 2000. Synthesis of Allometrics, Review of Root Biomass and Design of future woody Biomass Sampling Strategies. National Carbon Accounting System technical report no. 17. Australian Greenhouse Office.
36. Shepherd D., Montagnini F., 2001. Above ground carbon sequestration potential in mixed and pure tree plantations in the humid tropics. *J. Trop. For. Sci*., 13 (3): pp 450–459.

37. Thenkabail P. S., Stucky N., Griscom B. W., Ashton M. S., Diels J., Meer B. Van Der & Enclona E., 2004. Biomass estimations and carbon stock calculations in the oil palm plantations of African derived savannas using IKONOS data. Int. J. Remote Sensing, 25(23): pp 5447–5472.
38. Tiepolo Gilberto, Calmon Miguel, Feretti André Rocha, 2002. Measuring and Monitoring Carbon Stocks at the Guaraqueçaba Climate Action Project, Paraná, Brazil. Taiwan Forestry Research Institute. International Symposium on Forest Carbon Sequestration and Monitoring. Extension Serie No. 153: pp 98-115

TABLE VII: WESTERN GHATS

EQUATIONS	REFERENCE
1. Standing biomass (in Kg) =b+(aD^2H) Where, D=Diameter at breast height, H=Height of the tree, a and b=Constants	Ramachandra et al. (2004)
2. Tree fractions Boles (B): **log B = -1.39 + 2.28 log (dbh)** r^2=0.93, n=465 Branches (Br) **log Br = -1.24 + 1.98 log (dbh)** r^2=0.84, n=229 Leaves (Lo) **log Lv = 0.829 + 0.482 log (dbh)** r^2=0.17, n=229 Current year's twings (Tw) **log Tw = 1.18 - 0.108 log (dbh)** r^2=0.001, n=229 Total aboveground biomass *(T)* **log T = - 0.435 + 2.12 log (dbh)** r^2=0.92, n=9 Roots(≥5 cm girth) (R): **log R = - 2.30 + 1.63 log (dbh)** r^2=0.74, n=91	Rai & Proctor (1986)
3. $W_T = F \times H \times G \times D$ Where, W_T=Sum of the branch and bole biomass (g),	Cannell (1984)

F=Form factor, H=Tree height (cm), G=Basal area at breast height (cm^2), D=Specific gravity (gm^{-3})	
4. log y = a + b log x Where, y=Above ground biomass (kg), x=D^2H (D, cm × 10, H, m), a and b=Constants.	Rai (1984)
5. For over wood species **log y = - 0.6150 + 0.8315 log x** N=105, r=0.9138, F=1521.2	Rai (1984)
6. For Underwood species **log y = -0.4917 + 0.7935 log x** N=78, r=0.9175, F=404.5	Rai (1984)
7. For the whole forest **log y = -0.6206 + 0.8315 log x** N=183, r=0.9579, F=2014.6	Rai (1984)
8. y = a + b x Where, y=Above ground biomass in kg, x=D^2H (D, cm × 10, H, m× 10), a and b = constants.	Rai (1984)
9. For over wood species **y = 250.96 + 0.000036x** N=78, r=0.842, F=2.436	Rai (1984)
10. For Underwood species **y = 34.195 + 0.000047x** N=80, r=0.953, F=9.92	Rai (1984)
11. For the whole forest **y = 111.293 + 0.00004x** N=158, r=0.911, F=4.891	Rai (1984)
12. y = a + b x Where, y=Above ground biomass in kg, x=DBH (cm × 10), a and b=constant	Rai (1984)
13. For over wood species **y = -755.356 + 6.023x** N=78, r=0.874, F= 3.25	Rai (1984)
14. For Under wood species **y = - 322.13 + 3.661x**	Rai (1984)

N=80, r=0.935, F=6.92	
15. For the whole forest **y = - 635.412 + 5.578*x*** N=158, r=0.923,F= 5.789	Rai (1984)

References:

1. Cannell M. G. R., 1984. Woody biomass of forest stands, *Forest Ecology and Management,* 8: pp 299-3 12.
2. Ramachandra T. V., Kamakshi G. and Shruthi B. V., 2004. Bioresource status in Karnataka, *Renewable and Sustainable Energy Reviews*, 8(1): pp 1-47.
3. Rai, S. N., 1984. Above ground biomass in tropical rainforests of Western Ghats, *Indian For*., 110: pp 754–764.
4. Rai S. N., Proctor, 1986. Ecological Studies on Four Rainforests in Karnataka, India: I. Environment, Structure, Floristic and Biomass, *The Journal of Ecology*, 74(2): pp 439-454.

TABLE VIII: WESTERN GHATS (SPECIESWISE)

Species	**Biomass Equation**	**Reference**
1. *Calophyllum elatum*	**log y = a + b log x** N=20, a= - 0.9942, b=0.8866, r=0.9808, F=457.8 Where, y=Above ground biomass (kg), x=D^2H (D,cm × 10,H,m)	Rai (1984)
2. *Canarium strictum*	N=19, a= - 0.8233, b=0.8865, r=0.9646, F=227.3	Rai (1984)
3. *Carallia brachiata*	N=10, a= - 0.8398, b=0.8901, r=0.9664, F=116.7	Rai (1984)
4. *Dipterocarpus indicus*	N=10, a= - 0.8493, b=0.8897, r=0.8859, F=29.2	Rai (1984)
5. *Holigarna spp.*	N=16, a= - 0.7028, b=0.8355, r=0.9448, F=116.5	Rai (1984)
6. *Persea macrantha*	N=20, a= - 0.4252, b=0.8176, r=0.9235, F=104.3	Rai (1984)
7. *S. utilis*	N=10, a= - 1.2066, b=0.9872, r=0.9790, F=184.2	Rai (1984)
8. *Garcinia cambogia*	N=20, a= - 1.0883, b=0.9445, r=0.9581, F=404.5	Rai (1984)
9. *Garcinia indica*	N=20, a= - 0.3350, b=0.5624, r=0.7330, F=20.6	Rai (1984)
10. *L. anamallayanum*	N=20, a= - 0.6158, b=0.8189, r=0.9758, F=357.7	Rai (1984)

11. *Euphoria longana*	N=18, a= - 0.5181, b=0.8195, r=0.9915, F=925.7	Rai (1984)
12. *Calophyllum elatum*	**y = a + b x** N=19, a= - 572.09, b=4.59, r=0.961 Where, y=Above ground biomass in kg x=DBH in cm×10, a and b= constant	Rai (1984)
13. *Canarium strictum*	N=19, a= - 1045.18, b=7.30, r=0.954	Rai (1984)
14. *Dipterocarpus indicus*	N=10, a= - 899.76, b=6.49, r=0.822	Rai (1984)
15. *Persea macrantha*	N=20, a= - 1302.60, b=8.46, r=0.916	Rai (1984)
16. *S. utilis*	N=10, a= - 1070.5, b=7.19, r=0.962	Rai (1984)
17. *Garcinia cambogia*	N=20, a= - 288.79, b=3.18, r=0.955	Rai (1984)
18. *Garcinia indica*	N=20, a= - 352.08, b=3.70, r=0.957	Rai (1984)
19. *L. anamallayanum*	N=20, a= - 344.51, b=3.70, r=0.946	Rai (1984)
20. *Euphoria longana*	N=20, a= - 325.69, b=3.97, r=0.951	Rai (1984)

Reference:

Rai S. N., 1984. Above ground biomass in tropical rainforests of Western Ghats, *Indian For*., 110: pp 754–764.

Solar Potential Assessment in the Himalayan Landscape

Abstract

Estimation of solar energy reaching the earth's surface is essential for solar potential assessment, design of solar energy based applications, meteorology, climatology, oceanography, agriculture, forestry and for many other domains. Global insolation measured using data obtained from satellites provides higher spatial and temporal coverage of regions compared to ground based data from radiation stations or models based on other meteorological parameters. Solar potential of the Indian hill state of Himachal Pradesh has been assessed using NASA's Surface Meteorology and Solar Energy (SSE) data over 1°x1° global grid for 22 years. Monthly global insolation contour maps have been computed through interpolations and Geographical Information System (GIS). The results have been validated with ground data (Root Mean Square Error of 4.88%). Influences of seasons, meteorological parameters and topography on global insolation have also been analysed. It is observed that, during the period of March to October, the state receives global insolation above 4 kWh/m²/day throughout its eclectic topography with a peak of ~6.84 kWh/m²/day seen in the months of May and June encouraging viable solar devices. However high altitude regions such as of Kullu, Kinnaur and Lahul Spiti, have lesser global insolation below 4 kWh/m²/day with a minimum of 2.57 kWh/m²/day during winter months of November - February. Compared to this, low and medium altitude regions receive an average global insolation of ~ 4.5 kWh/m²/day during November - February and lesser than high altitude regions during December and January.

Keywords

Solar potential assessment, Himachal Pradesh, India, Global insolation, Spatial data, Geographic Information System (GIS), Geoinformatics, Renewable Energy

1. Introduction

Energy plays a pivotal role in the development of a region. However, energy shortages in recent times, the imminent energy crisis and threat of climate change have focused the attention for a viable sustainable alternative through renewable sources of energy. Sun is the vital source of energy manifested in different forms in the solar system. Solar energy intercepted by the earth at the rate of 1.7 X 10^{14} kW is many times greater than its present rate of overall energy consumption. Approximately 99% of the solar energy is contained in the wavelength band of 0.15 - 4.0 μm consisting of the ultraviolet, visible and near infrared regions of the solar spectrum. The geometry of the earth-sun movements causes large spatial, diurnal and seasonal variations in the amount of solar radiation received on earth. The 23.5° tilt of the earth's rotational axis with respect to the plane of orbital revolution causes larger annual variations near the poles and smaller variations near the equator [1]. Due to the variations in the sun-earth distance, intercepted solar radiation fluctuates by ±3.3 % around its mean value. The variations due to sunspots, prominences and solar flares, can be neglected as they constitute small fraction compared to the total energy emitted by the sun. The average solar radiation falling on the earth's atmosphere called the solar constant is estimated to be 1.36 kW/m^2. The presence

of clouds, suspended dust, gas molecules and aerosols in the atmosphere, through absorption and scattering, attenuates the incident solar energy radiation (also called insolation). A fraction of 0.3 of the total incident solar energy called the albedo of the earth-atmosphere system is reflected back to the space [2]. The remaining fraction of solar energy in the form of direct and diffuse insolation which comprises the global insolation is utilized in many processes like heating and illuminating the earth, photosynthesis, growth of vegetation, evapotranspiration, snow ablation as well as solar energy based applications. Solar radiation data is essential for solar energy potential assessment for designing solar energy based applications, meteorology, climatology, oceanography, agriculture, forestry and many other domains. Solar energy applications like photovoltaic based off-grid and utility grid power generation, solar water heaters, thermal concentrators, solar cookers, desalination plants, passive building heating etc. demand reliable information on surface global insolation measurements at different regions of interest. This could be estimated from insolation data procured from on-ground pyranometric networks, models based on meteorological parameters or those based on satellite data.

1.1. Solar potential assessment

Insolation data from pyranometric networks: Conventionally, solar potential of a region has been assessed using the insolation data obtained from ground based radiation stations. There are more than 500 radiation stations in 56 countries which provide global, diffuse and direct insolation data on hourly, daily or monthly basis to the World Meteorological Organisation apart from other archived data from radiation stations around the world [3]. An efficient and reliable pyranometric network, incurs heavy investment in terms of capital, maintenance and manpower. Developing countries like India with a vast land area of 3287263 km^2, find it hard to have a sufficient spatial coverage for insolation measurements. The Indian radiation network under the Indian Meteorological Department (IMD) has merely 43 radiation stations spread across the country. Data from ground based solar radiation monitoring stations are liable to errors due to calibration drift, manual data collection, soiling of sensors and non-standardization of measuring instruments [4]. The World Climate Research Program in 1989 had estimated an end to end uncertainty of 6% -12% in measurements from common solar radiation stations [5]. Most of the data available from radiation stations are at non- uniform and interrupted periods as shown by Alberto Ortega et al [6] for Chile which was reported to be 3 months to 21 years. In the case of India, its radiation network expanded from 4 stations in 1957 to 43 as of today, measuring one or more parameters like Global, Direct or Diffuse radiation at different locations. These datasets provide temporal information (in minutes) which are essentially important for solar energy applications and design [7]. Annual insolation varies with change in angle of incidence of the solar radiation. It is reported that a minimum of 7-10 years of solar radiation data is required to get a long term mean within 5 % [8].

Insolation data from meteorological parameters: Insufficient insolation data consequent to sparse radiation networks, lead to different parametric (Iqbal and ASHRAE Model) and decomposition models (Angstrom, Hay, Liu and Jordan, Orgill and Hollands Model). These models employ theoretical or empirical methods for interpolation or extrapolation of measured meteorological values to derive insolation data [1].These models use parameters like sunshine duration [9, 10], temperature [11],

rainfall [12], cloud cover [13], extraterrestrial radiation [14], etc. for estimating solar radiation over a given location. Artificial Neural Networks (ANN) have also been utilized for deriving insolation data based on climatological and geographical parameters [15]. These methods show low Root Mean Square Errors (RMSE) of 5% on validation with in-situ measurements and still are inadequate for large spatial and temporal scale studies.

Insolation data from satellites: Remote sensing data from polar satellites at ~850 km with higher spatial resolution and geostationary satellites at ~36000 km with higher temporal resolution are being utilized for different studies [16]. The LANDSAT – MSS/TM, SPOT – VHR, NIMBUS – CZCS, NOAA – AVHRR, INSAT- VISSR, GOES –VISSR instruments [17] provide information for estimation of insolation based on different subjective, empirical and theoretical methods.

Subjective methods involve subjective interpretation of cloud cover from the satellite images and its statistical relationship with atmospheric transmittance. Empirical methods depend on functional relations based on satellite derived data and available solar radiation data which are customized for any place and time. Empirical methods are classified into two models: statistical and physical. Statistical models use independent variables including brightness levels, solar zenith angle, precipitable water and cloud amount inferred from satellite data on the basis of their ability to explain the variability in solar radiation. They depend on ground networks for parameterization and do not require satellite sensor calibration. Physical models are originated from the radiation balance of the earth atmospheric system. They deduce surface insolation by physical simulation of radiation transfer through the atmosphere and are independent of the ground data while demanding sensor calibration. Another method which simulates radiant energy exchanges taking place within the earth atmospheric system, hypothetically not demanding empirical calibration of model parameters is called theoretical method. The broadband and spectral models are attached to this method [18].

The solar potential of Kampuchea was estimated based on a statistical model [19] with the visible and infrared images obtained from Japanese Stationary Meteorological Satellite GMS-3 along with ground based regression parameters and concluded that seasonal average of daily insolation depended more on the topography of the region than on seasonal variations. The Root Mean Square Error (RMSE) of the monthly average insolation were shown to vary from 5.7% to 11.6% as the cloudiness of the region increased. The solar potential of Pakistan was estimated by employing a physical model [17] based on the images collected from the Geostationary Operational Environmental Satellite (GOES) INSAT which scanned the region four times per day. The results indicate that the desert and plateau regions received favourable global insolation while the monsoon had its influence on reduced insolation in the eastern and southeastern Pakistan, for the months of August, October and May.

Daily global insolation in Brazil was assessed for cloudy, partially cloudy and clear sky conditions based on a statistical model on images from GOES- VISSR instrument and verified it to obtain standard

errors of 27%, 15% and 11% respectively [20]. Attempt was made to obtain a reliable solar map for Chile [6] based on a physical model applied to the GOES-8 and GOES-12 images validated with the ground data. They reported regional and temporal variations in global insolation due to the diverse topography and climate of Chile. Stretched Visible Infrared Spin Scan Radiometer (S-VISSR) images of Geostationary Meteorological Satellite (GMS) of 15 minute interval high spatial resolution (0.01^0X0.01^0) for a period of 3 months in 1996 [21] were analysed to develop a bispectral threshold technique with respect to earth-atmosphere albedo and infrared temperature and performed a parameter tuning of the model at 67 weather stations. It was shown that more the number of higher resolution images used, lower is the Root Mean Square Error (RMSE) of hourly insolation compared to ground data and was more evident for regions with rapid variations in insolation due to topography. The RMSE was calculated to be 25 % for daily and 12% for hourly insolation data obtained. Similar endeavor generated hourly and monthly basis global as well as direct insolation maps using SOLARMET physical model applied over 7 years high resolution Meteosat satellite images [22]. They also employed a smoothing procedure over each 3X3 km pixels so as to obtain regular insolation contour lines over the maps produced. It was found that the modeled insolation data showed a yearly average relative difference of 7.6% when compared to the data from 51 ground stations. A physical model based on visible range satellite images considering the climatological aspects of hourly global insolation useful for designing solar energy systems was designed [23]. The importance of aerosols in solar radiation depletion has been studied and a method to address it in the model is discussed. The model is specifically applicable for tropical regions like South East Asia and Thailand is taken as the study area. In the study, 8 years 3X3 km resolution GMS 5 visible images are used to obtain monthly average hourly insolation datasets with RMSE ~10% when validated with 25 pyranometric stations. Evaluation of the direct beam insolation in Abudhabi for a year is about $400W/m^2$ based on the monitored ground data [24]. This data was validated with the 22 year average data from NASA's Surface Meteorology and Solar Energy (SSE) datasets, which proved that the region was a high potential area for solar energy based applications. Satellite-data based models do not show much difference in performance as the primary source of ambiguity for all these models is the influence of cloud pattern. It has been proved that interpolations and extrapolations of available ground data for predicting solar radiation over distances beyond 34 km show higher RMSE compared to satellite-data based measurements [25]. RMSE for different models have been found to be within 20% for daily values and 10% for hourly values [26]. Today satellite data for about 20 years are available, which reduces the possibility of error due to annual variations in insolation. Nevertheless, ground data is indispensable at this juncture for validation and model improvement of satellite based data.

2. Objective

The prime objective of this study is to assess the solar energy potential of the Indian federal state of Himachal Pradesh using higher spatial and temporal scale satellite derived monthly average global insolation datasets.

3. Study area

3.1. Geography and climate

Himachal Pradesh (Figure 1) is located between 30.38° to 33.21° North latitudes and 75.77° to 79.07° East longitudes, in the western Himalayas, covering a geographical area of 55673 km^2. The State is divided into 12 districts surrounded by Jammu and Kashmir in the North, Tibet in the Northeast, Uttarakhand in East/Southeast, Haryana in South and Punjab in Southwest/West, with an abundance of snow fed perennial rivers and rivulets. Out of the total area, 37,033 km^2 is managed by the forest department and 16,376 km^2 is under permanent snow cover [27].

Figure 1: Study area - Himachal Pradesh, India

The agro-climatic zones of Himachal Pradesh are divided based on its elevation above mean sea level. Parts of Una, Bilaspur, Hamirpur, Kangra, Solan and Sirmaur districts in the Western and Southern regions lie below 1000m with a tropical climate and respective vegetation. Some portions of Solan, Sirmaur, Mandi, Chamba and Shimla districts at altitude between 1000-3500 m have climate conditions varying from sub-tropical to wet- temperate with elevation. Lahaul Spiti, Kullu and Kinnaur districts ranging between 3500-6700 m are part of the dry temperate, sub-alpine and alpine zones with very sparse rainfall of less than 80cm annually. The Digital Elevation Model (DEM) of the state provides a clearer understanding of its topography (Figure 2).

Figure 2: Digital Elevation Model of Himachal Pradesh

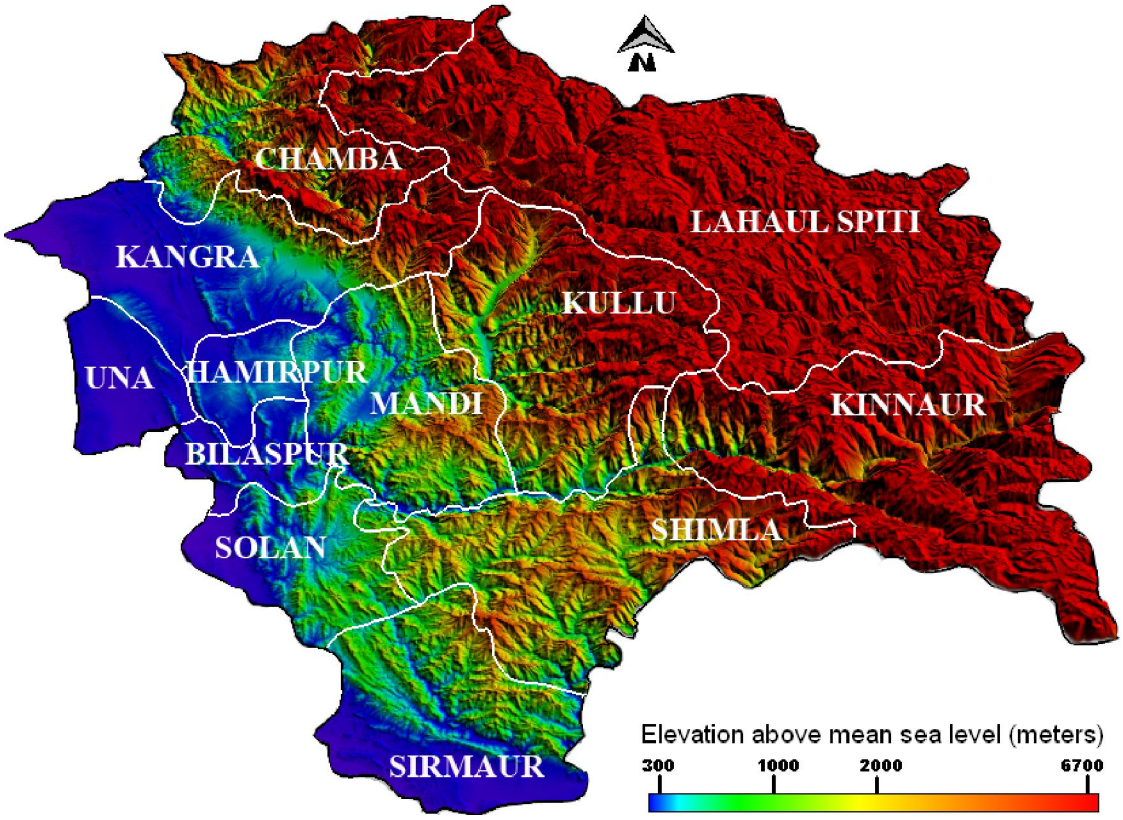

The spatial and monthly variations of average rainfall (Figure 3) and temperature (Figure 4) over Himachal Pradesh have been observed from a 100 years meteorological dataset. The monthly average temperature decreases with altitude and shows a regional difference of approximately 15° C from higher elevations (above 3500 m) to lower (below 1000 m). Winter season commences in the month of October, reaches its peak in January and continues till February. The months of March, April, May and June are comparatively warmer. Figure 3 clearly shows the onset of Southwest monsoon in June with average rainfall uniformly reaching higher values in all the regions. The highest annual average rainfall is recorded in the district of Kinnaur and the least in Una. The rainfall slows down towards the end of September marking the end of the southwest monsoon season.

Figure 3: Monthly average rainfall variation in Himachal Pradesh

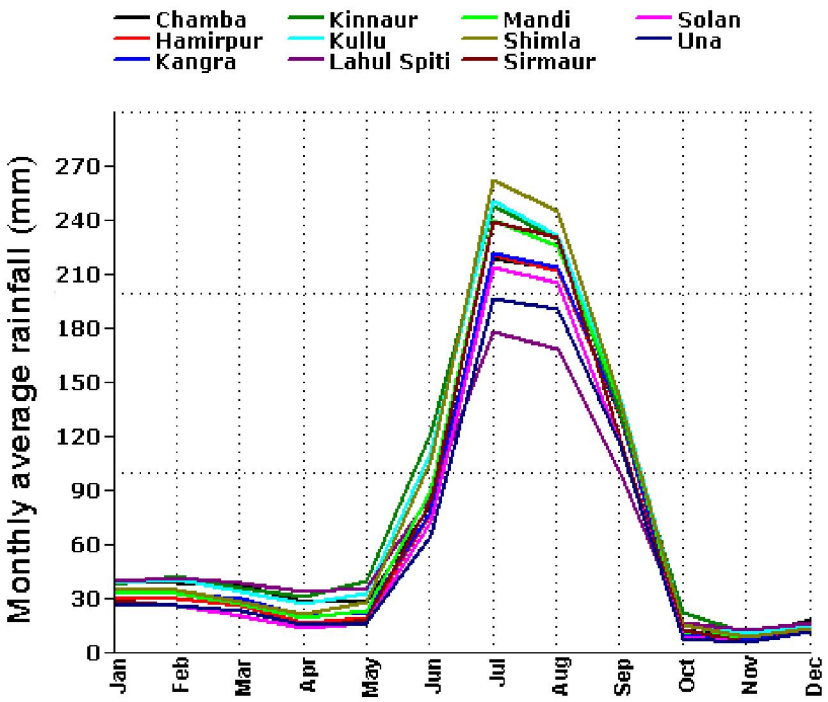

Figure 4: Monthly average temperature variation in Himachal Pradesh

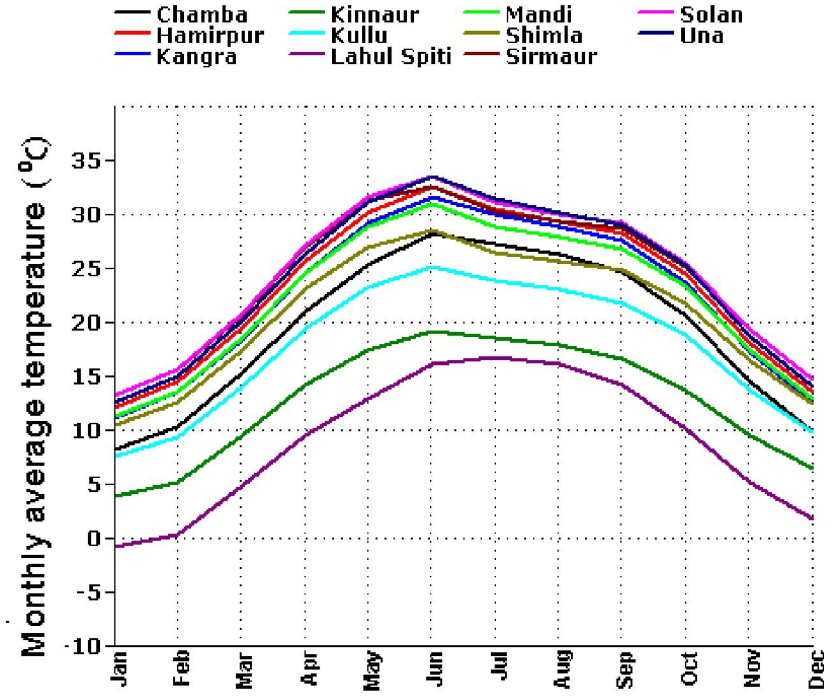

3.2. Availability of ground radiation data

Himachal Pradesh has an IMD's ordinary radiation station which is situated in Manali at 32.27° North latitude and 77.17° East longitude measuring gobal insolation. The data from the station do not suffice for a higher temporal and spatial scale study of solar energy availability throughout the state. Hence 22 year average satellite data with 1° X 1° resolution have been used apart from validating with ground based estimations.

4. Data and methodology

4.1. Data source

Surface Meteorology and Solar Energy (SSE) datasets provided by the National Aeronautics and Space Administration (NASA) Langley Research Center give solar radiation and meteorological data collected by a variety of earth-observing satellites from different countries. These datasets are global and contiguous in time and are accessible (http://gewex-srb.larc.nasa.gov) in user friendly formats. The solar radiation parameters were validated with the Baseline Surface Radiation Network (BSRN) while the meteorological parameters were validated with the National Climate Data Center (NCDC). SSE data was validated with BSRN data (RMSE 10.28% for global horizontal insolation). SSE Release 6.0 datasets of 2008 were used for this work. The data is of spatial resolution of 1°x1° on a global grid and temporal coverage of solar radiation parameters for 22 years from July 1st, 1983 to June 30th, 2005 [5].

4.2. Model

The SSE datasets are derived from a physical model based on the radiative transfer theory employing a modeled atmosphere along with parameterization of its absorption and scattering properties. Primary inputs to the model include visible and infrared radiation, inferred cloud and surface properties, temperature, precipitable water, column ozone amounts and atmospheric state variables such as temperature and pressure [28]. The parameters have been measured using instruments like CERES (Clouds and the Earth's Radiant Energy System), MODIS (Moderate-resolution Imaging Spectro Radiometer), TOMS (Total Ozone Mapping Spectrometer) etc mounted on GMS, NIMBUS, METEOR, GOES, METEOSAT, NOAA and many other satellites. Insolation at a given location on the earth's surface is inferred based on the shortwave (0.2 to 4um) and longwave (4 to 100um) solar radiation reflected to the satellite sensors from the Top of Atmosphere (TOA). A calculative TOA solar radiation is iteratively compared to the values measured by the satellite sensors. Iterations are carried on parameters like aerosol distribution until the error is within a marginal value. Global insolation on the

surface for each such iteration is also computed. This forms the dataset for global insolation incident on a horizontal surface for given durations [5].

Shortwave and longwave solar radiation datasets were derived (discussed in the next section) based on primary algorithms by Pinker and Lazlo (1992) and Fu et al (1997) respectively. The quality check algorithms called the Langley Parameterized Shortwave Algorithm (LPSA) and Downward Longwave Algorithm by Gupta et al (2001 and 1992 respectively) validates the primary algorithms [29]. All the released datasets in SSE have undergone validation based on these four algorithms. Here we have discussed the quality check algorithms which forms the foundation for shortwave and longwave datasets.

Shortwave algorithm: The LPSA by Gupta et al [30] gives the downward shortwave flux as

$$F_{SD} = F_{TOA} T_A T_C \quad \text{…….. (1)}$$

where F_{TOA} is the corresponding shortwave insolation at the TOA, T_A is the transmittance of the clear atmosphere, and T_C is the transmittance of clouds in which all parameters are computed on a daily average basis.

Insolation at TOA is given by,

$$F_{TOA} = S(d_m / d)^2 \cos Z \quad \text{..... (2)}$$

where S is the solar constant, d is the instantaneous Sun-Earth distance, d_m is the mean Sun-Earth distance and *Z* is the solar zenith angle.

Clear-sky transmittance is given by,

$$T_A = (1+B)e^{-\tau z} \quad \text{……..(3)}$$

where the term B accounts for the reflected solar radiation from the surface that is backscattered by the atmosphere (calculated with surface albedo as a parameter) and τz accounts for all absorption and scattering properties of gases and aerosols in the clear sky.

Cloud transmittance T_c is given by,

$$T_c = 0.05 + 0.95 (R_{ave} - R_{meas})/(R_{ave} - R_{clr}) \quad \text{…….(4)}$$

where R_{ave}, R_{clr} and R_{meas} represent daily average values of overcast, clear and measured reflectance respectively, corresponding to an overhead sun. Even for the thickest clouds T_c is not reduced to zero.

Longwave algorithm: Based on the quality check algorithm by Gupta et al [31] the surface downward long wave flux is given by

$$F_{LD} = C_1 + C_2 A_c \quad \text{.....(5)}$$

where C_1 is the clear sky flux, C_2 is the cloudy sky flux (also called cloud forcing factor) and A_c is the fractional cloud cover. C_1 and C_2 are parameterized based on radiative transfer calculations on a range of meteorological inputs. While C_1 is calculated over total precipitable water and effective emitting temperature of the atmosphere, C_2 is a function of total water vapour content and temperature at the cloud base for the layer considered.

4.3. Data Procurement

The global insolation data for horizontal surfaces are available as daily, monthly and annual averages obtained from daily 3 hourly datasets for UTC (Coordinated Universal Time) 0, 3, 6, 9, 12, 15, 18, 21 hrs on any 1° X 1° global grid from the SSE web portal. Within a 1° X 1° grid, any points which do not lie on its Northern or Eastern boundaries share a common insolation value corresponding to the midpoint of the grid. The study area of Himachal Pradesh lies between 30.38° to 33.21° North latitudes and 75.77° to 79.07° East longitudes. Out of 13 optimal grids (regions) from 29.5° to 33.5° North latitudes and 75.5° to 79.5° East longitudes (Table 1) , 10 grids provide a complete coverage of the land area of the state while the other 3 are used to support an optimal interpolation through Geographic Information System (GIS). Out of the 13 selected grids, 6 grids cover Chamba, Lahaul-Spiti, Krishnaganj/Kinnaur, Hamirpur, Kullu and Sirmaur districts of Himachal Pradesh, 5 grids cover the districts of Kargil, Kathua (Jammu & Kashmir), Fatehgarh Sahib (Punjab), Muzaffarnagar (Uttarpradesh), Tehri Garhwal (Uttarakand) and 2 grids cover the Tibetan region (Figure 5).

Figure 5: Selected regions (star marked) for obtaining monthly average insolation maps in GIS

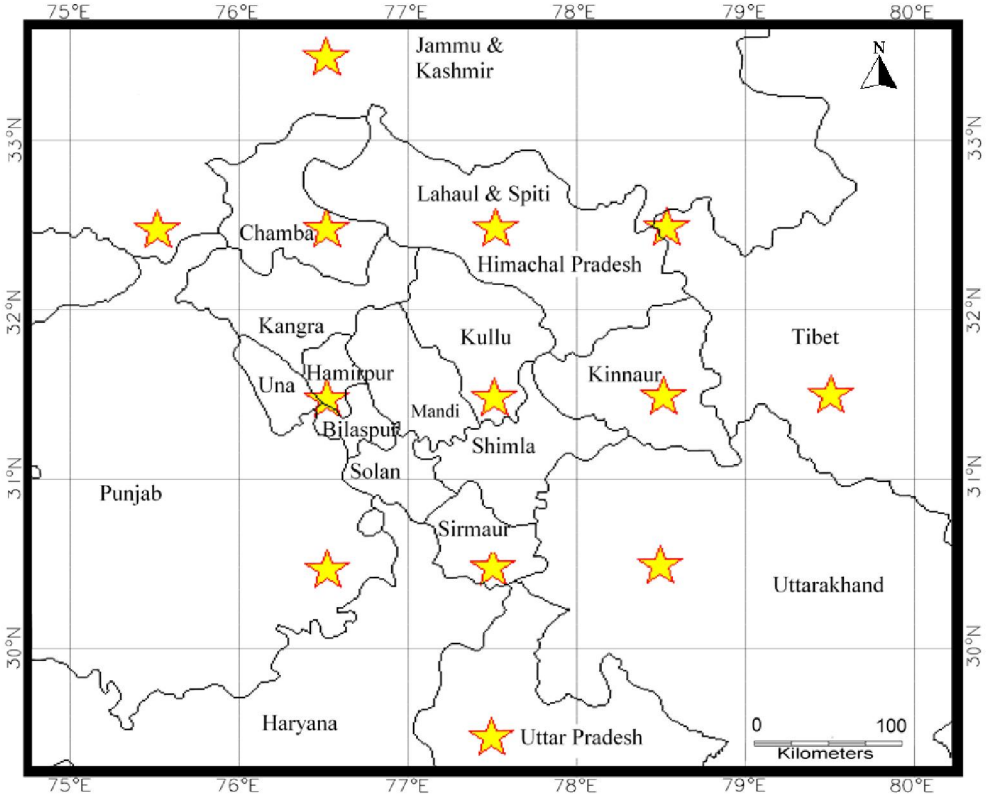

5. Results and discussion

The average global insolation datasets of 22 years (Table 1) were analysed spatially using GIS to understand monthly global insolation variations. Season wise analysis show that Himachal Pradesh receives an average insolation of 5.99 kWh/m²/day in the warm summer months of March, April and May; 5.89 kWh/m²/day in the wet monsoon months of June, July, August and September; 3.94 kWh/m²/day in the colder winter months of end October, November, December, January and February. It is observed that the period from March to October which covers the summer and monsoon seasons, over the entire physiographic zones of Himachal Pradesh receives insolation above 4 kWh/m²/day. This indicates favourable solar potential for commercial as well as domestic energy applications. The insolation throughout Himachal Pradesh drops down (<kWh/m²/day) with the onset of winter by the end of October, and a low insolation period prevails till the end of February. This potential is suitable for domestic appliances like solar cookers, solar water heater, etc.

Table 1 : Monthly average insolation (kWh/m^2/day) data collected for the study

Longitude	Latitude	Jan	Feb	Mar	Apr	May	Jun	Jul	Aug	Sep	Oct	Nov	Dec
77.5^{0}E	**29.5^{0}N**	3.68	4.56	5.80	6.84	7.31	6.71	5.57	4.93	5.25	5.05	4.26	3.54
76.5^{0}E	**30.5^{0}N**	3.57	4.61	5.71	6.81	7.42	7.12	5.89	5.46	5.62	5.29	4.32	3.45
77.5^{0}E	**30.5^{0}N**	3.66	4.55	5.75	6.92	7.53	6.93	5.65	5.08	5.43	5.40	4.44	3.57
78.5^{0}E	**30.5^{0}N**	3.75	4.50	5.64	6.76	7.42	6.73	5.36	4.83	5.25	5.42	4.49	3.69
76.5^{0}E	**31.5^{0}N**	3.41	4.31	5.45	6.68	7.43	7.17	5.68	5.29	5.55	5.30	4.23	3.36
77.5^{0}E	**31.5^{0}N**	3.58	4.26	5.38	6.49	7.21	6.87	5.59	5.15	5.41	5.41	4.42	3.52
78.5^{0}E	**31.5^{0}N**	2.85	3.37	4.28	5.09	6.03	6.10	5.63	5.33	5.15	4.89	3.88	2.97
79.5^{0}E	**31.5^{0}N**	3.10	3.62	4.41	5.26	6.57	7.02	6.64	6.09	5.80	5.15	4.04	3.11
75.5^{0}E	**32.5^{0}N**	3.25	4.15	5.22	6.55	7.32	7.33	5.86	5.48	5.75	5.29	4.13	3.18
76.5^{0}E	**32.5^{0}N**	3.23	3.84	4.98	6.02	6.85	6.87	5.66	5.22	5.40	5.16	4.11	3.21
77.5^{0}E	**32.5^{0}N**	2.67	3.29	4.23	5.05	5.80	6.33	6.01	5.53	5.19	4.67	3.55	2.66
78.5^{0}E	**32.5^{0}N**	3.17	3.86	4.66	5.44	6.42	7.02	6.67	6.20	5.78	5.11	3.86	3.01
76.5^{0}E	**33.5^{0}N**	2.59	3.20	4.04	4.88	5.83	6.49	6.10	5.76	5.35	4.58	3.41	2.57

Cloud cover increases with increasing elevation as a consequence of the cloud-topography interactions and orographically-induced convection [32], evident from the monthly average cloud cover data procured from a 100 year meteorological dataset (Figure 6). Lahul Spiti district in the high altitude alpine zone has the highest average cloud cover and solan district in the low altitude tropical zone has the least (Table 2). This also highlights the fluctuation in cloud amount over the advection facing and opposite sides of the mountains [32]. The relief elevation of the region and the resultant cloud cover influences the regional variation in insolation to a bigger extent even while considering the seasonal influences. These variations in insolation are apparent in the box plots given in figures 7, 8 and 9. The insolation in Himachal Pradesh is observed to increase from high altitude cold and dry alpine zone to the low altitude warmer tropical regions (below 1000 m). This regional variation in the magnitude of insolation is seen for a major part of the year from November to June while the trend reverses during July to October, with the high altitude zone receiving comparatively higher insolation. This could be attributed to the Southwest monsoon and the increase in cloud cover over the low as well as middle altitude regions (below 3500m) and the northeast dry monsoon winds from Central Asia setting in October.

Table 2: Regional variations, monthly average and standard deviations of global insolation

Month	Variation of monthly average insolation (kWh/m²/day)	Monthly average insolation (kWh/m²/day)	Standard deviation
January	2.59 – 3.75	3.27	±0.39
February	3.20 – 4.62	4.01	±0.51
March	4.04 – 5.80	5.04	±0.64
April	4.88 – 6.92	6.06	±0.80

May	5.80 – 7.53	6.86	±0.65
June	6.10 – 7.33	6.82	±0.35
July	5.36 – 6.77	5.87	±0.40
August	4.83 – 6.20	5.41	±0.41
September	5.15 – 5.80	5.46	±0.23
October	4.58 – 5.42	5.13	±0.27
November	3.41 – 4.49	4.09	±0.34
December	2.57 – 3.69	3.22	±0.35

Figure 6: District wise monthly average cloud cover (%)

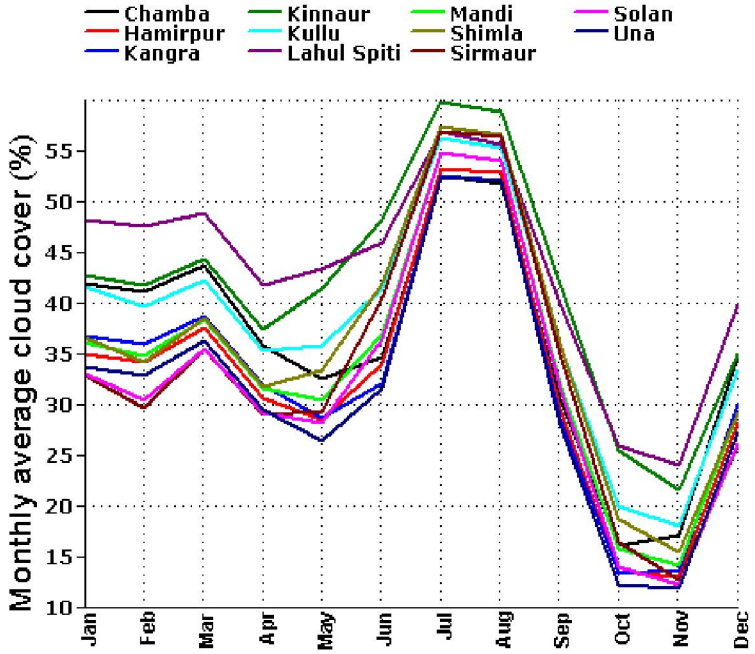

It has already been noted that March to October is a favourable period when the state receives good incident solar energy. In November, while low and middle altitude districts of Una, Bilaspur, Hamirpur, Kangra, Solan, Sirmaur, Mandi, Chamba and Shimla (below 3500m) enjoy insolation above 4 kWh/m²/day, the high altitude districts of Kullu, Lahaul Spiti and Kinnaur receive insolation below that. December and January witness the least insolation values in Himachal Pradesh with a maximum of ~3.75 kWh/m²/day even in the potential low altitude districts of the hill state. While the low and middle altitude districts pick up with increasing magnitude of insolation towards the end of January, the higher regions continue receiving lower insolation till the end of February. The low as well as middle altitude districts

receive the highest average insolation above 7 kWh/m²/day in the month of May. In the case of high altitude districts, the highest insolation is observed in the month of June with an average of ~6.60 kWh/m²/day. Solar potential contours were developed based on the spatial distribution to explore the regional variations, and are illustrated in Figures 10 and 11 respectively. The global insolation spatial data indicate the monthly variations in insolation over the diverse topography of Western Himalayas. These variations could be attributed to the influence of the season, elevation and orography.

Table 3: Solar radiation data through ground based pyranometer [2]

Months	**Jan**	**Feb**	**Mar**	**Apr**	**May**	**Jun**	**Jul**	**Aug**	**Sep**	**Oct**	**Nov**	**Dec**	**Annual**
Average insolation (kWh/m²/day)	3.55	4.19	5.32	6.33	7.10	6.5	5.48	5.81	5.33	5.20	4.00	3.23	5.17

Figure 7: Variation of monthly average insolation in high altitude (above 3500 m) regions

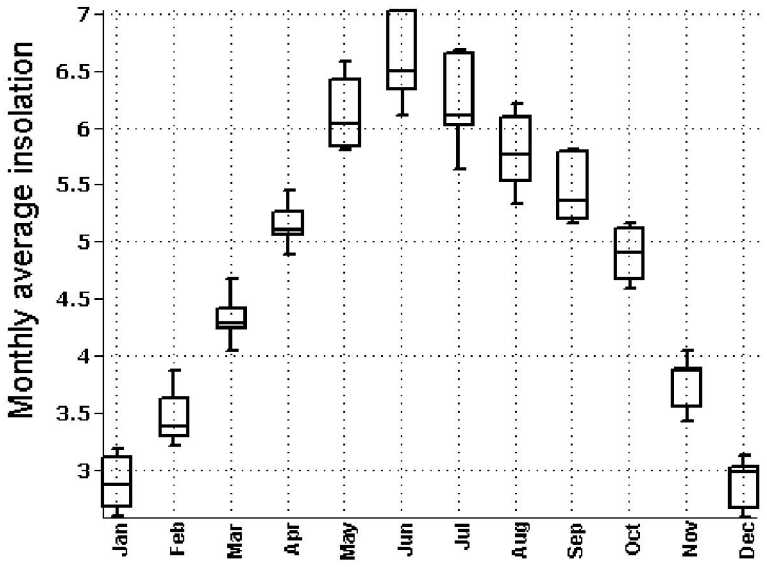

Figure 8: Variation of monthly average insolation in middle altitude (1000-3500m) regions

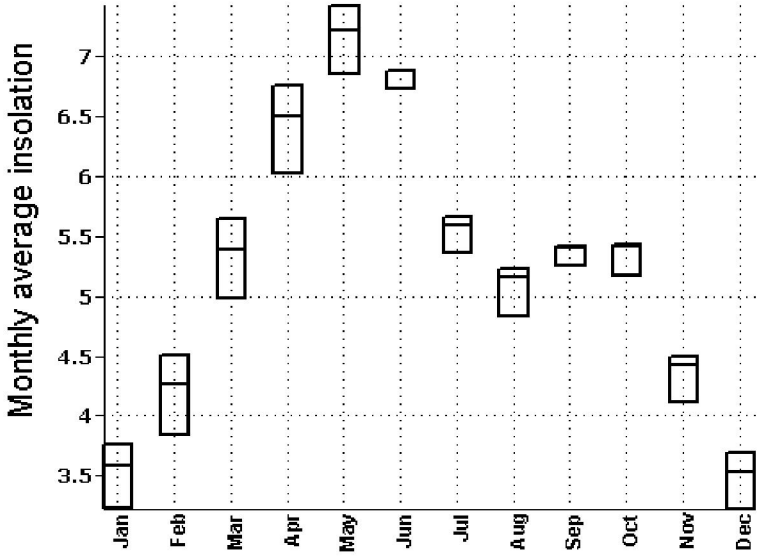

Figure 9: Variation of monthly average insolation in low altitude (below 1000m) regions

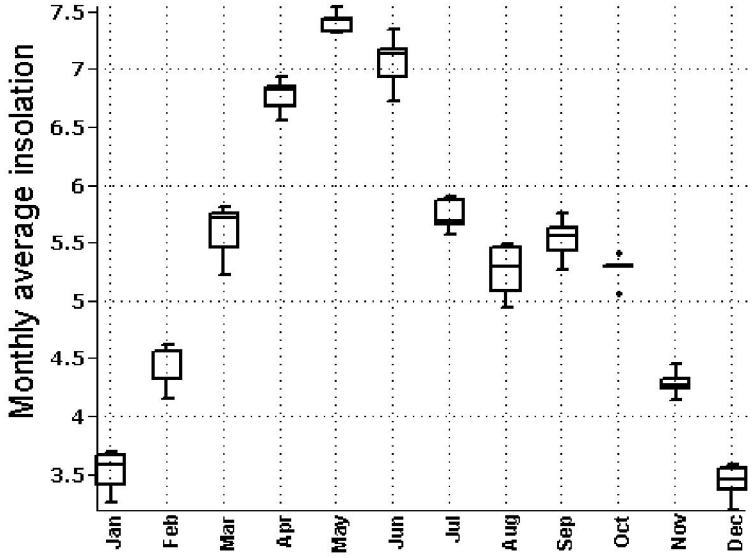

5.1. Validation with ground data

Spatial variation of Global insolation with the regional variation contours for the months of January – June is given in Figure 10, while Figure 11 presents the variation during July-December. These were validated with the monthly Global insolation data based on pyranometric data from ground radiation stations [2], given in table 3 (RMSE of 4.88%).

Figure 10: Spatial variation of Global insolation with the regional variation contours for the months of January - June

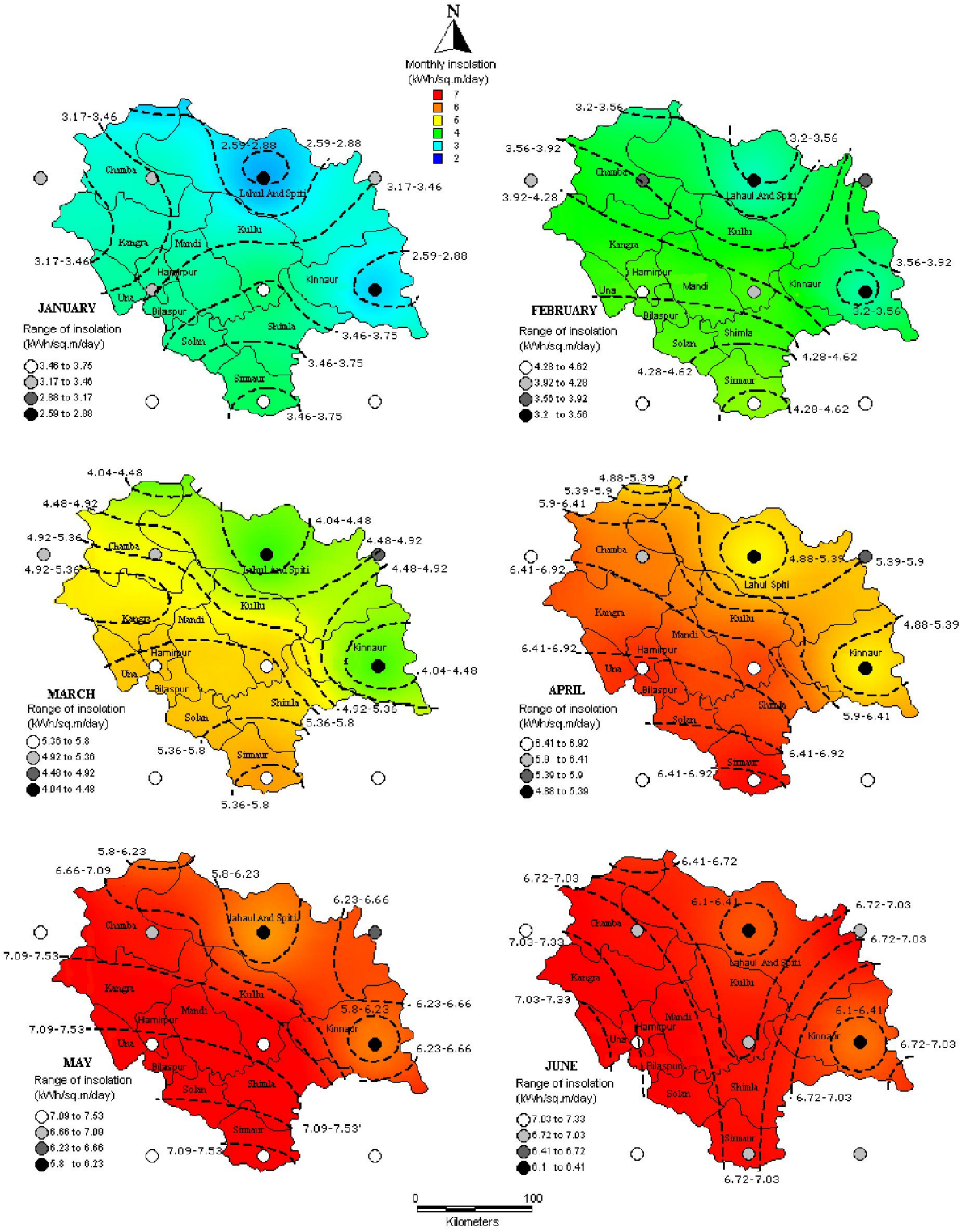

Figure 11: Spatial variation of Global insolation with the regional variation contours for the months of of July – December

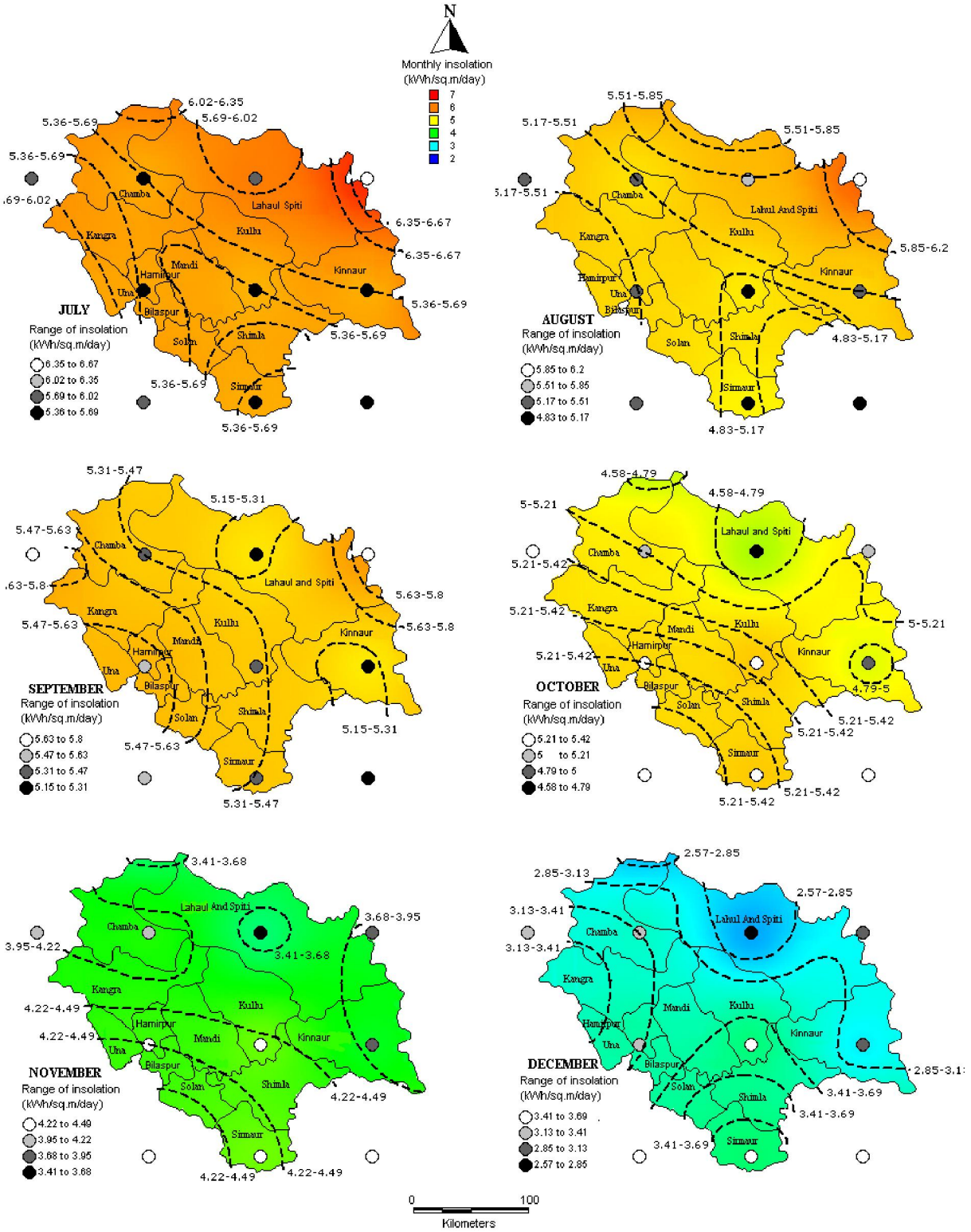

6. Conclusion

Spatial analysis of global insolation data aided in identifying the localities suitable for implementation of solar technologies. Satellite derived datasets available in user friendly formats based on time tested and realistic models provide solar radiation data on higher spatial and temporal scales, evident from the current endevour based on the 22 year average monthly global insolation data obtained from NASA SSE datasets. Solar potential of Himachal Pradesh was mapped and validated with the ground data obtained from radiation stations in India. The study demonstrates that the hill state receives global insolation (above 4 kWh/m²/day during the period of March to October) favourable for commercial solar applications. The low and middle altitude regions (below 3500vm) receive similar global insolation during the months of February and November as well. The low and middle altitude regions receive similar Global insolation during the months of February and November as well. The state witness low average insolation values in the cold months of December and January mostly favouring domestic solar appliances like solar cooker, solar water heater etc. The solar maps obtained help in the design of appropriate solar energy devices for Himachal Pradesh which is facing ecological disasters in the wake of depleting resources. Conspicuously, they also provide suitable information for areas like meteorology, agriculture, forestry etc. This regional level understanding of solar potential will aid the policy makers, entrepreneurs as well as researchers especially in the context of the National Solar Mission of the Government of India.

7. Acknowledgement

We thank NASA for making available the SSE datasets for renewable energy potential assessment throughout the world. The India Water Portal provides 100 years district wise meteorological data for India. We are grateful to NRDMS division, the Ministry of Science and Technology, Government of India and Indian Institute of Science for the financial and infrastructure support.

8. References

[1] Kishore V V N, Renewable Energy Engineering and Technology : A knowledge compendium , TERI Press, New Delhi, 2008

[2] Mani A., Handbook of solar radiation, Allied Publishers, New Delhi, 1981

[3] World Meteorological Organisation, Viewed on July 29 2010, <http://www.wmo.int/pages/prog/arep/gaw/solar-radiation.html>

[4] Varshita R D and Gupta M K, Modernisation of Radiation Network, Indian Meteorological Department, Pune, India, Viewed July 29 2010, <http://www.wmo.int/pages/prog/www/IMOP/publications/IOM-82-TECO_2005/Posters/P1%2810%29_India_Vashistha.pdf>

[5] NASA, Surface Meteorology and Solar Energy Release 6.0 Methodology, Viewed 29 July 2010, <http://eosweb.larc.nasa.gov/sse/documents/SSE6Methodology.pdf>
[6] Alberto Ortega, Rodrigo Escobar, Sergio Colle, Samuel Lunade Abreu, The state of solar energy resource assessment in Chile, Renewable energy, 35, (2010) 2514 – 2524
[7] Gayathri Vijayakumar, Michael Kummert, Sanford William A. Beckman, Analysis of short-term solar radiation, Solar Energy, 79, (2005) 495–504
[8] Pitz-Paal, R, Geuder Norbert, Hoyer-Klick Carsten, Schillings Christoph, 2007, How to get bankable meteodata ? DLR solar resource assessment, NREL 2007 parabolic trough technology workshop, Golden, Colorado, Viewed August 1 2010, <http://www.nrel.gov/csp/troughnet/pdfs/2007/pitz_paal_dlr_solar_resource_assessment.pdf >
[9] Ramachandra T V and Subramanian D K, Potential and prospects of solar energy in Uttara Kannada district of Karnataka State, Energy Sources, 19, (1996) 945 – 988
[10] Kun Yang, Toshio Koike, Baisheng Ye, Improving estimation of hourly, daily, and monthly radiation by importing global data sets, Agricultural and Forest Meteorology, 137, (2006) 43–55
[11] Xiaoying Liu, Xurong Mei, Yuzhong Li, Qingsuo Wang, Jens Rauns Jensen, Yanqing Zhang, John Roy Porter, Evaluation of temperature-based global solar radiation models in China. Agricultural and Forest Meteorology, 149, (2009) 1433–1446
[12] Liu D.L. and Scott B.J., Estimation of solar radiation in Australia from rainfall and temperature observations, Agricultural and Forest Meteorology, 106, (2001) 41–59
[13] Jimmy S G, Ehnberg, H.J. Math, Simulation of global solar radiation based on cloud observations, Solar Energy, 78, (2005) 157–162
[14] Ramachandra T V, Solar energy potential assessment using GIS, Energy Education Science and Technology, 18, Issue 2, (2007) 101-114
[15] Adnan Sozen, Erol Arcaklioglu, Solar potential in Turkey, Applied Energy, 80, (2005) 35 – 45
[16] Kishtawal C.M., Meteorological Satellites, Satellite Remote Sensing and GIS Applications in Agricultural Meteorology, pp. 67-79, viewed August 1 2010 <http://www.wamis.org/agm/pubs/agm8/Paper-4.pdf>
[17] Malik A.Q., Mufti A., Hiser H.W., Veziroglu N.T.and Kazi L., Application of Geostationary data for determining solar radiation over Pakistan, Renewable Energy, 1, (1991) 455-461
[18] John E Hay, Satellite based estimates of solar irradiance at the earth's surface - I Modelling approaches, Renewable energy, 3, (1993) 381- 393
[19] Chumnong Sorapipatana, An assessment of solar energy potential in Kampuchea, Renewable and Sustainable Energy Reviews, 14, (2010) 2174–2178
[20] Frulla L.A., Grossi Gallegos, Gagliardini T.D.A. and Atmnzai G., Analysis of satellite measured insolation in Brazil, Solar & Wind Technology, 7, (1990) 501-509
[21] Tanahashi S., Kawamura H., Matsuura T., Takahashi T, and Yusa H., Improved estimates of hourly insolation from GMS S-VISSR data, Remote sensing of environment, 74, (2000) 409 – 413
[22] Cogliani E., Ricchiazzi P. and Maccari A., Generation of operational maps of global solar irradiation on horizontal plan and of direct normal irradiation from meteosat imagery by using SOLARMET, Solar energy, 82, (2008) 556 – 562
[23] Janjai S., Pankaew P. and Laksanaboonsong J., A model for calculating hourly global solar radiation from satellite data, Applied Energy, 86, (2009) 1450 – 1457
[24] Islam M.D., Alili A.A., Kubo I and Ohadi M., Measurement of solar-energy (direct beam radiation) in Abu Dhabi, UAE, Renewable Energy, 35, (2010) 515–519

[25] Richard Perez, Robert Seals, Antoine Zelenka, Comparing satellite remote sensing and ground network measurements for the production of site/time specific irradiance data, Solar Energy, f50, (1997) 89-96

[26] Illera P., Fernfindez A, and Perez A., A simple model for the calculation of global solar radiation using geostationary satellite data, Atmospheric Research, 39, (1995) 79 – 90

[27] Statistical Data of Himachal Pradesh upto 2009-10, Himachal Pradesh Planning Department, Govt. of Himachal Pradesh, Viewed on August 2, 2010, <http://hpplanning.nic.in/Statistical data of Himachal Pradesh upto 2009-10.pdf>

[28] SRB Data and Information, Atmospheric Science Data Center, NASA, Viewed August 2, 2010 <http://eosweb.larc.nasa.gov/PRODOCS/srb/table_srb.html>

[29] NASA/GEWEX Surface Radiation Budget Project, Viewed August 2 2010, <http://gewex-srb.larc.nasa.gov/>

[30] Gupta S.K., Wilber A.C., Kratz D.P. aand Stackhouse Jr. P.W., The Langley Parameterized Shortwave Algorithm (LPSA) for Surface Radiation Budget Studies, NASA/TP-2001-211272, 2001

[31] Gupta S.K., Whitlock C.H., Ritchey N.A. and Wilber A.C., An Algorithm for Longwave Surface Radiation Budget for Total Skies, CERES ATBD Subsystem 4.6.3 , Viewed August 2 2010, http://ceres.larc.nasa.gov/documents/ATBD/pdf/r2_2/ceres-atbd2.2-s4.6.3.pdf

[32] Andrzej Z. Kotarba, Satellite-derived cloud climatorlogy over high elevation areas based on circulation types: A 2007 analysis of the Tatra Mountains, Physics and chemistry of the earth, 35, (2010) 462 – 468

SPATIAL ANALYSIS OF WIND ENERGY POTENTIAL IN HIMACHAL PRADESH

ABSTRACT

India ranks fifth in terms of installed capacity (14 GW) of global wind power systems (~200 GW). Commercial wind power based on large-scale wind turbines picked up in the country in 90's. Improvement in small wind technologies will now provide further impetus to the development of wind based power systems for decentralized applications in a major expanse in India. This study explores wind resource potential in the federal state of Himachal Pradesh characterized by undulating terrain in Himalaya based on validated long term reliable synthesized wind data. Spatial wind profiles based on high resolution data provide insights to the wind regime that helps in identifying potential sites for wind prospecting. The higher altitude alpine zone in Himachal Pradesh has relatively higher wind speeds compared to lower altitude zones. The minimal but reliable surface measurements in the lower altitude temperate and tropical zones indicate the micro climatic influences and spatial variability in the complex Himalayan terrain. The wind potential in Himachal Pradesh supports small wind technologies like agricultural water pumps, wind-photovoltaic hybrids, space/water heaters etc. This would help in meeting the decentralized energy demand sustainably.

KEYWORDS

Renewable energy, Wind resource, Potential assessment, Himachal Pradesh, Synthesized wind data, Small wind technologies

INTRODUCTION

Wind energy has been utilized as a driving source for grinding grains, pumping water and also for sailing. Wind turbines earned prominence in the 19th Century with the advent of electric power generation as local power sources. This renewable energy technology suffered a setback with the highly subsidized centralized fossil fuel based electricity generation and distribution. However, oil crisis of 70's revived the global interest in wind based decentralized systems. A policy shift was also noticed at this time in India for exploiting its abundant wind energy resource (Wiser, 2000). India has installed 14158 MW of commercial wind power systems since 1983 and the total potential is estimated to be 48561 MW. There is enormous scope of up-scaling through improved technologies. A large extent of the Deccan plateau, coastal states of the Western Ghats and small pockets in the Coromandel Coast have the highest recorded wind energy potential in the country. This includes the federal states of Rajasthan, Gujarat, Madhya Pradesh, Maharashtra, Andhra Pradesh, Karnataka and Tamil Nadu where majority of wind power

installations have been deployed (IWEA, 2010). A major expanse of the country is deemed as low wind energy potential areas since resource assessments were performed for large-scale wind turbines based on higher winds. However, a proficient understanding of local wind dynamics with the improvement in the technologies promises sustainable energy from this ubiquitous resource. The advancement in small wind technologies has given stimulus to the distributed energy generation and consumption. Wind energy also has high carbon offset capacity and support the Clean Development Mechanism (CDM) endorsed by the Kyoto Protocol (Indian Wind Energy Outlook, 2009).This reiterates the need for detailed regional wind resource assessment.

Wind resource assessment is the primary step towards understanding the wind dynamics of a region (Ramachandra et al. 1997). Wind flow developed due to the differential heating of earth is modified by its rotation and further influenced by the local topography. This results in annual (year to year), seasonal, synoptic (passing weather), diurnal (day and night) and turbulent (second to second) changes in wind pattern (Hester and Harrison, 2003). Increased heat energy generated due to industries and escalating population in urban areas result in heat islands which affects the wind flow as well. Wind characteristics like speed and direction measured at meteorological stations (surface) aid in assessing local wind resources. Wind patterns are observed to be tantamount for regions in proximity. However, local winds have high topographical and land cover influence, and assuming the wind data from a measured site applicable for a nearby site of interest calls for error. Monthly wind speed variation for regions within a radius of 30 km shows similar patterns but with difference in magnitude, and the study suggests using 6 years of long term wind data for satisfactory representation of monthly variations (Mani and Mooley, 1983). A one year wind speed data maintains an error within ± 10% which reduces to ± 3% for 3 years data but still burden the economics of a wind energy based project (Wind Energy, 2010). The surface wind datasets sometime fail to capture the diurnal variations especially during the night hours, giving an elevated estimate of the daily average as wind speeds are generally higher in the daylight (Bekele and Palm, 2009). Despite these complexities, wind resource assessment based on the available surface measurements at different sites using statistical tools have provided satisfactory results (Ramachandra and Shruthi, 2003; Mathew et al. 2002; Elamouri and Ben, 2008; Ullah et al. 2010).

The surface wind measurements being a reliable source of information on the wind regime of a region are available for only few sites and are found to be costly and also time consuming for acquiring the data. These gaps make a wider spatial and temporal coverage of wind characteristics difficult. In this regard, models like Wind Atlas Analysis and Application Program (WAsP) and Computational Fluid Dynamics (CFD) based on local topography and climate help in micro–scale (1–10 km) studies of wind resources. These models are validated with the dense surface measurements. They are not applicable for regions with thermally forced flows like sea breeze and mountain winds for which meso–scale (10–100 km) models are preferred. A combination of meso–scale and micro–scale models like the Karlsruhe Atmospheric Meso–scale Model (KAMM/WAsP), MesoMap and Windscape System along with geoinformatics provide reliable wind prospecting and has been tried for different regions (Wind Energy, 2010; Coppin et al. 2003).

Today, there are easily accessible wind datasets available from different organizations providing preliminary understanding of the wind regime of a region. High spatiotemporal resolution synthesized wind datasets based on various sources and models are available. Depending on the physiographical features and climatic conditions, these datasets would help for assessing wind potential in the region of interest along with surface wind measurements for validation. Wind resource atlas derived with the help of National Oceanic and Atmospheric Administration (NOAA) and National Aeronautical and Space Agency (NASA) Surface Meteorology and Solar Energy (SSE) data, validated with available surface

measurements, provide a range of mean wind speeds on a meso–scale wind atlas for the Newfoundland (Khan and Iqbal, 2004). Similarly an optimistic wind map was prepared with synthesized global datasets of NOAA and NASA SSE for Bangladesh along with many terrain specific characters from surface observations (Khan et al. 2004).The wind energy potential of the Saharan desert in Algeria was assessed based on NASA SSE data. This wind is expected to power an innovative brackish water greenhouse desalination plant and support agriculture in the arid study region (Mahmoudi et al. 2009). Kumar and Prasad (2010) demonstrated the application of NASA SSE data for wind power prospecting in two islands of Fiji. These studies substantiate the advantage and increasing interest in high resolution synthesized data for wind resource assessment.

STUDY AREA AND OBJECTIVE

Himachal Pradesh is an Indian federal state in the Western Himalayas located between 30.38°– 33.21° North latitudes and 75.77°–79.07° East longitudes, covering a geographical area of 55673 km^2 with 12 districts (Statistical Data, 2010). It has a complex terrain with elevation ranging from ~300 m to 6700 m as shown by the Digital Elevation Model (DEM) in Figure 1. Topography, climate, soil and vegetation clearly define the agro–climatic zones in the state. Parts of Una, Bilaspur, Hamirpur, Kangra, Solan and Sirmaur districts less than 1000 m above mean sea level represent the tropical zone. Certain segments of Solan, Sirmaur, Mandi, Chamba and Shimla districts located between 1000 m – 3500 m have climate conditions varying from sub–tropical to wet–temperate. Lahaul Spiti, Kullu and Kinnaur districts ranging between 3500 m – 6700 m are part of the dry temperate, sub–alpine and alpine zones with sparse vegetation and rainfall.

Figure 1: Digital Elevation Model (DEM) of Himachal Pradesh

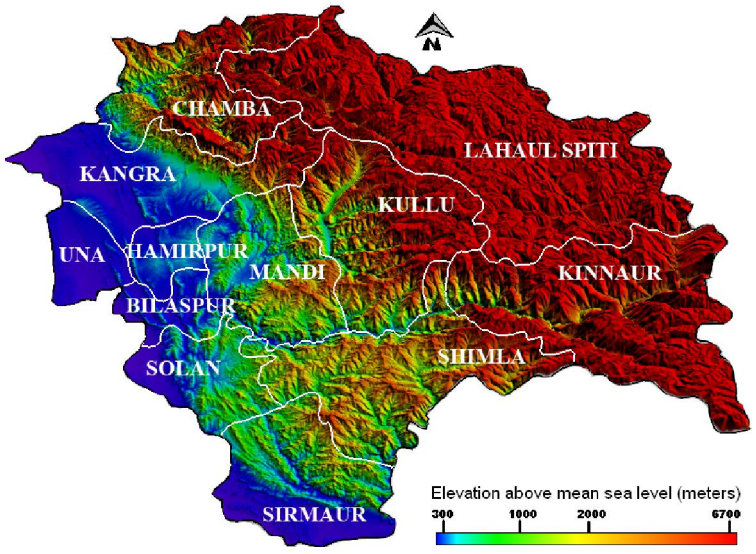

The hill state of Himachal Pradesh represents one of the rich biodiversity zones in the country adversely impacted by unplanned development. Dependence on the forests for fuel wood has resulted in decline of vegetation cover, fragmentation of forests and associated ecological imbalance in an ecologically fragile region such as Himalaya, etc.. In recent times, there has been increase in fossil–fuel based energy consumption, with resultant pollution and glacial melting (Aggarwal and Chandel, 2010). This necessitates exploration for clean renewable energy sources like wind etc. Even so, marginality and negligence of this region in the past has led to scarcity of reliable data which hinders efficient resource planning (Bhagath et al. 2006).

Historical wind speed records maintained by the Indian Meteorological Department (IMD) are available for 13 stations (Figure 2) in Himachal Pradesh. These data are characterized by large data gaps and non–standard measurement heights. Measurement heights, commencement of wind measurement exercises and duration vary abruptly (Table 1) for 7 stations. The topography of the region renders enormous variation to the micro–climate, wind speed and its direction adding further to the complexity of wind resource assessment. Capturing the wind regime of a diverse geographical entity like Himachal Pradesh using the limited available long term surface data cannot be a desirable option. The Automatic Weather Stations (AWS) installed at 22 locations in Himachal Pradesh (Figure 2) at 2 m has started operating since early 2011 (AWS, 2011). However a minimum one year long data is essential to explore the wind energy in the state which the AWS fail to provide at this point of time. The present study explores the wind resource potential in Himachal Pradesh based on synthesized wind data validated with the select surface wind data of Indian Meteorological Department (IMD).

Table 1: Wind stations in Himachal Pradesh maintained by the Indian Meteorological Department (IMD)

Index	Station	Longitude	Latitude	Elevation(m)	Anemometer height(m)	Wind Data availability (period, source)
08003	Nahan	76 44'	30 24'	959	-	1977-1998, IMD
08204	Sundernagar	76 88'	31 53'	861	-	1981-1997, IMD
08205	Chamba	76 07'	32 34'	996	-	1977-1990, IMD
08207	Simla CPRI	77 10'	31 06'	~2202	-	1989-2003, IMD
42059	Dalhousie	75 58'	32 32'	1959	1.7	1951-1988, IMD
42062	Dharmshala	76 23'	32 16'	1211	7	1952-1998, IMD
42065	Manali	77 10'	32 16'	2039	5	1968-1998, IMD
42080	Bilaspur	76 40'	31 15'	587	9.7	1956-1992, IMD
42081	Bhuntar	77 10'	31 50'	1096	-	1960-2003, IMD
42083	Shimla	77 10'	31 06'	2202	26.5	1933-1992, IMD
42063	Kyelong	77 04'	32 35'	3348+	26	1978, IMD

42078	Mandi	76 58'	31 43'	761	-	1958-1967, Mani and Mooley, 1983
42107	Dharmpur	77 01'	30 54'	1986+	-	-

Figure 2: Available wind stations in Himachal Pradesh as on January 11, 2011

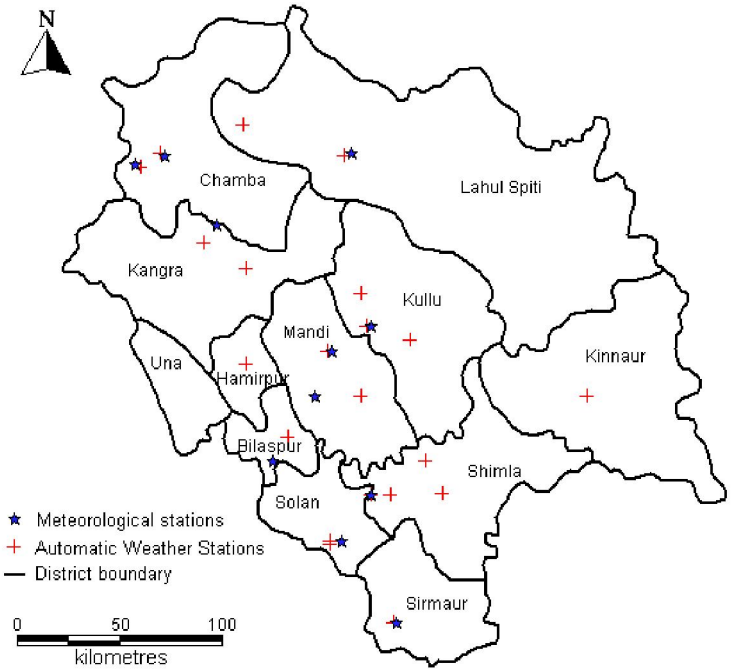

DATA, MODELS AND METHODS

Wind speeds at different spatial and temporal resolutions were compiled from various sources. NASA SSE datasets include 10 years (1983–1993) average wind speed at 1^0X1^0 global grid derived based on a Global Circulation Model (GCM) applied on satellite data. Every 1^0X1^0 grid represents the average of all data points within that grid (Takacs et al. 1994; NASA, 2010). Based on the NASA SSE wind speeds collected for 10 m, the annual average varies from 2.5±0.6 m/s to 5.8±0.8 m/s at 13 data locations in the state. Studies have shown that NASA SSE wind data exceeds the 25% error margin even for plain regions when compared to surface measurements with consequent errors in the wind power estimates (Kumar and Prasad, 2010). The wind regime obtained for the study region given in Figure 3 shows a latitudinal increase in wind speed from South to North. Himachal Pradesh is a complex terrain with features like vegetation and local relief influencing the wind regime. The NASA SSE wind data has been derived for plain landscapes (airport–like) and hence minimally used for further analyses.

NOAA–CIRES 20^{th} Century Reanalysis Version 2 data for 138 years (1871–2008) based on a global data assimilation system and surface pressure observations is available at 2^0X2^0 spatial resolution (NOAA,

2011). Long term wind speed average illustrated in Figure 4 shows annual values of 3.6 m/s for Himachal Pradesh. While the NOAA–CIRES annual wind speed values are not exaggerated like NASA SSE, the low resolution of the data (with only 9 data points) inherently neglects the topographical influences of the study region. However, the wind regime shows an increase in wind speed with the altitude of the region coherent with the changing agro–climate zones. However, for Himachal Pradesh with undulating terrain, a higher spatial resolution wind speed data addressing the geographical parameters would be desirable.

Figure 3: Annual average wind speed based on 1^0X1^0 resolution NASA SSE data

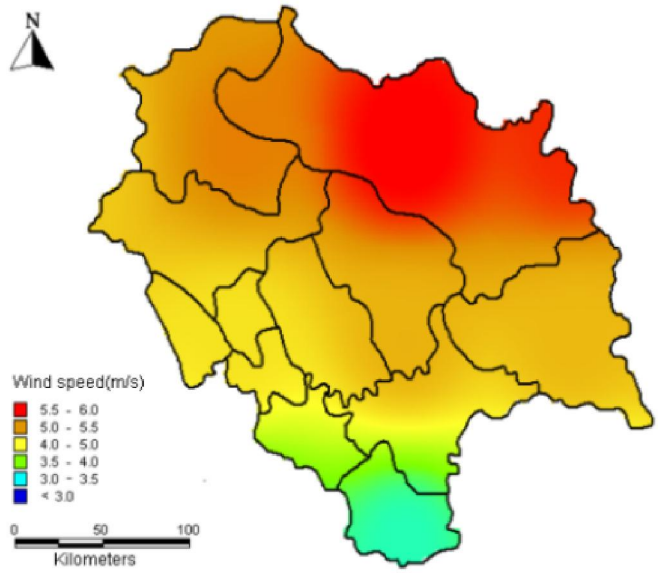

Figure 4: Annual average wind speed based on 2^0X2^0 resolution NOAA–CIRES reanalysis data

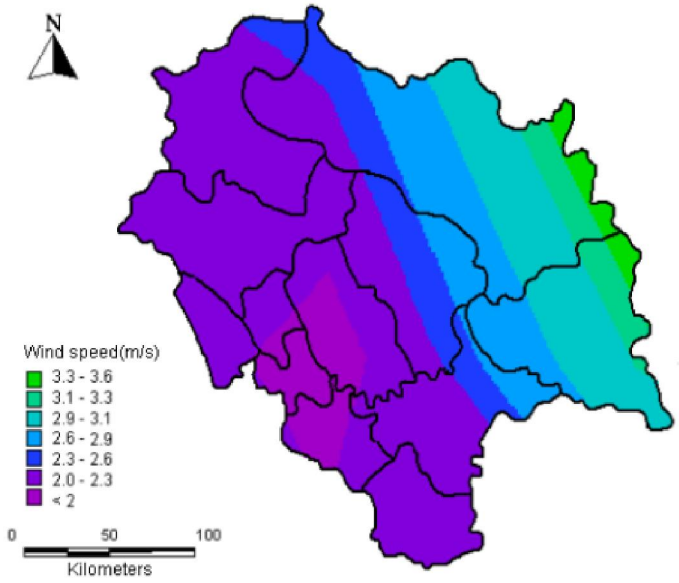

The Climate Research Unit (CRU) at the University of East Anglia maintains climatic averages of variables including wind speed for the period of 1961–1990 compiled from different sources with the inter and intra variable consistency checks to minimize data consolidation errors. The Gobal Land One–km Base Elevation Project (GLOBE) data of the National Geophysical Data Center (NGDC) were re–sampled to 10'X10' elevation grids where every cell with more than 25% land surface (those below 25% being considered water bodies) represent the average elevation of 100–400 GLOBE elevation points. The climatic average of wind speeds measured at 2 m to 20 m anemometer heights (assumed to be standardized during collection) collated from 3950 global meteorological stations together with the information on latitude, longitude and elevation were interpolated based on a geo–statistical technique called thin plate smoothing splines. Elevation as a co–predictor considers topographic influence on the wind speed and proximity of a region to the measuring station improves the reliability of the interpolated data. During interpolation inconsistent data were removed appropriately. This technique is identified to be steadfast in situations of data sparseness or irregularity. The wind speed as a climatic average is obtained for all global regions (excluding Antarctica) at 10'X10' resolution (New et al. 2002). This high resolution data mapped for the study region of Himachal Pradesh shows the annual average wind speed varying with the altitudinal gradient (Figure 5) as observed in the case of NOAA–CIRES data. On a preliminary observation, the wind speed values range well within the surface measurements obtained from IMD. Compared to other collated datasets, wind data from CRU is prudent for a meso–scale (10–100 km) study in the tough Himalayan terrain of Himachal Pradesh.

Figure 5: Annual average wind speed based on 10'X10' resolution CRU data

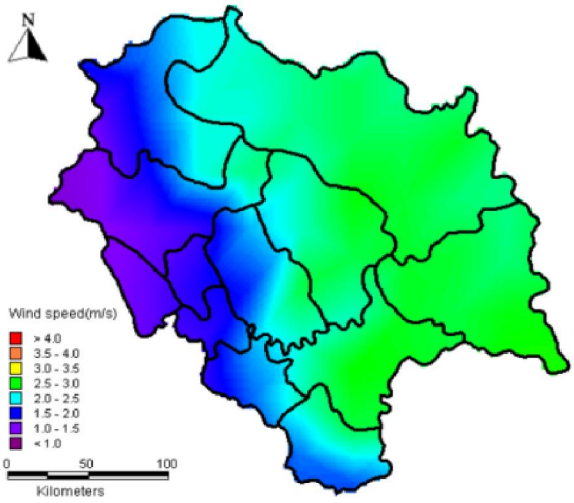

Wind resource potential assessment

The monthly average wind speed data obtained from the CRU databank were used to produce monthly wind atlases for Himachal Pradesh. Nearly 400 data points covering the entirety of the land area were

spatially analysed using Geographic Information Systems (GIS). The monthly average wind speed atlases for all the months hence obtained are enriched with isotachs (lines connecting regions with equal wind speed) showing regional wind speed variations.

The Indian Meteorological Department (IMD) provided surface wind data for 10 stations of Bilaspur, Sundernagar, Nahan, Chamba, Bhuntar, Dharmshala, Dalhousie, Manali, Simla CPRI and Shimla measured for different durations (Table 1). Wind speed at Mandi was obtained from a literature on wind climatology in India (Mani and Mooley, 1983). However, these locations are not representative of the diverse topography of Himachal Pradesh. The measured data include synoptic hour values (local time 8:30 and 17:30 hrs), daily averages for durations between synoptic hours and also monthly averages (not available for Mandi) of wind speed. Daily averages of wind speeds are obtained by averaging the mean for two 12 hour periods starting from 17:30 hrs capturing the diurnal variations of the resource. Wind measurements are standardized to 10 m using equation 1 as per World Meteorological Organization (WMO) norm (Ramachandra et al. 1997).

$$V/V_o = (H/H_o)^{\alpha} \qquad \ldots\ldots\ldots\ldots(1)$$

where V_o is the measured wind speed, V is the standardized wind speed, H_o is the measured height, H is the desired height (10 m) and α is the power law index. α is a measure of roughness due to frictional and impact forces on the ground surface which varies according to terrain, time and seasons. The valueof α calculated for most of the regions representing the Himalayan terrain are well above 0.40 based on long term observations and calculations (Mani and Mooley, 1983). In order to reduce extrapolation errors we consider the least value of 0.40 for Himachal Pradesh. The wind measurement heights varying widely from 1.7 m to 26.5 m for different sites in Himachal Pradesh are standardized based on the power law equation with α=0.4. It is observed that wind speed increases with height within the atmospheric boundary layer. Wind speed at 30 m is estimated to explore the possibility of energy utilization with the available wind technologies.

The meso–scale wind regime for Himachal Pradesh is generated using CRU data and validated with the surface measurements.

RESULTS AND DISCUSSION

The seasonal as well as spatial variation of average wind speed for Himachal Pradesh portrayed in Figure 6.1 and 6.2 respectively show increased wind speed during summer (February to June) which declines during southwest monsoon (June to September) and remains even during winter (November–February). The surface measurements from the IMD stations illustrated in Figures 7.1 and 7.2 conform with the earlier results (Figure 6.1 and 6.2). Most of the sites recorded peak wind speeds during the period of May–June. A minor influence of the northeast monsoonal winds originating from Central Asia is observed in the months of October and November in some sites recorded. The cold winter months of December and January witness calm breeze awaiting a surge in the forthcoming summer towards mid–February. The daylight average wind speed (at 8:30–17:30 hrs) is higher than the dark hours (at 17:30–

8:30 hrs) for all the months recorded by IMD. These trends are quite prevalent in most of the sites although exceptions due to the micro climatic influences on wind speed are also observed.

From the CRU wind atlases obtained, the spatial variation of wind speed is observed to be explicitly influenced by the elevation and resultant agro–climatic zones of Himachal Pradesh. It is known that the density of vegetation cover reduces with increasing elevation and facilitates higher wind flow. The dependence on elevation could be inherent from the interpolation technique followed by CRU. However, there are certain pockets of high wind speeds irrespective of elevation observed in the CRU wind regime distribution due to the complexity of the topography captured in the model.

According to the wind regime, an increasing trend of wind speed is observed from lower altitude tropical zone (< 1000 m) towards higher altitude alpine zone (> 3500m) with the monthly average varying from 0.6 to 4 m/s throughout the state. The lower altitude tropical zone including Kangra, Una, Bilaspur, Hamirpur and parts of Chamba, Mandi, Solan and Sirmaur experience wind speeds ranging from 0.6–3 m/s following the seasonal trends already discussed. The middle altitude zone (1000–3500 m) covering Shimla, Kullu and parts of Mandi, Chamba, Solan, Sirmaur and Kinnaur represent wet to dry temperate regions. The wind speed in this zone is seen to vary from 1.3–4 m/s. Further upwards, the high altitude zone of Lahaul Spiti, Kinnaur and Kullu report 2–4 m/s annually. This zone has appreciable wind potential compared to other regions. The wind speed ranges marked by altitudinal gradients of agro–climatic zones provide a preliminary insight into the wind regime of Himachal Pradesh. The NOAA–CIRES annual average wind atlas (Figure 3) also validates this trend.

The surface measurements aided in understanding the seasonal variations and dynamics. However, the magnitude of wind speeds obtained are not truly representative of the respective agro–climatic zones. Terrain and vegetation immensely influences the wind speed and hence each site represents a micro locality within the respective zone. These sites are mostly located in the low and middle altitude zones ranging from tropical to dry–temperate (< 3500m) which experience a wind speed range of 0.6–4 m/s as shown by the CRU data based wind atlases. The standardized monthly average wind speeds given in Figure 8 for these sites show the annual variation from 0.3–3.2 m/s. Most of these sites (except Shimla) measured wind speed below 10 m, and the assumption of standardized measurements for data sparse sites could be an underestimate according to equation 1. Hence, the actual wind speeds in many of the data sparse sites may be higher at 10 m. None of the available sites represent the higher altitude alpine zone where the highest wind speeds are observed in the wind atlases. These data gaps and ambiguities could be rectified in long term monitoring through recently installed AWS wind speed measurements with relatively better spatial coverage for 22 stations spread across Himachal Pradesh. Availability of more number of reliable wind measurement stations and detailed analysis of terrain features could facilitate micro–scale wind resource assessment in Himachal Pradesh.

In the case of surface measurements projected to a height of 30 m (Figures7.1–7.2), the annual average monthly wind speeds for Bilaspur, Nahan and Dalhousie are above 2 m/s with the highest average of 3 m/s at Dalhouise. At the same height more than 61% of measured hours in Nahan, 44% in Bhuntar and 18% in Dalhousie obtained wind speeds above 2 m/s, while more than 29% of the measured hours crossed 4 m/s wind speeds in Bhuntar (Figure 9). The annual averages of 1.9 m/s daily wind speed at 30 m for Bhuntar and Dharamshala are also significant. Most of the other sites recorded annual average daily and monthly wind speeds below 1.3 m/s. As noted earlier, there could be possible but unavoidable underestimations in these values.

Figure 6.1: Wind regime for the months of January – June

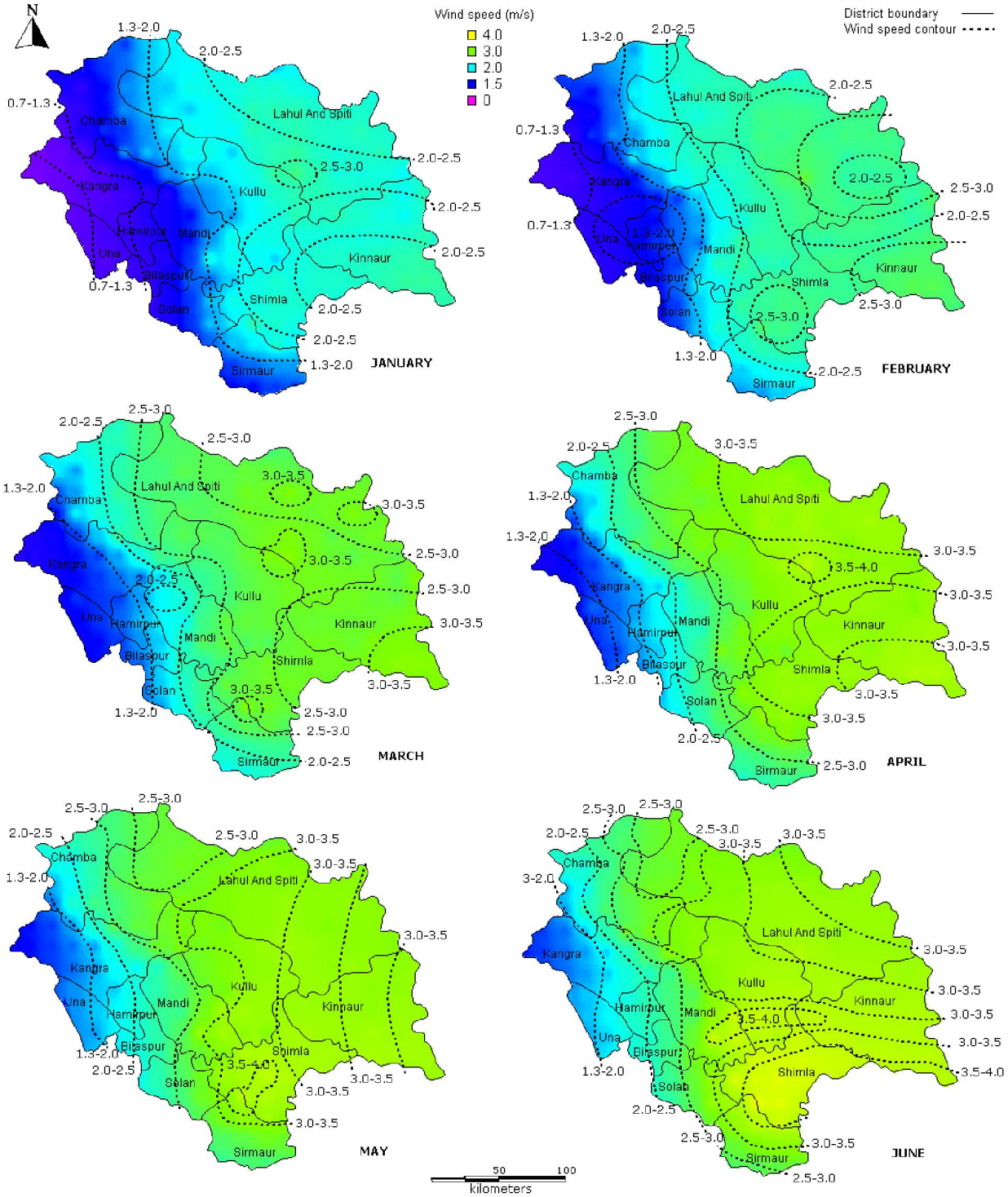

Figure 6.2: Wind regime for the months of July – December

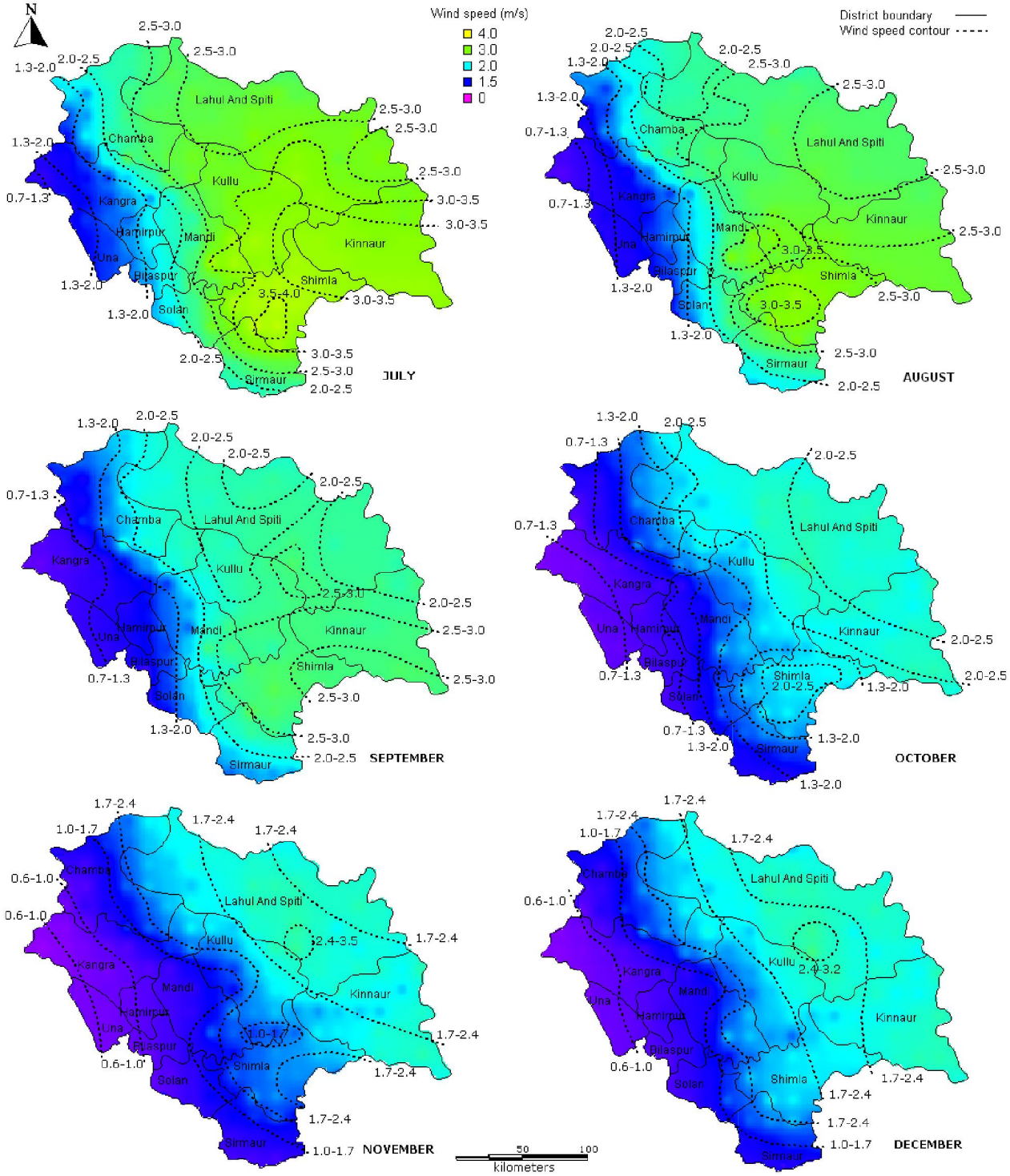

Figure 7.1: Daily average wind speeds at 10 m and 30 m for surface observations

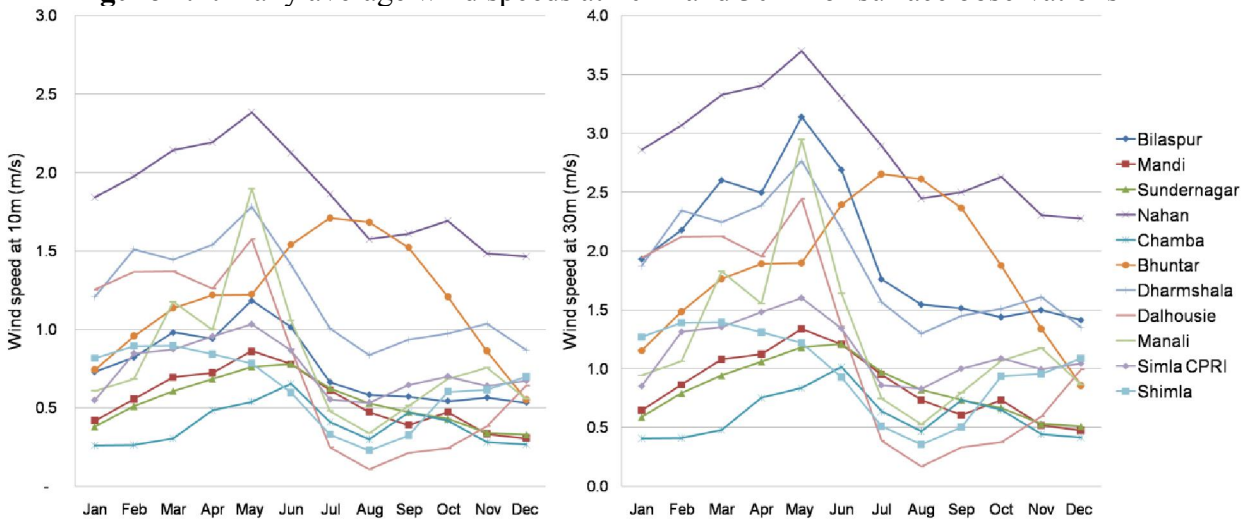

Figure 7.2: Monthly average wind speed at 10 m and 30 m for surface observations

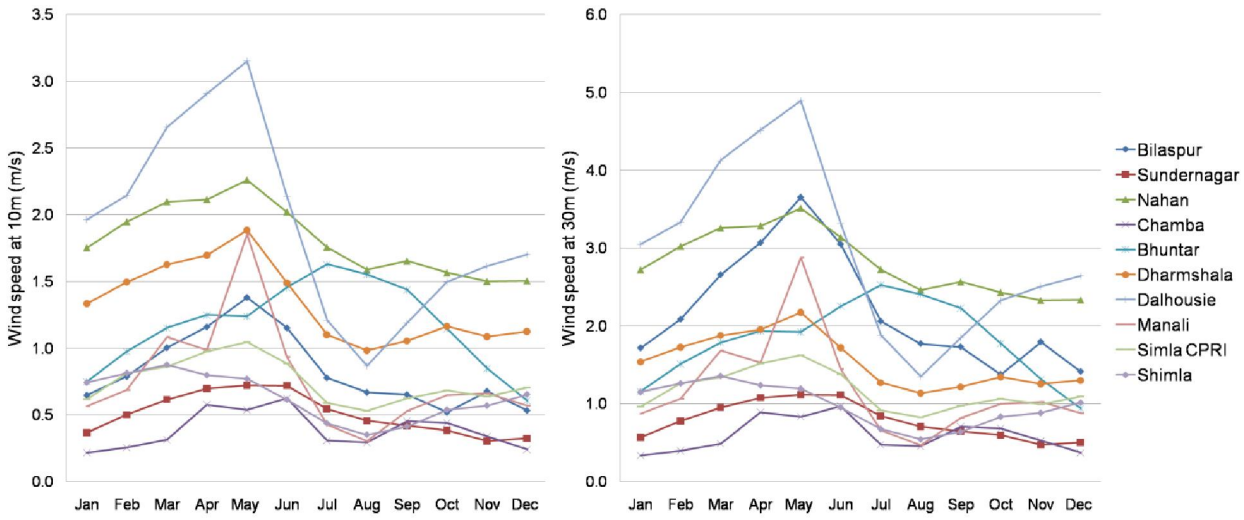

Figure 8: Wind speed variations for standardized surface observations

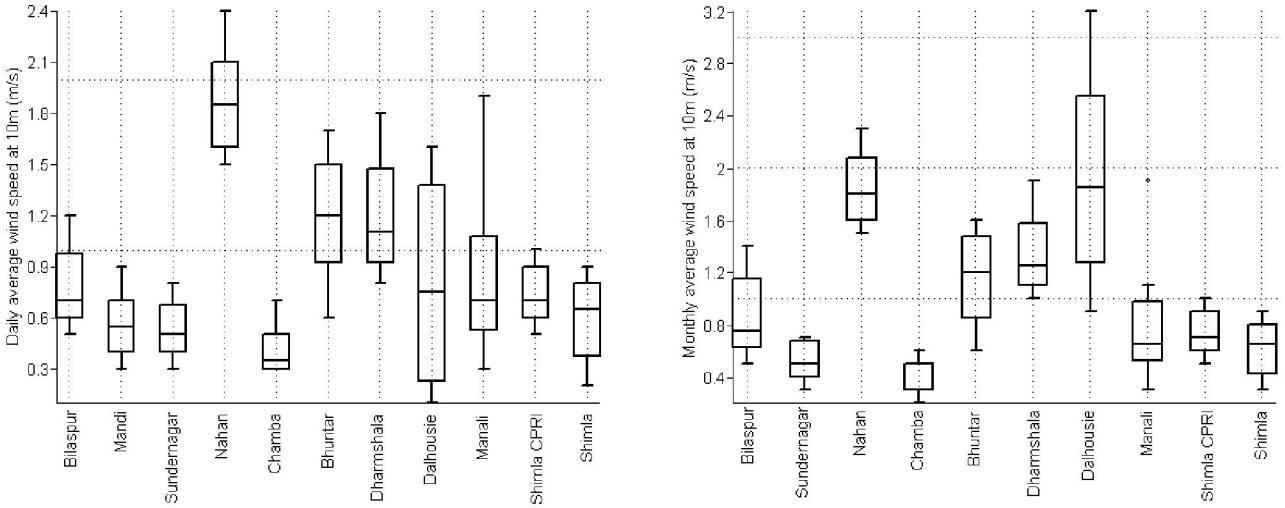

Figure 9: Percentage occurrence of winds above 2 m/s and 4 m/s from hourly readings projected to 30 m hub height

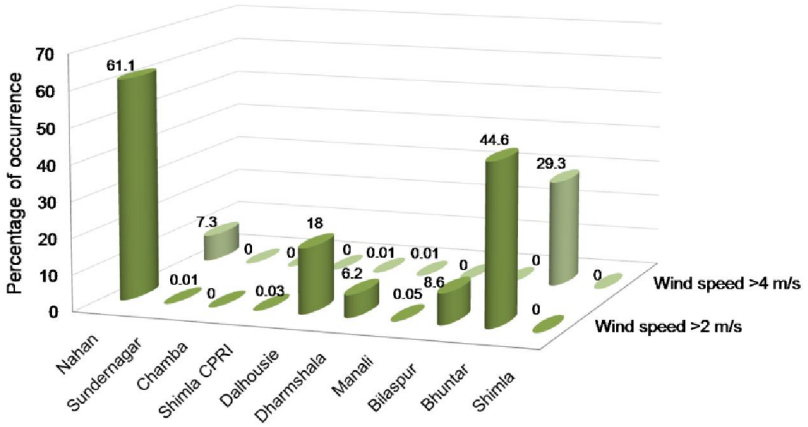

Utilizing the wind resource in Himachal Pradesh

With the advancements in wind turbine technologies listed in Table 2, small–scale power generation at moderately low wind speeds is now technically feasible and also economically viable. It has been shown that small–scale wind turbines are more attractive in terms of deployment, functioning and management compared to commercial setups (Ramachandra et al. 1997). Himachal Pradesh being well connected by the electricity grid could support grid–connected wind power in the state. The sparse population densities also demand decentralized energy generation. Small wind turbines are used in conjunction with diesel generators especially in remote areas (Clausen and Wood, 1999). However, wind–diesel hybrid solution cannot assure sustainability since reduction in wind speeds must be compensated with more fossil fuel supply so as to maintain the output.

High resolution spatial data from NASA SSE (NASA, 2010) shows that Himachal Pradesh receives monthly average global insolation (incoming solar radiation) above 4 kWh/m^2/day (Ramachandra et al. 2011) except for the winter months of December and January (Figure 10). Higher altitude alpine zone (> 3500 m) receive lower insolation values but higher wind speeds. This trends inverts in lower altitude

tropical zone i.e higher insolation and lower wind speeds. Hence wind–photovoltaic hybrids could be considered for decentralized power generation throughout the state. Similar proposals for wind–photovoltaic hybrids have been observed in regions with low wind speeds (Cabello and Orza, 2010; Ramachandra et al. 2011).

Wind pump for drawing water is an attraction for rural energy needs (Mathew et al. 2002). The agriculture intensive sub–tropical to wet–temperate zone of Himachal Pradesh gets benefited by wind pumps which function at wind speeds above 2 m/s. As seen in Nahan and Bhuntar, increased hub heights could deliver prolonged winds. Wind based space heating systems have been analysed to be cost effective compared to many conventional fuel sources like firewood and electricity (Jaber et al. 2008). The cold alpine zones of Lahaul Spiti and Kinnaur where the wind speeds are relatively higher, could meet their space heating requirements through wind energy. Development of wind energy based water heaters is promising for such regions (Tudorache and Popescu, 2009). This ensures reduced dependence on fuel wood and coke which currently warm them during harsh winters.

Table 2: Available small wind turbines

Rated power (kW)	Rotor swept area (m^2)	Sub-category
$P_{rated} < 1$ kW	$A < 4.9$ m^2	Pico wind
1 kW < P_{rated}< 7 kW	$A < 40$ m^2	Micro wind
7 kW < P_{rated}< 50 kW	$A < 200$ m^2	Mini wind
50 kW < P_{rated}< 100 kW	$A < 300$ m^2	(No clear definition adopted yet)

Source: (Wind Energy, 2010)

Figure 10: Global insolation (kWh/m^2/day) received in Himachal Pradesh

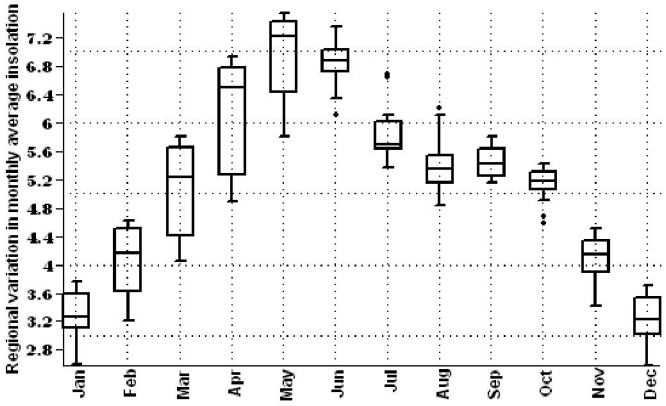

Constraints

Wind technologies could be deployed only after assessing the wind characteristics, land availability and socioeconomic impact. Wind characteristics like speed, power density, turbulence and vertical profile variations influence the design of wind turbines for purposes like power generation, battery charging,

water pumping or space heating. Technology deployment could be initiated only with long term surface wind measurements at specific locations which are invariably influenced by the local terrain features. This assessment of wind resource potential in Himachal Pradesh shows minimal potential for large scale power generation in the state. Land availability for small turbines may not be a serious constraint. However, increased hub heights even for small turbines could be at the cost of the soil strength and land stability. Success of wind technology demands regular monitoring and sustained maintenance. Employment generation through appropriate mechanisms mobilizes the local people in these efforts. More importantly, resolute organizational support will ensure smoother penetration of wind technologies for sustainable development in Himachal Pradesh.

CONCLUSION

This study addresses the increasing need for detailed wind energy resource assessment in remote regions like Himachal Pradesh which also faces serious ecological threats. Due to sparse and unreliable surface wind measurements available and expensive modeling alternatives, proven and authentic synthesized data were scrutinized for suitability in the study region. High resolution wind atlases hence generated, quantifies the increasing wind speed with altitudinal gradients and varying agro–climatic zones. While the higher elevation (> 3500) alpine zone is identified as a suitable candidate for further wind exploration, the lower elevation zones cannot be neglected as shown by the surface measurements. Certain small wind technologies suitable for the study region have been discussed, while also mooting the possible constraints of dissemination. Meeting the energy demands through clean resources like wind envisions a sustainable future for Himachal Pradesh as well as other regions neglected in the conventional wind assessment studies.

ACKNOWLEDGEMENT

We thank the Indian Meteorological Department (IMD) for providing the surface wind measurements for Himachal Pradesh and NASA, NOAA and CRU for making the global wind speed databanks available for use. We are grateful to NRDMS, Ministry of Science and Technology, DST, Government of India and Indian Institute of Science for the financial and infrastructure support.

REFERENCES

1. Aggarwal, R.K. (2010). Chandel S.S. Emerging energy scenario in Western Himalayan state of Himachal Pradesh. Energy Policy. 38, 2545–2551.
2. AWS (Automatic Weather Station). Indian Meteorogical Department. Government of India [Online] http://www.imdaws.com/ (accessed on 11 January 2011)
3. Bekele, G., Palm, B. (2009). Wind energy potential assessment at four locations in Ethiopia. Applied Energy. 86, 388–396.
4. Bhagat, R.M, Sharda, S., Virender, K. (2006) Agro–Ecological Zonation of Himachal Pradesh. Palampur: CSK Himachal Pradesh Agricultural University
5. Cabello, M., Orza, J.A.G. (2010) Wind speed analysis in the province of Alicante, Spain: Potential for small–scale wind turbines. Renewable and Sustainable Energy Reviews, 14, 3185–3191.
6. Clausen, P.D., Wood, D.H. (1999) Research and Development Issues for Small Wind Turbines. Renewable Energy, 16, 922–927.
7. Coppin, P.A., Ayotte, K.A., Steggel, N., CSIRO. Wind energy research unit [Online]. http://www.csiro.au/files/files/pis7.pdf (accessed on 16 August 2010).
8. Elamouri, M., Ben, F.A. (2008) Wind energy potential in Tunisia. Renewable Energy, 33, 758–768.

9. Hester, R.E., Harrison, R.M. (2003) Sustainability and Environmental Impact of Renewable Energy Resource United Kingdom: Royal Society of Chemistry
10. Indian Wind Energy Association. http://www.inwea.org (accessed on 16 August 2010)
11. Indian Wind Energy Outlook 2009. Global Wind Energy Council [Online]. http://www.gwec.net/fileadmin/documents/test2/GWEO_A4_2008_India_LowRes.pdf (accessed on 10 December 2010)
12. Jaber, J.O., Jaber, Q.M., Sawalha, S.A., Mohsenb, M.S. (2008) Evaluation of conventional and renewable energy sources for space heating in the household sector. Renewable and Sustainable Energy Reviews, 12, 278–289.
13. Khan, M.J, Iqbal, M.T. (2004) Wind energy resource map of Newfoundland. Renewable Energy, 29, 1211–1221
14. Khan, M.J., Iqbal, M.T., Mahboob, S. (2004) A wind map of Bangladesh. Renewable Energy. 2004, 29, 643–660.
15. Kumar, A., Prasad, S. (2010) Examining wind quality and wind power prospects on Fiji Islands. Renewable Energy, 35, 536–540.
16. Mahmoudi, H., Spahis, N., Goosen, M.F., Sablani, S. (2009) Assessment of wind energy to power solar brackish water greenhouse. Renewable and Sustainable Energy Reviews, 13, 2149–2155.
17. Mani, A., Mooley, D.A. (1983). Wind Energy Data for India New Delhi: Allied Publisher
18. Mathew, S., Pandey, K.P., Anil Kumar, V.C. (2002). Analysis of wind regimes for energy estimation. Renewable Energy, 25, 381–399.
19. NASA (National Aeronautics and Space Administration). Surface Meteorology and Solar Energy. [Online]. http://eosweb.larc.nasa.gov/sse/documents/SSE6Methodology.pdf (accessed on 10 August 2010)
20. New, M., Lister, D., Hulme, M., Makin, I. A high–resolution data set of surface climate over global land areas. Climate Research. 2, 1–25.
21. NOAA (National Oceanic and Atmospheric Administration). U S Deparment of Commerce [Online]. http://www.esrl.noaa.gov/psd/data/gridded/data.20thCentReanalysis.html (accessed on 18 January 2010)
22. Ramachandra, T.V., Subramanian, D.K., Joshi, N.V. (1997) Wind energy potential assessment in Uttara Kannada district of Karnataka India. Renewable Energy, 10, 585–611.
23. Ramachandra, T.V., Shruthi, B.V. (2003). Wind energy potential in Karnataka, India. Wind Engineering, 27(6), 549–553.
24. Ramachandra, T.V., Jain, R., Krishnadas, G. (2011). Hotspots of solar potential in India, Renewable and sustainable energy review, 15(6), 3178-3186.
25. SRTM (Shuttle Radar Topography Mission). [Online]. http://srtm.usgs.gov (accessed on 12 August 2010)
26. Statistical Data, Himachal Pradesh 2009–10. Government of Himachal Pradesh [Online]. http://hpplanning.nic.in/Statistical data of Himachal Pradesh upto 2009–10.pdf (accessed on 3 August 2010)
27. Takacs, L.L, Molod, A., Wang, T. (1994). Documentation of the Goddard Earth Observing System–General Circulation Model. Technical Memorandum, No: 104606. National Aeronatics and Space Administration
28. Tudorache, T., Popescu, M. (2009). FEM Optimal Design of Wind Energy–based. Acta Polytechnica Hungarica, 6(2).
29. Ullah, I., Chaudhry, Q., Chipperfield, A.J. (2010). An evaluation of wind energy potential at Kati Bandar, Pakistan. Renewable and Sustainable Energy Reviews, 14, 856–861.
30. Wind Energy: The Facts. European Wind Energy Association [Online]. cited 2010 August 16. Available from: http://www.wind–energy–the–facts.org
31. Wiser, W.H. (2000). Energy Resources: Occurrence, Production, Conversion, Use New York: Springer Verlag

REGIONAL BIOENERGY PLANNING FOR SUSTAINABILITY IN HIMACHAL PRADESH, INDIA

ABSTRACT

Energy system in mountain regions is complex due to the wide variations in availability and demand of energy resources. Mountain inhabitants are traditionally dependant on bioenergy resources like fuelwood, agro and animal residues for meeting their energy requirements for heating, cooking, etc. However, depleting forest resources limit availability of fuelwood while commercial sources like LPG and kerosene fail to meet the domestic energy demands due to logistic and economic constraints. Hence, the inhabitants are forced to follow inefficient and ad hoc usage of juvenile forest trees (thus hindering regeneration), agro and animal residues disregarding their alternative utilities. This deteriorates the ecological harmony and demands for sustainable resource planning in the regional level. The study assesses the bioresource availability and its potential to meet the bioenergy demands of three mountain districts in the Western Himalayan federal state of Himachal Pradesh. Regions of bioenergy surplus or deficit are identified for different scenarios. The ecological status of forests and actual availability along with the demand of fuelwood in villages are analyzed to highlight the significance of decentralized regional level bioenergy resource planning. BEPA: Bioenergy potential assessment – A Decision Support System (DSS) to facilitate compilation, analysis, representation, interpretation, comparison and evaluation of regional bioresource has been used to visualize bioenergy status. This supports energy planners and policy makers in efficient disaggregated bioenergy resource planning to meet the subsistence and development needs of mountain inhabitants at least cost to the environment and economy.

INTRODUCTION

Mountain regions are unique in terms of their landscape, climate, vegetation, economic activities and socio–cultural aspects. The mountain inhabitants are traditionally dependent on natural resources for their livelihood. Development in these regions historically neglected the diversity and heterogeneity of their ecosystems [1]. As a consequence of the landscape changes due to natural and anthropogenic influences the ecological integrity and resource sustenance are under serious threat. Clearance of forest resources for fuelwood, fodder, timber, industrial products and agriculture has ensued in forest fragmentation resulting in human–animal conflicts and scarcity of resources. Even though governmental regulations restrict illegal felling of forest trees, this process continue rampantly depleting forest cover, degrading soil fertility, eroding top productive soil layer and flooding the plains [2]. The holistic and sustainable development of mountain regions is essentially linked to the management of natural resources and improvements in the conversion and end use of energy through viable eco–friendly alternate technologies. Bioenergy from combustion of bioresources like fuelwood (including dry litter of leaves, twigs etc), agro residues (stalk, straw, cobs, husk, bagasse etc) and animal residues has been a traditional predominant energy source for heating and cooking in the mountainous rural energy system. Trees grown on agricultural margins and forests are the major source of fuelwood. It is observed that more than 70% of the total energy consumption of Western Himalayan mountain regions is met by traditional sources of which nearly 60% is fuelwood. Over 90% of this fuelwood is consumed in households for heating and cooking [3]. Agro residues classified as field–based residues (straw, stalk, cobs etc) are used sparingly as fuel apart from fodder and mulch while process–based residues (rice husk, sugarcane bagasse, etc) are usually discarded. Scarcity of fuelwood

in recent times has forced people to depend more on agro residues for domestic heating and cooking needs, leaving the crop lands unfertile. This subsequently has affected the crop yield resulting in further clearance of forests for cultivation. Apart from these, forced dependence on pine cones, tree bark and weeds with high ash content and low heating values has increased indoor pollution affecting especially women and children [4]. Livestock is the major source for manure, dairy, meat and draught. Due to the scarcity of fuel wood, rich dried dung–cake as alternative fuel deprives agriculture field of nutrients apart from causing pollution on direct burning. Stoves used for burning in mountain areas vary with altitude and most of them are traditional devices with low thermal efficiency [5]. Transition to commercial energy sources like kerosene and LPG at subsidized rates is noticed in urbanizing landscapes, although there are logistic and economic constraints in supply [3]. Thus, the alternative bioresources as well as commercial sources fail to reduce the burden on forest cover.

Energy demand and supply dynamics in mountain regions are complex due to the spatial variations in availability and accessibility of resources and their differing usage along altitudinal gradients. This complexity demands detailed studies for improving the regional energy system [2]. Reducing inefficient use of fuelwood and encouraging conservative use of alternative bioresources in meeting the energy demand ensures ecological sustainability. This necessitates the assessment of bioenergy availability (supply) and consumption (demand) to identify the bioenergy surplus or deficit status of mountain regions for efficient, integrated and sustainable resource planning.

Resource planning at aggregate level neglects the regional paucity of resources and the crisis faced by the inhabitants in meeting their domestic energy demands without feasible alternatives. Regional information on energy resources and patterns of human dependence is vital for efficient planning. The basis of regional integrated energy planning is the preparation of area based decentralized energy system to meet the subsistence and development needs at the least cost to the environment and economy. This considers all the socioeconomic and ecological factors of a region essential for long term success of the intervention. Decision making involves data compilation, analysis and visualization of various scenarios. In this context, regional energy plan through a Decision Support System (DSS) provides an interactive user friendly platform with options to compile, analyze, interpret and visualize the information. DSS essentially consists of database, modeling and dialogue management subsystems [6]. BEPA (Bioeneergy Potential assessment) – A DSS designed for bioresource assessment accounts for the bioenergy availability to demand status of realistic scenarios in the regional level. It facilitates the collection and analysis of available information, the projection of future conditions and the evaluation of alternative energy solutions for conservative resource planning [7]. DSS based bioenergy resource assessment and planning has been proposed in many regions [8, 9, 10, 11]. Regional bioenergy planning and execution through DSS potentially resolves the energy and environmental issues faced by the mountain regions. The present study assesses bioenergy resource status of three representative mountainous districts in the federal state of Himachal Pradesh located in Western Himalayas. This includes the causal factors for degradation of resources, levels of forest fragmentation etc.

Objectives: Main objectives of this study are

1. quantification of bioresources availability,
2. demand assessment,
3. assessment of levels of degradation through forest fragmentation analysis; and
4. visualization of levels of degradation

STUDY AREA

Himachal Pradesh is located between 30.38°– 33.21° North latitudes and 75.77° – 79.07° East longitudes, covering a geographical area of 5.57 million ha with 12 districts [12]. The agro–climatic zones in the state are defined by altitude, climate, soil, precipitation and other geophysical parameters. It has a complex terrain with altitude ranging from 300 to 6700 m as shown by the Digital Elevation Model (DEM) in Figure 1. Almost one–third of the area is snow covered for seven months and forms the origin for many rivers. Regions above 4500 m experience perpetual snowfall and rainfall vary from 50 to 2600 mm along different altitudinal zones [13]. Climate, soil as well as biotic factors in the past (forest fire, shifting agriculture, grazing, etc.) influences the type of vegetation along with other factors like solar radiation, temperature, moisture, geology etc. The major vegetation types found in Himachal Pradesh are tropical, sub–tropical, wet temperate, dry temperate, sub–alpine and alpine, varying with altitudinal gradients and often overlapping due to changes in climate [14].

The study area covers three districts of Solan, Shimla and Lahual Spiti, focusing on three watersheds of Mandhala, Moolbari and Megad inhabiting village clusters (Figure 1). These watersheds and districts are representative of the different agroclimatic zones in the hill state of Himachal Pradesh. The respective watersheds provide village level insight significant for the regional study. The physiographic information of the districts and watersheds are summarized in Table 1.

Table 3: Physiographic information of the study region

District	**Altitude (m)**	**Area (ha)**	**Rainfall (mm)**	**Population density (no:/sq km)**	
Solan	316 – 2209	193600	1179–1899	258.6	
Shimla	713 – 4984	513100	847–1330	141	
Lahaul Spiti	2043 – 6514	911165	332–803	2	
Watershed	**Latitude (°N)**	**Longitude (°E)**	**Altitude (m)**	**Area (ha)**	**River associated**
Mandhala(Solan)	30.87–30.97	76.82–76.92	400–1100	1453	Yamuna
Moolbari(Shimla)	31.07–31.17	77.05–77.15	1400–2000	1341	Yamuna
Megad(Lahaul Spiti)	32.64–32.74	76.46–76.74	2900–4500	1050	Chandrabhaga

Figure 1: Digital Elevation Model (DEM) representing the three districts and village clusters in respective watersheds

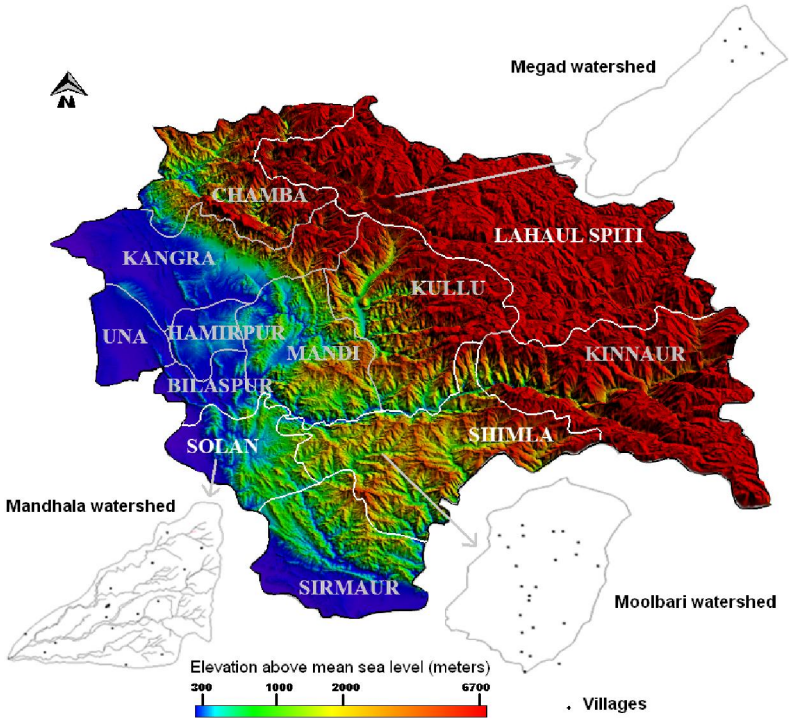

Woody biomass

Net Primary Productivity (NPP) of vegetation is the annual increment (t/ha/yr) in total standing biomass of the vegetation. Litterfall includes woody biomass shed from forests including leaves, twigs, branches etc used as fuelwood [15]. The biomass and NPP in Himalayan forests increases from tropical to temperate and then decreases towards alpine [16]. The above ground tree biomass ranges from 80 to 400 t/ha. Litterfall in Central Himalayas for an altitudinal range of 350–2250 m varies between 4.2–7.8 t/ha/yr. Of the litterfall in Himalayan forests, contribution of wood is 9–20% and leaves range between 54–82% [17]. The vegetation types as well as biomass and NPP of representative forests and tree species found in Himalayan terrain are summarized in Table 2 [18–36]. Tropical vegetation dominated by broadleaved tree species is found below 1000 m in major parts of Solan and minor parts of Shimla districts. The tree biomass ranges from 58.7 to 136.1 t/ha and NPP from 5.9 to 22.7 t/ha/yr. Dominance of *Lantana Camara* weed is noticeable in the hilly tracts degraded by anthropogenic activities. Plantations of *Acacia catechu* are frequented here. The sub–tropical vegetation found in Solan and Shimla at an altitude range of 900 to 1500 m is characterized by chirpine (*Pinus roxburgii*) forests. Chirpine has high regeneration potential and caters to the fuelwood needs of the dependants. The vegetation also includes mixed oak forest of *Quercus leucotricophora*, locally called as Banj oak. The tree biomass of sub–tropical vegetation ranges from 113 to 388 t/ha with NPP of 7.6 to 18.9 t/ha/yr. Beyond the transitional stage of sub–tropical vegetation, wet temperate vegetation is observed in minor parts of Solan and major parts of Shimla districts (1200 to 2500 m). The tree biomass ranges from

146.43 to 782 t/ha with NPP of 15.5 to 28.2 t/ha/yr. Further high, above 2200 m, the wet temperate vegetation gives way to dry temperate and sub–alpine vegetation which are coniferous and dry deciduous in nature. Dry temperate vegetation is found in Shimla and Lahaul Spiti and the tree biomass ranges from 40 to 502 t/ha with NPP of 7.3 to 24.6 t/ha/yr. Above 4000 m (timber limit or tree line) the alpine vegetation favours only short shrub species. Enormous diversity of undergrowths are observed throughout all types of vegetation, however of lesser fuelwood value. The representative fuel wood trees common in these regions with standing biomass and NPP are given in Table 2.

Table 4: Himalayan vegetation types, representative tree species, standing biomass and NPP found in the study regions

Vegetation		Standing biomass (t/ha)	NPP (t/ha/yr)	Ref
Tropical	**Forest type**			
	Broadleaved vegetation	276.79		[18]
	Dry deciduous forest	–	14.6–15.7	[19]
	Tropical seasonal forest	–	16	[20]
	Representative trees			
	Khair (*Acacia catechu*)	76.35	7.63	[21]
	Poplar (*Populus deltoides*)	–	5.9–22.7	[22]
	Bamboo (*Dendrocalamus strictus*)	–	15.8–19.3	[23]
	Siris (*Albizzia lebbeck*)	–	8.38	[24]
	Shisham (*Dalbergia sissoo*)	58·7–136·1	12·6–20·3	[25]
Subtropical	**Forest type**			
	Pine forest	210·8	9.9–21.2	[26]
	"	115.2–286.2	11.0–23	[27]
	"	200.8–	18.5–24.5	[2

		377.1		8]
	Mixed oak forest	163.4–432.6	14.4–18.9	[28]
	"	426	15.9	[29]
	Representative trees			
	Chirpine (*Pinus roxburghii*)	113–283	7.6–18.7	[29]
	"	117.53	18.9	[18]
	Banj oak (*Quercus leucotricophora*)	388	13.2	[29]
Wet temperate	**Forest type**			
	Oak forest	197.2–322.8	15.9–20.6	[30]
	Mixed oak	344	15	[29]
	Representative trees			
	Oak (*Quercus sp*.)	285–782	15.5–25.1	[29]
	Deodar (*Cedrus deodara*)	451	28.2	[29]
	"	146.43		[18]
Dry temperate to subalpine	**Forest type**			
	Temperate decidous forest	–	12	[20]
	Temperate broad leaved forest	–	7 – 15.6	[31]
	Sub alpine forest	–	4.76–19.68(ANP)	[32]
	Representative trees			

Silver fir (*Abies pindrow*)	–	18.9	[33]
Fir (*Abies sp*)	–	7.3–20.0	[33]
Blue pine (*Pinus wallichiana*)	–	13.08.	[34]
Spruce (*Picea sp*)	–	11–14.0	[35]
Maple (*Acer sp.)*	–	10.9 (ANP_{tree})	[36]
Horse chestnut (*Aesculus indica*)	502	16.5	[29]
"	–	19.6	[33]
Kharsu oak (*Quercus semicarpifolia*)	–	24.6	[33]
Birch (*Betula utilis*)	172	12.5	[29]
Rhododendron (*Rhododendron sp.*)	40	7.5	[29]

Agriculture

Agricultural systems in Himachal Pradesh vary with soil, climate, vegetation as well as socioeconomic factors like market proximity and government intervention. More than 90% of the cropped area in the districts are rain–fed and found on sloping marginal lands and small land holdings. Earlier subsistence based farming system has given way to cash crops and mechanization [13]. Mixed crop–livestock, vegetable based, perennial plantation and agro–pastoral systems are the common farming practices observed here. Including plantations, the net cropped area in Solan, Shimla and Lahaul Spiti are 39370 ha, 67857 ha and 3292 ha respectively [37]. Wheat, maize, rice, pulses and oil seeds are dominant in the tropical and sub–tropical regions, while crops such as millet, barley, buckwheat and dry nuts are common to temperate regions. Fruits and vegetables are profitable, generate more employment and are prominent in regions with access to roads and market. Apple orchards are predominant in wet temperate regions of Solan and Shimla. The sub–tropical and wet temperate regions are reported to be highly productive in terms of crop yield and are largely agriculture intensive. Farmers in dry temperate regions prefer more of mixed type of farming with livestock for sustenance. Due to unfavourable weather conditions agricultural productivity is low in upland cold districts like Lahaul Spiti [1].

Livestock

Livestock includes cattle, buffaloe, yak, mithun (bos frontalis), sheep, goat, horse, pony, mule, donkey, pig and camel which contribute nearly one–fourth of the total household farm income in Himachal Pradesh. Large animals are reared for dairy, draft power, transportation and manure while small animals provide meat, wool etc. Nearly 75–80% households in Himachal Pradesh keep dairy animals and 10% draught animals. The shift to plantation crops as well as mechanization has decreased the demand for draught. It is observed that the number of livestock per household has dwindled in the past few decades. Nevertheless, livestock owners are found to replace low productive cattle and buffaloes with more productive animals [38]. The tropical and subtropical regions have stall–fed and grazed cattle as the major livestock. Wet temperate regions prefer stall–fed cattle while dry temperate regions prefer more of sheep and goats which are grazed in open pastures. Transhumance farming with seasonal migration of people and livestock is observed in Lahaul Spiti and higher reaches of Shimla [1].

Bioenergy consumption

Over 90% of the population in Himachal Pradesh lives in rural areas (17495 villages). Electricity is the source of lighting in nearly 98% of these villages, the others depending on kerosene. Fuelwood satisfies nearly 70% of their heating and cooking needs. Himachal Pradesh is one of the major bioenergy consumer in India with annual fuelwood consumption of 3.2 million tonnes [39]. In rural areas, apart from household heating and cooking, fuelwood is consumed during festivals, marriages, funerals and also burned in margins of agricultural lands to drive away wild animals [40]. Increasing distance for fuelwood collection due to scarcity of forest resources in many cold tribal villages exhaust higher human energy and time [41]. Energy inefficient traditional cook stoves reported thermal efficiency of 8–13% contributing to the indoor pollution affecting women and children [5]. However, improved cook stoves disseminated through the federal program are being used in certain villages of Lahaul Spiti [40]. Certain studies suggest that kerosene and LPG distribution systems are well developed in rural areas while continued availability is not ensured and people are hesitant to switch due to lack of awareness and cost factors [42]. Hence these commercial sources minimally satisfy the rural domestic energy needs.

Fuelwood consumption patterns in different altitudinal gradients were ascertained through field surveys in the three watersheds – Mandhala, Moolbari and Megad apart from comprehensive literature survey of the Western and Central Himalayas given in Table 3 [3, 4, 39–41, 43–47]. The Per Capita Fuelwood Consumption (PCFC) ranges from 0.46 to 4.67 kg/day in Western Himalayas and 1.07 to 2.80 kg/day in Central Himalayas. Eastern Himalayas are the highest consumers of fuelwood reaching even beyond 4 kg/day [2]. Table 3 lists the regional fuelwood consumption studies. It highlights that PCFC in Solan is 0.46 to 1.32 kg/day, Shimla is 1.9 to 2.68 kg/day and Lahaul Spiti is 0.89 to 2.91 kg/day. This increase in consumption pattern along the altitudinal gradient is conspicuous due to higher demand for space and water heating in colder regions. This altitude based variation is observed irrespective of socioeconomic conditions. However, within an altitudinal range, large families consume less fuelwood per capita compared to smaller ones [40, 41].

Table 5: Fuelwood consumption patterns in different altitudinal gradients of Western and Central Himalayas

Region	PCFC (kg/day)	Elevation	Reference

Western Himalaya			
Himachal Pradesh (Rural areas)	1.562	300–6700	[39]
Mandhala watershed, Solan	0.68±0.22	400–1100	Present study (ground survey)
Moolbari watershed, Shimla	1.9–2.63	1400–2000	Present study (ground survey)
Megad waterhed, Lahaul Spiti	1.53±0.64	2900–4500	Present study (ground survey)
Solan district, Himachal Pradesh (HP)	1.32	316 – 2209	[3]
Shimla district, Himachal Pradesh	2.68	713 – 4984	[3]
Mandi district, Himachal Pradesh	2.99	–	[3]
Kullu valley	4.3±0.37	1200–1400	[43]
Hill forest (rural areas)	1.89	–	[44]
Hill forest (urban areas)	1.21	–	[44]
Hill non–forest (rural areas), HP	1.31	–	[44]
Khoksar, Lahaul Valley	1.06–3	3200	[40]
Jahlma, Lahaul Valley	1.02–2.91	3000	[40]
Hinsa, Lahaul Valley	0.98–2.74	2700	[40]
Kuthar, Lahaul Valley	0.91–2.68	2600	[40]
Central Himalaya			
Garhwal Himalaya	1.07–2.80	380–2500	[41]
Garhwal Himalaya, Tehri	1.12–2.44	500–2500	[45]
Garhwal, tropical	2.42–2.52	300–400	[4]
Garhwal, sub–tropical	1.63–1.7	900–1300	[4]
Garhwal, temperate	1.77–2.32	1900–2400	[4]
Kumaon Himalaya	1.49	–	[46]
Nepal Himalaya	1.23	–	[47]

METHODOLOGY

Bioenergy resource assessment in the district level

Bioenergy resource availability

We employ an integrated approach of compiling data from government agencies and biomass inventorying of fuelwood, agro and animal residues. Primary data includes information from ground survey and remote sensing data. Secondary data are collected from respective government departments and literatures of previous studies.

Multispectral moderate resolution (30 m) cloud–free satellite images from Landsat (TM/ETM/ETM+ sensors) obtained in September/October months of 1989/90, 2000 and 2005/2006 covering the three districts of Solan, Shimla and Lahaul Spiti are collected from Global Land Cover Facility [http://glcfapp.glcf.umd.edu]. Since boundaries of the districts derived from Survey of India (SOI) toposheets cover more than one scene, mosaicking (combining the satellite images) and subsequent histogram matching (synchronizing the spectral reflectance of different images) corrections are performed. Bands of geo–corrected (geographic coordinates of satellite images are compared with ground control points) satellite images are masked and cropped with the district boundary. Land use analysis is performed on the satellite images using supervised Gaussian Maximum Likelihood Classification (GMLC) method categorizing the natural features like vegetation, water bodies, snow and open spaces. Training data were obtained from field and higher resolution (at least 15 m) spatial images from Google Earth (http://earth.google.com) were used for pre–classification error correction and post–classification validation. Although we tried to distinguish the land used for agriculture from total vegetation cover and built–up from open space, the varying spectral reflectance in the complex hill terrain due to high relief and shadow deteriorated the performance of the classification algorithm. The extent and temporal change of tree cover (also including horticulture plantation crops like apple, orange, peach etc), short vegetation (shrubs, crops, grassland), water and others (barren land, fallows, rocky terrain, built–up etc) are quantified from the classified satellite images with overall accuracy in the range of 75–90%. Vegetation is observed to vary primarily based on altitudinal gradients although species mixing towards upper and lower ranges have occurred in due course of time due to anthropogenic activities and climatic changes [14]. Training data corresponding to the land use types were derived from field (using Global Positioning System – GPS) and Google Earth (http://www.googleearth.com) along with the elevation contours generated from DEM. Remote sensing data (2005/06) of these districts were classified using these training data with the Gaussian maximum likelihood classifier. Classified data were validated with field data and accuracy assessment (Figure 3). This provided the extent and type of vegetation in the district.

The Aboveground Net Productivity of tree biomass (ANP_{tree}) in forest vegetation has been quantified to assess the woody matter available for extraction. 70–90 % of the total forest biomass productivity is shared by trees and the rest by undergrowths of shrubs and herbs [17]. Nearly 60% and above of the total productivity of trees are attributed to the above ground biomass increment in the forests of Himachal Pradesh. Hence, ANP_{tree} of three practical scenarios of high (75%), medium (50%) and low (25%) for availability of resources are considered.

The Net Calorific Values (NCV) of different tree species is above 4000 kcal/kg (dry weight) as per the literatures [48]. This value is used as energy equivalent in the total bioenergy estimation of woody biomass. The annual bioenergy available (E_{tree}) from tree biomass resource of a particular vegetation type is calculated by equation 1

$$BE_{tree} = Area * ANP_{tree} * NCV \quad (1)$$

The extent of agricultural land use mapped from the remote sensing data and the data from Department of Economics and Statistics, Ministry of Agriculture, Government of India [37]. The agriculture data includes crop types (cereals, vegetables, pulses, oilseeds, horticulture plantation, oilseeds, cotton, sugarcane, fodder crops and narcotics) with yield of crops (final product) for the years 2000 to 2005 in the three districts. Horticulture plantations of apple, orange, peach etc have been included in the woody biomass estimated using remote sensing data. Biomass residues from vegetables are negligible on field. The agro residues (cereals, pulses, oilseeds, cotton and sugarcane) and their production are calculated from the Residue to Product Ratio (RPR) considering the yield of respective crops [49]. The NCV of crop residues identified in the region are observed to range from 3000 – 4200 kcal/kg [49–53] and NCV of crop residues for three scenarios (viz. 3000, 3500 and 4000 kcal/kg) were considered assuming efficient energy conversion. Considering the multiple uses of crop residues as fodder, manure, mulch etc, the final residue production per area (R) available as fuel is accounted for high (75%), medium (50%) and low (25%) availability scenarios. The annual bioenergy from a particular crop residue is computed by equation 2.

$$BE_{crop} = \text{Gross cropped area} * R * NCV \quad (2)$$

The district wise livestock population of cattle, buffaloe, yak, mithun, sheep, goat, horse, pony, mule, donkey and pig are collated from the livestock population census 2007, Department of Animal Husbandry, Government of Himachal Pradesh [54]. The dung yield per livestock type are given in Table 5 [15, 48, 56–58] and lower, moderate (average of lower and upper) and upper dung yield cases are considered. Biogas generated based on animal dung vary from 0.036 to 0.042 m^3/kg [15]. However, cold conditions in the study region suggest lower value of 0.036 m^3/kg biogas generation. NCV of biogas is consistently over 5000 kcal/m^3 [55]. Alternative uses of animal dung as direct manure and constraints of dung collection during grazing restrict its availability for biogas generation. Here three scenarios of high (75%), medium (50%) and low (25%) animal dung availability are considered for biogas generation. The annual bioenergy yield from livestock is calculated as

$$BE_{livestock} = \text{Total annual dung yield from livestock} * \text{Volume of biogas per mass of dung} * NCV \quad (3)$$

Total annual bioenergy available from bioresources including forests, agriculture residues and animal residues in a region is calculated using equation 4

$$BE_{available} = BE_{tree} + BE_{crop} + BE_{livestock} \quad (4)$$

The different scenarios of low (25%), medium (50%) and high (75%) fuel based availability of the bioresources account for practical constraints in satisfying alternative needs.

Table 4: Crop types, productivity, residue types, residue to product ratio and energy equivalents considered

Crop	Type	Productivity (t/ha/yr)	Residue type	Residue to product ratio	Energy equivalent (kcal/kg)
Cereals	Rice	1.84	Husk	0.29	3000
			Stalk	1.5	3000
	Wheat	1.47	Stalk	1.6	3500
	Bajra	0	Cobs	0.33	3500
			Husk	0.3	3000
			Stalk	2	3500
	Maize	1.97	Cobs	0.27	3500
			Husk	0.2	3000
			Stalk	2	4000
	Barley	0.86	Stalk	1.3	3000
	Others	0	Stalk	1.4	3000
Pulses	Gram	0.88	Stalks	1.1	3500
	Tur/arhar	0	Husk	0.3	3000
			Stalk	2.5	3000
	Kharif	0.76	Husk	0.18	3000
			Stalk	1.1	3500
	Rabi	0.67	Stalk	1.2	3500
Oilseeds	Groundnut	0.9	Shell	0.33	4000
			Stalk	2	4000
	Sesamum	0.2	Stalk	1.5*	3000
	Rapeseed & Mustard	0.49	Husk & Stalk	1.5	3500

	Soyabeen	1.37	**Stalk**	1.7	3000
	Others	0.2*	**Stalk**	2	3500
Others	**Cotton**	0.72	**Shell & husk**	2.2	3000
			Stalk	3t/ha	3000
	Sugarcane	0.87	**Bagasse**	0.33	3500
			Top & leaves	0.05	3500

*Data for which no references were available and hence approximated based on the conservative values

Table 5: Livestock in the study region and dung yield

Livestock	Dung yield (kg/head/day)	Reference
Cattle	2.87	[48]
	10	[56]
	3–7.5	[15]
Buffaloe	2.65	[48]
	15	[56]
	12–15	[15]
Yak	4.5	[57]
Mithun (Bos frontalis)	–	[48]
Sheep	0.32	[48]
	0.1	[15]
Goat	0.35	[48]
	0.1	[15]
Horse	1.72	[48]
	6.08	[58]

Pony	–	–
Mule	0.94	[48]
Donkey	–	–
Pig	0.34	[48]
Camel	2.49	[48]

Bioenergy resource demand

The PCFC in Solan, Shimla and Lahaul Spiti was computed from the data compiled from household surveys and literatures (Table 3). Bioenergy resource availability is assessed for the period 2005/2006 and the district–wise population is projected for the year 2006 from 2001 census [59, 60]. Considering 4000 kcal/kg energy equivalence of woody biomass, the domestic heating and cooking energy (majorly bioenergy) demand is given by

$$BE_{demand} = \text{Annual PCFC} * \text{Population} * \text{NCV} \quad (5)$$

Bioenergy resource status

The total woody biomass production in each district compared to the heating and cooking energy demand of the population indicate the ecological health of the region. The total bioenergy availability (including woody biomass, agro residues and animal dung) to bioenergy demand ratio gives the bioenergy resource status of the region.

$$BE_{status} = BE_{available} / BE_{demand} \quad (6)$$

The different scenarios of high (75%), medium (50%) and low (25%) biomass availability are compared with the lower, moderate and upper case bioenergy demand. If the value of E_{status} is above one, the region is surplus in bioenergy resources while a ratio below one denotes deficit. A bioenergy deficit status emphasizes adopting innovative and sustainable practices of enhancing the resources while improving the end use efficiency of the devices [15].

Bioenergy resource assessment in the village level: Bioresource assessment at district level provides an overview of the bioenergy status. However, the availability and consumption vary spatially and regionally. In order to understand the bioresource availability dynamics, the ecological status of the forest as well as the actual availability of the bioresources in the villages for meeting their bioenergy requirements have been studied. Fragmentation of forests is one of the decisive parameters in the

availability of bioresources. Also an attempt is made to spatially analyse the degradation levels with the demand centre – villages in the watersheds of Solan and Shimla districts.

Fragmentation of forests: Forest fragmentation is a process by which a contiguous area of forest is reduced and divided into multiple fragments ultimately leading to deforestation. Fragmentation of forests is assessed using remote sensing data for Moolbari and Mandhala watersheds of Shimla and Solan districts respectively. Multispectral and temporal satellite images covering Moolbari watershed (1341 ha) are downloaded from GLCF (http://glcf.umiacs.umd.edu/data/) and also procured from National Remote Sensing Agency, Hyderabad, India. These include images with diverse spatial and spectral resolutions acquired from Landsat MSS (1972), Landsat TM (1989), Landsat ETM+ (2000) and IRS LISS–III (2007). SOI toposheets of 1:50000 and 1:250000 scales are digitized to derive boundary layer of the watershed which is used to mask and crop the region out of the satellite image. Land use (type of features like crops, built–up etc associated to human activities) and land cover (natural features like tree cover, water body, snow etc) analyses are performed on these satellite images using various classification algorithms like GMLC. Ground control points (GCPs) for geo–correction and training data for classification of remote data are collected through field investigations using a handheld GPS (Global Positioning System). Google Earth data (http://earth.google.com) are used for pre–classification and post–classification validation. Similar methodology is followed for Mandhala watershed (1453 ha) in Solan district. The extent of forest fragmentation is assessed using FRAGSTATS®

Biomass degradation analysis

Biomass degradation analysis maps the resource availability with respect to the bioenergy demand of inhabiting villages in the vicinity. The extent of woody biomass meeting the bioenergy requirements of 7 villages in Moolbari watershed is mapped using remote sensing (IRS LISS III) and Geographical Information Systems (GIS) tools. Classification of remote sensing data provided the land use and also helped in mapping the resource availability around each village. The watershed is divided in to 7 zones using theissen polygon method (based on the proximity of the village to the resource availability) such that each zone represents corresponding villages' proximity area (village zonation theme). Multiple ring buffers are drawn around villages at 100 m interval up to 1000 m (10 rings). The buffer themes are clipped using village zonation theme and those falling on other village zones are deleted. ANP_{tree} of forest cover is taken to be 3.6 t/ha/yr and PCFC as 2.3 kg/day and 1.9 kg/day in lower and upper case demand scenarios respectively. Finally, thematic maps are created for both the scenarios to understand the level of bioresources degradation.

DSS for regional bioenergy resource planning

A DSS for assisting regional bioenergy resource planning is developed using Microsoft Visual Basic 6.0 as frontend and Microsoft Access database as backend [6, 7]. It comprises of different modules enabling data management, processing, interpretation, modeling, projection and visualization (Figure 2). In the database module, the data collected from primary (ground surveys, spatial data) and secondary sources (Government departments, records, literatures) are stored in a database which is easily accessible for retrieval, updating or editing. This includes information on forest vegetation, plantation, crops, cattle and other sources of bioenergy. Data redundancy is minimized through normalized data tables. GIS provides the capabilities such as spatial and temporal analysis, querying

and visualization which helps the location based decentralized planning. Land cover land use (LCLU) analysis module calculates the extent of vegetation cover in a region using remote sensing data. Temporal changes in land cover have been analyzed for studying trends of resource availability or degradation. Land use module helps in mapping the extent of different land use pattern (agriculture, plantation, forests etc.) in a region. The flexibility to enrich the database with spatial aspects helps to identify and quantify the local constraints in the resource management. Level of analysis module helps in hierarchical data input and analysis. Bioresource yield module computes sector–wise resource yield based on spatial extent (forest, agriculture, plantation etc.) and productivity. Energy module computes the available energy for the selected bioresource at selected level. Forecasting module helps in projecting the resource status to future conditions and facilitates alternative approaches so as to reduce possible resource crunch. This enables the planner to access and study bioenergy resource status in the village level to national level in a bottom up approach of resource planning [7]. The method flow diagram of DSS designed for regional bioenergy resource estimation and planning is given in Figure 3.

RESULTS AND ANALYSIS

LCLU analyses of Solan, Shimla and Lahaul Spiti districts are performed and the types of vegetation are identified spatially (Figures 4a–c). The temporal land cover changes for the districts are given in Table 6. Based on analysis of the latest available spatial data (2005/06), the total tree cover in Solan is 43.51%, Shimla is 48.85% and Lahaul Spiti is 0.36% of the respective total geographic areas (Table 7). The ANP_{tree} estimated for the vegetation types are given in Table 8. The annual woody biomass produced ranges as 517.3–1111.7, 1253.8–3029.8, and 18.9–63.8 kilo tonnes for Solan, Shimla and Lahaul Spiti districts respectively. The lower, moderate and uppercase scenarios of availability are listed in Table 9. In all cases, the total availability of woody biomass is the highest in Shimla, followed by Solan and Lahaul Spiti. The district–wise fuelwood demand for lower, moderate and upper PCFC cases is given in Table 10. PCFC in Solan is 0.48–1.32 kg/person/day, Shimla is 1.9–2.68 and Lahaul Spiti is 0.89–2.91 kg/person/day. Evidently, the higher case of fuelwood demand in Lahaul Spiti cannot be met even by the moderate case productivity of woody biomass in the region. Moreover, the actual availability of woody biomass as fuelwood considering its alternative use as timber is lower than the total productivity in any region. Hence practically available fuelwood may not meet the bioenergy requirements of these regions for different demand cases.

Figure 2: Design of DSS for bioenergy resource assessment and planning

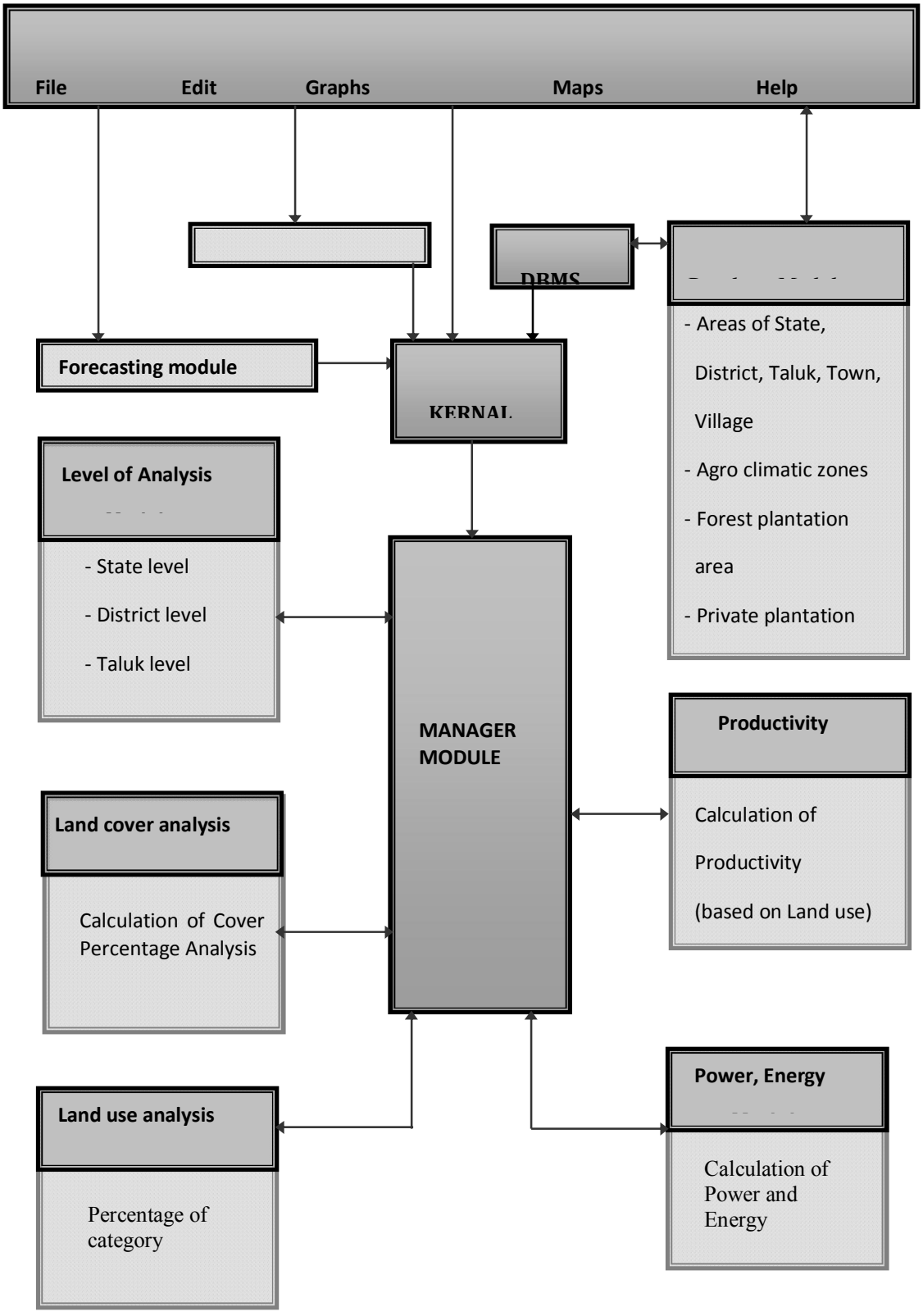
File
Edit
Graphs
Maps
Help
DBMS
- Areas of State,
District, Taluk, Town,
Village
- Agro climatic zones
- Forest plantation
area
- Private plantation
Forecasting module
KERNAL
Level of Analysis
- State level
- District level
- Taluk level
MANAGER
MODULE
Productivity
Calculation of
Productivity
(based on Land use)
Land cover analysis
Calculation of Cover
Percentage Analysis
Power, Energy
Calculation of
Power and
Energy
Land use analysis
Percentage of
category

Figure 3: DSS methodology for bioenergy resource assessment and planning

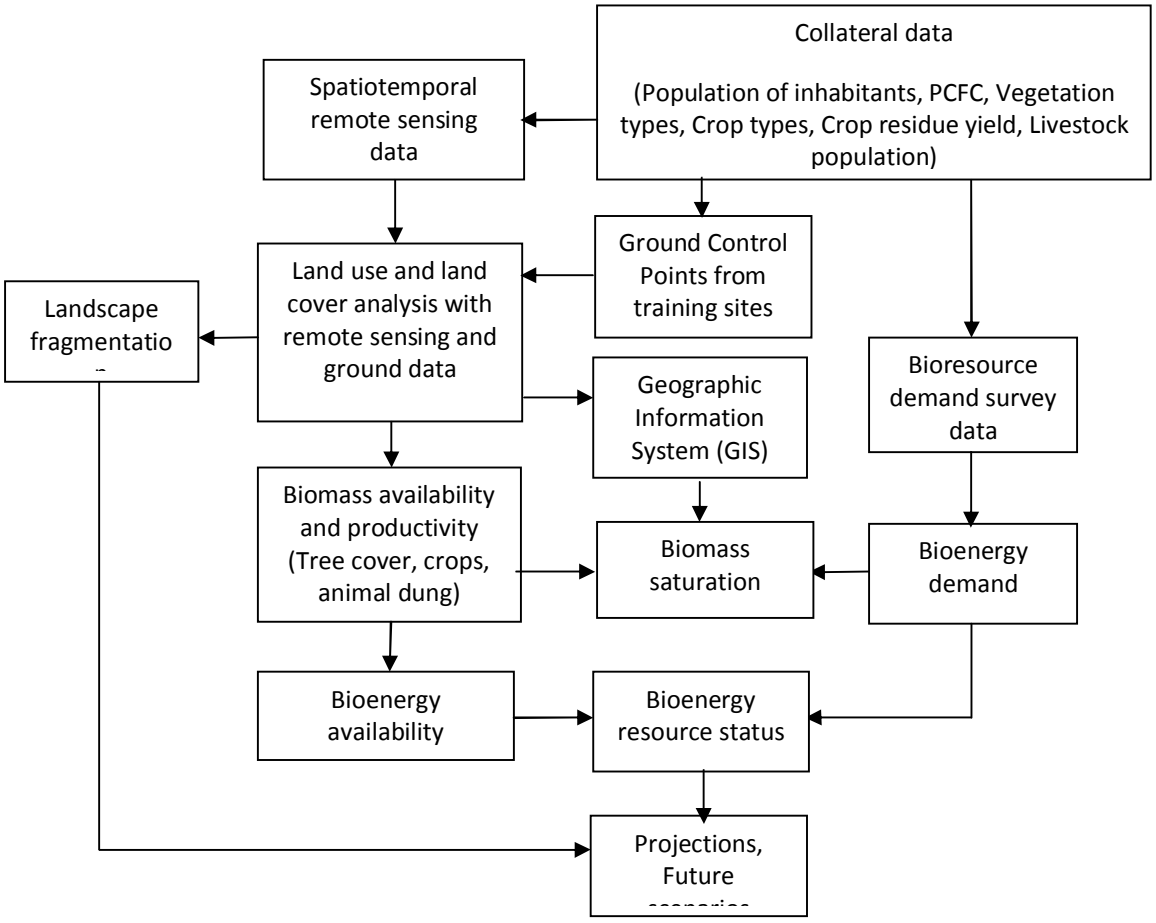

Figure 4a: Land cover classification of 2005/06 satellite image with vegetation type identified for Solan

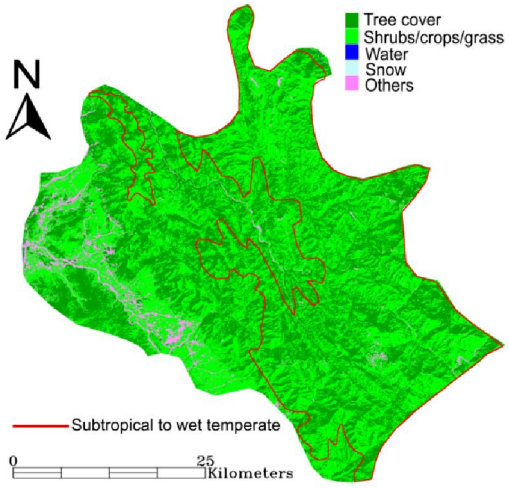

Figure 4b: Land cover classification of 2005/06 satellite image with vegetation type identified for Shimla

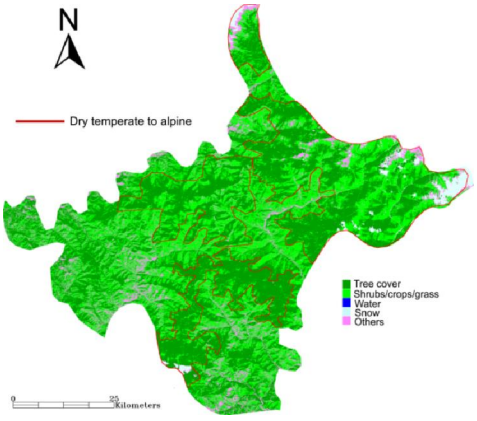

Figure 4c: Land cover classification of 2005/06 satellite image for Lahaul Spiti

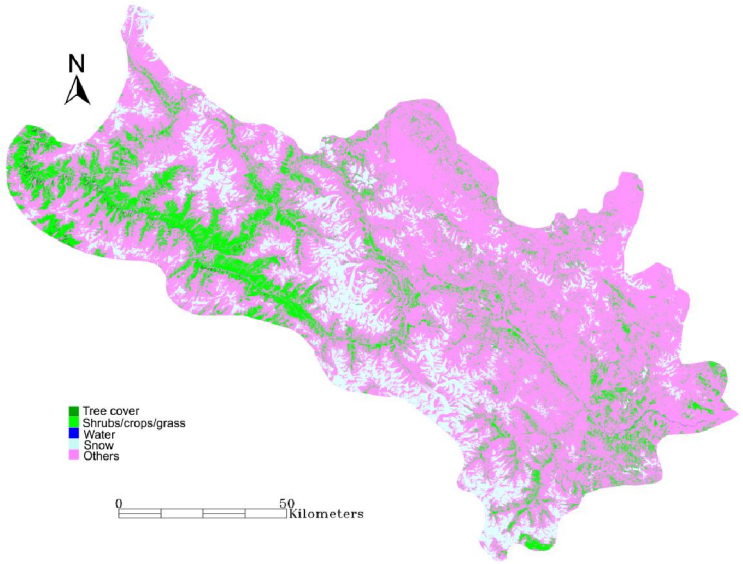

Table 6: GMLC based temporal land cover classification results for Solan, Shimla and Lahaul Spiti

District	Year	Tree cover		Shrubs/crops/grass		Water		Snow		Others	
		ha	%	ha	%	ha	%	ha	%	ha	%
Solan	1989	97665.43	47.70	101291.19	49.47	24.37	0.01	0.00	0.00	5774.69	2.8
	2000	94508.19	46.02	102382.68	49.85	24.39	0.01	0.00	0.00	8469.95	4.1
	2005	89354.01	43.51	107318.57	52.26	26.28	0.01	0.00	0.00	8669.05	4.2
Shimla	1989	249589.62	52.55	190807.40	40.17	10.88	0.00	9373.37	1.97	25176.71	5.3
	2000	232780.26	48.98	191295.96	40.25	28.98	0.01	9092.59	1.91	42074.63	8.8
	2005	231767.28	48.85	189457.75	39.93	1.44	0.00	9499.76	2.00	43766.50	9.2
Lahaul Spiti	1989	7215.61	0.51	166665.31	11.67	290.46	0.02	253642.97	17.77	999896.33	70.0
	2000	8060.11	0.56	226480.31	15.86	478.74	0.03	216714.47	15.18	976327.38	68.3
	2005	5187.92	0.36	203383.35	14.24	497.75	0.03	200516.52	14.04	1018475.48	71.3

Table 7: Types of vegetation identified and extent of tree cover (in hectares) mapped in different districts

District	Tropical to subtropical	Wet temperate	Dry temperate to subalpine	Total
Solan	40051.97	49302.04	0.00	89354.01
Shimla	0.00	99474.43	132292.85	231767.28
Lahaul Spiti	0.00	0.00	5187.92	5187.92

Table 8: The lower, moderate and upper case ANP_{tree} (t/ha/yr) values of different vegetation

Scenario	Tropical to subtropical	Wet temperate	Dry temperate to subalpine
Lower case	3.375	7.75	3.65
Moderate case	6.8875	10.93	7.98
Upper case	10.4	14.10	12.30

Table 9: Woody biomass availability (kilo t/yr) from different vegetation types of three districts for lower, moderate and upper case ANP_{tree}

District	Scenario	Tropical to subtropical	Wet temperate	Dry temperate to subalpine	Total
Solan	Lower case	135.18	382.09	0.00	517.27
	Moderate case	275.86	538.62	0.00	814.48
	Upper case	416.54	695.16	0.00	1111.70
Shimla	Lower case	0.00	770.93	482.87	1253.80
	Moderate case	0.00	1086.76	1055.04	2141.79
	Upper case	0.00	1402.59	1627.20	3029.79
Lahaul Spiti	Lower case	0.00	0.00	18.94	18.94
	Moderate case	0.00	0.00	41.37	41.37
	Upper case	0.00	0.00	63.81	63.81

Table 10: PCFC estimated and total fuelwood demand for different scenarios in three districts projected for the year 2006

District	Scenario	PCFC (kg/day)	Total fuelwood demand (kilo tonnes/yr)

Solan	Lower case	0.46	97.50
	Moderate case	0.89	188.65
	Higher case	1.32	279.79
Shimla	Lower case	1.9	544.28
	Moderate case	2.29	656.00
	Higher case	2.68	767.72
Lahaul	Lower case	0.89	11.13
	Moderate case	1.9	23.76
	Higher case	2.91	36.39

The annual bioenergy equivalent of agro residues (from cereals, pulses, oilseeds, cotton and sugarcane) in Solan is 698925 million kcal, Shimla is 443124 million kcal and Lahaul Spiti is 5356 million kcal. However, we have considered only 50% of the agro residues available for energy purposes (fuel ratio). The total annual production of agro residues and agro bioenergy availability in the three districts are given in Table 11. Figure 5 shows that total annual bioenergy from agro–residues is the highest in Solan and least in Lahaul Spiti. Cereals and oilseeds are the only sources of agro bioenergy in Lahaul Spiti. Among all crops, cereals have the highest bioenergy potential in all districts, followed by pulses.

Table 12 gives the different cases of dung yield from livestock found in Himachal Pradesh. Considering the moderate case of dung yield, total dung generation is the highest in Shimla and least in Lahaul Spiti. Cattles, buffaloes and goats are the major sources of animal dung in Solan and contributes nearly 615.3 kilo tonnes annually. Since these are mostly stall fed, the actual availability is higher in the district. Apart from these animals, Shimla has additional livestock varieties of sheep, horses and mules, together generating 778.7 kilo tonnes of dung annually. The cold district of Lahaul Spiti has cattle, yak, sheep, buffaloe, goat and horses generating 36.6 kilo tonnes of annual dung. Total annual dung yield from livestock, their biogas generation potential and energy equivalents are estimated for lower, moderate and upper case dung yield values (Table 13). The annual biogas generation in Solan is 8.7–35.6 million m^3, Shimla is 12.9–43.2 million m^3 and Lahaul Spiti is 0.8–1.9 million m^3.

Figure 5: Total energy equivalent of agro residues produced in Solan, Shimla and Lahaul Spiti

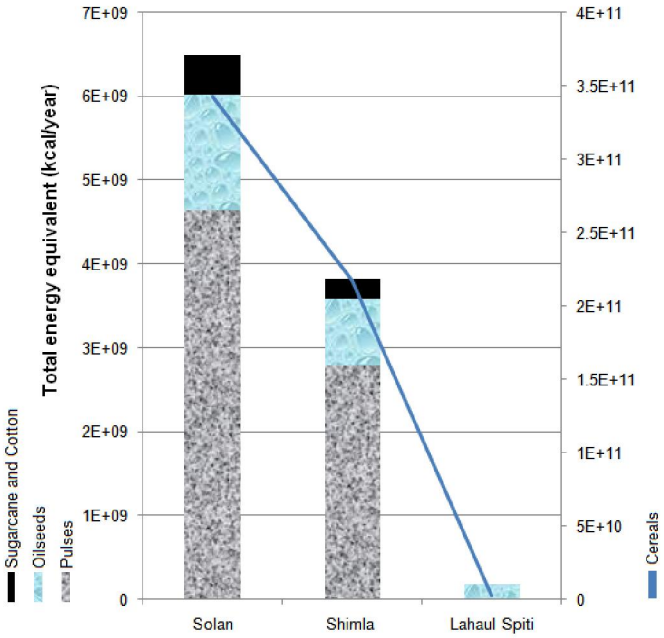

Table 11: Area, residue production and energy equivalent for different crops in Solan, Shimla and Lahaul Spiti

CROP	NAME	Residue type	Solan			Shimla			Lahaul Spiti	
			Area (ha)	Residue produced (t/yr)	Energy equivalent (kcal/yr)	Area (ha)	Residue produced (t/yr)	Energy equivalent (kcal/yr)	Area (ha)	Residue produced
CEREALS	Rice	Husk	4742	2530	4.00E+09	1981	586	9.00E+08	0	
		Stalk		13088	2.00E+10		3031	5.00E+09		
	Wheat	Stalk	24694	58080	1.00E+11	15104	24891	4.00E+10	81	
	Bajra	Cobs	0	0	0	3	1	1.00E+06	0	
		Husk		0	0		1	1.00E+06		
		Stalk		0	0		5	9.00E+06		
	Maize	Cobs	22852	12290	2.00E+10	13896	8763	2.00E+10	64	

		Husk		9004	1.00E+10		6420	1.00E+10		
		Stalk		90037	2.00E+11		64200	1.00E+11		2
	Barley	Stalk	1682	1880	3.00E+09	4704	6054	9.00E+09	592	9
	Others	Stalk	0	0	0	4049	4195	6.00E+09	107	
PULSES	**Gram**	Stalk	315	305	5.00E+08	29	33	6.00E+07	0	
	Tur/arhar	Husk	0	0	0	70	4	6.00E+06	0	
		Stalk		0	0		35	5.00E+07		
	Kharif	Husk	1695	232	3.00E+08	4416	215	3.00E+08	27	
		Stalk		1417	2.00E+09		1312	2.00E+09		
	Rabi	Stalk	908	730	1.00E+09	48	32	6.00E+07	0	
OILSEEDS	**Groundnut**	Shell	14	4	8.00E+06	8	1	1.00E+06	0	
		Stalk		25	5.00E+07		4	8.00E+06		
	Sesamum	Stalk	320	96	1.00E+08	40	13	2.00E+07	0	
	Rapeseed & Mustard	Husk & Stalk	414	304	5.00E+08	601	361	6.00E+08	68	
	Soyabeen	Stalk	46	107	2.00E+08	39	89	1.00E+08	0	
	Others	Stalk	684	274	5.00E+08	7	3	5.00E+06	0	
MISCELLANEOUS	**Cotton**	Shell & husk	53	84	1.00E+08	0	0	0	0	
		Stalk		159	2.00E+08		159	2.00E+08		
	Sugarcane	Bagasse	189	54	9.00E+07	0	0	0	0	
		Top & leaves		8	1.00E+07		0	0		

Table 12: Lower, moderate and upper case dung yield (kg/head/day) considered for livestock

Livestock	Cattle	Buffaloe	Yak	Mithun	Sheep	Goat	Horse	Pony	Mule	Donkey	Pig	Camel
Lower case	2.87	2.65	4.50	4.50	0.10	0.10	1.72	1.72	0.94	0.94	0.34	2.49
Moderate case	6.44	8.83	4.50	4.50	0.21	0.23	3.90	3.90	0.94	0.94	0.34	2.49
Upper case	10.00	15.00	4.50	4.50	0.35	0.35	6.08	6.08	0.94	0.94	0.34	2.49

Table 13: Livestock types, biogas generation and energy equivalent for different dung yield scenarios (L–lower case, M–Moderate case, U–Uppercase) in Solan, Shimla and Lahaul Spiti

Livestock		Solan			Shimla			Lahaul Spiti		
		Total dung (kg/yr)	Biogas(m 3/yr)	equivalent (kcal/yr)	Total dung (kg/y)	Biogas(m 3/yr)	equivalent (kcal/y)	Total dung (kg/y)	Biogas (m3/yr)	equivalent (kcal/y)
Cattle	L	2.E+08	5.E+06	3.E+10	3.E+08	1.E+07	6.E+10	1.E+07	5.E+05	2.E+09
	M	3.E+08	1.E+07	6.E+10	7.E+08	3.E+07	1.E+11	3.E+07	1.E+06	5.E+09
	U	5.E+08	2.E+07	9.E+10	1.E+09	4.E+07	2.E+11	4.E+07	2.E+06	8.E+09
Buffaloe	L	8.E+07	3.E+06	1.E+10	1.E+07	5.E+05	2.E+09	0	0	0
	M	3.E+08	1.E+07	5.E+10	4.E+07	2.E+06	8.E+09	0	0	0
	U	5.E+08	2.E+07	8.E+10	7.E+07	3.E+06	1.E+10	0	0	0
Yak	L	0	0	0	3.E+04	1.E+03	5.E+06	2.E+06	8.E+04	4.E+08
	M	0	0	0	3.E+04	1.E+03	5.E+06	2.E+06	8.E+04	4.E+08
	U	0	0	0	3.E+04	1.E+03	5.E+06	2.E+06	8.E+04	4.E+08
Mithun	L	0	0	0	0	0	0	3.E+03	1.E+02	6.E+05
	M	0	0	0	0	0	0	3.E+03	1.E+02	6.E+05
	U	0	0	0	0	0	0	3.E+03	1.E+02	6.E+05
Sheep	L	3.E+05	1.E+04	5.E+07	1.E+07	4.E+05	2.E+09	4.E+06	2.E+05	8.E+08
	M	2.E+05	7.E+03	3.E+07	7.E+06	3.E+05	1.E+09	3.E+06	1.E+05	5.E+08
	U	9.E+04	3.E+03	2.E+07	3.E+06	1.E+05	6.E+08	1.E+06	5.E+04	2.E+08
Goat	L	1.E+07	4.E+05	2.E+09	1.E+07	4.E+05	2.E+09	1.E+06	4.E+04	2.E+08
	M	7.E+06	2.E+05	1.E+09	8.E+06	3.E+05	1.E+09	7.E+05	2.E+04	1.E+08
	U	3.E+06	1.E+05	5.E+08	3.E+06	1.E+05	6.E+08	3.E+05	1.E+04	6.E+07
Horse	L	2.E+05	7.E+03	3.E+07	7.E+05	2.E+04	1.E+08	1.E+04	4.E+02	2.E+06
	M	4.E+05	2.E+04	8.E+07	2.E+06	6.E+04	3.E+08	2.E+04	9.E+02	4.E+06
	U	7.E+05	2.E+04	1.E+08	2.E+06	9.E+04	4.E+08	4.E+04	1.E+03	7.E+06
Pony	L	3.E+04	1.E+03	6.E+06	6.E+05	2.E+04	1.E+08	6.E+05	2.E+04	1.E+08
	M	8.E+04	3.E+03	1.E+07	1.E+06	5.E+04	2.E+08	1.E+06	5.E+04	2.E+08

	U	1.E+05	4.E+03	2.E+07	2.E+06	8.E+04	4.E+08	2.E+06	8.E+04	4.E+08
Mule	**L**	3.E+05	9.E+03	5.E+07	1.E+06	3.E+04	2.E+08	0	0	0
	M	3.E+05	9.E+03	5.E+07	1.E+06	3.E+04	2.E+08	0	0	0
	U	3.E+05	9.E+03	5.E+07	1.E+06	3.E+04	2.E+08	0	0	0
Donkey	**L**	6.E+04	2.E+03	1.E+07	3.E+05	1.E+04	5.E+07	7.E+05	2.E+04	1.E+08
	M	6.E+04	2.E+03	1.E+07	3.E+05	1.E+04	5.E+07	7.E+05	2.E+04	1.E+08
	U	6.E+04	2.E+03	1.E+07	3.E+05	1.E+04	5.E+07	7.E+05	2.E+04	1.E+08
Pig	**L**	2.E+04	9.E+02	4.E+06	3.E+04	1.E+03	5.E+06	0	0	0
	M	2.E+04	9.E+02	4.E+06	3.E+04	1.E+03	5.E+06	0	0	0
	U	2.E+04	9.E+02	4.E+06	3.E+04	1.E+03	5.E+06	0	0	0
Camel	**L**	9.E+02	3.E+01	2.E+05	3.E+03	1.E+02	5.E+05	0	0	0
	M	9.E+02	3.E+01	2.E+05	3.E+03	1.E+02	5.E+05	0	0	0
	U	9.E+02	3.E+01	2.E+05	3.E+03	1.E+02	5.E+05	0	0	0

Considering the multiple uses of woody biomass, agro residues and animal dung, the actual availability of these bioresources for fuel purposes are accounted in high (75%), medium (50%) and low (25%) supply scenarios. Figure 6 highlights these bioenergy availability scenarios (considering moderate case production for woody biomass and animal dung) and their prospects of meeting the lower, moderate and upper case bioenergy demands in the three districts. The bioenergy resource status of the three districts are represented in Figure 7. In solan, higher case bioenergy demand cannot be met by the low (25%) bioenergy availability scenario even after including agro residues and biogas energy from animal dung. This scenario points at a bioenergy deficit status for the region (Figure 7). However, moderate and lower case demand is being met by the fuelwood resources. In Shimla, even lower case bioenergy demand is met by the low (25%) availability scenario of woody biomass. Additional bioenergy from agro and animal residues (low) fail to meet the moderate and higher case demand. As seen in Figure 7, this scenario represents a critical bioenergy status for Shimla. However, medium (50%) availability of woody biomass is sufficient for a higher case demand. In Lahaul Spiti, high (75%) availability of woody biomass sustains at least moderate case demand, while medium (50%) availability sustains only lower case demand. Even a high total bioenergy availability scenario, cannot sustain the higher case demand of the region. This indicates a very critical bioenergy deficit status in the cold district of Lahaul Spiti.

Figure 6: Different availability scenarios of bioenergy resources and cases of bioenergy demand in Solan, Shimla and Lahaul Spiti

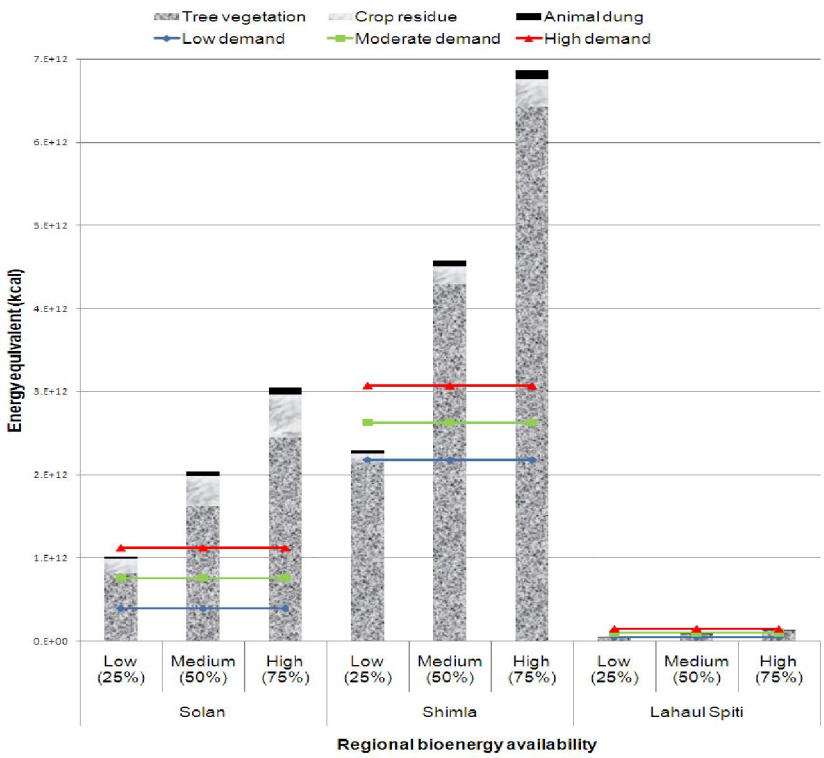

Figure 7: Bioenergy resource status of Solan, Shimla and Lahaul Spiti

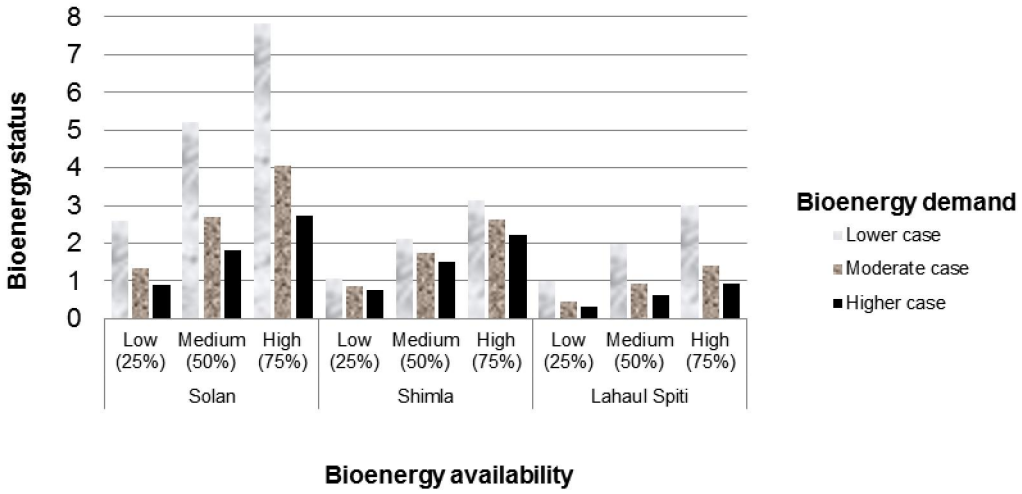

Figures 8a and 8b represent biomass saturation in the proximity of 7 villages in Moolbari watershed for higher (2.63 kg/day) and lower (1.9 kg/day) case bioenergy demand scenarios respectively. It is observed that the villages of Moolbari, Ganeog, Kiuru and Dochi have limited availability of fuelwood resource in their vicinity and people traverse longer distances to meet their needs. The villages of Tikri and Niaog have relatively higher fuelwood availability while Shanohal has the highest among all. The

forest fragmentation study conducted in the same watershed reveals the extent of forest degradation that has occurred from 1972 to 2007 (Figure 9a). The overall accuracy of image classification is between 81–89% and results show that the extents of forest cover which was high in 1972 eventually declined by 5.59% in 2007. It is observed that the regions prone to higher forest fragmentation levels inhabit villages like Moolbari, Ganeog, Kiuru and Dochi with lower biomass saturation. This highlights the anthropogenic influence in forest fragmentation occurred over a period of time. A similar analysis of the tree cover changes in Mandhala watershed during the period 1972 to 2007 also exposes the forest fragmentation in its landscape (Figure 9b). Such grassroots level resource constraints are not discerned in the district level bioresource assessment and hence call for further disaggregation in assessment studies.

Figure 8a: Bio–mass saturation map for Moolbari, Case–I

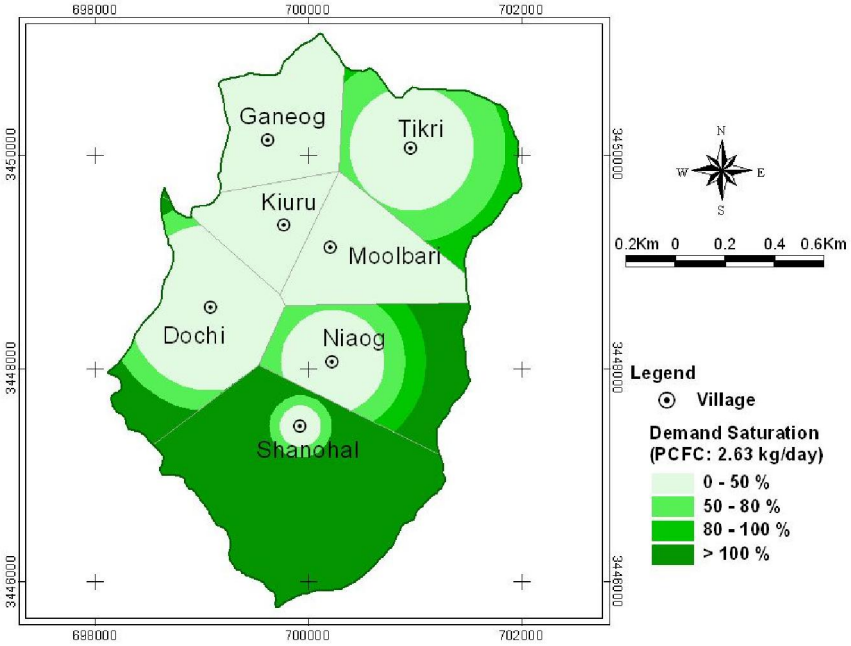

Figure 8b: Bio–mass saturation map for Moolbari, Case–II

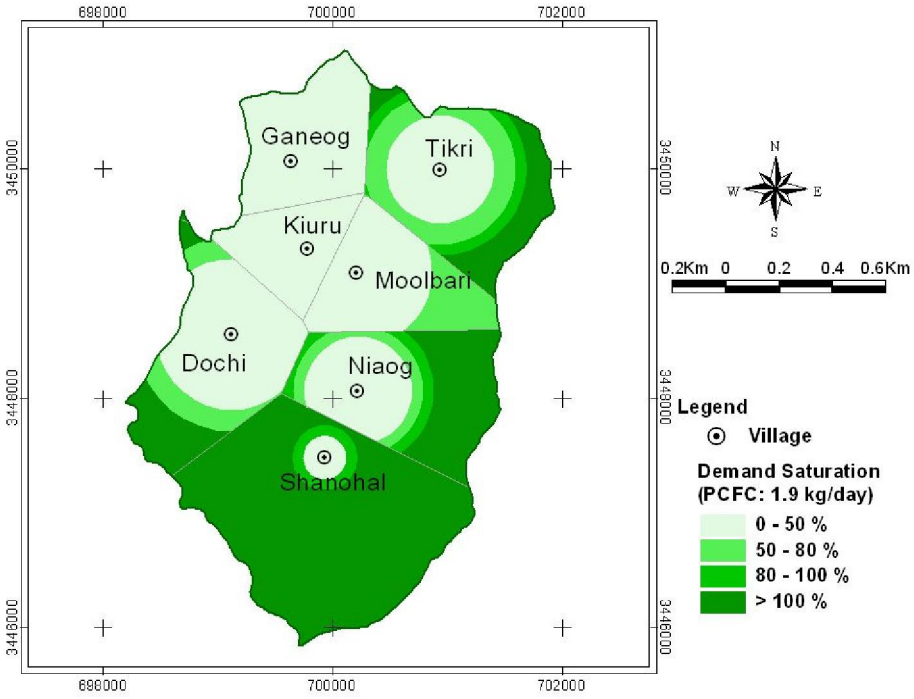

Figure 9a: Classified images of Mandhala watershed showing land cover and land use changes from 1972 to 2007

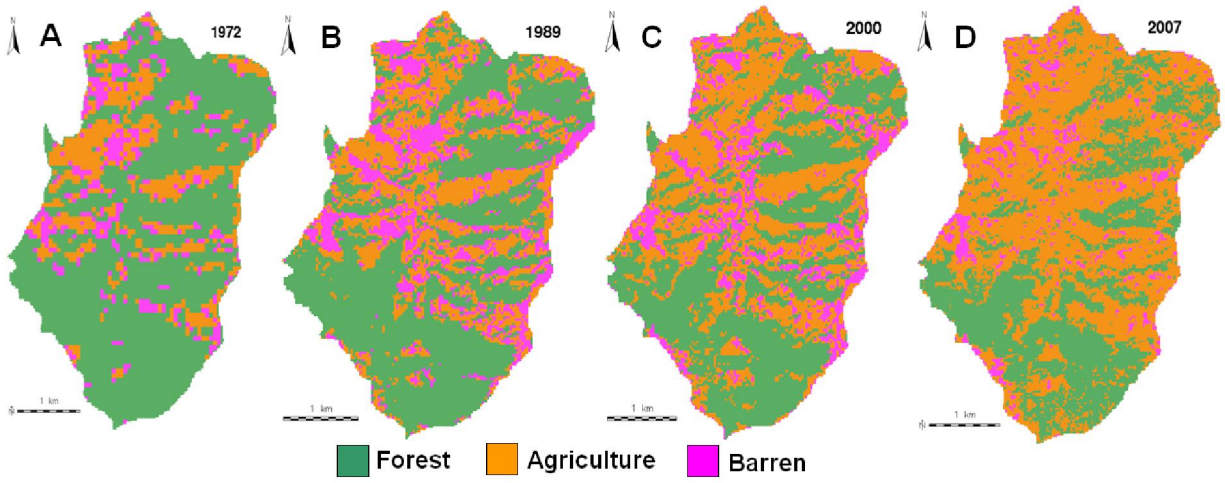

Figure 9b: Tree cover change from 1972 to 2007 in Mandhala watershed

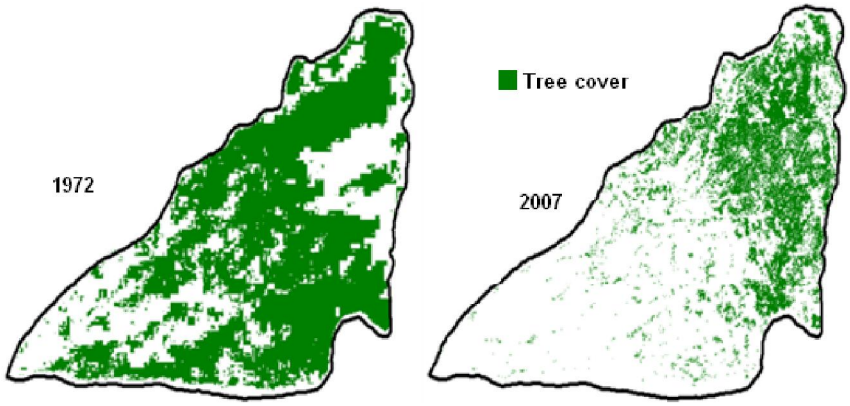

DISCUSSION

The bioenergy resource status of the three districts highlights highly pronounced scarcity of bioresources. The estimations are based on the moderate (average of upper and lower) case of bioenergy production. A possible lower case of production worsens the bioenergy status further. Increase in population results in increasing bioenergy demand and its impact is felt more on regions with higher PCFC. Especially in critical bioenergy deficit regions like Lahaul Spiti, with the highest PCFC an energy crisis is imminent. The dwindling forest resources may not suffice the domestic, commercial and industrial needs of an ever increasing population. This results in shortage of fuelwood availability even for sustenance. In such situations people tend towards alternative bioenergy resources in an inefficient and ad hoc manner with dire consequences of pollution and conflicts with other traditional utilities. Efficient utilization of fuelwood, agro residues and animal dung could however reduce the pressure on forest resources. This demands site specific and innovative solutions with ultimate priority for the bioenergy deficit regions where even the total estimated bioenergy availability cannot meet the demands of an ever increasing population. Nevertheless, the regions deemed as bioenergy surplus in these estimations should not be marginalized while adopting such methodologies since they are under pressure. Potential bioresource crunch is imminent in the absence of immediate intervention perceptibly leading to deforestation.

Traditional stoves used for burning wood in these hill regions are thermally inefficient. They emit more smoke causing health hazards to women and children. Energy efficient, smokeless and innovative ASTRA cookstoves with thermal efficiency above 30% will reduce the fuel consumption by 42% [61, 65]. In mountains regions the demand as well as utility of fuelwood varies with altitude and hence the traditional designs differ zone–wise. The National Program on Improved Cookstoves (NPIC) introduced in Himachal Pradesh in 1983, has not given the desired results due to technical and institutional problems. The improved and efficient designs were not accepted by the inhabitants who were used to their traditional models. In recent times, need and location specific cookstoves are being designed so as to improve the prospects of social acceptance. Improvements in technical knowhow, institutional support, women awareness, publicity campaigns and subsidies are proposed for long term success of the national program [5].

Biogas from animal residues is an important alternative energy source in fuelwood deficient regions. Compared to traditional burning of animal dung cakes, biogas is efficient, cleaner and easier to

distribute in a community based system. The potential of small 1 m^3 capacity biogas plants in rural regions is enormous [62]. Dung from stall–fed livestock could be used for biogas generation and the slurry as nitrogen rich manure which is not available during direct burning of dung–cakes. The state has an estimated potential to install nearly 0.332 million family size (2 m^3) biogas plants which could produce 0.515 million m^3 of biogas per day with energy equivalent to about 1801.1 tonnes of fuelwood. However due to the lacunae in planning, technical, organizational and social aspects, biogas program introduced in the state in 1982 has not been successful [63, 61]. Performance of biogas plants in colder regions is relatively poor. Warmer climate in lowland regions of Solan and Shimla is conducive for biogas generation with the existing technology. The annual energy from biogas generation is 55373 million kcal in Solan, 70081 million kcal in Shimla and 3291 million kcal in Lahaul Spiti, considering the moderate case of production, medium scenario (50%) of availability and lower energy equivalent for conversion. Biogas has enormous potential to replace fuelwood and can save up to 13843, 17520 and 823 tonnes of fuelwood annually in Solan, Shimla and Lahaul Spiti respectively. Livestock in Shimla and Lahaul Spiti also include horse and pony which are mostly stall–fed. It has been observed that a 20 % replacement of cattle dung can be made by horse dung for operating family size biogas plants without much reduction in their gas production or encountering any operational problem [64]. The increased grazing based livestock farming in Lahaul Spiti results in lesser actual availability of animal dung for biogas generation. Stall–fed livestock facilitate dung collection as well as reduce grazing in forests [61]. Hence site specific innovative solutions need to be introduced to revamp and enhance the biogas prospects in these hill regions.

Agro residues generated are to be judiciously utilized for energy without compromising their alternative utilities as fodder, manure and mulch. The annual energy from agro residues is 349463 million kcal in Solan, 221562 million kcal in Shimla and 2678 million kcal in Lahaul Spiti, considering the medium scenario (50%) of availability and lower energy equivalents for conversion. This can save up to 87366, 55390 and 669 tonnes of trees annually in Solan, Shimla and Lahaul Spiti respectively. Process based residue like rice husk has high energy potential if utilized effectively. Commercial energy sources like LPG and kerosene distribution system need revitalization so as to ensure wider absorption into the local energy system. As observed in the land cover analyses, Solan, Shimla and Lahaul Spiti have large open spaces. The extent of waste lands could be prospected through government records for energy plantations. Multiple tree species with high growth and regeneration potential need to be introduced in the regions with bioenergy deficit status as high priority. Species level mapping of fuelwood trees could be carried out using remote sensing and geospatial tools [66]. The exotic *Lantana camara* weeds spread in the hills of Solan could be replaced with native trees as energy plantations. The upland regions of Lahual Spiti with critical bioenergy deficit support lesser vegetation. Hence certain studies suggest energy plantations in lower altitude tribal villages to sustain the higher energy demands in the higher altitude villages [40]. Energy plantation provides employment opportunities for the mountain people, provides sufficient time for the natural restoration of degraded forests and helps sequester more carbon dioxide from the atmosphere. Joint forest management practices need to be strengthened through local support.

Importantly, the ultimate benefit of regional bioenergy resource assessment exercise is realized through an efficient and user friendly BEPA DSS. An executable file is provided for this application and by running this, a form with Login, Level of Analysis and Resources Menu options are displayed. After logging with the user information, the Level of Analysis option is enabled for hierarchical administrative levels of analysis such as state, district, taluk, town and village levels. This option also enables user to either input retrieve or edit data in the database. This includes data entry of forest type, productivity, year of estimate and spatial extent of the forest. Similar options are available for

computing bioenergy from agriculture and livestock sectors. The GIS enabled features of the DSS facilitates simpler interpretation of spatial resource and demand variations as well as their quantification. Figures 10a–b demonstrate some of the visual features of BEPA DSS. The complexity in collating, processing, analyzing, interpreting and outputting information on bioenergy resources is simplified through the DSS designed. This helps the planner to act according to the regional energy scenarios which are often diluted in the national decision making process.

Figure 110a: BEPA DSS visualization of forest bioresource

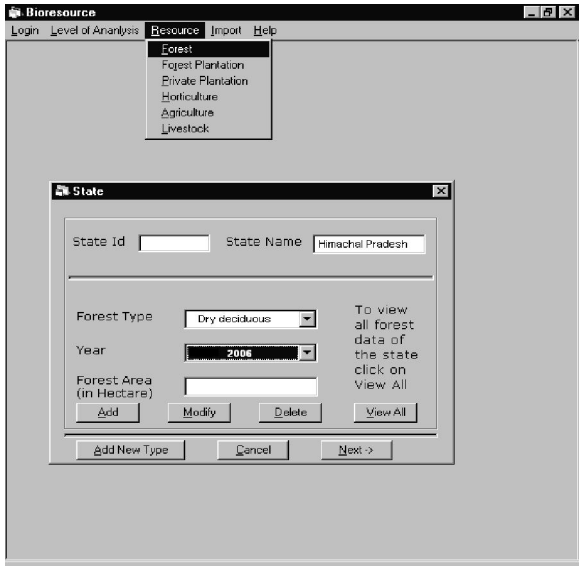

Figure 10b: BEPA DSS visualization of agricultural bioresource

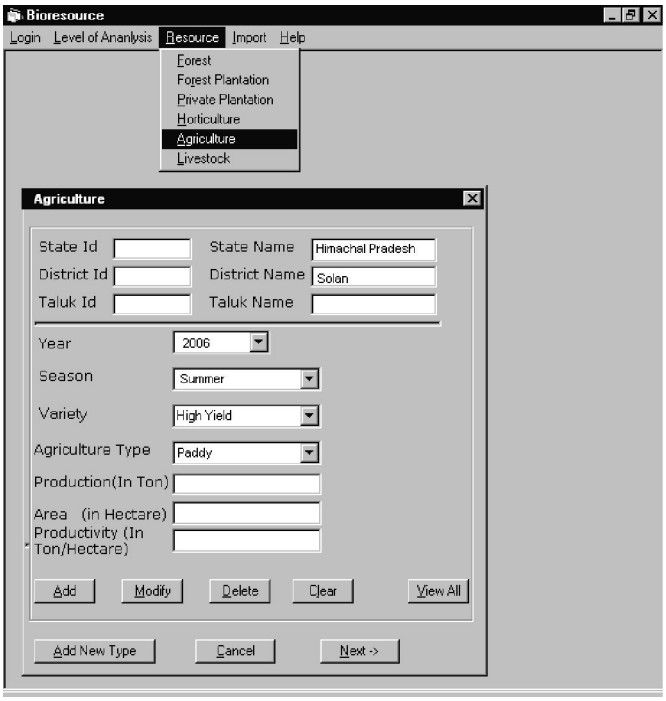

CONCLUSION

The bioenergy resource statuses of Solan, Shimla and Lahaul Spiti districts are assessed for different resource availability scenarios and demand cases. PCFC varies with seasons and regions as 0.48–1.32 kg/person/day (Solan), 1.9–2.68 (Shimla) and 0.89–2.91 kg/person/day (Lahual Spiti). The total tree cover in the study area is 43.51% (Solan), 48.85% (Shimla) and 0.36% (Lahaul Spiti) providing annual woody biomass of 517.3–1111.7 kilo tonnes (Solan), 1253.8–3029.8 kilo tonnes (Shimla) and 18.9–63.8 kilo tonnes (Lahaul Spiti). The annual bioenergy potential of agro residues (considering 50% for fuel purpose) is 349463 million kcal (Solan), 221562 million kcal (Shimla) and 2678 million kcal (Lahaul Spiti). The annual biogas generation potential is 8.7–35.6 million m^3 (Solan), 12.9–43.2 million m^3 (Shimla) and 0.8–1.9 million m^3 (Lahaul Spiti). Bioenergy resource crunch is more pronounced in the higher elevations while scarce resource availability scenarios create similar conditions in lower elevations as well. Possible alternatives are proposed for ensuring proper ecological health in the mountain areas. Reiterating the importance of further disaggregated bioresource analysis, village level forest fragmentation and biomass saturation studies are also performed. Proximity of energy demand centers like villages create shortage of fuelwood and increase deforestation. Enhancing the possibility of regional bioenergy resource planning, a DSS has been designed to support energy planners and policy makers.

ACKNOWLEDGEMENT

We are grateful to NRDMS division, Ministry of Science and Technology (DST), Government of India and Indian institute of Science for the financial and infrastructure support.

REFERENCES

1] Bhati JP, Singh R, Rathore MS, Sharma LR, Diversity of mountain farming systems in Himachal Pradesh, India. Sustainable mountain agriculture – Farmers'strategies and innovative approaches. ICIMOD 1992, Kathmandu: Oxford and IBH Publishing Co Pvt Ltd;2

2] Rijal K, Energy use in mountain areas–emerging issues and future priorities. ICIMOD 1997, Kathmandu

3] Rijal K, Energy use in mountain areas–trends and patterns in China, India, Nepal and Pakistan. . ICIMOD 1999, Kathmandu

4] Kumar M, Sharma CM, Fuelwood consumtion patterns at different altitudes in rural areas of Garhwal Himlayas. Biomass and Bioenergy 2009; 33:1413 – 1418

5] Aggarwal RK, Chandel SS, Review of Improved Cookstoves Programme in Western Himalayan State of India, Biomass and Bioenergy 2004;27:131 – 144

6] Ramachandra TV, RIEP:Regional Intergrated Energy Plan, Renewable and Sustainable Energy Reviews 2009;13(2):285–317

7] Ramachandra TV,Vamsee Krishna S, Shruthi BV, Decision Support System to assess regional biomass energy potential, International Journal of Green Energy 2004;11(4):407–428.

8] Perimenis A, Walimwipi H, Zinoviev S, Muller–Langer F, Miertus S, Development of a decision support tool for the assessment of biofuels, Energy Policy 2011;39:1782–1793

9] Noon CE, Daly MJ, GIS–based biomass resource assessment with BRAVO, Biomass and Bioenergy 1996;10:101–109

10] Ayoub N, Wang K, Kagiyama T, Seki H, Naka Y, A planning support system for biomass–based power generation, 16th European Symposium on Computer Aided Process Engineering and 9th International Symposium on Process Systems Engineering, Elsevier 2006

11] Frombo F, Minciardi R, Robba M, Sacile R, A decision support system for planning biomass–based energy production, Energy 2009;34:362–369

12] Statistical Data of Himachal Pradesh upto 2009–10, Himachal Pradesh Planning Department, Govt. of Himachal Pradesh, Accessed on August 2 2010 < http://hpplanning.nic.in/Statistical data of Himachal Pradesh upto 2009–10.pdf>

13] Bhagat RM, Singh S, Kumar V, Kalia V, Sood C, Pradhan S, Immerzeel W, Shrestha B, Developing Himachal Pradesh Agricultural Systems Information Files (HASIF) and Tools for Decision Support Systems for Niche Based Hill Farming, CSKHPAU–ICIMOD 2006,Palampur, Himachal Pradesh

14] Champion HG, Seth SK, A revised survey of the forest types in India, Govt of India press 1968, Nasik

15] Ramachandra TV, Kamakshi G, Shruthi BV, Bioresource status in Karnataka, Renewable and Sustainable Energy Reviews 2004;8:1–47

16] Singh SP, Singh JS, Analytical conceptual plant to reforest Central Himalaya for sustainable development, Environmental Management 1991;15(3):369–379.
17] Singh JS, Singh SP, Forest vegetation of the Himalaya, The Botanical Review 1987;53(1);80–192
18] Sharma DP, Biomass distribution in sub tropical forest of solan forest division (HP), Indian J Ecol 2009; 36(1):1–5,
19] Singh R.P, Primary production and energy dynamics of tropical deciduous forest in Chandraprabha region, Varanasi, Ph.D. thesis, Banaras Hindu University, Varanasi. India.
20] Holdgate M, The ecological significance of biological diversity, Ambio 1996, 25(6)
21] Agarwal SK, Swarnalata Tiwari, Dubey PS, Biodiversity and environment, APH Publishing corporation, New Delhi
22] Singh B, A study of silvicultural practices, biomass,productivity and nutrient cycling in poplar plantations of sub–Himalayan tract of U.P. State, Ph.D. thesis. Kumaun University 1989, Nainital.
23] Tripathi SK, Singh,KP, Productivity and nutrient cycling in recently harvested and mature bamboo savannas in the dry tropics, Journal of Applied Ecology 1994;31(1): 109–124
24] Das DK, Chaturvedi OP, Mandal MP, Kumar R, Effect of tree plantations on biomass and primary productivity of herbaceous vegetation in Eastern India, Tropical Ecology 2008;49(2): 95–101
25] Lodhiyal N, Lodhiyal LS, Pangtey YPS, Structure and Function of Shisham Forests in Central Himalaya, India: Dry Matter Dynamics, Annals of Botany 2001;89(1):41–54
26] Chaturvedi OP, Singh, JS, The structure and function of pine forest in Central Himalaya: I. Dry matter dynamics, Annals of Botany 1987;60:237–252.
27] Chaturvedi OP, Biomass structure, productivity and nutrient cycling in Pinus roxburghii forest. Ph.D. Thesis. Kumaun University 1983, Nainital.
28] Singh SP, JS Singh, An integrated ecological study of eastern Kumaun Himalaya,with emphasis on natural resources, Kumaun University 1982, Nainital
29] Singh SP, Adhikari BS, Zobel DB, Biomass, Productivity, Leaf Longevity, and Forest Structure in the Central Himalaya, Ecological Monographs 1994, 64:401–421
30] Rawat YS, Plant biomass, net primary production and nutrient cycling in oak forests. Ph.D. Thesis. Kumaun University 1983, Nainital.
31] Nihlgard B, Lindgren L, Plant biomass, primary production and bioelements of three mature beech forest in southern Sweden. Oikos 1977;28: 95–104
32] Dhaulakhandi M, Rajwar GS, Kumar P, Primary productivity and system transfer functions in an alpine grassland of Western Garhwal Himalaya Tropical Ecology 2000;41(1): 99–101
33] Adhikari BS, Rawat YS, Singh SP, Structure and function of high altitude forests of central Himalaya, I.Dry matter dynamics, Annals of botany 1995;75:237–248
34] Bhutan Energy Data Directory 2005, Department of Energy 2007, Thimphu
35] Chenghui M, Liqiang M, Zhongliang Y, Peng L, Jianfeng S, Biomass and net productivity for spruce plantation, Journal of Forestry Research 1999; 10(1)
36] Garkot SC, Singh SP, Variation in NPP and biomass of forest in high mountains of central himalayas, Journal of vegetation Science 1995; 6:23–28
37] Crop production statistics information system, Directorate of Economics and Statistics, Government of India. Accessed on January 3 2011 <http://dacnet.nic.in/apy/>

38] Tulachan PM, Neupane A, Livestock in mixed farming systems of the Hindukush–himalayas– trends and sustainability, FAO– ICIMOD 1999, Kathmandu, Nepal
39] Teri Energy Data Directory and Yearbook 2010, TERI Press 2011, New Delhi
40] Rawat YS, Vishvakarma SCR, Todaria NP, Fuel wood consumption pattern of tribal communities in cold desert of the Lahaul valley, North–Western Himalaya, India, Biomass and Bioenergy 2009; 33:1547 – 1557
41] Bhatt BP, Sachan MS, Firewood consumption along an altitudinal gradient in mountain villages of India. Biomass and Bioenergy 2004; 27:69–75
42] Parikh J, The energy poverty and gender nexus in Himachal Pradesh, India– the impact of clean fuel access policy on women's empowerment, integrated research and action for development (IRADe) WECS, Energy Sector Synopsis Report, Government of Nepal, Accessed ob February 26 2011 <http://www.dfid.gov.uk/r4d/PDF/Outputs/Energy/R8346_finrep_parikh.pdf>
43] Vishvakarma SCR, Kuniyal JC, Singh GS, Indigenous Agroforestry system of North Western Himalaya. research for mountain development– some initiatives and accomplishments, gyanodaya prakashan, Nainital 1998; 99–118.
44] Rai SN, Chakrabarti SK. Demand and supply of fuel wood and timber in India, Indian Forester 2001; 263–79.
45] Bhatt BP, Negi AK, Todaria NP, Fuel wood consumption pattern at different altitudes in Garhwal Himalaya. Energy 1994; 19(4):465–8.
46] Pandey V, Singh JS. Energy flow relationship between agro and forest ecosystem in central Himalaya, Environment Conservation 1984;11:45–53.
47] Mahat TBS, Grigflin DM, Shephered KP. Human impacts on some forests of the middle hills of Nepal. Part 4: A detailed study in South–east Sindhu Palanchock and Northeast Kabhere Palanchock, Mountain Research and Development 1987;7: 114–34.
48] Kishore VVN, Renewable energy engineering and technology, TERI press 2008, New Delhi
49] Ramachandra TV, Joshi NV, Subramanian DK. Present and prospective role of bioenergy in regional energy system. Renewable and Sustainable Energy Reviews 2000;4:375–430.
50] Bhattacharya SC, Salam PA, Runqing H, Somashekar HI, Racelis DA, Rathnasiri PG, Yingyuad R, An assessment of the potential for non–plantation biomass resources in selected Asian countries for 2010, Biomass and Bioenergy 2005; 29:153–166
51] Abdallah MH, Energy potential from economically available crop residues in the sudan, Energy 1991;16(8):1153–1156
52] Gemtos TA, Tsiricoglou T, Harvesting of cotton residue for energy production, Biomass and Bioenergy 1999; 16: 51–59
53] Wilaipon P, Physical characteristics of maize cob briquette under moderate die pressure, American Journal of Applied Sciences 2007;4(12): 995–998
54] Department of Animal Husbandry, Government of Himachal Pradesh, Accessed on January 3 2011 <http://hpagrisnet.gov.in/animal–husbandry/Ahd%20Docs/18th%20Livestock%20Census–2007.aspx>
55] Recent trends in biogas technology for poverty reduction and sustainable development, United Nations ESCAP, Accessed on March 14 2011 < http://www.unapcaem.org/publication/F–Biogas.PDF>
56] Energy Sector Synopsis Report 2010, Water and Energy Commission Secretariat, Kathmandu, 2010, Accessed on March 14 2011 < http://www.wec.gov.np/>

57] Rhode D, Madsen DB, Brantingham PJ, Dargye T, Yaks, yak dung, and prehistoric human habitation of the Tibetan Plateau, Developments in Quaternary Science 2007;9:205–224
58] Tao J, Mancl K, Estimating manure production, storage size, and land application area, Accessed on March 17 2011 <http://ohioline.osu.edu/aex–fact/pdf/0715.pdf>
59] Mapping Himachal Pradesh Census Indicators 2001 and trends, CSKHPAU–ICIMOD 2006,Palampur, Himachal Pradesh
60] Mehta AC, National Institute of Educational Planning and Administration , Accessed on March 17 2011 <http://www.educationforallinindia.com/New%20Modules/module%20on%20enrolment%20and%20population%20projections.pdf>
61] Ramachandra, TV, Sreekantha , Purnima GB, Bioenergy status of Sharavathi river basin,Western Ghats, India, Energy & Environment 2007;18(5):591–613.
62] Ramachandra TV, Geographical System Information approach for regional biogas potential assessment, Research Journal of Environmental Sciences 2008;2(3):17–184
63] Singh,SP, Vatsa DK, Verma HN, Problems with biogas plants in Himachal Pradesh Bioresource Technology 1997;59:69–71
64] Kalia AK, Singh SP, Horse dung as a partial substitute for cattle dung for operating family–size biogas plants in a hilly region, Bioresource Technology 1998; 64:63–66
65] Ramachandra TV, Subramanian DK, Joshi NV, Gunaga SV, Harikantra RB, End use efficiencies in the domestic sector of Uttara Kannada District, Energy Conversion & Management 2000; 41: 833–845
66] Ramachandra TV, Mapping of fuelwood trees using geoinformatics, Renewable and Sustainable Energy Reviews 2010; 14: 642–654
67] Ramachandra TV, Vijaya Prasad BK, Samapika Padhy, Bioresource inventory using remote sensing for regional energy planning, *Proceedings of ISRS National Symposium on Remote Sensing Applications for Natural Resources Retrospective & Perspective, Bangalore* 1999*:* 245-256.

Publications

1. Ramachandra T.V., Uttam Kumar and Joshi N. V, 2012. Landscape Dynamics in Western Himalaya - Mandhala Watershed, Himachal Pradesh, India, Asian Journal of Geoinformatics, 12(1):22-35, http://www.geoinfo.ait.ac.th/ajg/index.php/journal/article/view/31/14
2. Ramachandra T V, Gautham Krishnadas and Rishabh Jain, 2012, Solar potential in the Himalayan Landscape, International Scholarly Research Network, ISRN Renewable Energy, 2012 (ID203149):13 pages, http://www.isrn.com/journals/re/aip/203149/, doi:10.5402/2012/203149
3. Ramachandra T V and Gautham Krishnadas, 2012. Prospects and Challenges of Decentralized Wind Applications in the Himalayan Terrain, Journal of Energy Bioscience, 3(1); http://bio.sophiapublisher.com/jeb-13
4. Ramachandra T. V., Gautham Krishnadas, Bharath Setturu, Uttam Kumar, 2012. Regional Bioenergy Planning for Sustainability in Himachal Pradesh, India, Journal of Energy, Environment & Carbon Credits, 2(1): 13-49
5. Ramachandra T V, Bharath H Aithal and Sanna Durgappa, 2011. Land Surface Temperature Analysis in an Urbanising Landscape through Multi-Resolution data, Research & Reviews : Journal of Space Science & Technology, http://www.stmjournals.com/sci/index.php/RRJSST 1(1): 1-12
6. Rajasri Ray, Gururaja K V and Ramachandra T V, 2011. Predictive distribution modeling for rare Himalayan medicinal plant *Berberis aristata* DC. Journal of Environment Biology, 32 (2011):725-730
7. Ramachandra T. V. and Uttam Kumar, 2011. Characterisation of Landscape with Forest Fragmentation Dynamics, *Journal of Geographic Information System*, 2011, 3, 242-254 doi:10.4236/jgis.2011.33021

Ecological Modelling and Energy DSS

Energy & Wetlands Research Group
Centre for Ecological Sciences, TE 15
New Biology Building, Third Floor, E Wing
[Near D Gate], Indian Institute of Science,
Bangalore - 560012, INDIA
Web: http://ces.iisc.ernet.in/energy/
http://ces.iisc.ernet.in/biodiversity
Email: cestvr@ces.iisc.ernet.in,
energy@ces.iisc.ernet.in
Tel: 91-080-22933099/22933503-extn 107